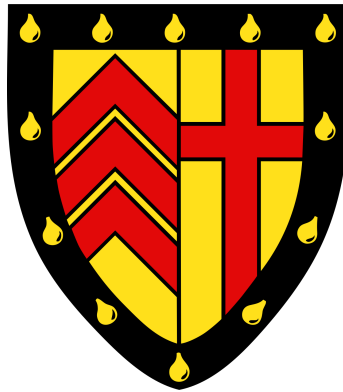


Metabolic regulation of denitrification in the
opportunistic pathogen *Pseudomonas aeruginosa*



Stephen Byron Trigg

Clare College

March 2022

This thesis is submitted for the degree of Doctor of Philosophy

Declaration

This dissertation is the result of my own work carried out under the supervision of Professor Martin Welch in the Department of Biochemistry and includes nothing which is the outcome of work done in collaboration except as specified in the text.

It is not substantially the same as any that I have submitted, or, is being concurrently submitted for a degree or diploma or other qualification at the University of Cambridge or any other University or similar institution.

I further state that no substantial part of my dissertation has already been submitted, or, is being concurrently submitted for any such degree, diploma or other qualification at the University of Cambridge or any other University or similar institution.

This dissertation does not exceed the word limit specified by the Biology Degree Committee.

Summary

Pseudomonas aeruginosa is a World Health Organization Priority 1 human pathogen and is one of the leading bacterial species implicated in nosocomial infections, posing a significant risk to immunocompromised patients due to its high level of intrinsic antimicrobial resistance and diverse metabolic physiology. Denitrification allows *P. aeruginosa* to utilise N-oxides as alternative electron acceptors to enable maintenance of proton motive force and thus the generation of ATP under nutrient- and oxygen-limited scenarios, and may also act as a defence mechanism against nitrosative attack by host immune cells. Traditionally, denitrification is thought of as an anaerobic process. However, recent work in the Welch laboratory has shown that when grown aerobically with acetate as a sole carbon source, genes involved in the denitrification pathway are highly up-regulated, despite there being no change in the transcript level of known regulators of denitrification. This is intriguing since fatty acids, such as acetate, are a preferred energy source for *P. aeruginosa* during infection, and furthermore, the known regulators of denitrification are inactivated in the presence of oxygen. In this work, I investigate the regulation of denitrification under aerobic conditions. The data revealed that the oft-reported master regulator of (anaerobic) denitrification, Anr, is of limited utility under aerobic conditions. I then examined how a loss of denitrification capabilities affects the redox state of the cell. I hypothesised that under conditions that promote rapid growth, I would observe an increase in NADH accumulation, and that this might be decreased through the use of aerobic denitrification. I found that this redox-balancing activity was independent of Anr, but was dependent on its subordinate, Dnr, and the NarG nitrate reductase. I also investigated the impact of denitrification on *P. aeruginosa* survival in a polymicrobial community using an *in vitro* continuous-flow system developed in the Welch laboratory with subsequent analysis using a Lotka-Volterra competition model. This analysis revealed that denitrification mutants are considerably less “tolerant” towards competing species and begin to rapidly dominate the culture medium, highlighting a potentially significant role for denitrification in maintaining stable population dynamics during an infection scenario.

Acknowledgements

Countless people have influenced my time in Cambridge, and each has contributed to my experience in unique, unqualifiable ways. The culmination of these interactions over the years has truly shaped me as a person and made this period of my life memorable.

I would like to thank my supervisor, Professor Martin Welch, for his invaluable feedback and forthrightness throughout my project and time in the Welch laboratory. I would like to thank Dr Rita Monson for her kindness and generosity, Dr Stephen Dolan for “spirited” scientific discussion, and Dr Shunsuke Numata for being an icon of experimental efficiency.

I also thank all the members of the Welch and Salmond groups, past and present, not only for the many happy interactions and general shenanigans, but for their tolerance and assistance with numerous things over the years. I would like to especially express my gratitude to the following people: Maria Stroyakovski for being a fantastic friend and companion in academic misery, Dr Wendy Figueroa for excellent technical advice and guidance, Dr Éva Bényei and Pok-Man Ho for their collaboration, and Dr Mel Lawson for introducing me to microbiological research.

My appreciation also goes to George for his friendship over the many, many years leading to this point, to Dom for introducing me to so many new and interesting people across Cambridge, and to Shoby for always being enthusiastic accomplices.

My family have also supported me tremendously during this project, I appreciate their belief in me and words of encouragement during the best and worst times. I could not have embarked on this journey without their love, help, and assurance.

Lastly, I would like to express unbounded gratefulness to Ayuko for her unwavering love, limitless patience, and for inspiring me each day.

*In the dark times
Will there also be singing?
Yes, there will also be singing
About the dark times.*

Bertolt Brecht

Contents

List of Figures	i
List of Tables	iii
1 Introduction	1
1.1 Ancient and modern history	1
1.2 <i>P. aeruginosa</i> in infection	3
1.2.1 Cystic fibrosis	3
1.2.2 Quorum sensing	7
1.2.3 Virulence factors	11
1.2.3.1 Phenazines	11
1.2.3.2 Siderophores	12
1.2.3.3 Hydrogen cyanide	13
1.2.4 Biofilms	14
1.2.5 Denitrification in polymicrobial infections	16
1.3 Central metabolism	17
1.4 Electron transport	19
1.4.1 Denitrification	20
1.4.1.1 Regulators of denitrification	21
1.4.1.2 The nitrate reductases	23
1.4.1.3 Nitrite reductase	24
1.4.1.4 Nitric oxide reductase	24
1.4.1.5 Nitrous oxide reductase	25
1.4.2 Terminal oxidases	25
1.4.3 Aerobic denitrification	26
1.5 Redox homeostasis	27
2 Thesis	29

3	Materials and Methods	30
3.1	Microbial strains and culture conditions	30
3.2	Media preparation	33
3.2.1	Artificial sputum medium	35
3.2.1.1	Day 1	35
3.2.1.2	Day 2	35
3.2.1.3	Day 3	37
3.3	CFU enumeration	37
3.4	DNA extraction	38
3.5	PCR and gel electrophoresis	38
3.6	Promoter:: <i>lux</i> transcriptional fusion strain generation	39
3.6.1	Vector construction	39
3.6.2	Preparation of electrocompetent <i>P. aeruginosa</i> cells	40
3.6.3	Electroporation of <i>P. aeruginosa</i>	41
3.6.4	Identification of <i>P. aeruginosa</i> transformants	41
3.7	NAD(P)(H) extraction and measurement	41
3.8	Nitrate/nitrite measurement	43
3.9	Quorum sensing molecule measurement	44
3.10	Siderophore measurement	44
3.11	Pyocyanin extraction and measurement	45
3.12	Biofilm assays	46
3.12.1	XTT assay	46
3.12.2	Crystal violet staining	46
3.12.3	CFU enumeration	47
3.13	Continuous-flow system	47
3.14	General statistical analysis	48
3.15	Lotka-Volterra competition model	48
3.15.1	General equation	48
3.15.2	Parameter estimation	48
3.15.3	Bayesian inference with Markov Chain Monte Carlo	49

METABOLIC CONTROL

4	Batch culture growth	50
4.1	Background and rationale	50
4.2	Minimal media (MOPS with a single carbon source)	51

4.3	Artificial sputum medium (single species)	55
4.4	Artificial sputum medium (triple species)	55
4.5	Discussion	59
5	Expression of respiration associated genes	61
5.1	Background and rationale	61
5.2	Differential expression of <i>acsA</i> and <i>ccoN1</i>	62
5.3	Expression of <i>anr</i> and <i>dnr</i>	62
5.4	Expression of N-oxide reductases	63
5.5	Expression of <i>fbp</i> and <i>stb</i>	64
5.6	Discussion	65
6	Measurement of redox ratios	67
6.1	Background and rationale	67
6.2	NAD(H) concentrations	68
6.3	NADP(H) concentrations	68
6.4	NAD(H) ratios	69
6.5	NADP(H) ratios	73
6.6	Discussion	73
7	Nitrate reduction	75
7.1	Background and rationale	75
7.2	MOPS acetate with nitrate	76
7.3	Artificial sputum medium	76
7.4	Discussion	79
 SIGNALLING, VIRULENCE, AND BIOFILMS		
8	Extracellular profile	82
8.1	Quorum sensing	82
8.1.1	Background and rationale	82
8.1.2	Batch culture (MOPS acetate ± nitrate)	83
8.1.3	Batch culture (artificial sputum medium)	85
8.1.4	Continuous-flow system culture (artificial sputum medium)	85
8.1.5	Discussion	88
8.2	Siderophore production	89
8.2.1	Background and rationale	89

8.2.2	Batch culture (MOPS acetate ± nitrate)	90
8.2.3	Batch culture (artificial sputum medium)	91
8.2.4	Continuous-flow system culture (artificial sputum medium)	91
8.2.5	Discussion	95
8.3	Pyocyanin production	97
8.3.1	Background and rationale	97
8.3.2	Batch culture (artificial sputum medium)	97
8.3.3	Continuous-flow system culture (artificial sputum medium)	100
8.3.4	Discussion	100
9	Biofilm formation	103
9.1	Background and rationale	103
9.2	XTT assay	104
9.3	Crystal violet staining	105
9.4	CFU distribution: biofilm vs planktonic	107
9.5	Discussion	109
 POLYMICROBIAL INTERACTIONS		
10	Continuous-flow system population dynamics	111
10.1	Background and rationale	111
10.2	CFU enumeration	112
10.3	Lotka-Volterra Markov Chain Monte Carlo analysis	114
10.3.1	Wild type analysis	114
10.3.2	Δanr analysis	115
10.3.3	Δdnr analysis	115
10.3.4	$\Delta narG$ analysis	116
10.3.5	$\Delta roxSR$ analysis	116
10.4	Discussion	116
11	Final conclusions	121
11.1	Regulation of denitrification genes	122
11.2	Denitrification in redox homeostasis	123
11.3	Denitrification and fitness in a polymicrobial community	124
11.4	Future perspectives	126
	References	128

Appendices	161
Appendix A: NAD(P)(H) measurements	161
Appendix B: quorum sensing gene promoter activity measurements	165
Appendix C: continuous-flow system CFUs (single species) and additional sta- tistical analyses of LVC model interactions (triple species)	171

List of Figures

1	Healthy and cystic fibrosis airways	6
2	<i>P. aeruginosa</i> 's quorum sensing network	8
3	Typical <i>in vitro</i> model of biofilm formation	14
4	Overview of the <i>P. aeruginosa</i> citric acid cycle and glyoxylate shunt	18
5	The branched respiratory chain of <i>P. aeruginosa</i>	20
6	The denitrification apparatus of <i>P. aeruginosa</i>	21
7	The anaerobic denitrification regulatory cascade of <i>P. aeruginosa</i>	22
8	NAD(P)(H) standard curves	42
9	Nitrite standard curve	43
10	Deferoxamine mesylate salt standard curve	45
11	Continuous-flow system setup	47
12	Growth curves: MOPS minimal medium containing single carbon sources	52
13	Growth rates: MOPS minimal medium containing single carbon sources	53
14	Growth curves: MOPS acetate ± nitrate	54
15	Growth curves: artificial sputum medium	56
16	Growth rates: artificial sputum medium	56
17	Growth curves: artificial sputum medium (96-hour batch culture, single species)	57
18	Growth curves: artificial sputum medium (96-hour batch culture, triple species)	58
19	Lux assay: <i>acsA</i> and <i>ccoN1</i>	63
20	Lux assay: <i>anr</i> and <i>dnr</i>	63
21	Lux assay: <i>narK1</i> , <i>nirS</i> , <i>norC</i> , and <i>nosR</i>	64
22	Lux assay: <i>fbp</i> and <i>sth</i>	65
23	Total NAD(H) concentrations: MOPS acetate ± nitrate	69
24	Total NADP(H) concentrations: MOPS acetate ± nitrate	69
25	Peak NADH:NAD ⁺ ratios: MOPS acetate ± nitrate	70
26	NADH:NAD ⁺ ratios: MOPS acetate ± nitrate	71
27	NADPH:NADP ⁺ ratios: MOPS acetate ± nitrate	72
28	Nitrite concentrations: MOPS acetate ± nitrate	77

29	Nitrate and nitrite concentrations: artificial sputum medium	78
30	Summary: redox balancing via denitrification	81
31	PQS promoter activity: multiple media (24-hour batch culture, <i>P. aeruginosa</i>) . .	84
32	PQS promoter activity: artificial sputum medium (96-hour batch culture, single and triple species)	86
33	PQS promoter activity: artificial sputum medium (96-hour continuous-flow cul- ture, single and triple species)	87
34	Siderophore concentrations: multiple media (24-hour batch culture, <i>P. aeruginosa</i>)	92
35	Siderophore concentrations: artificial sputum medium (96-hour batch culture, single and triple species)	93
36	Siderophore concentrations: artificial sputum medium (96-hour continuous-flow culture, single and triple species)	94
37	Pyocyanin concentrations: artificial sputum medium (96-hour batch culture, single and triple species)	98
38	Pyocyanin concentrations: artificial sputum medium (96-hour continuous-flow culture, single and triple species)	99
39	Biofilm assay: XTT (wild types; single-, dual-, and triple-species)	104
40	Biofilm assay: XTT (mutants; single-, dual-, and triple-species)	105
41	Biofilm assay: crystal violet (wild types; single-, dual-, and triple-species)	106
42	Biofilm assay: crystal violet (mutants; single-, dual-, and triple-species)	107
43	Biofilm assay: CFUs (batch culture, single species)	108
44	Biofilm assay: CFUs (batch culture, dual species)	108
45	Biofilm assay: CFUs (batch culture, triple species)	109
46	Continuous-flow system: CFUs (triple species)	113
47	Summary: ecological interactions	120

List of Tables

1	CF mutation type frequency	4
2	Classes of <i>CFTR</i> mutations	4
3	Microbial strains	30
4	General growth media	33
5	MOPS minimal media	33
6	Species-selective media	34
7	Artificial sputum medium: amino acid stock solutions	36
8	Artificial sputum medium: buffered base stock solutions	36
9	Artificial sputum medium: nutrients	37
10	Artificial sputum medium: solids	37
11	PCR master mixture	38
12	PCR thermocycling conditions	38
13	Primers	40
14	Siderophore assay reagents	44
15	XTT assay reagents	46
16	Continuous-flow system: ecological interactions	115
17	Summary: phenotypes observed in Chapters 4-8	127

Introduction

1.1 Ancient and modern history

The history of *Pseudomonas aeruginosa* begins in 1849, when a French military surgeon, Charles-Emmanuel Sédillot, described observing a blue-grey pus present in wound dressings (Sédillot, 1849). In the 1860s, Mathurin-Joseph Fordos identified the agent causing the discolouration as pyocyanin, and this was then associated with rod-shaped bacteria by Georg Albert Lücke (Fordos, 1860; Lücke, 1862). It wasn't until 1882 that a pure culture of *P. aeruginosa*, then called *Bacillus pyocyaneus*, was first obtained by Carle Gessard (Gessard, 1882).

Following these landmark discoveries, attention turned to the utilisation of *P. aeruginosa* in a medical context. In 1889, Albert Charrin and Georges Henri Roger revealed that resistance to *P. aeruginosa* could be achieved by prior exposure, after demonstrating the reduced reinfection of previously *P. aeruginosa*-infected animals (Charrin and Roger, 1889). Advancing the theory of protective inoculation further, Charles Jacques Bouchard injected small quantities of cell-free *P. aeruginosa* culture into rabbits and found that this inhibited the development of anthrax, establishing that a *P. aeruginosa* secretion has an antimicrobial effect (Bouchard, 1889). Additionally, German Sims Woodhead and George Edward Cartwright Wood noted that the same result could be achieved using sterilised cultures (Woodhead and Wood, 1889). In pursuit of a purer treatment, Rudolph Emmerich and Oscar Löw showed that a culture extract that they named pyocyanase—a moniker given as it was initially believed to be an enzyme, but was later revealed to be pyocyanin and a range of “pyo compounds” that today are recognised as 4-hydroxy-2-alkylquinolines—was able to inhibit the growth of *Bacillus anthracis*, *Corynebacterium diphtheriae*, *Neisseria gonorrhoeae*, *Staphylococcus* spp., *Streptococcus pneumoniae*, *Shigella dysenteriae*, and *Vibrio cholerae* (Emmerich and Löw, 1899; Wells, 1952).

Subsequently, pyocyanase was produced as eyedrops, mouthwash, and topical sprays that were used in a clinical setting, before falling out of favour in the following decades due to its incon-

sistent efficacy, short shelf life, and troublesome production, since not all strains of *P. aeruginosa* were apparently able to produce pyocyanase (Hays *et al.*, 1945). Interestingly, in Selman Waksman's final publication, entitled *History of the Word 'Antibiotic'*, pyocyanase is listed first, followed by penicillin and actinomycin, acknowledging *P. aeruginosa* as an originator of the field of antimicrobial discovery (Waksman, 1973).

Today, we recognise *P. aeruginosa* as a Gram-negative opportunistic pathogen that can flourish throughout diverse aerobic and anaerobic environments, ranging from soil and water in the greater biosphere to distinct microenvironments in animal, human and plant hosts (Hardalo and Edberg, 1997; Ahearn *et al.*, 1999; Costerton, Stewart and Greenberg, 1999). In the human host, *P. aeruginosa* has been identified in the respiratory system, burn wounds, and the gastrointestinal and urinary tracts (Bodey *et al.*, 1983). These locations underscore *P. aeruginosa* as an important human pathogen, but additionally its ability to colonise the surfaces of medical equipment, such as catheters and ventilators, highlight its exquisite capacity to thrive in varied clinical settings (Bodey *et al.*, 1983). *P. aeruginosa* poses little threat to the healthy population. However, the elderly and immunocompromised, particularly those in the hospital environment, are at particular risk. *P. aeruginosa* is a leading nosocomial pathogen, accounting for 10% of all hospital acquired infections in Europe and an carrying an estimated mortality rate 40-60% of all infections resulting in hospitalisation (Lister, Wolter and Hanson, 2009; De Bentzmann and Plésiat, 2011). Public Health England recently introduced mandatory reporting of *P. aeruginosa* infections and the World Health Organization reclassified it as a Priority 1 pathogen—therefore, there is significant interest in the physiology of this bacterial species (Lister, Wolter and Hanson, 2009).

The ability of *P. aeruginosa* to resist antimicrobial treatment and host immune defences, use a variety of energy sources, and outcompete a number of microbial species to dominate the local environment may be attributed to its large genome size of 6.3 Mbp arranged in more than 5000 open reading frames (Stover *et al.*, 2000). The *P. aeruginosa* genome includes the largest predicted suite of regulatory proteins observed in any sequenced bacterial species, comprising some 9% of the genome, and a considerable number of genes involved in chemosensing, chemotaxis, nutrient import, and metabolism. It is this density of transcriptional regulators that enables *P. aeruginosa* to be able to adapt to such diverse environments and has placed it as a model organism for many bacterial processes, such as quorum sensing, biofilm formation, and antimicrobial resistance (Toole, Kaplan and Kolter, 2000; Poole, 2001; Withers, Swift and Williams, 2001; Juhas, Eberl and Tümmler, 2005).

P. aeruginosa is renowned for its high level of intrinsic resistance to a number of chemotherapeutic agents, a phenotype conferred by the broad range of resistance genes and efflux pumps encoded in its genome (Stover *et al.*, 2000). Additionally, *P. aeruginosa* synthesises a diverse suite of toxins and virulence factors that permit the organism to damage host cells and dominate lo-

cal microenvironments, allowing it to consolidate its colonisation of the host. Virulence factors produced by *P. aeruginosa* include LPS, exotoxin A, proteases, type III secretion systems, lectins, flagella, type IV pili, pyocyanin, pyoverdine, rhamnolipids, and cystic fibrosis transmembrane conductance regulator (CFTR) inhibitory factor (Cif). *P. aeruginosa* is able to thrive under numerous conditions in part due to its highly adaptive metabolism that allows for the efficient use of various carbon sources, appropriately directing flux through a number of energy-generating pathways to minimise carbon-loss during growth on poor nutrient sources. Furthermore, *P. aeruginosa* utilises aerobic and anaerobic respiration, enabling it to adjust and fine-tune its electron transport chain in rapidly changing oxygen-limited environments. These abilities are underscored by its efficiency in maintaining a highly persistent lung infection in cystic fibrosis (CF) patients, where a major carbon source for *P. aeruginosa* is often fatty acids and polyols derived from the metabolism of lipids contained in lung surfactant (Sun *et al.*, 2014).

1.2 *P. aeruginosa* in infection

1.2.1 Cystic fibrosis

P. aeruginosa is one of the major bacterial species that infects the airways of CF patients. CF is the most common life-limiting disease in the Caucasian population and affects more than 70,000 people worldwide (Chen, Shen and Zheng, 2021). CF is caused by a mutation in the *CFTR* gene, inherited in an autosomal recessive manner (Riordan *et al.*, 1989). The most common mutation in the Caucasian population is an in-frame deletion of phenylalanine at position 508, however, more than 1950 *CFTR* mutations have been identified to date and these can be grouped into 6 distinct classes (Table 1 and Table 2; Boyle and De Boeck, 2013; Chen, Shen and Zheng, 2021). Despite the wide range of mutations and classes of mutations, only 450 of these mutations have been classified to date as pathogenic, according to the CFTR2 database, and these mutations co-segregate with 96% of CF patients with northern European ancestry (*CFTR2 Variant List History*, 2022).

CFTR encodes a transmembrane protein that facilitates the transport of chloride across epithelial cell membranes (Riordan *et al.*, 1989). In normal healthy lungs, there is a mucus layer that, coupled with ciliary movement, aids in the capture and removal of bacteria from the respiratory tract. The CFTR channel's primary function is to transport anions (for example, chloride and bicarbonate) across epithelial cell apical membranes, but it also interacts with the amiloride-sensitive sodium channel, or ENaC. These two channels work together to regulate the hydration of mucins and airway secretions in the airway.

TABLE 1. CF mutation type frequency.

Mutation type	Count	Frequency (%)
Missense	815	38.74
Frameshift	342	16.25
Splicing	230	10.93
Nonsense	177	8.41
In frame in/del	43	2.04
Large in/del	59	2.8
Promoter	17	0.81
Sequence variation	269	12.79
Unknown	152	7.22

TABLE 2. Classes of *CFTR* mutations.

Class	Defect	Mutation type	Common mutations
I	No functional CFTR protein	Nonsense	Gly542X
		Frameshift	Arg553X
		Canonical splice	621+1G→T
II	CFTR trafficking defect	Missense	Phe508del
		Amino acid deletion	Ile507del
			Arg560Thr
III	Defective channel regulation	Missense	Gly551Asp
		Amino acid change	Gly178Arg
			Ser549Asn
IV	Decreased channel conductance	Missense	Arg117His
		Amino acid change	Arg347Pro
			Arg117Cys
V	Reduced synthesis of CFTR	Missense	3849+10kbC→T
		Splicing defect	3120+1G→A
			5T
VI	Decreased CFTR stability	Missense	4326delTC
		Amino acid change	Gln1412X
			4279insA

Since epithelial cells also line the liver, pancreas, intestines, and sweat glands, defective CFTR can affect multiple organ systems, therefore the pathophysiology of CF is not limited just to reduced lung function (Vallières and Elborn, 2014; O'Neal and Knowles, 2018)., However, regardless of the organ affected, mutations in *CFTR* lead to a defect in chloride and bicarbonate transport, in addition to modified sodium (through ENaC) and water transport, disrupting ion and fluid homeostasis, and ultimately resulting in acidification of the apical surface microenvironment. In sweat glands, this defect diminishes the recovery of salt from sweat. However, in the lungs, liver, pancreas, and intestines, impaired CFTR function results in dehydration of the mucosal surface, and a thickened, viscous mucus build up that obstructs luminal compartments and ducts (Derichs, 2013; Gentsch and Mall, 2018). In the lung, airway surface liquid is a two-part protective system usually serves to sequester and clear unwanted entities from the airways, comprising an outer mucus layer that initially serves as a sticky trap for pathogens and other particles, and the periciliary layer, that acts as a lubricated surface to facilitate ciliary beating and the movement of the outer mucus layer from the airway (Button *et al.*, 2012; Button and Button, 2013). Therefore, the hydration and volume of the airway surface liquid is extremely important to mucociliary clearance. When the CFTR channel is dysfunctional, the osmotic gradient between the mucus and epithelium is altered as a result of altered anion transport and sodium and water absorption. These transport changes manifest as a depletion of the airway surface liquid volume and changes to the osmotic gradient that affects the two layers differently. The reduction in airway surface liquid volume increases the osmotic pressure in the outer mucus layer, which in turn pulls water from the periciliary layer and compresses cilia (Button *et al.*, 2012; Henderson *et al.*, 2014). This results in impaired mucociliary clearance in the respiratory system, the first line of defence against pathogens, ultimately leading to the lung being colonised by various microbial species (Figure 1; Govan and Deretic, 1996).

Typically, *Staphylococcus aureus* and *Haemophilus influenzae* are common early colonisers during early childhood, before *P. aeruginosa* becomes the dominant infection from adolescence onwards, with *P. aeruginosa* found in 93% of CF patients between the ages of 18 and 24 years old, and present in 80% of all adults with CF (Greenberg and Stutman, 1991; Döring, 1997; Lyczak, Cannon and Pier, 2000; Tang *et al.*, 2014). Additionally, *Achromobacter* spp., *Aspergillus* spp., *Burkholderia cepacia*, *Candida* spp., *Granulicatella* spp., non-tuberculous *Mycobacteria*, *Neisseria* spp., *Pandoraea* spp., *Prevotella* spp., *Ralstonia* spp., methicillin-resistant *Staphylococcus aureus*, *Stenotrophomonas maltophilia*, and *Veillonella* spp. are all emerging in recent years as important cystic fibrosis-associated pathogens, highlighting the range of species that colonise the CF lung as highly diverse (Sajjan *et al.*, 2001; Pihet *et al.*, 2009; Bittar and Rolain, 2010; Field *et al.*, 2010; LiPuma, 2010; Chiappini, Taccetti and de Martino, 2014; Parkins and Floto, 2015; Frayman *et al.*, 2017; Ahmed *et al.*, 2019).

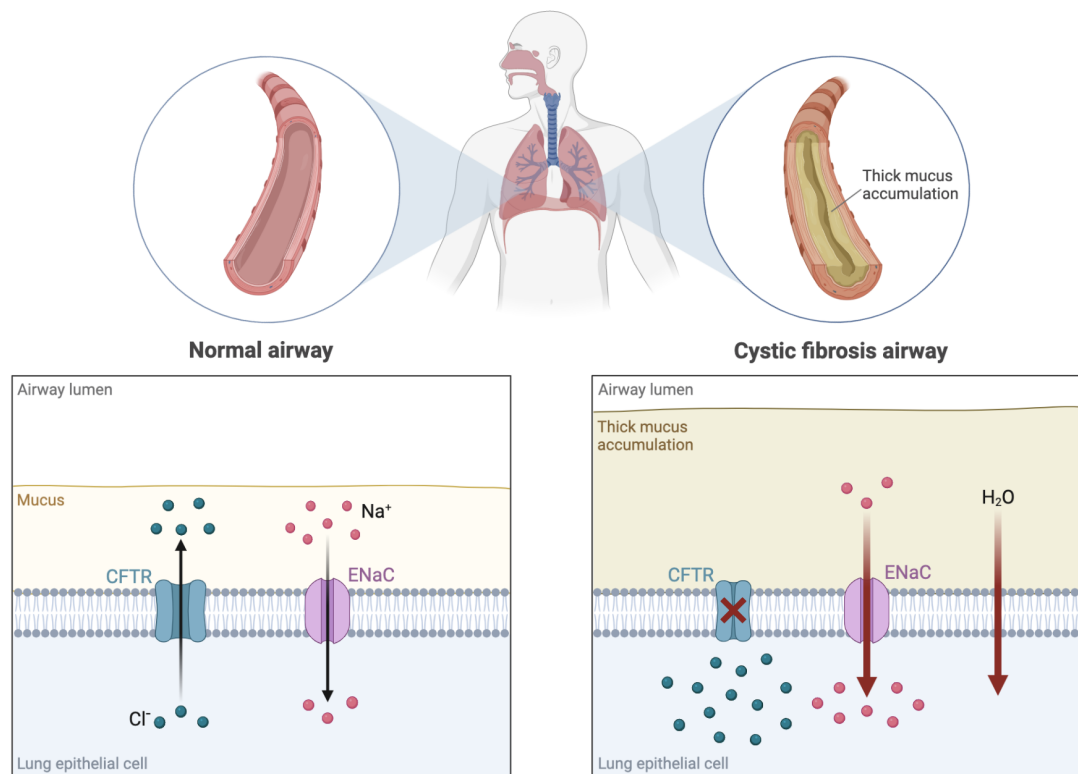


FIGURE 1. The normal human airway compared with the cystic fibrosis airway. Mutations in the *CFTR* gene result in impairment of chloride transport, disrupting the ionic balance across the lung epithelium. This results in increased sodium import, shifting the osmotic gradient and subsequently drawing water out of the lumen, increasing the thickness and stickiness of secreted mucus.

With so many species present in the CF lung, a complex network of interspecies interactions must exist in order to permit these species to live alongside each other. Species can communicate by several means, for example through the recognition of cell-surface elements (for example, proteins or cell wall components), the secretion and uptake of metabolites, or the detection of quorum sensing molecules. The net effect of these interactions may be beneficial or detrimental to one species or the community as a whole, and while this is a fascinating avenue of research, it is not clear how new species and strains interact with the pre-existing lung microbiota, which species comprise the beneficial commensal population that protect the airways, and which species promote colonisation (Bjornson *et al.*, 1982; Kirketerp-Møller *et al.*, 2008; Conrad *et al.*, 2013). However, gene expression profiles have been obtained for species cultured axenically and in co-cultivation that could shed some light on this area. For example, comparisons between *S. aureus* and *P. aeruginosa* co-cultures and axenic growth of these species have revealed that *S. aureus* differentially expresses as much as 25% of its core genome during growth in the presence of *P.*

aeruginosa (Ibberson *et al.*, 2017; Briaud *et al.*, 2019). Interestingly, there is evidence to suggest that *P. aeruginosa* generally outcompetes *S. aureus* in the CF lung, but if given enough time, these species co-evolve and exist in an uneasy truce (Yung, Sircombe and Pletzer, 2021).

After *P. aeruginosa* becomes established in the CF lung, it may undergo several physiological changes that render infections almost impossible to eradicate. Prime among these is the over-expression of alginate, resulting in the conversion to a mucoid phenotype that is associated with loss of flagella (and thus motility), signalling the onset of chronic infection (Lyczak, Cannon and Pier, 2002). Additionally, mutations in DNA mismatch repair genes lead to a hypermutable phenotype that has an increased mutation frequency (>20-fold compared with wild type), allowing for the selection of advantageous genotypes (Hogardt *et al.*, 2007; Oliver and Mena, 2010). These adaptations culminate in the characteristic persistence of *P. aeruginosa* in the CF lung that is coupled with exceptional resistance to a wide range of antimicrobials.

The treatment of CF has dramatically improved over the years and has greatly extended the projected lifespan of CF patients. For example, the use of the Orkambi combination therapy in patients homozygous for the Phe508del mutation—which contains ivacaftor, a CFTR potentiator that increases channel opening, and lumacaftor, a protein folding chaperone that assists in CFTR trafficking to the cell membrane—has been shown to improve patients' forced expiratory volumes, decreases lung clearance indexes (which are increased when airways narrow due to inflammation or mucus build-up), and decreases the amount of chloride present in sweat (whose presence is an measure of defective chloride transport) (Konstan *et al.*, 2017). However, in spite of these successful novel treatments, there is still the lingering issue of chronic *P. aeruginosa* infections in CF, which reduce life expectancy in Europe to 12-40 years (Klepac-Ceraj *et al.*, 2010). Of course, *P. aeruginosa* is not the only pathogen found in the lungs and airways of CF patients, however, its impressive adaptability and resistance to chemotherapeutic intervention mean that it comes to dominate the lung microflora, and its range of secreted virulence factors can provoke widespread inflammation (Paranjape and Mogayzel, 2014). This, coupled with declining lung function and infection-induced scarring, exacerbates the CF condition, and emphasises the need for effective treatments of chronic *P. aeruginosa* infections.

1.2.2 Quorum sensing

In order to flourish in such a variety of environments, *P. aeruginosa* requires a comprehensive regulatory network not just to control its metabolic network at a single-cell level, but also to coordinate the bacterial population at large. Cell-to-cell communication between bacterial communities is mediated by quorum sensing (QS), an intracellular communication system based on cell density and the production of signalling molecules that have a population-wide effect upon accumulation.

QS was first proposed in the 1990s, based on population-density dependent mechanisms found in *Aliivibrio fischeri* (Fuqua, Winans and Greenberg, 1994). Typically, QS molecules will accumulate as the bacterial population increases. When this happens, eventually a threshold effective concentration of QS molecules will accumulate. Depending on the distribution and diffusion rate of these molecules through the population, transcription of various QS-regulated genes will be initiated. *P. aeruginosa*'s QS system is mediated by two chemically distinct classes of signalling molecules: acylhomoserine lactones and 4-quinolones.

The importance of *P. aeruginosa* as a nosocomial human pathogen has led to it becoming a model system for examining the functionality of QS. *P. aeruginosa* has an elaborate QS network, comprising at least three distinct signalling systems (*las*, *rhl*, and *pqs*), that function together to form an efficient, self-regulatory, looping feedback system (Figure 2). A fourth (proposed) QS system, *iqs*, has in recent years been a controversial subject of debate, with its pervasive inclusion in many QS reviews leading to acceptance of its role in QS in spite of contradictory evidence (Cornelis, 2020). For this reason, the *iqs* system will not be discussed here.

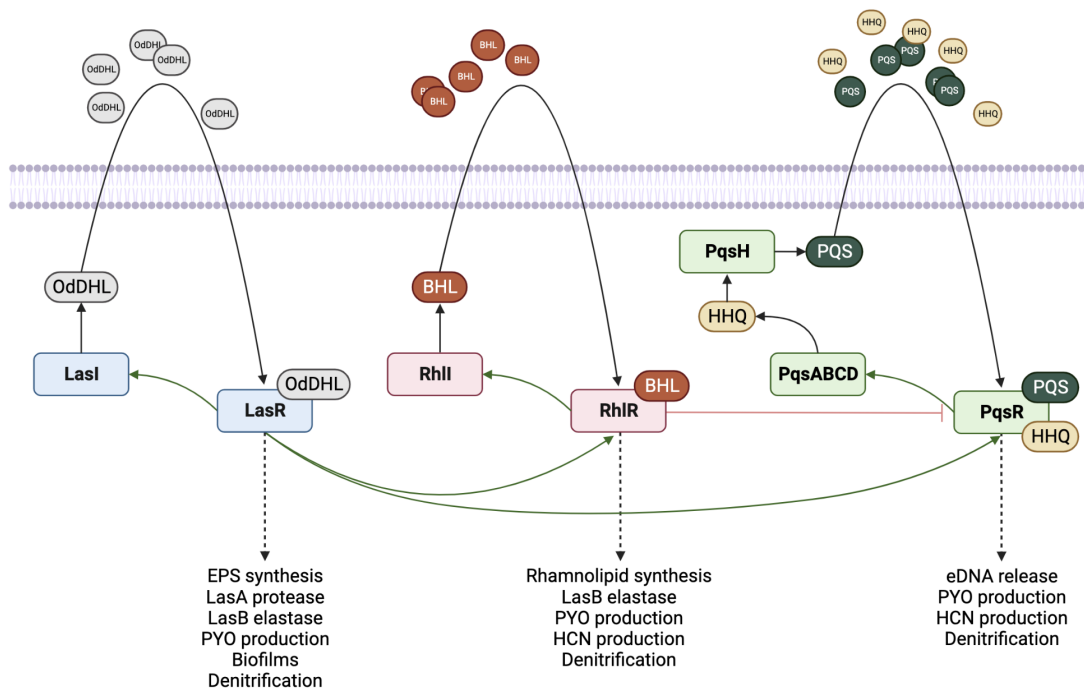


FIGURE 2. The feedback loop of interlinked quorum sensing systems in *P. aeruginosa*, comprising autoinducer synthases (LasI, RhlI, and PqsABC) and their cognate receptors (LasR, RhIR, and PqsR).

The *las* system comprises the transcriptional activator LasR and the acylhomoserine lactone (AHL) synthase LasI. The latter catalyses the synthesis of the *as* autoinducer molecule, OdDHL

(3-oxo-C₁₂-HSL or PAI-1), which binds to LasR and activates or represses its target genes (Gambello and Iglewski, 1991; Pearson *et al.*, 1994). LasR recognises the *las* box, a conserved dyad symmetry DNA motif that is found upstream of many genes known to be directly regulated by this system, such as exopolysaccharide synthesis, proteases, elastases and biofilm regulation (Rust, Pesci and Iglewski, 1996; Anderson, Zimprich and Rust, 1999; Whiteley and Greenberg, 2001).

The *rhl* system connects with the previously characterised *rhlABR* gene cluster, which encodes a rhamnosyltransferase (RhlAB) and a regulatory protein (RhlR) that are all required for rhamnolipid biosynthesis (Ochsner and Reiser, 1995). The RhlI autoinducer synthetase produces BHL (C₄-HSL or PAI-2) which binds to RhlR, activating its activity against target genes, such as those involved in rhamnolipid synthesis. Together the *las* and *rhl* systems coordinate the production of elastase (Brint and Ohman, 1995; Ochsner and Reiser, 1995; Pearson *et al.*, 1995). The RhlR ligand-free form functions as a transcriptional repressor, demonstrating that both forms of RhlR can moderate the expression of QS-regulated genes (Medina *et al.*, 2003). Interestingly, RhlR was also recently shown to have transcriptional activity even in the absence of RhlI, suggestive of RhlR regulation by a different, unknown ligand. Furthermore, $\Delta rhlI$ mutants display full virulence in animal models, in contrast with the $\Delta rhlR$ mutant (Mukherjee *et al.*, 2017).

The *pqs* system was identified through the addition of spent culture supernatant from *P. aeruginosa* wild type PAO1 cultures to $\Delta lasR$ mutant cultures, which resulted in significant transcription from the *lasB* promoter. This could not be replicated by the addition of OdDHL or BHL, therefore suggesting the existence of an uncharacterised QS signalling molecule, which turned out to be an alkylquinolone, aptly named *Pseudomonas* quinolone signal (2-heptyl-3-hydroxy-4-quinolone or PQS) (Pesci *et al.*, 1999). The genes required for PQS biosynthesis were identified and as *pqsABCD*, *phnAB*, *pqsH*, and a LysR family regulator encoded by *pqsR* (Cao *et al.*, 2001; Gallagher *et al.*, 2002). PQS biosynthesis is initiated by anthranilate-CoA ligase, PqsA, which then activates the anthranilate synthesised by PhnAB to form anthraniloyl-CoA. This is then processed by the 3-oxoacyl-ACP synthases, PqsB, PqsC and PqsD, generating 2-heptyl-4-quinolone (HHQ) (Gallagher *et al.*, 2002; Déziel *et al.*, 2004; Collman, Hudson, *et al.*, 2008). HHQ is subsequently converted into PQS by PqsH, a predicted flavin-dependent monooxygenase (Déziel *et al.*, 2004; Schertzer, Boulette and Whiteley, 2009). The PQS system has been demonstrated to be involved in the regulation of multiple virulence determinants including elastases, rhamnolipids, lectins, and pyocyanin—the blue-green phenazine pigment that gives *P. aeruginosa* its distinctive hue (Pesci *et al.*, 1999; Diggle *et al.*, 2003). The PQS gene cluster also contains a fifth ORF, *pqsE*. The role of PqsE is relatively unclear, as $\Delta pqsE$ mutants do not affect the biosynthesis of PQS, do not respond to PQS, and do not produce PQS-regulated molecules, such as pyocyanin. In contrast however, overexpression of PqsE results in enhanced pyocyanin and rhamnolipid biosyn-

thesis; two phenotypes that are dependent on PQS signalling (Gallagher *et al.*, 2002; Diggle *et al.*, 2003; Farrow *et al.*, 2008). PqsE was finally characterised as a thioesterase, which catalyses the production of the HHQ precursor, 2-aminobenzoylacetate (Drees and Fetzner, 2015). As one might come to expect from the complex metabolic network of *P. aeruginosa*, there is some redundancy built into the HHQ biosynthetic pathway. The thioesterase TesB has been shown to sustain HHQ production in the absence of *psqE*, therefore clarifying how the *pqsE* mutant can still synthesise both HHQ and PQS (Drees and Fetzner, 2015). However, blocking the thioesterase activity of PqsE does not block pyocyanin production, indicating that regulatory activity of PqsE is independent of this activity (Zender *et al.*, 2016).

Upon first glance at the hierarchy of the *P. aeruginosa* QS network, it appears that the *las* system may be the most important component, considering it promotes the expression of the *rhl* system. LasR also positively regulates the expression of the *pqs* system genes *pqsR* and *pqsH*, initiating the production of HHQ and its derivative, PQS (Pesci *et al.*, 1999; McKnight, Iglewski and Pesci, 2000). Elegantly, a feedback loop involving PQS stimulates the production of BHL and thus the *rhl* system regulon, which eventually leads to the inhibition of *pqs* expression. This highlights the importance of a finely-tuned ratio between OdDHL and BHL in the regulation of PQS signaling (Cao *et al.*, 2001). Additionally, the small RNA, ReaL, has been shown to regulate synthesis of PQS via a positive post-transcriptional interaction with *pqsC*, and ReaL is also negatively regulated by LasR, further highlighting the complexity of QS in *P. aeruginosa* (Carloni *et al.*, 2017). Interestingly, deletion of *lasR* does not preclude PQS production or indeed result in significant impediment of QS in *P. aeruginosa* (Diggle *et al.*, 2003). In fact, many clinical isolates are in fact LasR-null and retain RhlR activity, possibly rerouting the QS network through PqsE or the stringent response (Van Delden *et al.*, 1998; Smith *et al.*, 2006; Feltner *et al.*, 2016).

There is abundant literature surrounding the role of QS in the expression of virulence factors. Most relevant to this dissertation perhaps is the role of QS in denitrification. In oxygen-limited environments, *P. aeruginosa* survives by respiring N-oxides in lieu of molecular oxygen, catalysing the four-step conversion of nitrate to dinitrogen gas via a series of reductases (Henry and Bessières, 1984; Zumft, 1997; Cutruzzolà and Frankenberg-Dinkel, 2016). Crucial in this cascade is the production of the toxic intermediates, nitric oxide and nitrous oxide (Fang, 1997). QS involvement in denitrification was first demonstrated in anaerobic biofilms, where *rhl*-deficient mutants were committing what was termed as ‘metabolic suicide’ as a result of nitric oxide accumulation, effectively showing that *rhl*-mediated nor regulation was required in order to maintain low nitric oxide during anaerobic respiration (Yoon *et al.*, 2002). Further work showed that the *las* and *rhl* systems repress denitrification, in a *rhl*-dependent manner, and additionally that under aerobic conditions PQS affects denitrification enzyme activities through its iron-chelating activity, which is especially relevant considering many of the enzymes and reg-

ulators involved in denitrification have iron-sulphur clusters and haem groups (Zumft, 1997; Toyofuku *et al.*, 2007). The addition of FeCl₃ to the medium alongside PQS reversed the suppression of nitrate reduction (Toyofuku *et al.*, 2008). A transcriptomic study investigated a QS-deficient clinical isolate, J215, compared with the *P. aeruginosa* wild type, and revealed that the denitrification machinery was expressed at a higher level in the clinical isolate (Hammond *et al.*, 2015). More recently, Cui *et al.* demonstrated that addition of OdDHL or BHL to $\Delta lasI$ or $\Delta rhlI$ mutant cultures, respectively, restored a wild-type phenotype with respect to denitrification. Furthermore, the addition of an acylase, which degrades acylhomoserine lactones, increased denitrification activity (Cui *et al.*, 2021).

1.2.3 Virulence factors

1.2.3.1 Phenazines

P. aeruginosa produces a wide range of virulence factors, some with multiple activities in the context of infection or polymicrobial interaction. Among these virulence factors are the phenazines. *P. aeruginosa* can synthesise four phenazines: pyocyanin, phenazine-1-carboxylic acid, phenazine-1-carboxamide, and 1-hydroxyphenazine. Phenazines have been linked to a range of processes: iron acquisition, biofilm formation, persister formation, colony morphology, and the support of anaerobic growth by maintaining proton motive force through redox cycling (Möker, Dean and Tao, 2010; Wang, Kern and Newman, 2010; Wang *et al.*, 2011; Dietrich *et al.*, 2013; Glasser, Kern and Newman, 2014). Perhaps the best recognised phenazine is pyocyanin, to which the blue-green colour of *P. aeruginosa* stationary-phase cultures may be attributed. Pyocyanin is the most abundant phenazine produced and has both antimicrobial and redox-active properties (Kerr *et al.*, 1999; Mavrodi *et al.*, 2001; Price-Whelan, Dietrich and Newman, 2006, 2007; Das *et al.*, 2013; Raji El Feghali and Nawas, 2018). In addition, the low molecular weight and zwitterionic state of pyocyanin enables it to permeate cells with relative ease and cause widespread oxidative stress and inflammation in multiple organ systems during an infection, further reinforcing its relevance as an important virulence factor (Lau *et al.*, 2004; Hall *et al.*, 2016).

Most relevant to this dissertation are the redox-active capabilities of phenazines and their involvement in denitrification. In phenazine-null mutants, an increase in transcripts relating to denitrification, specifically the up-regulation of *napA* during stationary phase growth has been observed (Y.-C. Lin *et al.*, 2018). The previously cited work also highlights that in a biofilm cross-section, the denitrification regulator Anr has an inverse relationship between its expression and the abundance of phenazines. Additionally, the work indicates that phenazine-null mutants also displayed increased intracellular oxidation of the redox pool, raising the possibility of a redox-cycling loop balanced by phenazines and denitrification activity.

1.2.3.2 Siderophores

In addition to phenazines, *P. aeruginosa* produces siderophores, metal-chelating molecules that obtain the iron that is essential to a wealth of biological processes in bacteria. Iron is a key component in the catalytic activity of many enzymes and sensing proteins, including the denitrification apparatus, and is commonly used in two oxidation states: Fe^{2+} and Fe^{3+} . This difference in oxidation state makes iron perfectly suited for oxido-reduction reactions, though its availability can be impinged by the degree of oxidation. For example, Fe^{3+} has low solubility in oxygenated environments (Andrews, Robinson and Rodríguez-Quiñones, 2003). *P. aeruginosa* has several strategies that it uses to acquire iron, mainly utilising extracellular reduction of Fe^{3+} to Fe^{2+} , thus increasing solubility (for example by reduction by phenazines and the Feo system), or by using siderophores to directly intake Fe^{3+} (Andrews, Robinson and Rodríguez-Quiñones, 2003; Cornelis, 2010; Lau, Krewulak and Vogel, 2016).

P. aeruginosa produces two iron-chelating siderophores with differing affinities, pyoverdine (high affinity) and pyochelin (low affinity). These siderophores bind specifically to Fe^{3+} before being imported to the cell by the cytoplasmic membrane protein TonB (Cornelis and Dingemans, 2013). The different affinities of these molecules, in addition to their stoichiometric values of iron binding (pyoverdine binds 1:1 with Fe^{3+} , pyochelin binds 2:1 with Fe^{3+}), cement the positioning of pyoverdine as the dominant siderophore used in iron acquisition. Fe^{3+} is toxic to mammals even at low concentrations, therefore transferrin—a vertebrate iron transport protein—is used to sequester Fe^{3+} . Interestingly, pyoverdine's iron affinity is strong enough to remove iron from transferrin, therefore it is perhaps not surprising that iron-acquiring actions by bacteria are often associated with disease severity. Indeed, pyoverdine alongside TonB has been demonstrated to be essential for infection in a mouse model (Takase *et al.*, 2000). Additionally, pyoverdine is an extracellular signalling factor that stimulates the production of exotoxin A and the transferrin-cleaving protease, PrpL (Wilderman *et al.*, 2001; Lamont *et al.*, 2002; Visca, Imperi and Lamont, 2007; Cornelis and Dingemans, 2013). Due to the low iron affinity of pyochelin, its production is generally limited to conditions of higher iron concentration, and when iron becomes critically low *P. aeruginosa* switches to production of the higher affinity siderophore, pyoverdine (Dumas, Ross-Gillespie and Kümmerli, 2013). Interestingly, however, the pyochelin-iron complex has been demonstrated to be active in redox cycling activity. Furthermore, in conjunction with the presence of pyocyanin, pyochelin activity can lead to the generation of hydroxyl radicals that damage the lung epithelium. Therefore, whilst its utility in iron acquisition may be limited, pyochelin's relevance in infections is not negligible (Coffman *et al.*, 1990; Britigan *et al.*, 1992; Lyczak, Cannon and Pier, 2002).

As previously mentioned, Fe^{3+} accumulation can be toxic due to generation of reactive oxygen

species, therefore the uptake of iron is under stringent regulation. Iron acquisition is regulated by Fur (shortened from ferric uptake regulator), which binds to target DNA at defined “Fur boxes” depending on the environmental iron concentration (Pasqua *et al.*, 2017). In iron-rich conditions, Fur, in conjunction with a bound Fe^{2+} , acts as a transcriptional repressor of genes involved in iron uptake, therefore precluding a toxic accumulation of iron (Troxell and Hassan, 2013). In iron-poor conditions, Fur inhibition of iron acquisition promoters ceases, and the biosynthesis of siderophores and uptake machinery is initiated (Youard, Wenner and Reimann, 2011). In the context of *P. aeruginosa* respiration Fur is also known to repress expression of some of the iron-containing terminal oxidases in the presence of Fe^{2+} , and it loses this repression in the presence of nitric oxide, emphasising the role of iron acquisition in maintaining functional respiratory branches under diverse conditions (D’Autr aux *et al.*, 2002; Kawakami *et al.*, 2010).

1.2.3.3 Hydrogen cyanide

P. aeruginosa is also a well-known producer of hydrogen cyanide (HCN). Detection of HCN produced by *P. aeruginosa* is a common biomarker of a new *P. aeruginosa* infection in children with CF, and it is the only organism found in the CF lung known to produce HCN (Williams, Zlosnik and Ryall, 2006; Ryall *et al.*, 2008; Smith *et al.*, 2013; Gilchrist *et al.*, 2015).

Considering that HCN binds tightly to haem iron and thus prevents ligand binding (Sugishima *et al.*, 2007), *P. aeruginosa* has a strictly controlled regulatory network around HCN production that prevents it from inhibiting its own respiratory system (denitrification enzymes and cytochrome *c* oxidase have haem groups). HCN production is catalysed by HCN synthase, encoded by the *hcnABC* operon, which converts glycine into HCN and CO_2 .

The expression of the *hcnABC* operon is controlled by four regulators: Anr, GacA, AlgR, and RhIR (Williams, Zlosnik and Ryall, 2006; Anderson *et al.*, 2010). Anr positively regulates *hcnABC* expression at low oxygen tension (HCN synthase is inactivated by exposure to oxygen), resulting in the production of HCN and the inhibition of all of the terminal oxidases, except for the cyanide insensitive oxidase CIO (Castric, 1983, 1994; Laville *et al.*, 1998). CIO is then used for aerobic respiration, until the environment is depleted of oxygen and denitrification is required for continued respiration. In fully aerobic conditions when nitrate is utilised as an electron acceptor, HCN is not produced, and therefore only residual HCN produced in aerobic conditions can inhibit denitrification enzymes (Castric, 1983, 1994).

Another important regulator of HCN is the *rhl* quorum sensing system. In this regulatory pathway, RhIR upregulates HCN production, highlighting an additional mechanism by which quorum sensing control denitrification (Blumer and Haas, 2000; Williams, Zlosnik and Ryall, 2006).

1.2.4 Biofilms

In the field of biofilms, *P. aeruginosa* is one of most extensively studied organisms in the context of clinical relevance, earning it the “accolade” of being the archetypal biofilm-forming organism (Costerton, Stewart and Greenberg, 1999). Biofilms are effectively surface-associated microbial communities that live in a self-synthesised extracellular polymeric substance (EPS) composed of polysaccharides, extracellular DNA (eDNA), and proteins. In biofilms, species also have altered gene expression profiles, therefore it follows that biofilms may be especially plastic with respect to their phenotypes, affording them exceptional resilience to perturbation (Donlan, 2002). The formation of biofilms within the laboratory setting (Figure 3) follows four sequential steps: the initial attachment of planktonic cells to a surface, coupled with loss of motility; the subsequent growth of the biofilm through formation of microcolonies, alongside EPS secretion; maturation, in which the biofilm begins to adopt a mushroom-like shape (during growth utilising glucose) comprising multiple species coadapted to living together; and finally, dissemination, in which the biofilm (partially) disperses and species return to planktonic life (Klausen *et al.*, 2003; Msken *et al.*, 2010; Maunders and Welch, 2017).

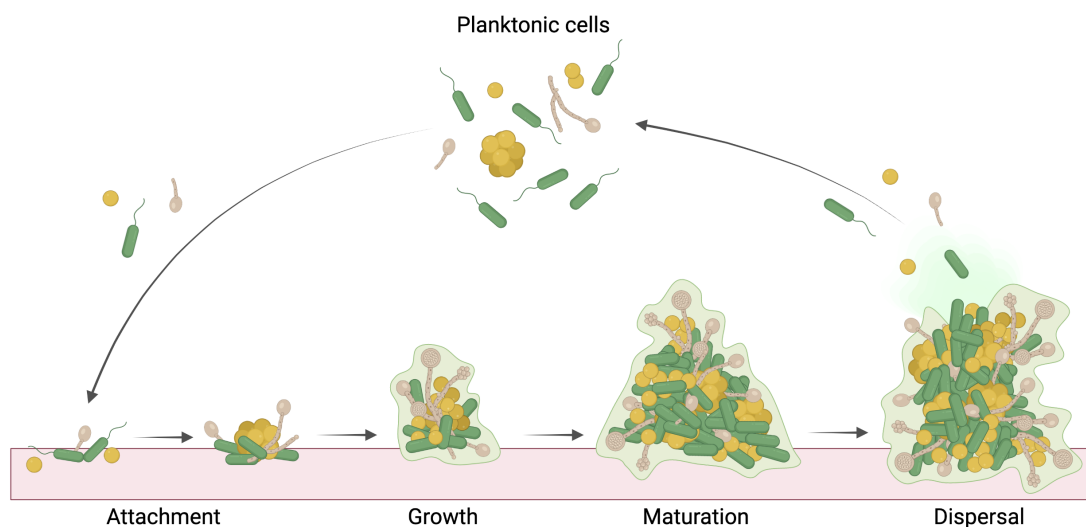


FIGURE 3. Typical *in vitro* model of biofilm formation (Recreated from Maunders and Welch, 2017).

The EPS of biofilms comprises three major polysaccharides, Psl, Pel, and alginate. The latter is commonly produced by CF isolates with the distinct mucoid phenotype, with its overproduction considered pathognomonic of CF (Pulcrano *et al.*, 2012). Psl and Pel are most common in non-mucoid phenotypes, forming a scaffold to which cells and other molecules can attach, leading to increased aggregation of biofilm constituents. Psl overexpression is attributed to pellicle formation in at the air-liquid interface (Friedman and Kolter, 2004; Wang *et al.*, 2013). Extracellular

DNA attaches to Psl, forming thick strand-like structures in the biofilm, and also facilitates the migration of cells at the leading edge of biofilm formation. During movement along a surface, a trail of Psl is deposited that acts as a framework for attachment and microcolony formation (Zhao *et al.*, 2013). Though axenic *in vitro* experiments can only attribute the eDNA component of biofilms to *P. aeruginosa* cells, *in vivo* eDNA is largely derived from leukocytes (Wang *et al.*, 2015; Wilton *et al.*, 2016). The protein CdrA has been associated with cross-linking Psl, assisting in matrix formation and the subsequent aggregation of cells (Borlee *et al.*, 2010).

Biofilms are incredibly resistant to chemotherapeutic intervention and are often named the primary reason for ineffective clearance of an infection, especially in CF where the *P. aeruginosa* biofilm is the best described reason behind poor treatment outcomes. The formation of numerous sputum-associated microcolonies and disparate polymicrobial aggregates, in addition to the dense meshwork of biofilm composites, defines biofilms as extremely difficult to penetrate chemically whilst avoiding toxicity to the host, thus rendering chronic infections extremely difficult to eradicate (Sriramulu *et al.*, 2005). In fact, some biofilms exhibit antimicrobial tolerance some 1000 times higher than planktonic culture of the same species (Parsek and Singh, 2003). Furthermore, approximately 60% of global bacterial infections are associated with biofilm formation, therefore investigation into the survival mechanisms of species—especially *P. aeruginosa*—in biofilms is particularly pertinent.

The diffusion coefficient of biofilms is reported to be much lower than a comparable aqueous solution (Stewart, 2003). Therefore, oxygen-free respiration is an invaluable aid to *P. aeruginosa*'s survival, especially considering that the CF lung is an oxygen-limited environment owing to the accumulation of mucus restricting oxygen transfer from the lumen to the bloodstream (Ratjen and Döring, 2003; Bjarnsholt *et al.*, 2009). Under these conditions, *P. aeruginosa* displays remarkable heterogeneity that is linked to oxygen availability, with protein synthesis decreased at increasing depth inside the biofilm (Xu *et al.*, 1998). Denitrification transcripts are known to be increased in anoxic conditions, especially in biofilms (Härtig and Zumft, 1999; Schreiber *et al.*, 2007). Several publications recently detail that the individual steps of the denitrification pathway are differentially expressed at various depths of aerobically grown biofilms, hinting that in the biofilm architecture, electron acceptor availability is likely to fluctuate dramatically, resulting in the absolute requirement for metabolic cross-feeding between the composite subpopulations of a mature aggregates and biofilm (Y.-C. Lin *et al.*, 2018; Livingston *et al.*, 2022; Schwermer, Beer and Stoodley, 2022). Additionally, anaerobic biofilms are found to be thicker, with a larger proportion of viable cells, compared with aerobic biofilms, further supporting that expression of denitrification is crucial to biofilm survival (Yoon *et al.*, 2002).

1.2.5 Denitrification in polymicrobial infections

With the majority of microbial research focused on the culture of species in isolation, it is sometimes difficult to appreciate the relevance of various systems in a polymicrobial community, for example, quorum sensing, siderophore production, and respiration. Especially in the context of the CF lung, where the airways are colonised by complex ecosystems with myriad species-species interactions, and species have multiple means by which they may communicate with each other. The exact nature of these interactions is also not always clear, with some species waging chemical warfare against each other in antagonistic interactions, others cooperating in mutualistic support, and some behaving altruistically by producing “public goods”. Regardless of the exact nature of these interactions, it is clear that species-species interactions can have profound effects on the phenotypes of parties involved, which can affect the wider microbial community in a manner akin to the ripple effect. In addition, it is not fully clear which species in the CF lung contribute to promoting or protecting the airway from colonisation by different species, though the depth of knowledge on these interactions is expanding through use of ecological theory and ‘omics-based studies (Bjornson *et al.*, 1982; Kirketerp-Møller *et al.*, 2008; Conrad *et al.*, 2013; Quinn *et al.*, 2016). For example, recent transcriptomic investigation of *P. aeruginosa* and *S. aureus* clinical isolate co-cultures uncovered that *P. aeruginosa* interacts antagonistically with *S. aureus*, dysregulating some 200 genes linked to metabolism, virulence, and even antimicrobial resistance (Briaud *et al.*, 2019). Additionally, *Rothia mucilaginosa*, usually resident in the oral cavity, was recently demonstrated to be present in the lower airways where it inhibits NF- κ B pathway activation, resulting in a decrease of pro-inflammatory markers in a cohort with chronic bronchiectasis (Rigauts *et al.*, 2021).

More recent work has developed a continuous-flow culture system that permits the steady state growth of *P. aeruginosa*, in a physiologically relevant artificial sputum medium, alongside other common CF lung pathogens, *C. albicans* and *S. aureus* (Haiko *et al.*, 2019; O’Brien and Welch, 2019). To date, few publications focus on the impact of denitrification in the polymicrobial community, despite ‘omics studies identifying nitrate reductase genes as the most abundant electron acceptor genes in CF sputa and that a loss of nitrite reductase impinges on the survival of *P. aeruginosa* in co-culture with *S. parasanguinis*, another organism found in the CF lung (Gaston *et al.*, 2002; Schobert and Jahn, 2010; Quinn *et al.*, 2014; Scofield and Wu, 2016). Alongside this data, it has been reported that nitric oxide levels are decreased in CF sputum in comparison to other inflammatory airway diseases, likely due to the utilisation of denitrification by dominant and competent denitrifiers, such as *P. aeruginosa* (Grasemann *et al.*, 1998, 2000; Zheng *et al.*, 2004). To attempt to address this gap in the literature, future sections in this dissertation will explore the relationship between denitrification (or lack thereof) and interspecies interactions.

1.3 Central metabolism

The increased-viscosity mucus found in the CF lung and lack of ciliary clearance provides an optimal environment for the formation of persistent biofilms. The lung is ordinarily rich in surfactant that is composed of approximately 90% lipids and 10% proteins. Dipalmitoylphosphatidylcholine (DPPC), a phospholipid, contributes around 30% from the lipid fraction and plays a primary role in the surface-tension lowering capabilities of surfactant (Glasser and Mallampalli, 2012). In *P. aeruginosa*, DPPC and other phospholipids may be cleaved by phospholipase C and other lipases to generate long-chain fatty acids and glycerol. These molecules may then be further metabolized using β -oxidation and GlpD, respectively (Sun *et al.*, 2014). The short-chain fatty acid acetate, obtained from β -oxidation pathways, feeds into the tricarboxylic acid cycle, and glycerol contributes to the generation of Entner-Doudoroff and pentose phosphate pathway precursors. These two metabolites feed into considerably different metabolic pathways and begin to highlight the diversity in carbon-processing by *P. aeruginosa*.

The citric acid cycle, first discovered by Krebs, Kornberg and Monod, is central to *P. aeruginosa* carbon metabolism, where its main function is the generation of key metabolic intermediates and generate electron carriers for oxidative phosphorylation and thus ATP synthesis at the final stage of cellular respiration (Campbell and Stokes, 1951; Krebs, 1970a, 1970b). Diverse carbon sources such as glucose and fatty acids are oxidized to two-carbon acetyl-groups, which in the form of acetyl-CoA is then fed into the citric acid cycle (Figure 4).

There are eight reactions in the citric acid cycle: (1) acetyl-CoA and oxaloacetate are condensed to citrate by citrate synthase, releasing a CoA group; (2) citrate is converted to isocitrate by aconitase; (3) isocitrate is oxidised to α -ketoglutarate, releasing one carbon to the environment in the form of CO₂ and reducing NADP⁺ to NADPH; (4) α -ketoglutarate is oxidised to succinyl-CoA by α -ketoglutarate dehydrogenase, losing a second carbon to CO₂ and reducing NAD⁺ to NADH; (5) succinyl-CoA is converted to succinate by succinyl-CoA synthetase, a CoA group is liberated, and one molecule of ATP is generated from the concomitant dephosphorylation of GTP; (6) succinate is oxidised to fumarate by succinate dehydrogenase, reducing FAD⁺ to FADH₂; (7) fumarate is hydrated by fumarase, producing malate; and finally (8) malate is oxidised by malate dehydrogenase to form oxaloacetate, and NAD⁺ is reduced to NADH.

There is also a shortcut through the citric acid cycle, the glyoxylate shunt, first discovered in *P. aeruginosa* (Kornberg and Krebs, 1957; Kornberg and Madsen, 1958). This shortcut uses isocitrate lyase to convert isocitrate to glyoxylate and succinate, and glyoxylate is then converted to malate by malate synthase in a condensation reaction with acetyl-CoA. The glyoxylate shunt allows the conservation of carbon, as might be essential for growth on short chain fatty acids, such as acetate, at the expense of NADPH generation. The partitioning of flux between the glyoxylate shunt and

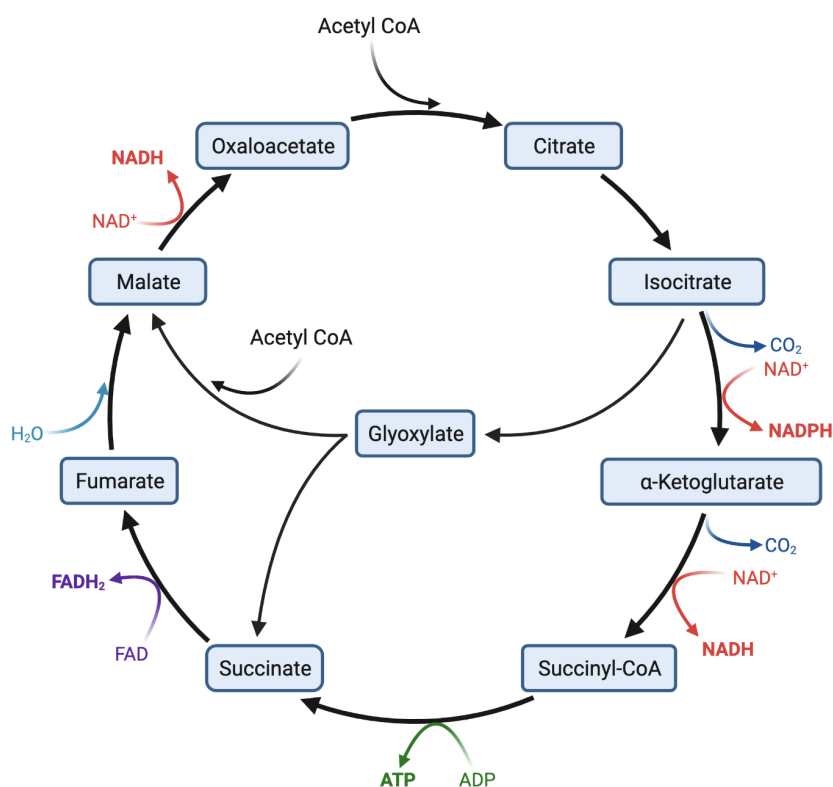


FIGURE 4. Overview of the *P. aeruginosa* citric acid cycle and glyoxylate shunt.

the complete citric acid cycle is regulated by a kinase-phosphatase, AceK. In *Escherichia coli*, if an alternative carbon source becomes available, such as glucose, ICD is dephosphorylated and flux may redistribute to the complete citric acid cycle, effectively driven by the K_m values of ICD and isocitrate lyase for isocitrate, which are approximately $8 \mu\text{M}$ and $600 \mu\text{M}$, respectively. This is essential for growth on acetate, with approximately 75% of the carbon flux being directed through the glyoxylate shunt (Walsh and Koshland, 1984, 1985). In contrast to other species in which the glyoxylate shunt is relatively well studied, *P. aeruginosa* has two isocitrate dehydrogenases, ICD and IDH, as well as isocitrate lyase, meaning three enzymes compete for isocitrate (Crousilles *et al.*, 2018; Dolan and Welch, 2018). Only one of these dehydrogenases, ICD, is sensitive to AceK-mediated regulation, where AceK phosphorylates and inactivates the enzyme, resulting in increased carbon flux through the glyoxylate shunt (Borthwick, Holms and Nimmo, 1984; La-Porte, Walsh and Koshland, 1984; Crousilles *et al.*, 2018). Furthermore, the kinetic enzymology of the citric acid cycle-glyoxylate shunt branch point is markedly different to species such as *E. coli*, where in stark contrast, isocitrate lyase has a higher affinity for isocitrate ($K_m = 12 \mu\text{M}$) than either ICD or IDH ($K_m = 26 \mu\text{M}$ and $K_m = 18 \mu\text{M}$, respectively) (Crousilles *et al.*, 2018). These

data highlight the fine-tuned regulation of *P. aeruginosa* central carbon metabolism and the importance of tightly-regulated partitioning between the complete citric acid cycle, which provides the reducing equivalents required anabolism and mitigating oxidative stress, and the glyoxylate shunt, which provides a pathway to conserve carbon during growth on short-chain fatty acids.

1.4 Electron transport

The diversity and flexibility of bacteria is perhaps best demonstrated by the various ways in which they are able to generate energy based on the resources around them. Work in the Welch laboratory has drawn attention to the remarkable plasticity of *P. aeruginosa* central carbon metabolism, highlighting the broad range of substrates and their related pathways that are used to ensure their survival (Davenport, Griffin and Welch, 2015; Crousilles *et al.*, 2018; Abdelhamid *et al.*, 2019, 2021; Dolan, Kohlstedt, *et al.*, 2020; Dolan, Pereira, *et al.*, 2020; McVey *et al.*, 2020). A branched respiratory network utilising both oxygen and nitrate as terminal electron acceptors, as well as arginine and pyruvate fermentation, provide the necessary ATP—and importantly the proton gradient that drives its synthesis—by directing flux through various respiratory pathways (Figure 5).

P. aeruginosa encodes three types of NADH dehydrogenases in its genome: NDH-1, NDH-2, and Nqr. NDH-1 is a proton-translocating NADH dehydrogenase and is effectively the bacterial version of the eukaryotic mitochondrial complex I. NDH-2 does not translocate protons. Nqr translocates sodium. The NDH-1 NADH dehydrogenases are key to respiration as they couple the oxidation of NADH to the donation of electrons via the ubiquinone pool and various cytochromes to terminal acceptors, nitrate or oxygen, simultaneously translocation protons and generating the necessary gradient for ATP synthesis. Depending on the oxygen tension in the immediate environment, *P. aeruginosa* controls the expression of either N-oxide reductases or terminal oxidases. By controlling the expression of these two sets of enzymes separately, *P. aeruginosa* ensures efficient distribution of membrane space to the appropriate respiratory branch. The transition between oxic and anoxic conditions requires the restructuring of the electron transport chain from aerobic to anaerobic respiration, thus *P. aeruginosa* has evolved to possess a considerable number of regulators to differentiate these conditions.

A thickened mucus layer, mucoid *P. aeruginosa* phenotypes and the formation of biofilms leads to the generation of steep oxygen gradients in the CF lung (Worlitzsch *et al.*, 2002). Furthermore, the environment around mucoid biofilms is rich with polymorphonuclear leukocytes which further deplete local O₂ levels via the reduction of O₂ to O₂⁻ in respiratory burst activity (Fang, 2004; Kolpen *et al.*, 2014). This creates hypoxic to anoxic microenvironments, presenting a challenge to the respiratory chain of *P. aeruginosa*.

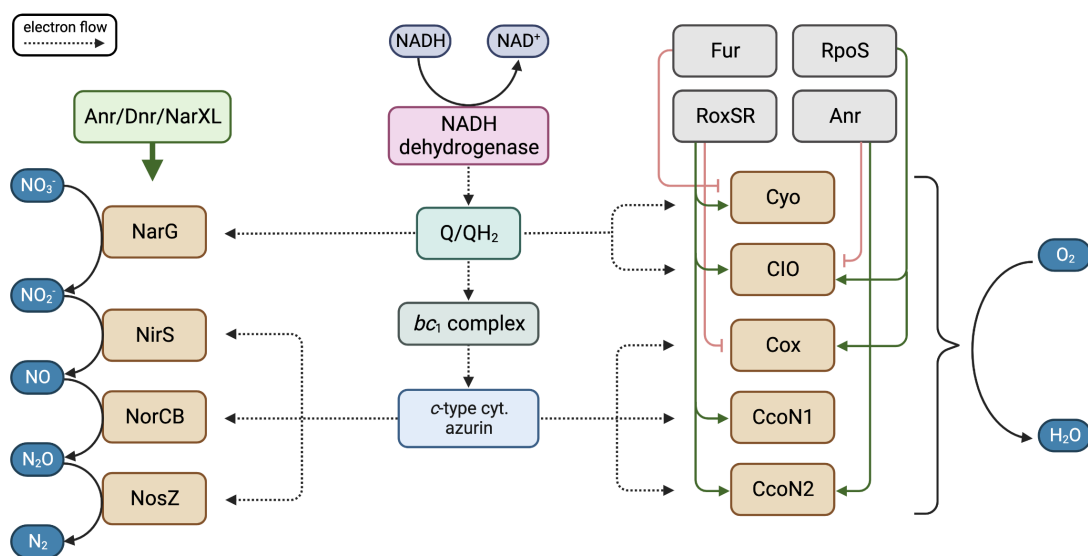


FIGURE 5. The branched respiratory chain of *P. aeruginosa*. Under anaerobic conditions, nitrate is sequentially reduced to dinitrogen by a series of reductases. Under aerobic conditions, oxygen is converted to water by oxidases. In each case, electrons are received from either the ubiquinone pool or cytochrome *c* and/or azurin.

1.4.1 Denitrification

P. aeruginosa is able to use denitrification as a method of anaerobic respiration, with the use of N-oxides in lieu of oxygen as terminal electron acceptors; this process is absolutely vital to survival and growth in microaerobic to anaerobic conditions (Yoon *et al.*, 2002). Denitrification was first documented as a respiratory process in bacteria in the 19th century (Gayon and Dupetit, 1886). Denitrification is the stepwise reduction of NO_3^- to N_2 , via the intermediate formation of NO_2^- , NO and N_2O (Zumft, 1997). The use of N-oxides as terminal electron acceptors maintains the generation of the electrochemical gradient across the cytoplasmic membrane and is therefore critical to respiration and generation of ATP under anaerobic conditions.

Denitrification is catalysed by four primary enzymes: nitrate reductase, nitrite reductase, nitric oxide reductase and nitrous oxide reductase. NarK₁ transports nitrate to the cytoplasm where it may be converted by NarG, the cytoplasmic membrane bound nitrate reductase, to nitrite ($\text{NO}_3^- + 2e^- + 2\text{H}^+ \rightarrow \text{NO}_2^- + \text{H}_2\text{O}$) (Sharma, Noriega and Rowe, 2006). Following this, nitrite is transported back to the periplasm via NarK₂, where NirS, periplasmic nitrite reductase, converts nitrite to nitric oxide ($\text{NO}_2^- + e^- + 2\text{H}^+ \rightarrow \text{NO} + \text{H}_2\text{O}$). NorBC, the cytoplasmic membrane-bound nitric oxide reductase, combines two molecules of NO to produce N_2O ($2\text{NO} + 2e^- + 2\text{H}^+ \rightarrow \text{N}_2\text{O} + \text{H}_2\text{O}$). Finally, NosZ, the periplasmic nitrous oxide reductase, converts N_2O to dinitrogen gas ($\text{N}_2\text{O} + 2e^- + 2\text{H}^+ \rightarrow \text{N}_2 + \text{H}_2\text{O}$) (Figure 6; Borrero-de Acuña *et al.*,

2016). NarG receives electrons from Q/QH₂, and all other denitrification enzymes receive electrons from cytochrome *c*.

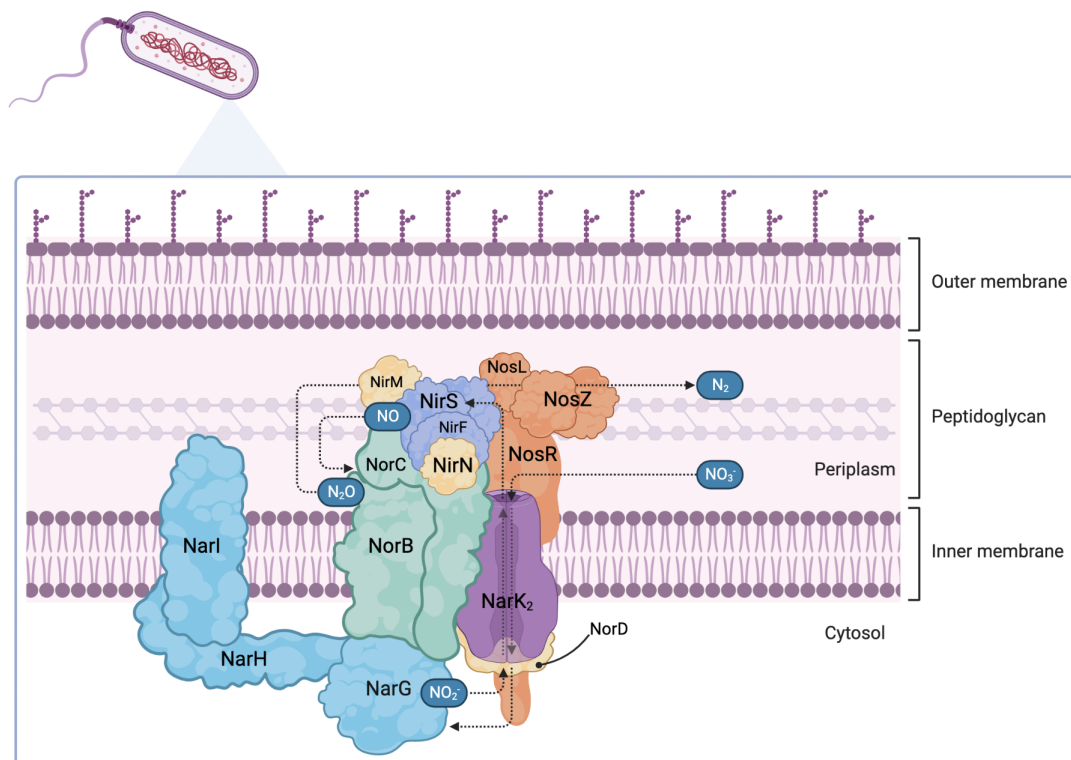


FIGURE 6. The *P. aeruginosa* denitrification apparatus anchored in the cytoplasmic membrane/periplasmic space (Recreated from Borrero-de Acuña *et al.*, 2016).

1.4.1.1 Regulators of denitrification

The regulation of denitrification is controlled by a complex hierarchy of triggers and sensors (Figure 7). The presence of nitrate is detected by the two-component system NarXL (Zumft, 1997). Aerobically, *narXL* is constitutively expressed, however, under anaerobic conditions Anr (anaerobic regulation of arginine deiminase and nitrate reduction) and Dnr (dissimilatory nitrate respiration regulator) may be required for transcription of *narXL* (Schreiber *et al.*, 2007). The two top-level regulators, Anr and Dnr, also respond to low oxygen tension (the primary activator of denitrification) and the presence of NO, respectively (Sawers, 1991; Zimmermann *et al.*, 1991; Arai, Kodama and Igarashi, 1997).

Anr is an Fnr-type regulator, sharing 51% sequence identity with *E. coli* FNR (fumarate and

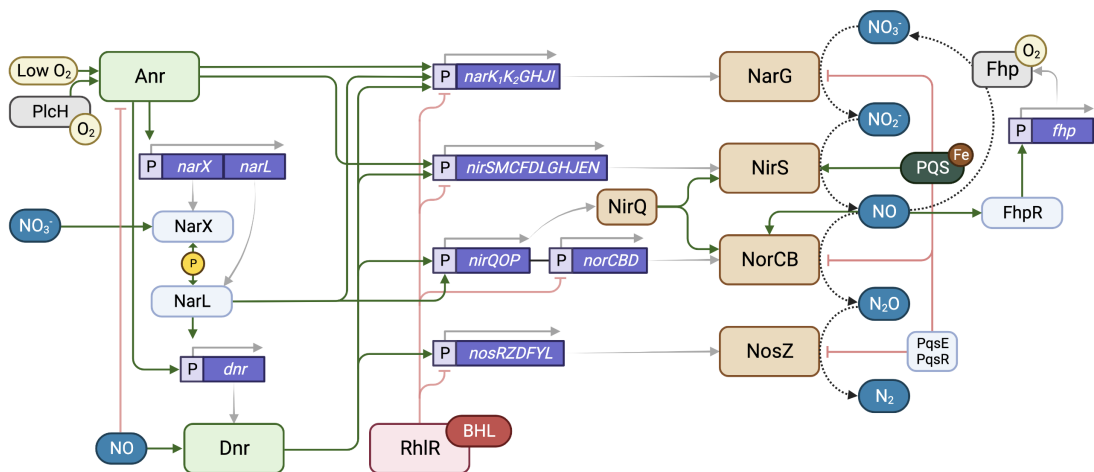


FIGURE 7. The anaerobic denitrification regulatory cascade of *P. aeruginosa*.

nitrate reductase regulatory protein), and is absolutely required for anaerobic denitrification, as its name suggests (Ye *et al.*, 1995). Dimeric Anr has a $[4\text{Fe}-4\text{S}]^{2+}$ cluster in its active form that enables it to bind to DNA. In the presence of oxygen or nitric oxide, the iron sulphur cluster is partially destroyed and Anr can no longer bind to its DNA target sequence (Yoon *et al.*, 2007; Kuroki *et al.*, 2014). However, recent work has indicated there may be means to activate Anr in the presence of oxygen. Haemolytic phospholipase C (PlcH) can degrade phosphatidylcholine found in lung surfactant to choline and glycine betaine. Interestingly, Jackson *et al.* demonstrated that choline derived from PlcH activity increased Anr regulon expression in an Anr-dependent manner in the presence of oxygen, however, the details of this remain to be revealed (Jackson *et al.*, 2013). They then demonstrated that Anr can also repress *plcH* transcription in low oxygen conditions, and that *plcH* transcription was enhanced in an Δanr mutant (Jackson *et al.*, 2014).

Anr controls the expression of *narXL*, which encodes a nitrate-sensing two component system, NarXL. In the presence of nitrate, NarX phosphorylates NarL, releasing a sequestered C-terminal output domain and allowing it to bind to its DNA targets. In some species, NarL has been shown to be regulated by nitrite-sensing proteins, however, this has not been fully elucidated for *P. aeruginosa* (Schroder *et al.*, 1994; Gupta, 1997; Härtig *et al.*, 1999; Yamamoto *et al.*, 2005; Constantinidou *et al.*, 2006; Katsir *et al.*, 2015; Durand and Guillier, 2021). The NarL regulon is yet to be defined for *P. aeruginosa*, however it is known that NarL activates expression of *dnr* and the *nar/nirQ* operons, and represses *nap* in anaerobic conditions (Arai, Kodama and Igarashi, 1997; Schreiber *et al.*, 2007; Van Alst *et al.*, 2009).

Anr and NarXL induce the expression of *dnr*, encoding another regulator of denitrification, Dnr, that contains a haem cofactor that is responsive to nitric oxide. Dnr dimerises and controls

the expression of all enzymes involved in the stepwise reduction of nitrate to nitrogen gas (Arai, Kodama and Igarashi, 1997; Hasegawa, Arai and Igarashi, 1998). Halfway through this process, nitric oxide is generated. Nitric oxide binds to the haem cofactor and through conformational changes permits DNA binding and subsequent transcription (Arai, Kodama and Igarashi, 1999; Giardina *et al.*, 2008, 2009; Castiglione *et al.*, 2009). Interestingly, Anr and Dnr share consensus binding sites that are indistinguishable from each other, highlighting some of the redundancy in the denitrification regulatory network, for example they both regulate the expression of *nar* and *nirS* operons (Gamper, Zimmermann and Haas, 1991; Hasegawa, Arai and Igarashi, 1998; Kuroki *et al.*, 2014).

Additionally, recent work by Cui *et al.* (2021) has shown that aerobic nitrate reduction is repressed by the *las/rhl* quorum sensing networks, which inhibit the expression of *napA*, *nirS*, *norCB*, and *nosZ*. In addition, they show that these QS systems repress *dnr* expression, and that a decrease in AHL concentration in the medium results in an increase in nitrate reduction. The relationship between AHLs and denitrification gene expression has been previously established. In brief, anaerobic denitrification activity is regulated by AHL-*rhl*-dependent transcriptional inhibition (Yoon *et al.*, 2002; Toyofuku *et al.*, 2007). However, the reported regulatory role of Dnr in mediating *napA* expression claimed by Cui *et al.* has not been experimentally demonstrated. Further investigation using a Δdnr mutant would have been invaluable in interrogating this claimed relationship.

NirQ is an ATP-binding protein, reported to be involved in the maturation of the NorCB complex, and its presence enhances nitrite reductase and nitric oxide reductase activity. In contrast, a loss of *nirQ* results in decreased nitrite and nitric oxide reduction (Hayashi *et al.*, 1998; Borrero-de Acuña *et al.*, 2016). These findings suggest that NirQ is a post-translational regulator of denitrification and may potentially function as a supplementary nitrite reductase.

1.4.1.2 The nitrate reductases

The *nar* locus' *narXL*-*narK1* intergenic region is the site of transcriptional control for the first step of denitrification, and its expression is regulated by the concerted action of Anr (with the help of the DNA-bending protein IHF), NarXL, and Dnr (Hasegawa, Arai and Igarashi, 1998; Arai, Mizutani and Igarashi, 2003; Schreiber *et al.*, 2007). The cytoplasmic membrane-bound iron-sulphur-containing nitrate reductase, NarG, is coexpressed with the NarK₂ nitrate/nitrate antiporter. When nitrate is imported to the cytoplasm, NarG catalyses its reduction to nitrite, and nitrite is then returned to the periplasm. Importantly, NarG is electrogenic, i.e. it generates proton motive force across the cytoplasmic membrane (Zumft, 1997).

A periplasmic nitrate reductase, NapA, is under the transcriptional control of RpoS, and is

therefore generally considered to be expressed only in stationary phase (Schuster *et al.*, 2004). However, recent evidence has suggested that under oxygen limitation NapA may be expressed during exponential growth (Alvarez-Ortega and Harwood, 2007), and an absence of narXL (but not narG) results in compensatory activity by NapA (Van Alst *et al.*, 2009). Nitrate reduction by NapA is also not coupled to quinol oxidation, therefore, NapA is not considered to contribute to the generation of proton motive force (Berks *et al.*, 1995).

Both the NarG and NapA enzymes contain a molybdenum cofactor, and like Anr, also possess an iron-sulphur cluster (Zumft, 1997; Jormakka *et al.*, 2004).

1.4.1.3 Nitrite reductase

The nitrite reductase of *P. aeruginosa*, NirS, is a haem-containing enzyme located in the periplasmic space. The activity of NirS reduces nitrite to nitric oxide, and also reduces oxygen to water. *P. aeruginosa*'s NirS contains a *c*-haem group which accepts electrons, and an unusual *d*₁-haem group which then receives these electrons for use in reduction of the *d*₁-haem-bound nitrite, producing nitric oxide (Zumft, 1997; Rinaldo and Cutruzzola, 2007). Nitric oxide is reported to bind tightly to reduced haems compared with oxidised haems (Moore and Gibson, 1976; Brown and Cooper, 1994; Boon and Marletta, 2005). Interestingly, the reduced *d*₁-haem group found in NirS has a relatively low affinity for nitric oxide, allowing for the rapid release of an otherwise inhibitory product that would prevent the further turnover of nitrite (Rinaldo *et al.*, 2011).

1.4.1.4 Nitric oxide reductase

The *P. aeruginosa* NorCB enzyme catalyses the conversion of nitric oxide to nitrous oxide. Nitric oxide is a toxic by-product of denitrification, therefore its production must be tightly maintained at a suitable level, estimated to be between 1 and 65 nM in bacterial species (Goretski, Zafriou and Hollocher, 1990). Consequently, nitric oxide detoxification is extremely important. Without effective detoxification, the iron-sulphur cluster in Anr is disabled, and expression of the denitrification genes should be curtailed, thus limiting the further production of nitric oxide (Yoon *et al.*, 2007).

When levels of nitric oxide increase, nitrosative species derived from nitric oxide damage DNA, bind to haem groups, iron-sulphur clusters and other enzymatically important groups (Mayburd and Kassner, 2002; Soum and Drapier, 2003; Woodmansee and Imlay, 2003). Furthermore, nitric oxide reductase activity is essential to survival of macrophage-delivered nitrosative attacks on *P. aeruginosa* (Kakishima *et al.*, 2007). The work of Yoon *et al.* has also shown that overproduction of nitric oxide in a *rhlR* mutant resulted in death of *P. aeruginosa*, and interestingly, that acidified nitrite enhanced killing of the *P. aeruginosa* mucoid variant, suggesting that

this was due to nitrosation of metal centres in enzymes (Yoon *et al.*, 2002, 2006). NorCB contains a haem-group and a non-haem iron at its binuclear catalytic centre, where a nitric oxide molecule binds to both, before electron donation from both iron centres facilitates the cleavage of a bound hyponitrite intermediate to nitrous oxide and H₂O (Collman, Yang, *et al.*, 2008; Hino *et al.*, 2010; Shiro, 2012; Cordas *et al.*, 2013).

Interestingly, *P. aeruginosa* can not only reduce NO to N₂O, but may also oxidize NO to NO₃⁻ with the use of nitric oxide dioxygenase, encoded by *fbp* (Arai *et al.*, 2005). This additional pathway may aid in mitigating the effects of the host's immune cells, which are known to use nitrosative stress to combat *P. aeruginosa* (Darling and Evans, 2003; Fang, 2004; Kakishima *et al.*, 2007). Interestingly, NO production by NirS is strongly implicated in the expression of virulence factors and dispersal of biofilms (Barraud *et al.*, 2006, 2009). Therefore, it becomes clear that the denitrification apparatus of *P. aeruginosa* is not only essential for anaerobic growth but may play important roles in infection and survival in the lung. However, *P. aeruginosa* has various escape mechanisms, such as a nitric oxide dioxygenase, to allow its continued growth even in compromised situations.

1.4.1.5 Nitrous oxide reductase

Nitrous oxide is a non-toxic gas, that is relatively inert and poses no direct biological threat to *P. aeruginosa*, however its utility as an electron acceptor is beneficial. The nitrous oxide reductase of *P. aeruginosa*, NosZ, is a copper-containing metalloprotein homodimer (McGuirl *et al.*, 2001). The general mechanistic scheme is that each monomer has two domains, each with a C-terminal electron transfer Cu centre (CuA) and an N-terminal catalytic Cu centre (CuZ). Nitrous oxide then binds to CuZ and accepts an electron from CuA and is subsequently released as the environmentally harmless dinitrogen gas (Pauleta, Dell'Acqua and Moura, 2013).

1.4.2 Terminal oxidases

The *P. aeruginosa* genome encodes five terminal oxidases (Kawakami *et al.*, 2010; Arai *et al.*, 2014). Each catalyses the reduction of molecular oxygen to water, and each is differentially regulated depending on oxygen availability and growth phase (Figure 5).

There are two haem-copper *cbb*₃-type oxidases with high oxygen affinity, CcoN1 and CcoN2. CcoN1 is constitutively positively regulated by RoxSR, in contrast, CcoN2 is only expressed in stationary phase or low oxygen tension and is positively regulated by RoxSR and Anr. A single haem-copper *aa*₃-type oxidase, CoxB, is expressed under conditions of nutrient starvation and has a low oxygen affinity. CoxB is positively regulated by RpoS and negatively regulated by RoxSR. CcoN1, CcoN2, and CoxB all receive electrons from cytochrome *c*. A final haem-copper oxidase,

Cyo, is a low oxygen affinity bo_3 -type oxidase with low oxygen affinity, regulated positively via RoxSR during iron starvation, and repressed by Fur. Lastly, a low oxygen affinity cytochrome *bd* family oxidase, CIO (or cyanide insensitive oxidase), is expressed during copper starvation, in the presence of cyanide, and in stationary phase, positively regulated by RoxSR and RpoS, and negatively regulated by Anr. Both Cyo and CIO receive electrons from Q/QH₂.

This range of variability of oxygen affinity and expression characteristics are an excellent example of the complex differential metabolism of *P. aeruginosa* and undoubtedly contribute to its environmental ubiquity. The integration of terminal oxidase and denitrification reductase expression is elegantly evolved, with the expression of CIO, the cyanide insensitive oxidase, coinciding with the production of hydrogen cyanide by *P. aeruginosa* at the entry to stationary phase, just as the remaining oxidases would be disabled and oxygen would become limited prior to the canonical takeover of anaerobic denitrification.

1.4.3 Aerobic denitrification

The exquisite balance between aerobic and anaerobic metabolism hints at the coevolution of these two systems together, and the potential for a hybrid electron transport chain to be utilised by *P. aeruginosa* in potentially challenging, rapidly changing environments. The literature surrounding *P. aeruginosa* denitrification and its complex regulatory network suggests that denitrification, or even the expression of the complete denitrification suite, should not occur in the presence of oxygen during exponential growth. Recent RNA-seq data obtained in the Welch laboratory revealed that when grown on MOPS acetate and in the presence of oxygen, transcripts for the denitrification apparatus were some of the most highly up-regulated in the cell compared with when grown on MOPS glycerol, yet neither of the known master regulators were up-regulated (Dolan, Kohlstedt, *et al.*, 2020). This is intriguing on three fronts.

First, the presence of oxygen should preclude transcription of denitrification enzymes since the key regulator, Anr, contains a sensitive [4Fe-4S]²⁺ cluster that converts to [2Fe-2S]²⁺ in the presence of oxygen, reducing its DNA-binding activity (Lazazzera *et al.*, 1996; Yoon *et al.*, 2007). Certainly, the *nar* locus should not be so highly transcribed since *anr* expression was not modulated at all and the growth medium did not contain an exogenous nitrate source for induction of NarXL activity.

Second, acetate is a potential breakdown product of phospholipid metabolism in the lung. Growth rates on acetate do not appear to be dissimilar to glucose, and metabolic flux is directed through the glyoxylate shunt pathway in order to conserve carbon, since two carbons (thus the contribution of carbon from acetate) are lost in decarboxylation steps carried out by the isocitrate dehydrogenase and α -ketoglutarate dehydrogenase enzymes of the tricarboxylic acid cycle

(Figure 4; Kornberg, 1966; Renilla *et al.*, 2012; Murima *et al.*, 2016). Curiously, when grown with glycerol as a sole carbon source, *P. aeruginosa* has an extremely long lag phase and glycerol inhibits glycerol metabolism via GlpR after glycerol is imported to the cell, pushing the cell into a temporary dormant state (Schweizer and Po, 1996). Simultaneous with flux through the glyoxylate shunt is the up-regulation of type III secretion systems (Chung *et al.*, 2013). Although a simplistic conclusion, metabolism of phospholipids, such as DPPC, could provide a branch point for *P. aeruginosa*: commit to increased virulence or conserve resources.

Third, with oxygen present there is no need to activate aerobic denitrification and to do so would impinge a metabolic cost on *P. aeruginosa*. Production of the denitrification apparatus alongside aerobic respiration enzymes would occupy more space in the membrane, reducing the number of respective complexes, and consume more resources. Additionally, NosZ activity is reduced 60-80% in the presence of oxygen, further limiting the capabilities for complete denitrification and potentially leading to an accumulation of N₂O (Zumft and Kroneck, 2006). A comprehensive review of evidence supporting aerobic respiration by Chen and Strous concluded that although aerobic denitrification may occur, the majority of electron flow still appears to be directed through the canonical respiratory chain with oxygen, rather than via N-oxide reductases, perhaps acting as a supplementary pathway when the rate of NADH formation outpaces oxygen availability (Chen and Strous, 2013). This scenario may be likely in the steep oxic to anoxic gradient found in biofilms that can form in the lung.

The concept of operating a dual-respiratory network alongside the direction of flux through alternative carbon metabolism pathways presents as a potentially interesting behaviour. Considering the highly flexible nature of *P. aeruginosa* metabolism, the aerobic expression of denitrification apparatus could be a form of bet-hedging, in which various cues that are present in the CF lung environment (for example, low oxygen tension, phospholipid breakdown products, and reactive nitrogen species) trigger a pre-emptive metabolic shift to give *P. aeruginosa* an advantage in an infective scenario (Kawakami *et al.*, 2010).

1.5 Redox homeostasis

Redox homeostasis is essential to the cell, with many redox-active compounds playing a role in accepting and donating electrons to certain reactions. The ratio of NADH to NAD⁺ is critical to efficient electron transfer and is a good indicator of the metabolic state of the cell. In contrast, NADP(H) is associated with anabolic redox reactions, typically in biosynthesis and repair pathways. Therefore, the pools of NAD(P)(H) cofactors must be maintained in the appropriate state in order to promote efficient growth of the cell, with NAD(H) ratios tending towards being primarily oxidized, and NADP(H) ratios reduced. The NADH/NAD⁺ redox pair accepts electrons

from reduced carbon sources and donates electrons to the electron transport chain to generate the proton gradient required for ATP synthesis.

Perturbation of NAD(P)(H) pools can affect cellular metabolism, and therefore the ratio of reduced to oxidised species need to be sensed and corrected through the modulation of key enzyme expression with the end-goal of restoring redox balance. Catabolic reactions, for example those catalysed by the isocitrate dehydrogenases, can also contribute to maintaining redox balance by producing reducing equivalents, such as NADPH, required for antioxidation. Indeed, NADPH is an indispensable cofactor in the maintenance of reduction potential for anabolic reactions. In a biological context, redox stress can be induced by host-immune defences, nutrient availability, or antimicrobial treatment. Alongside Anr, the redox state may be detected by RoxSR, a two-component system whose *Rhodobacter sphaeroides* homologue, PrrBA, is modulated directly through an inhibitory signal received from a *ccb3* cytochrome *c* oxidase sensing electron flow either through the electron transport chain/ubiquinone pool, or an as yet unknown mechanism (Oh and Kaplan, 2000; Kawakami *et al.*, 2010; Arai *et al.*, 2014). Additionally, PrrBA has been shown to regulate *nirK* expression in *R. sphaeroides* (Laratta *et al.*, 2002). By using the ubiquinone pool as a checkpoint for redox status, the cell can then direct electron through either aerobic or anaerobic respiration at the top level (Figure 5).

Though the full functions of RoxSR are currently unknown, recent work has shown that expression of *cox* genes is regulated by RoxSR. The *cox* genes encode cytochrome *c* oxidase *aa3* (CoxB), the most efficient of *P. aeruginosa*'s five terminal oxidases for the generation of a proton gradient (Kawakami *et al.*, 2010; Arai *et al.*, 2014). Additionally, a Δ *roxSR* mutant showed reduced fitness when challenged with cyanide, caused by the failed induction of *cioAB* expression, with *cioAB* encoding a cyanide-insensitive oxidase (Comolli and Donohue, 2002). Recent RNA-seq analyses in the Welch lab found *coxB* to have one of the highest transcript levels in the cell when grown on MOPS with acetate. This is not unexpected given that the *cox* genes are only induced under nutrient starvation, however, it is worth noting that *cox* expression is repressed by RoxSR. Osamura *et al.* recently demonstrated using Δ *cox* and Δ *roxSR* mutants that overexpression of CoxB actually inhibits aerobic growth under 'normal' nutrient conditions, but that under nutrient starvation the use of CoxB enhanced survival, perhaps acting as a supplementary enzyme to maintain redox homeostasis (Osamura *et al.*, 2017). Furthermore, a Δ *roxR* mutant has also been shown to have reduced ability to interact with lung epithelial cells, an important virulence determinant in this organism (Hurley *et al.*, 2011). Homologues of RoxSR in *R. sphaeroides*, *M. tuberculosis*, and *B. abortus* have been shown to influence expression of a number of enzymes that aid in adaptation to low oxygen conditions, including those involved in denitrification (Comolli and Donohue, 2002; Laratta *et al.*, 2002; Nowak *et al.*, 2006; Carrica *et al.*, 2013).

Thesis

I propose that aerobic denitrification in *P. aeruginosa* is a form of overflow metabolism used to correct redox imbalance, controlled separately from the known denitrification regulatory network.

My hypotheses are:

- Expression of denitrification enzymes may be initiated independently from the canonical master regulator of denitrification, Anr.
- Aerobic denitrification may confer a growth advantage under denitrification-permissive conditions (i.e. nitrate availability), regardless of the presence of oxygen.
- Aerobic denitrification may be sufficient to permit reduction of the NADH pool during exponential growth of *P. aeruginosa* to such an extent that it may correct redox imbalance. Conversely, a loss of denitrification may lead to increased accumulation of NADH.
- A loss of denitrification in *P. aeruginosa* in a polymicrobial culture may lead to behavioural changes in *P. aeruginosa* in order to remain ecologically competitive.

Materials and Methods

3.1 Microbial strains and culture conditions

P. aeruginosa PAO1 was used for all *Pseudomonas* work. *E. coli* DH5 α was used for preparation and maintenance of promoter::*lux* transcriptional fusion vectors. For short term storage, strains on LB agar plates were kept at room temperature. For long term storage, strains were stored in sterile 25% v/v glycerol solution at -80°C.

Overnight liquid cultures were prepared by inoculating a single colony into 10 mL of the appropriate medium in a 30 mL screw-cap plastic tube. Strains were incubated at 37°C on a rotary drum at 120 rpm for 18-24 hours. Batch culture was carried out in 2 L deep-baffled Erlenmeyer flasks, filled no more than 10% of their capacity, at 37°C with 250 rpm orbital shaking. Microtitre plate culture was carried out at 37°C with no more than 50% of the well volume occupied and 500 rpm orbital shaking, unless otherwise stated. All liquid cultures were normalised to a starting OD₆₀₀ of 0.05.

TABLE 3. Microbial strains used in this study.

Name	Description	Source/reference
<i>P. aeruginosa</i> PAO1	Used worldwide as a laboratory reference strain. Spontaneous chloramphenicol-resistant isolate first identified in in Melbourne, Australia (1954).	Holloway (1955)
<i>C. albicans</i> SC5314	<i>Candida albicans</i> clinical isolate commonly used as a wild-type laboratory reference strain. First isolated in New York, USA (1980s).	Gillum, Tsay and Kirsch (1984)

<i>S. aureus</i> ATCC 25923	<i>Staphylococcus aureus</i> Rosenbach (ATCC 25923-D5). A methicillin-sensitive clinical isolate lacking <i>mecA</i> and recombinases commonly used as a laboratory reference strain. First isolated in Seattle, USA (1945).	Treangen <i>et al.</i> (2014)
<i>E. coli</i> DH5 α	<i>E. coli</i> K-12 derivative commonly used for laboratory cloning.	NEB
<i>E. coli</i> DH5 α pUC18-mini-Tn7T-Gm- <i>lux</i>	<i>E. coli</i> hosting a mini-Tn7 transposable vector containing the <i>luxCDABE</i> operon preceded by a multiple cloning site and a gentamicin resistance cassette.	Choi and Schweizer (2006)
<i>E. coli</i> Pir1 pTNS2	<i>E. coli</i> hosting a helper plasmid, pTNS2, which contains a transposase for inserting a mini-Tn7 backbone into the <i>Pseudomonas</i> genome and an ampicillin resistance cassette.	Choi and Schweizer (2006)
<i>P. aeruginosa</i> PQS biosensor	<i>P. aeruginosa</i> $\Delta pqsA$ <i>pqsA::luxCDABE</i> . Luciferase-based PQS biosensor integrated at a neutral site in the <i>P. aeruginosa</i> genome.	Fletcher <i>et al.</i> (2007)
<i>E. coli</i> BHL biosensor	<i>E. coli</i> JM109 pSB536. Luciferase-based BHL biosensor via an <i>abyR+PabyI::luxCDABE</i> fusion. Ampicillin resistant.	Swift <i>et al.</i> (1997)
<i>E. coli</i> OdDHL biosensor	<i>E. coli</i> JM109 pSB1075. Luciferase-based OdDHL biosensor containing a <i>lasR+PlasI::luxCDABE</i> fusion. Tetracycline resistant.	Winson <i>et al.</i> (1998)
<i>P. aeruginosa</i> Δanr	<i>P. aeruginosa</i> with denitrification regulator <i>anr</i> deletion in PAO1 background.	Welch laboratory
<i>P. aeruginosa</i> Δdnr	<i>P. aeruginosa</i> with denitrification regulator <i>dnr</i> deletion in PAO1 background.	Welch laboratory
<i>P. aeruginosa</i> $\Delta narG$	<i>P. aeruginosa</i> with nitrate reductase <i>narG</i> deletion in PAO1 background.	Welch laboratory
<i>P. aeruginosa</i> $\Delta nirS$	<i>P. aeruginosa</i> with nitrite reductase <i>nirS</i> deletion in PAO1 background.	Welch laboratory

<i>P. aeruginosa</i> $\Delta norB$	<i>P. aeruginosa</i> with nitric oxide reductase <i>norB</i> deletion in PAO1 background.	Welch laboratory
<i>P. aeruginosa</i> $\Delta roxSR$	<i>P. aeruginosa</i> with terminal oxidase regulator <i>roxSR</i> deletion in PAO1 background.	Welch laboratory
<i>P. aeruginosa</i> $\Delta aceK$	<i>P. aeruginosa</i> with isocitrate dehydrogenase kinase/phosphatase <i>aceK</i> deletion in PAO1 background.	Welch laboratory
<i>P. aeruginosa</i> <i>anr::lux</i>	Transcriptional fusion between the promoter region of <i>anr</i> and the <i>luxCDABE</i> cassette. Generated in PAO1 and $\Delta roxSR$.	Welch laboratory
<i>P. aeruginosa</i> <i>dnr::lux</i>	Transcriptional fusion between the promoter region of <i>dnr</i> and the <i>luxCDABE</i> cassette. Generated in PAO1, Δanr , and $\Delta roxSR$.	Welch laboratory
<i>P. aeruginosa</i> <i>narK1::lux</i>	Transcriptional fusion between the promoter region of <i>narK1</i> and the <i>luxCDABE</i> cassette. Generated in PAO1, Δanr , Δdnr , and $\Delta roxSR$.	Welch laboratory
<i>P. aeruginosa</i> <i>nirS::lux</i>	Transcriptional fusion between the promoter region of <i>nirS</i> and the <i>luxCDABE</i> cassette. Generated in PAO1, Δanr , Δdnr , and $\Delta roxSR$.	Welch laboratory
<i>P. aeruginosa</i> <i>norC::lux</i>	Transcriptional fusion between the promoter region of <i>norC</i> and the <i>luxCDABE</i> cassette. Generated in PAO1, Δanr , Δdnr , and $\Delta roxSR$.	Welch laboratory
<i>P. aeruginosa</i> <i>nosR::lux</i>	Transcriptional fusion between the promoter region of <i>nosR</i> and the <i>luxCDABE</i> cassette. Generated in PAO1, Δanr , Δdnr , and $\Delta roxSR$.	Welch laboratory
<i>P. aeruginosa</i> <i>fbp::lux</i>	Transcriptional fusion between the promoter region of <i>fbp</i> and the <i>luxCDABE</i> cassette. Generated in PAO1, Δanr , Δdnr , and $\Delta roxSR$.	Welch laboratory
<i>P. aeruginosa</i> <i>sth::lux</i>	Transcriptional fusion between the promoter region of <i>sth</i> and the <i>luxCDABE</i> cassette. Generated in PAO1, Δanr , Δdnr , and $\Delta roxSR$.	Welch laboratory

3.2 Media preparation

For general microbial growth, Luria-Bertani broth (LB) and LB agar was used, and phosphate buffered saline (PBS) was used as a dilution and washing medium (Table 4). MOPS media was prepared as in LaBauve and Wargo (2013) for use in experiments in sections 4-8 (Table 5). Selective media was used to isolate *P. aeruginosa*, *C. albicans*, and *S. aureus* from each other in mixed-species experiments (Table 6). A modified artificial sputum medium was prepared for use in experiments in sections 4 and 7-10 (Tables 7-10).

TABLE 4. General growth media. All solutions should be sterilised by autoclaving at 121°C for 15 minutes.

Media	Components	g L ⁻¹
LB	Tryptone	10
	NaCl	10
	Yeast extract	5
LB agar (1.5% w/v)	Tryptone	10
	NaCl	10
	Yeast extract	5
	Agar	15
PBS (Oxoid)	Premixed 10x tablet:	
	NaCl	8
	KCl	0.2
	Na ₂ HPO ₄	1.44
	KH ₂ PO ₄	0.24

TABLE 5. MOPS minimal media. All solutions should be sterilised by filtration using a 0.22 µm pore filter and protected from light. The 1x MOPS working medium was stored for a maximum of six months.

Stock solutions and working medium	Components	Concentration
100x micronutrient	(NH ₄) ₆ Mo ₇ O ₂₄ •4H ₂ O	3 µM
	H ₃ BO ₃	400 µM
	CoCl ₂	30 µM
	CuSO ₄	10 µM
	MnSO ₄	80 µM
	ZnSO ₄	10 µM

10x MOPS	MOPS pH 7.5	400 mM
	Tricine pH 7.5	40 mM
	FeSO ₄	0.18 mM
	NH ₄ Cl	95 mM
	CaCl ₂	5.3 μ M
	MgCl ₂ ·6H ₂ O	5.1 mM
	NaCl	500 mM
	100x micronutrient	1x
1x MOPS working medium	10x MOPS	1x
	Carbon source:	
	Acetate	40 mM
	Glucose	15 mM
	Succinate	30 mM
	Glycerol	30 mM
	K ₂ SO ₄	0.29 mM
K ₂ HPO ₄	1.32 mM	

TABLE 6. Species-selective media for isolation of *P. aeruginosa*, *C. albicans*, and *S. aureus*.

Media	Species	To make 1 L	Composition (L ⁻¹)
<i>Pseudomonas</i> Isolation Agar (PIA; Oxoid)	<i>P. aeruginosa</i>	48.4 g PIA powder 10 mL glycerol	11 g Bacto agar 10 g casein hydrolysate 16 g peptone 1.4 g MgCl ₂ 10 g K ₂ SO ₄ 1% v/v glycerol pH 7.1
		Autoclave and pour immediately	
BiGGY agar (Oxoid)	<i>C. albicans</i>	45 g BiGGY agar powder	16 g Bacto agar 5 g bismuth ammonium citrate 10 g dextrose 10 g glycine 3 g Na ₂ SO ₃ 1 g yeast extract pH 6.8
		Gently boil and pour immediately	

			15 g Bacto agar
		115 g MSA	10 g mannitol
Mannitol		powder	75 g NaCl
Salt Agar	<i>S. aureus</i>		1 g beef extract
(MSA; Oxoid)		Autoclave and	10 g peptone
		pour immediately	0.025 g phenol red
			pH 7.4

3.2.1 Artificial sputum medium

Artificial sputum medium was prepared using a combination of SCFM2 formulations published by Kirchner *et al.* (2012) and Turner *et al.* (2015). This preparation was used as it combined one of the most recently published artificial sputum medium compositions with a simpler DNA element preparation (i.e. no organic extraction step), and would also aid in comparisons to ongoing work within the Welch laboratory using the same methodology.[†]

3.2.1.1 Day 1

Add 5 g of mucin from porcine stomach, type-II (Sigma-Aldrich, M2378) to 250 mL of sterile 1x PBS (Oxoid) and leave to dissolve with stirring overnight at 4°C. Mucin can be dissolved in sterile dH₂O, however solubility is low and may take an extremely long time. Add 4 g of deoxyribonucleic acid from fish sperm (Sigma-Aldrich, 74782) to 250 mL of sterile dH₂O and leave to dissolve overnight in a shaking incubator set to 180 rpm and 35°C.

3.2.1.2 Day 2

Combine the mucin and DNA, then separate undissolved particles by centrifugation at 4000 rcf for 30 minutes at 4°C. Filter-sterilise (0.22 µm pore size) the supernatant and store at room temperature. Prepare amino acid stocks (Table 7), buffered base stocks (Table 8), and nutrients (Table 9).

[†]Since this work was completed it has been demonstrated that there may be significant differences in secondary metabolite production as a result of different artificial sputum medium formulations. Some components are undefined with regards to their exact composition (e.g. commercial porcine gastric mucin), therefore, the findings in this dissertation must be considered in the context of the formulation used and how that aligns with the wider literature (Neve, Carrillo and Phelan, 2021).

TABLE 7. Amino acid stock solutions (all 50 mL at 100 mM). All solutions should be sterilised by filtration using a 0.22 μm pore filter. All solutions (except those that must be freshly prepared) can be stored for maximum of 1 month at 4°C.

Amino acid	MW (g mol ⁻¹)	Mass for stock solution (g)	Volume of stock to add to beaker (mL)	Final conc. (mM)
Ala	89.09	0.445	17.80	1.780
Arg	174.20	0.871	3.06	0.306
Asp ^a	133.10	0.666	8.27	0.827
Cys•HCl ^b	157.60	0.788	1.60	0.160
Glu	147.13	0.736	15.49	1.549
Gly	75.07	0.375	12.03	1.203
His•HCl•H ₂ O ^b	209.60	1.048	5.19	0.519
Ile	131.17	0.656	11.21	1.121
Leu	131.17	0.656	16.09	1.609
Lys•HCl	182.60	0.913	21.28	2.128
Met	149.21	0.746	6.33	0.633
Orn•HCl	168.62	0.843	6.76	0.676
Pro	115.13	0.576	16.61	1.661
Phe ^b	165.19	0.826	5.30	0.530
Ser	105.09	0.525	14.46	1.446
Thr ^b	119.12	0.596	10.72	1.072
Trp ^c	204.23	1.021	0.13	0.013
Tyr ^{bd}	181.19	0.906	8.02	0.802
Val	117.15	0.586	11.17	1.117

^a Prepare in 0.5 M NaOH; ^b Prepare fresh; ^c Prepare in 0.2 M NaOH; ^d Prepare in 1 M NaOH

TABLE 8. Buffered base stock solutions (all 25 mL). All solutions should be sterilised by filtration using a 0.22 μm pore filter.

Item	Stock conc. (M)	MW (g mol ⁻¹)	Mass for stock solution (g)	Volume of stock to add to beaker (mL)	Final conc. (mM)
NaH ₂ PO ₄	0.2	119.980	0.599	6.500	1.300
Na ₂ HPO ₄	0.2	141.960	0.710	6.252	1.250
KNO ₃	1	101.103	2.528	0.348	0.348
K ₂ SO ₄	0.25	174.259	1.089	1.084	0.271

TABLE 9. Nutrients (all 50 mL at 1 M, except for FeSO₄·7H₂O). All solutions except egg yolk emulsion should be sterilised by filtration using a 0.22 μm pore filter.

Item	MW (g mol ⁻¹)	Mass for stock solution (g)	Volume of stock to add to beaker (mL)	Final conc. (mM)
CaCl ₂ ·2H ₂ O	147.01	7.350	1.754	1.754
Dextrose	180.16	9.008	3	3
Egg yolk emulsion ^a			5	
FeSO ₄ ·7H ₂ O ^b	278.01	0.050	1	0.0036
Lithium L-lactate ^c	96.01	4.801	9.3	9.3
MgCl ₂ ·6H ₂ O	203.31	10.166	0.606	0.606
<i>N</i> -acetylglucosamine	221.21	11.064	0.3	0.3

^a Sigma-Aldrich, 17148; ^b Prepare fresh, 50 mL at 3.6 mM; ^c Adjust to pH 7.0 with NaOH

3.2.1.3 Day 3

In a large clean beaker, add 250 mL of dH₂O, dissolve the solids detailed in Table 10, and add the appropriate volumes of amino acid and buffered base stocks according to Table 7 and Table 8. Add the combined filtered mucin and DNA solution and adjust to pH 6.8. Add nutrients according to the volumes detailed in Table 9. Adjust the final volume to 1 L with dH₂O and sterilise by filtration (0.22 μm pore size). Artificial sputum medium can be stored for up to one month in the dark at 4°C.

TABLE 10. Solids. Add directly to large beaker for final artificial sputum medium composition.

Item	MW (g mol ⁻¹)	Mass for 1 L solution (g)	Final conc. (mM)
KCl	74.551	1.116	14.943
MOPS	209.263	2.092	10
NaCl	58.440	3.032	51.848
NH ₄ Cl	53.491	0.124	2.281

3.3 CFU enumeration

Colony forming units were determined by serial diluting culture aliquots and subsequent plating onto the required media using the single plate–serial dilution spotting method described by Thomas *et al.* (2015). Plates were then incubated at 37°C for 16–48 hours, depending on the species cultured.

3.4 DNA extraction

Genomic DNA was extracted from bacterial cells using a GeneJET genomic DNA purification kit (Thermo Scientific). DNA concentration was measured using a Nanodrop (ND-1000, Thermo Scientific) PCR products were purified using a GeneJET PCR purification kit (Thermo Scientific). DNA fragments were purified from agarose gels with a GeneJET gel extraction kit (Scientific). All DNA samples were stored at -20°C .

3.5 PCR and gel electrophoresis

PCR products were obtained from either genomic DNA, plasmid DNA, or directly from bacterial colonies using “colony PCR”. A PCR master mixture was prepared as suggested by the manufacturer (Table 11; NEB). PCR thermocycling conditions (Table 12) varied depending on the melting temperature of primers, length of the DNA fragment being amplified, and the source of the template DNA.

TABLE 11. PCR master mixture.

Component	50 μL reaction	Final concentration
5x Phusion HF Buffer	10 μL	1x
10 mM dNTPs	1 μL	200 μM
10 μM forward primer	2.5 μL	0.5 μM
10 μM reverse primer	2.5 μL	0.5 μM
Phusion DNA polymerase	0.5 μL	1 unit
Template DNA	1 μL	250 ng
Nuclease-free water	32.5 μL	N/A

TABLE 12. PCR thermocycling conditions.

Step	Temperature ($^{\circ}\text{C}$)	Time
Initial denaturation	98	30 seconds or 5 minutes for “colony PCR”
25-35 CYCLES:		
[Denaturation	98	10 seconds
Annealing	55-72	20 seconds
Extension]	72	20 seconds per kb
Final extension	72	5 minutes
Hold	12	∞

PCR-amplified DNA was separated by electrophoresis through a 1% agarose gel (1% w/v agarose dissolved in Tris-Acetate-EDTA buffer). Ethidium bromide ($0.4 \mu\text{g mL}^{-1}$ final concentration) was added to molten agarose before gel casting. DNA migration was performed using a Bio-Rad Mini-Sub Cell GT Cell set to 80-110 volts for 45 minutes to 1 hour. DNA fragments were separated and sized using BioLine Hyperladder I (200-10,000 bp) as a reference. DNA fragments were visualised using a UV transilluminator (365 nm).

3.6 Promoter::*lux* transcriptional fusion strain generation

3.6.1 Vector construction

The LuxCDE complex is a fatty acid reductase complex which converts and supplies a fatty aldehyde substrate to the luciferase, LuxAB. In brief, LuxD is an acyltransferase which liberates myristic acid bound to acyl carrier protein, providing an acyl moiety to LuxCE. LuxE is an acyl-protein synthetase which, consuming ATP, generates a free fatty acid and acyl-AMP. LuxC is an NADPH-dependent acyl protein reductase, which generates the final fatty aldehyde product. LuxAB then oxidises the fatty aldehyde produced by LuxCDE, consuming molecular oxygen and reduced flavin mononucleotide, and emitting light as a by-product (Brodl, Winkler and Macheroux, 2018). The luciferase system is convenient as no exogenous substrate needs to be supplied since the bacterial cell provides all the required precursors.

Insert sequences encompassing promoter regions upstream of genes of interest (determined from RNA-seq data; Dolan, Kohlstedt, *et al.*, 2020) were PCR amplified from *P. aeruginosa* PAO1 genomic DNA with primers containing BamHI and XhoI restriction sites (Table 13). The pUC18-mini-Tn7T-Gm-*lux* plasmid vector was recovered from *E. coli* host cultures using a GeneJET Plasmid Miniprep kit (Thermo Scientific). Inserts and recovered plasmid were digested with two restriction enzymes, FastDigest BamHI and FastDigest XhoI (Thermo Scientific), to ensure correct promoter directionality during ligation. Inserts were ligated into pUC18-mini-Tn7T-Gm-*lux* using T4 DNA ligase ($5 \text{ U } \mu\text{L}^{-1}$; Thermo Scientific) and the ligation mixture was incubated with $100 \mu\text{L}$ of *E. coli* DH5 α competent cells (prepared by washing three times with ice-cold 10% v/v glycerol) on ice for 20 minutes. Next, cells were electroporated (2.5 kV pulse) and resuspended in $500 \mu\text{L}$ of prewarmed LB, followed by 1 hour recovery at 37°C on a rotary wheel. The entire recovery culture was then plated onto prewarmed 37°C LB agar plates with $10 \mu\text{g mL}^{-1}$ gentamicin. Plates were incubated at 37°C until colonies appeared, up to a maximum of 24 hours. Colony PCR was used to identify transformants, then plasmids were recovered and sequenced (GATC Biotech) to confirm correct construction.

TABLE 13. Primers used in this study.

Primer name	Direction	Sequence
<i>acsA::lux</i> F BamHI	Forward	AAACGCGGATCCCCTGGGCATCGTCATGGT
<i>acsA::lux</i> R XhoI	Reverse	AAAACCTCGAGCACGGGGTACAGGGATGC
<i>anr::lux</i> F BamHI	Forward	AAACGCGGATCCGCTGGGAAAGCTGTACATG
<i>anr::lux</i> R XhoI	Reverse	AAAACCTCGAGGGCCAGACTGCAATCCTT
<i>ccoN1::lux</i> F BamHI	Forward	AAACGCGGATCCCCCAGCTCCAACAAACCATC
<i>ccoN1::lux</i> R XhoI	Reverse	AAAACCTCGAGGACACCGAGACCCATTCCAA
<i>dnr::lux</i> F BamHI	Forward	AAACGCGGATCCTCTATCCTGACATCCGTGCT
<i>dnr::lux</i> R XhoI	Reverse	AAAACCTCGAGCGAACAGGTGGTGGCTTTG
<i>fbp::lux</i> F BamHI	Forward	AAACGCGGATCCGTAGGGATCGGGCAGGCCG
<i>fbp::lux</i> R XhoI	Reverse	AAAACCTCGAGACATGCTTGTTCACCACCTTGG
<i>lux</i> PCR check F	Forward	AACAAGCCATGAAAACCGCC
<i>lux</i> PCR check R	Reverse	AGTCATGCTCTTCTCTAATGCG
<i>narK1::lux</i> F BamHI	Forward	AAAAGGATCCGGAATTCCCGGCGTGGTTGATA
<i>narK1::lux</i> R XhoI	Reverse	AAAACCTCGAGTTCAAGCTTAGGCCAGGCCGTA
<i>nirS::lux</i> F BamHI	Forward	AAACGCGGATCCCATGTACTGGACGAAGCGG
<i>nirS::lux</i> R XhoI	Reverse	AAAACCTCGAGCGGCTTTCATGTCGTCCTTG
<i>norC::lux</i> F BamHI	Forward	AAACGCGGATCCCTTGACGATGGGGAGGAGC
<i>norC::lux</i> R XhoI	Reverse	AAAACCTCGAGTTCTCGGTGTGGTAGGTGAG
<i>nosR::lux</i> F BamHI	Forward	AAAAGGATCCCCTGGTACCGTTACCTGAAGGC
<i>nosR::lux</i> R XhoI	Reverse	AAAACCTCGAGCCCAAGCTTGGATCACCTGCAG
<i>sth::lux</i> F BamHI	Forward	AAACGCGGATCCGAGGTGCGACCGAGCCTTGC
<i>sth::lux</i> R XhoI	Reverse	AAAACCTCGAGGCGTACTCCTCAGAACAGGCCG

3.6.2 Preparation of electrocompetent *P. aeruginosa* cells

P. aeruginosa cells were prepared as in Huang and Wilks (2017). One colony was inoculated into 25 mL LB broth and incubated overnight at 42°C without shaking in order to inhibit the DNA restriction-modification system of *P. aeruginosa*. Cells from overnight cultures were recovered by centrifugation (3220 rcf for 15 min at 20°C) and resuspended in 5 mL of room temperature 1 mM MgSO₄. Cells were centrifuged again, and the supernatant discarded before washing once more. The cell pellet was finally resuspended in 250 μL of room temperature 1 mM MgSO₄.

3.6.3 Electroporation of *P. aeruginosa*

Chromosomal integration of pUC18-mini-Tn7T-Gm-*lux* plasmids was achieved by methods previously described (Choi and Schweizer, 2006; Damrom *et al.*, 2013). Approximately 0.5-1 μg of construct plasmid DNA and 150 μg of pTNS2 helper plasmid required to integrate transcriptional fusion constructs into the *P. aeruginosa* genome at a single *att*Tn7 site downstream from *glnS* was added to 50 μL of electrocompetent cells and the final mixture was transferred to a 2mm gap electroporation cuvette. Cells were pulsed at 2.2 kV, followed by the immediate addition of 1 mL LB broth and incubation at 37°C for 2 hours. Transformed cells were then pelleted, 700 μL of supernatant was discarded and the pellet was resuspended in the remaining media before plating on LB agar containing 50 $\mu\text{g mL}^{-1}$ gentamicin. Plates were incubated at 37°C for up to 24 hours.

3.6.4 Identification of *P. aeruginosa* transformants

Colonies that appeared following electroporation were isolated and inoculated in a microcentrifuge tube containing 500 μL of LB broth with 50 $\mu\text{g mL}^{-1}$ gentamicin, and incubated at 37°C. After 1 hour, a 100 μL sample was removed and added to a 96-well microtitre plate (Greiner Bio-One 655090). OD₆₀₀ and luminescence values were then read every 15 minutes using the BMG LABTECH FLUOstar Omega plate reader, with orbital shaking (200 rpm) during idle time. After 4-6 hours, samples that increased in both OD₆₀₀ and luminescence values were deemed successful transformants, and glycerol stocks were prepared from the remaining microcentrifuge tube cultures. Colonies were confirmed by PCR.

3.7 NAD(P)(H) extraction and measurement

P. aeruginosa PAO1 cultures were grown in MOPS media containing a single carbon source (40 mM acetate, 15 mM glucose, 30 mM glycerol, or 30 mM succinate) \pm 20 mM KNO₃ at 37°C with shaking at 250 rpm, using a culture volume of 150 mL in a 2 L deep-baffled Erlenmeyer flask. For each NAD(P)(H) extraction, 1.8 mL of culture was removed and immediately centrifuged for 1 minute at 15,800 rcf to obtain a cell pellet. The pellet was resuspended in 0.2 M HCl for NAD(P)⁺ or 0.2 M NaOH for NAD(P)H extraction, before incubation at 55°C for 10 minutes, followed by incubation on ice for 5 minutes. HCl or NaOH was then neutralised by the dropwise addition of 0.1 M NaOH or 0.1 M HCl, respectively, whilst vortexing at low speed. The mixture was then centrifuged for 5 minutes at 15,800 rcf and 135 μL of the supernatant was removed for immediate NAD(P)(H) measurement or storage at -80°C. Samples were stored for a maximum of one week before measurement.

NAD(P)(H) concentrations were measured using an enzyme cycling assay in a black flat-bottomed 96-well microtitre plate (Thermo Scientific 167008) as previously described by Kern, Price-Whelan, and Newman (2014). A reagent master mix containing 2 volumes 1 M bicine (pH 8.0), 1 volume 100% ethanol, 1 volume 40 mM EDTA (pH 8.0), 1 volume 4.2 mM thiazolyl blue, 2 volumes 16 mM phenazine ethosulfate, and 1 volume dH₂O was prepared. The reagent mix was incubated at 30°C and primed to injectors in a BMG Labtech FLUOstar Omega microplate reader. Aliquots (15 μ L) of NAD(P)(H) extracts were added to individual wells of a 96-well microtitre plate, which was then incubated in the microplate reader at 30°C. Reagent master mix (80 μ L) was added via a microplate reader injector (300 μ L s⁻¹) and vigorously mixed (200 rpm, 3 s) followed by static incubation for 10 min. Immediately before measurement, a solution of alcohol dehydrogenase (1 mg mL⁻¹ in 0.1 M bicine) was prepared for NAD(H) measurement or glucose 6-phosphate dehydrogenase (0.1 mg mL⁻¹ in 0.1 M bicine) for NAD(P)(H) measurement and primed to a second injector. To start the reaction, each well was injected (300 μ L s⁻¹) with 5 μ L of enzyme solution, followed by vigorous shaking (200 rpm, 1 s). The absorbance at 570 nm was then recorded every 30 to 60 s for 20 min, with vigorous shaking (200 rpm, 1 s) before each read. Slopes from plots representing change in absorbance over time were calculated for known NAD(H) and NADP(H) concentrations and were then used to calculate concentrations and ratios in experimental data (Figure 8).

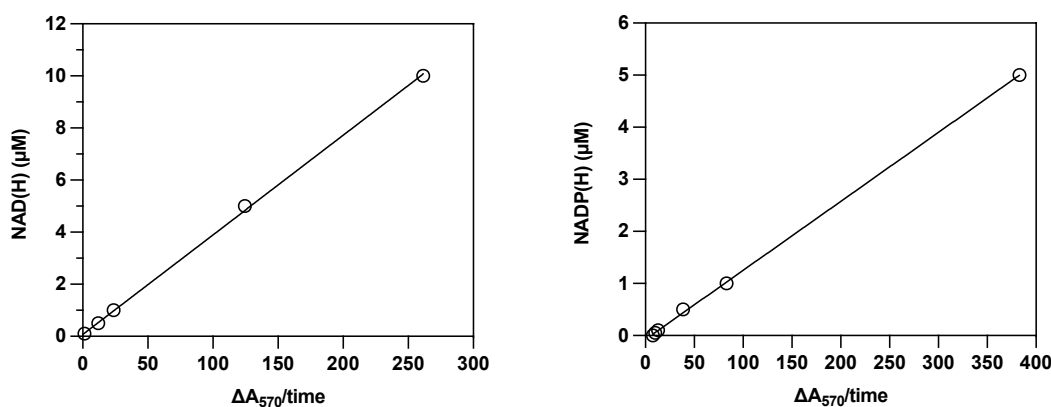


FIGURE 8. Representative standard curves of known concentrations of NAD(H) and NADP(H) used as substrates for the enzyme cycling assay.

3.8 Nitrate/nitrite measurement

Nitrate and nitrite concentrations in *P. aeruginosa* cultures were determined using the Griess reagent system (Promega G9230). Aliquots (1 mL) of culture were centrifuged (15000 rcf, 4°C, 5 minutes) and the supernatant was filter sterilized and stored at -80°C until use. Sulfanilamide and *N*-1-naphthylethylenediamine dihydrochloride (NED) solutions were equilibrated to room temperature before use. A fresh nitrite standard curve was used in each assay in triplicate (Figure 9). To measure nitrite (nitrite only), 50 μL of each experimental sample was pre-loaded to a flat-bottomed 96-well plate, and 50 μL of sulfanilamide was added to each well using a multichannel pipette, and the plate was then incubated for 10 minutes protected from light. Next, 50 μL of NED was dispensed to each well using a multichannel pipette, and the plate was incubated in the dark for a further 10 minutes. Absorbance was then measured at 548 nm and the concentration interpolated from the standard curve. To measure nitrate (nitrate from nitrite), samples were first processed using the Roche Nitrite/Nitrate Colorimetric Test Kit (Roche 11 746 081 001). In brief, this kit was only used to convert nitrate in experiment samples to nitrite with the supplied nitrate reductase. Nitrite concentration in these samples was then measured as described above. To determine the nitrate concentration of samples, the corresponding nitrite concentration in “nitrite only” measurements was subtracted from the “nitrite from nitrate” measurement.

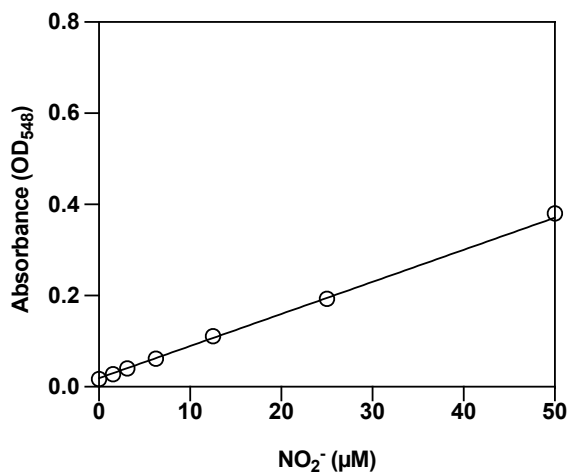


FIGURE 9. Representative standard curve of nitrite used in the Griess reagent system used for detection of nitrite.

3.9 Quorum sensing molecule measurement

QS molecules were extracted and quantified using luciferase reporter strains relevant to the desired molecule measurement (Table 3). Aliquots (1 mL) of culture were centrifuged (15000 rcf, 4°C, 5 minutes) and the supernatant was filter sterilized and stored at -80°C until use. Reporter strains were grown overnight in LB at 37°C with shaking and were then subcultured and grown to $OD_{600} = 1.0$. Following this, 60 μL of normalized culture was added to a white flat-bottomed 96-well microtitre plate (Thermo Scientific 136101) with 60 μL of thawed culture supernatant. The 96-well plate was then incubated for 3 hours with 100 rpm shaking before luminescence measurements were taken. N.B. This method does not directly quantify the concentration of QS molecules, rather it uses induction of QS system promoters by their cognate QS molecules as a proxy measurement.

3.10 Siderophore measurement

Siderophores were extracted and quantified using a Chrome Azurol S liquid assay as previously described, except reaction mixture volumes were scaled for use in a flat-bottomed 96-well microtitre plate (Payne, 1994). All glassware for preparing solutions was washed before use using 6 M HCl, followed by rinsing with MilliQ water. Briefly, 1 mL aliquots of culture were centrifuged (15000 rcf, 4°C, 5 minutes) and the supernatant was filter sterilized and stored at -80°C until use. Supernatants were thawed on ice, and 100 μL of supernatant was added to 100 μL of CAS assay solution and 2 μL of shuttle solution (Table 14) in a clear, flat-bottomed 96-well plate. The mixture was then incubated in the dark for 15 minutes with 50 rpm shaking before measuring absorbance at 630 nm. Supernatants were diluted in sterile culture medium as required. Deferoxamine mesylate salt was dissolved in the relevant medium for using in constructing standard curves, and sterile culture medium was used as a zero reference (Figure 10).

TABLE 14. Siderophore assay reagents.

Stock solutions	Components	Storage
	HDTMA	
CAS assay solution	1 mM $\text{FeCl}_3 \cdot 6\text{H}_2\text{O}$ 2 mM Chrome Azurol S Piperazine (pH 5.6)	Room temperature, protected from light
Shuttle solution	0.2 M 5-sulfosalicylic acid	Prepare fresh

To prepare reliably working CAS assay and shuttle solutions, their component solutions *must* be made with MilliQ water (hereafter referred to as "water") in acid-washed glassware. First, dissolve 0.022 g HDTMA in 100 mL water and prepare the Fe solution in 10 mM HCl. Next, add 1.5 mL of Fe solution to 7.5 mL of 2 mM Chrome Azurol S, and then add the resulting Fe-CAS solution to the HDTMA solution. Then dissolve 4.307 g of piperazine in 30 mL water and adjust to pH 5.6 with 6.75 mL of concentrated HCl. Finally, add the piperazine solution to the HDTMA-Fe-CAS solution and adjust to a final volume of 100 mL with water.

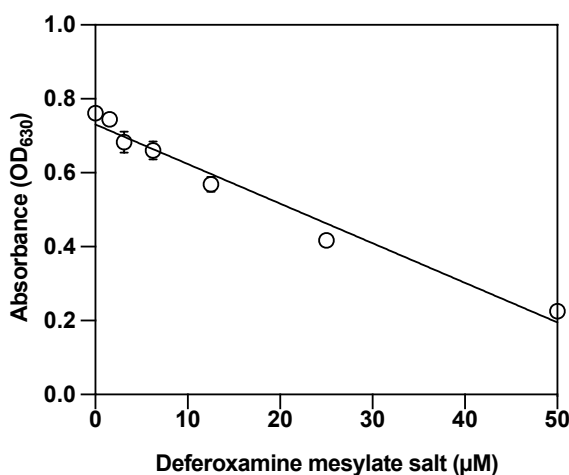


FIGURE 10. Representative standard curve of known concentrations of deferoxamine mesylate salt used as a substrate in the siderophore detection assay.

3.11 Pyocyanin extraction and measurement

Pyocyanin was extracted using a chloroform-acid separation technique that relies on the solubility of pyocyanin determined by pH (Essar *et al.*, 1990). Aliquots of culture were collected and centrifuged to separate cells from supernatant (3220 rcf, 4°C, 15 minutes). The supernatant was then filtered through a 0.22 µm pore size filter (Sartorius), and 7.5 mL of filtered supernatant was added to 4.5 mL of chloroform before vortexing vigorously for 1 minute. The supernatant and chloroform phase were separated by centrifugation (3220 rcf, 4°C, 15 minutes), and 3 mL of the cyan-blue chloroform phase was added to 1.5 mL of 0.2 M HCl. The HCl and chloroform layers were separated by further centrifugation, and 1 mL of the rose-pink HCl layer was transferred to a 1 cm pathlength spectrophotometer cuvette. Absorbance was then measured at 520 nm and converted to µg mL⁻¹ using the molar extinction coefficient of 17.072 (Kurachi, 1958; Essar *et al.*, 1990) and an adjustment factor of 1.5 to account for dilution.

3.12 Biofilm assays

Biofilm assays were carried out in round-bottom 96-well microtitre plates and were prepared using overnight cultures grown in artificial sputum medium. Cultures were washed twice in sterile PBS before a final pellet was resuspended in artificial sputum medium and normalised to a starting OD₆₀₀ of 0.05. Normalised culture (100 μ L) was added to the 96-well plate, then the plate sealed with a gas-permeable membrane and placed into a plastic box lined with damp paper towel. The plastic box was sealed and placed into an orbital incubator set to 100 rpm. Plates were incubated at 37°C for 48 hours before processing. A separate plate was prepared for each individual experiment: XTT assays, crystal violet staining, and CFU enumeration.

3.12.1 XTT assay

To measure metabolic activity, XTT was used. The culture supernatant was carefully aspirated, with minimal disruption to the adhered biofilm. The adhered biofilm was carefully washed three times with 200 μ L dH₂O. After washing, 100 μ L of XTT-menadione solution (Table 15) was added to each well and incubated in the dark at 37°C for two hours with 100 rpm shaking. Absorbance was then measured at 450 nm.

TABLE 15. XTT assay reagents.

Solution	Components	Storage
XTT	4 mg XTT in 10 mL PBS	80°C filtered, single-use aliquots
Menadione	10 mM menadione in 100% acetone	-80°C
XTT-menadione working solution	1 μ L menadione solution in 10 mL XTT solution	Prepare fresh

3.12.2 Crystal violet staining

To measure biofilm formation, crystal violet was used. The culture supernatant was carefully aspirated, with minimal disruption to the adhered biofilm. The adhered biofilm was carefully washed three times with 200 μ L dH₂O. After washing, 150 μ L of 0.1% crystal violet solution was added to each well and incubated at room temperature for 15 minutes. The now stained biofilm was carefully washed three times with 200 μ L dH₂O, the final volume of 200 μ L was removed, and plates were left to dry. After drying, the crystal violet stain was solubilised by addition of 100 μ L of 30% acetic acid. Absorbance was then measured at 590 nm.

3.12.3 CFU enumeration

The supernatant and biofilm fractions were carefully separated, resuspended, and enumerated as previously described. The supernatant fraction was carefully separated from the biofilm fraction by pipette, removing as much culture medium as possible without disrupting the adhered biofilm, and transferred to a sterile microcentrifuge tube. The biofilm fraction was then resuspended in sterile PBS by pipetting before transferring to a separate sterile microcentrifuge tube. Species were then enumerated separately by plating on the appropriate selective media (Table 6), using the previously described technique (Section 3.3).

3.13 Continuous-flow system

A continuous-flow system (Figure 11) was used as previously described (O'Brien and Welch, 2019). A 100 mL culture vessel (Duran) was fitted with a 4-port HPLC GL80 screw cap (Duran). A 24-channel IPC ISM934C standard-speed digital peristaltic pump (Ismatec) was then used to supply sterile ASM to the culture vessel at a constant flowrate ($145 \mu\text{L min}^{-1}$) from a fresh medium reservoir through 1.5 mm bore sterilin silicon tubing (Fisher Scientific). A different channel of the peristaltic pump was then used to remove culture into a waste vessel at the same flowrate. The culture vessel contents were kept homogenous by stirring at 100 rpm using a magnetic stir bare. The entire continuous-flow system was maintained at 37°C . Cultures were inoculated into the system with a starting OD_{600} of 0.05 and left to grow for 3 hours before the peristaltic pump was switched on.

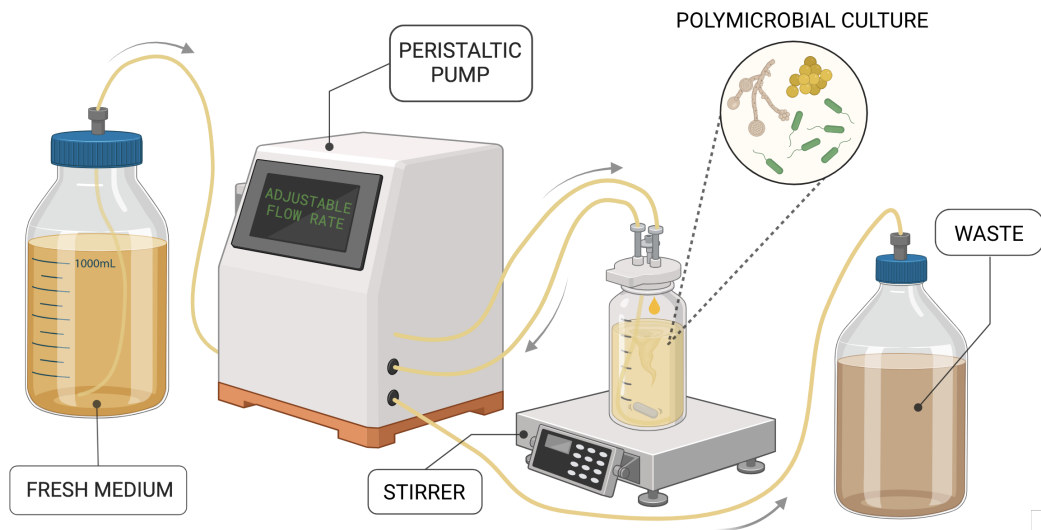


FIGURE 11. Continuous-flow system setup.

3.14 General statistical analysis

All data points represent the mean \pm standard deviation of at least three biological replicates. Unless otherwise stated, results were analysed by one-way ANOVA or Student's t-test (paired or unpaired) with significance considered as $p < 0.05$, using GraphPad Prism (v.9.1.1).

3.15 Lotka-Volterra competition model

3.15.1 General equation

Data was log-transformed with $\log(n+1)$ to return zero population sizes to zero, and log transformation was used as population growth follows a logistic equation. A Lotka-Volterra competition model was used as the culture environment was largely homogenous with no chemical gradients known, and used the general equation:

$$\dot{x}_i = \frac{dx_i}{dt} = r_i x_i \left(1 - \frac{\sum_{j=1}^n \alpha_{ij} x_j}{K_i} \right), \text{ where } \alpha_{ij} = 1 \text{ when } i = j$$

Where \dot{x}_i is the instantaneous rate of change of population i (CFU mL⁻¹ h⁻¹), r_i is the maximum growth rate of i (1/h), x_i is the population size of i at the instantaneous time (CFU mL⁻¹), α_{ij} is the density-dependent interaction coefficient of population i affected by population j , $\sum_{j=1}^n$ denotes that the total interaction is the sum of all individual effects without higher-order complications, and K_i is the carrying capacity of i in the culture medium (CFU mL⁻¹).

3.15.2 Parameter estimation

Initial growth rates were estimated from the rolling mean CFU mL⁻¹ of each species every hour. The starting value for mathematical optimisation was the maximum out of the rolling means, and half of the range value average was used as a buffer for constructing its prior. The initial carrying capacities were estimated as the mean of the data, considering every species at every time point, and the range was set as 0-120% of the maximum log-population value. This was chosen as the steady state population size of co-cultures may not necessarily reflect the true carry capacity of the system due to interspecies interactions. The interspecies interaction coefficients were not deducible directly from the data and were instead set at an initial value of 0, with a range from -2 to +2. The Lotka-Volterra competition model was mathematically optimised us-

ing model-fitting in R (v3.3.3) with deSolve (v1.30) and FME (v1.3.6.2) packages, following the suggested protocols in the FME user manual. For optimisation (“modFit” function), deviations of the simulation from experimentally collected data were minimised by the “modCost” function, using the best differential equation solver for the set of differential equations, which was selected using the minimum “cost value” derived from the starting parameter set. The optimised parameter set replaced the starting parameter set, and if any optimised value was outside of the parameter ranges a new prior boundary was defined (optimised value plus or minus the maximum or minimum starting value, respectively, for range maximums and minimums). These update ranges and starting parameter values were the priors used for Bayesian inference.

3.15.3 Bayesian inference with Markov Chain Monte Carlo

A Markov Chain Monte Carlo process (“modMCMC” function) was used to compare matching between the log-transformed experimentally collected data and the simulation trials with randomly selected parameter value sets. This process used a maximum of 10,000 iterations (option “niter=1e5”), and parameter co-variance was updated every 50 iterations (option “updatecov=50”), with no burn-in trials (option “burninlength=0”), and the chain was terminated after obtaining 100 best-fit parameter combinations (option “outputlength=1e2”). The 100 best-fit parameter combinations were arranged in species-species pairs for use in ecological relationship deduction (for example, species 1 influencing species 2 and species 2 influencing species 1), with the following interactions defined: competition (+,+), mutualism (-,-), predator or parasite (+,-), and prey or host (-,+). Note that the signs are the inverse of the usual ecological indications, as in the above equation the sum of influencing fractions was deduced. Pairwise Chi-square tests with Bonferroni p value correction were used to analyse the count of each ecological category, and pairwise t-tests with Bonferroni p value correction were used to analyse the growth rates and carrying capacities. All analyses used R (v.4.1.0).

METABOLIC CONTROL

Batch culture growth

4.1 Background and rationale

In this section I sought to determine the effects of denitrification gene deletion on the growth of *P. aeruginosa* in a minimal medium with various carbon sources, with and without additional nitrate. I anticipated that denitrification mutants may grow slower in the presence of nitrate as a result of insufficient restructuring of the respiratory network. That is, if *P. aeruginosa* is using denitrification under aerobic conditions, as our recent data supports (Dolan, Kohlstedt, *et al.*, 2020), then it could be hypothesised that the cell membrane contains both aerobic terminal oxidases and N-oxide reductases. In mutants that may be defective in expressing the full complement of denitrification proteins, it might be expected that an incomplete respiratory chain would subsequently be present in the cell membrane but the cell would have impaired respiratory capacity. As a result of this impairment, *P. aeruginosa* may have a decreased growth rate. Additionally, *P. aeruginosa* was cultured in artificial sputum medium axenically and in polymicrobial batch culture with *Candida albicans* and *Staphylococcus aureus*, to investigate growth in a physiologically relevant medium in a polymicrobial environment. Based on previous polymicrobial culture CFU data collected in the Welch laboratory (O'Brien, unpublished), I predicted that in these exper-

iments *P. aeruginosa* mutants defective in denitrification may outcompete the other species at a slower rate than the wild type.

We have demonstrated that when *P. aeruginosa* is cultured on a minimal medium with the only variation in composition being the carbon source, the carbon source used greatly affected the expression of numerous genes, most notably those involved in denitrification. Transcripts relevant to denitrification were in fact found to be among the most abundant when grown aerobically with acetate as the sole carbon source compared with glucose (Dolan, Kohlstedt, *et al.*, 2020).

This is an interesting observation for three main reasons. First, acetate is a two-carbon molecule, whereas glucose is a six-carbon molecule. When utilising acetate, *P. aeruginosa*, must use the glyoxylate shunt pathway in order to conserve carbon, otherwise the two carbons gained from acetate would be lost as CO₂ in the full citric acid cycle. Second, these culture conditions were highly aerobic, using deeply baffled flasks less than 10% full and shaking at 250 rpm. Denitrification is commonly thought of as the anaerobic complement to aerobic respiration, since the major regulator of denitrification—Anr—has an oxygen-sensitive Fe-S cluster, which, when exposed to oxygen becomes unstable and degrades, limiting the ability of the regulator to bind its DNA targets. Third, there was no nitrate present in the culture media in the RNA-seq experiments, therefore no apparent use for denitrification.

4.2 Minimal media (MOPS with a single carbon source)

The *P. aeruginosa* wild type was screened for growth differences in four single-carbon minimal media (acetate, succinate, glycerol, and glucose) to assess the impact of carbon source of growth rate. Day cultures were inoculated from an overnight culture using the same culture medium to ensure strains were pre-adapted to growth on the carbon source used. Cultures were normalised to a starting OD₆₀₀ of 0.05 and allowed to grow for 24 hours. There were no significant differences in final density in any of the cultures after 24 hours. However, when grown with glycerol there was a substantial lag phase of approximately 12 hours. Acetate, glucose, and succinate cultures all transitioned to stationary phase growth at approximately the same time point (5 hours), and glycerol at approximately 20 hours (Figure 12). The growth rate in glycerol (Figure 13) was significantly lower than that of growth in acetate, glucose, and succinate ($p = 0.0285$, $p = 0.0300$, and $p = 0.0270$, respectively).

The growth rates (Figure 13) and colony-forming units (Figure 14) were also measured and calculated for the *P. aeruginosa* wild type and a range of respiratory mutants cultured in MOPS with 40 mM acetate. These experiments were carried out with and without the addition of nitrate to determine if the presence of nitrate—and therefore further stimulation of denitrification gene expression via NarXL—would negatively impact growth rates.

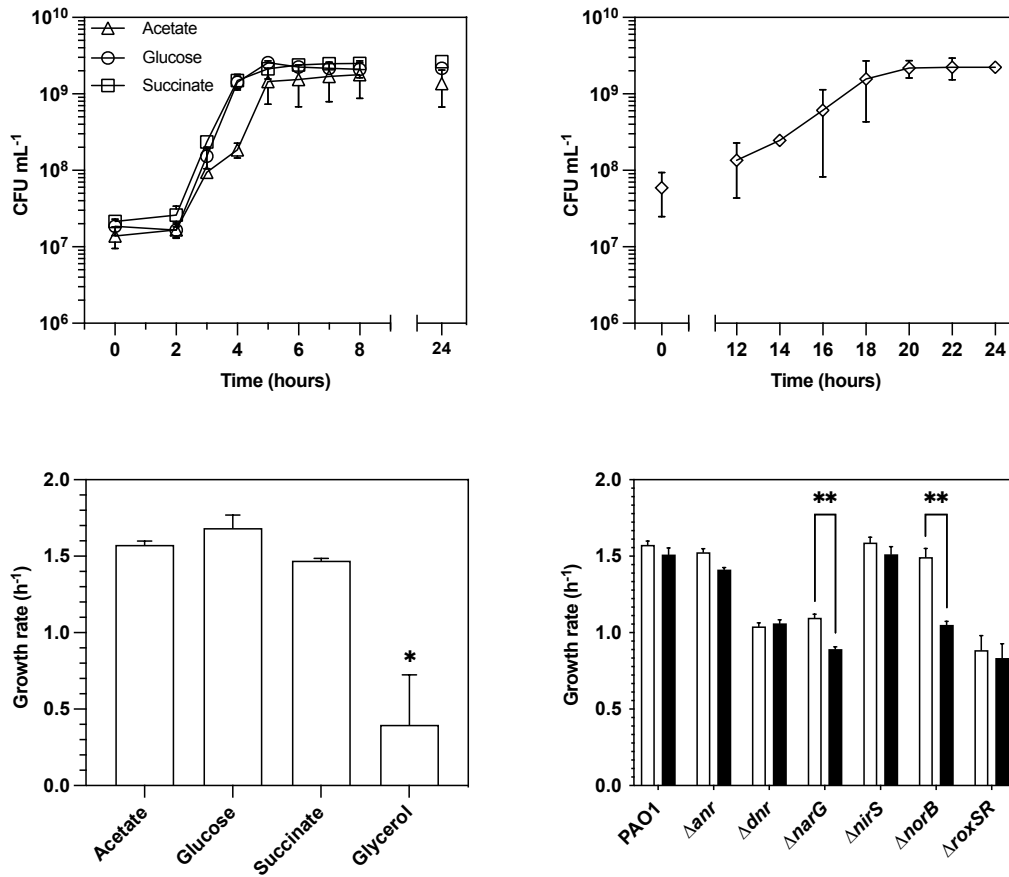


FIGURE 12. Growth curves for *P. aeruginosa* cultured in MOPS minimal medium containing single carbon sources. **LEFT** Acetate, glucose, and succinate. **RIGHT** Glycerol. Mean and standard deviation of at least three biological replicates.

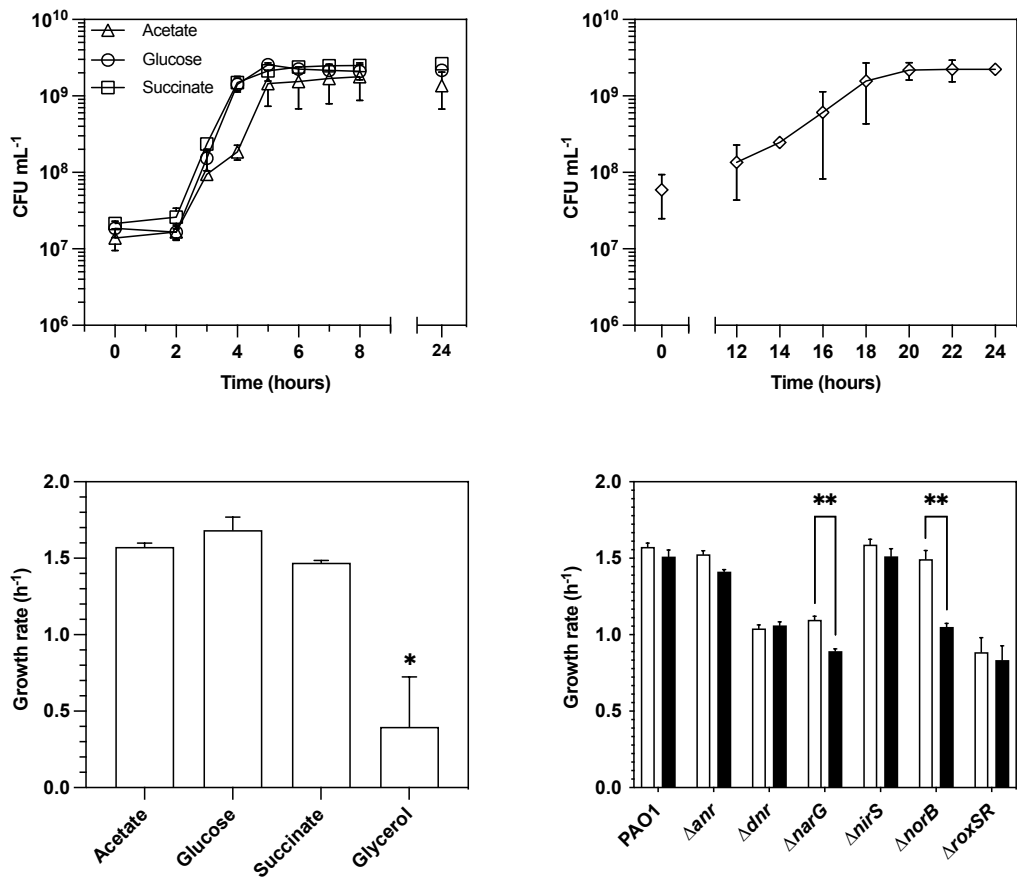


FIGURE 13. LEFT Growth rates of *P. aeruginosa* cultured in MOPS minimal medium with different single carbon sources. RIGHT Growth rates of *P. aeruginosa* wild type and respiratory mutants cultured in MOPS with 40 mM acetate (white bars) or MOPS with 40 mM acetate and 20 mM KNO₃ (black bars). Mean and standard deviation of at least three biological replicates.

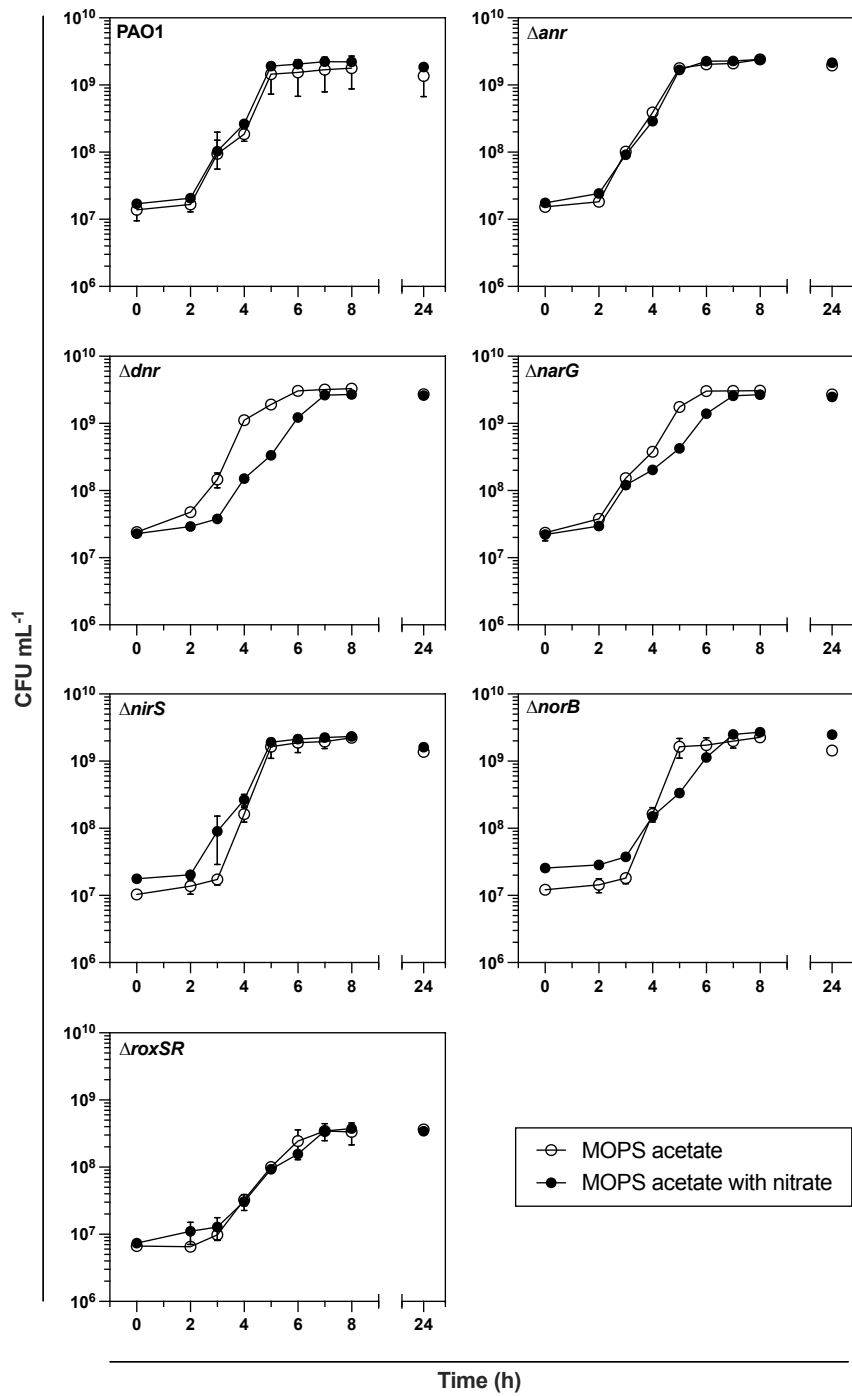


FIGURE 14. CFU enumeration of *P. aeruginosa* wild type and respiratory mutants cultured in MOPS with 40 mM acetate or MOPS with 40 mM acetate and 20 mM KNO₃. Mean and standard deviation of at least three biological replicates.

Only the Δdnr , $\Delta narG$, and $\Delta roxSR$ mutants had significantly slower growth rates than the wild type, in both MOPS with 40 mM acetate and MOPS with 40 mM acetate and 20 mM nitrate. The $\Delta narG$, and $\Delta norB$ mutant growth rates were all significantly decreased by the presence of nitrate ($p = 0.0011$, and $p = 0.0056$, respectively). Overall, the growth curves for the wild type and the respiratory mutants followed a general trend of a 2–3-hour lag phase, followed by short exponential phase of 3–4 hours, before finally transitioning to stationary phase at around 5–6 hours. All mutants achieved a final 24-hour density in the $1\text{--}3 \times 10^9$ CFU mL⁻¹ range, except for the $\Delta roxSR$ mutant which was slightly lower at approximately 3×10^8 CFU mL⁻¹.

4.3 Artificial sputum medium (single species)

The same mutants were also cultured in artificial sputum medium to assess the impact that defective denitrification may have on growth in a physiologically relevant medium (Figure 15).

The growth curves of the wild type and all mutants generally overlap with no major differences, with the exception of the $\Delta roxSR$ mutant. When comparing the exponential phase growth rates (Figure 16) there were also no significant differences between any of the mutants and the wild type, again, except for the $\Delta roxSR$ mutant, which was significantly lower than the wild type and the other mutant ($p = 0.0170$).

To assess long-term growth, *P. aeruginosa* wild type and selected mutants (Figure 17) were cultured over a four-day period to assess their performance in batch culture as resources become limited. Two other microbial species, *C. albicans* and *S. aureus*, were also cultured under the same conditions.

All *P. aeruginosa* cultures reached a density of approximately 1×10^9 CFU mL⁻¹ after 24 hours and maintained this density for the 96-hour duration of the experiment, except for the $\Delta roxSR$ mutant which grew slowly to a density of approximately 1×10^8 CFU mL⁻¹. The resolution of the growth curve was not sufficient to determine growth rates. *C. albicans* and *S. aureus* cultures both reached a lower culture density than the *P. aeruginosa* cultures. All cultures were able to maintain a steady population over the course of the 96-hour experiment.

4.4 Artificial sputum medium (triple species)

I hypothesised that in conditions without severe nutrient limitation, but with increased competition for those nutrients, *P. aeruginosa* mutants defective in denitrification may have impaired survival compared with the *P. aeruginosa* wild type. To test this, the wild type and selected mutants were then batch cultured with two other microbial species, *C. albicans* and *S. aureus*, to assess their performance under increased competition for resources (Figure 18).

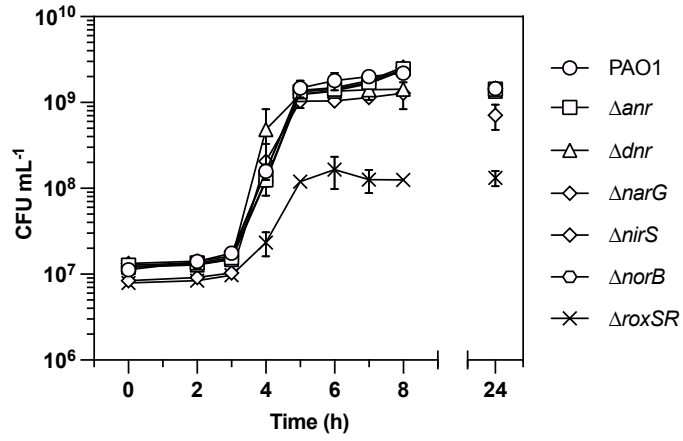


FIGURE 15. CFU enumeration of *P. aeruginosa* wild type and respiratory mutants cultured in artificial sputum medium. Mean and standard deviation of at least three biological replicates.

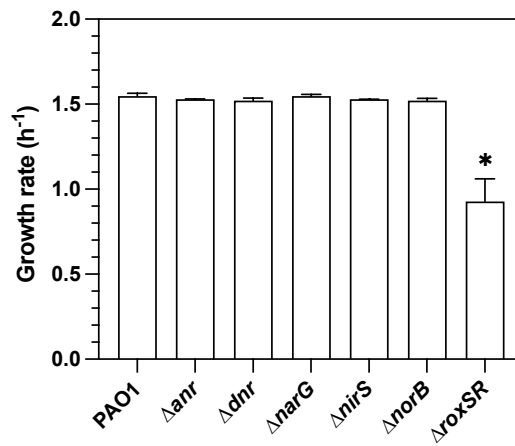


FIGURE 16. Growth rates of *P. aeruginosa* wild type and respiratory mutants cultured in artificial sputum medium. Mean and standard deviation of at least three biological replicates.

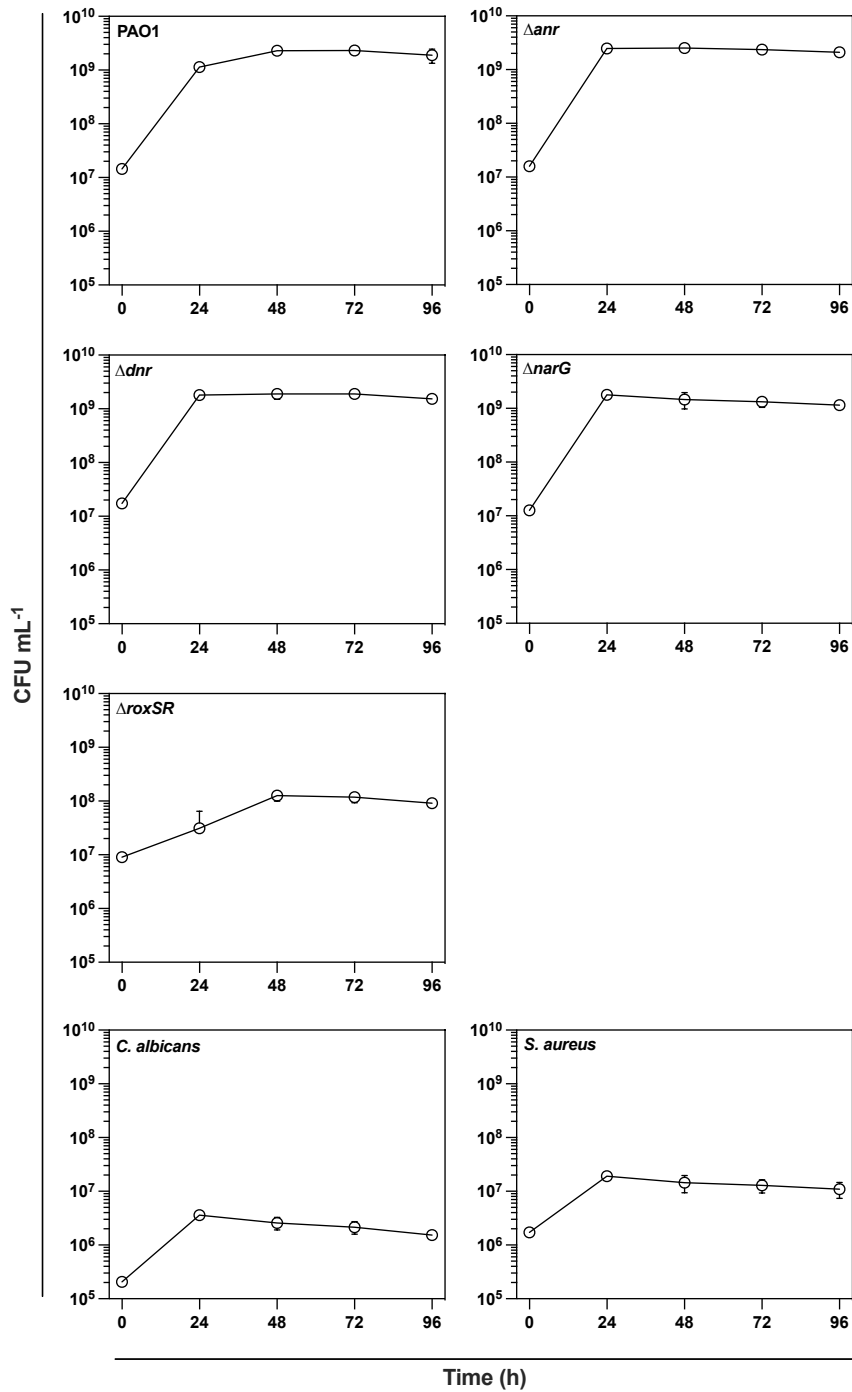


FIGURE 17. CFU enumeration of *P. aeruginosa* wild type and respiratory mutants, *C. albicans*, and *S. aureus* cultured in artificial sputum medium batch culture conditions. Mean and standard deviation of at least three biological replicates.

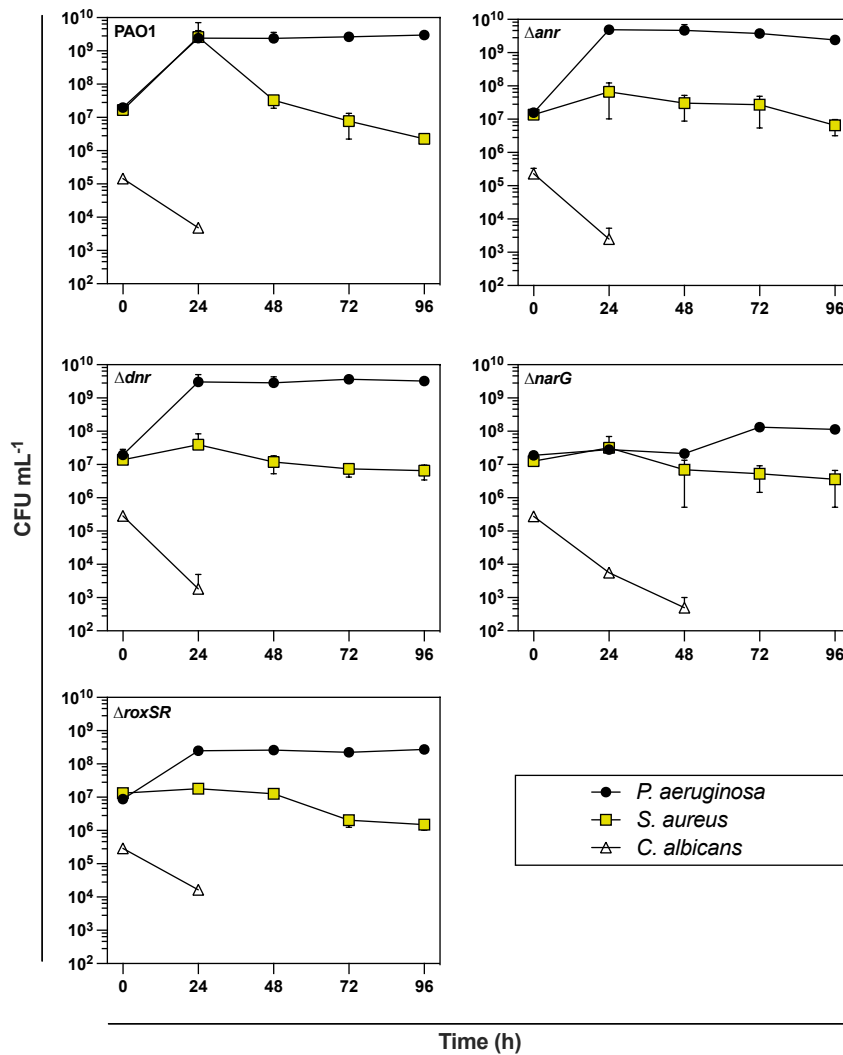


FIGURE 18. CFU enumeration of *P. aeruginosa* wild type and respiratory mutants cultured artificial sputum medium in triple-species batch format with *C. albicans* and *S. aureus*. Mean and standard deviation of at least three biological replicates.

The general trends observed were of population stability. Of the *P. aeruginosa* mutants tested, only the $\Delta roxSR$ mutant presented differently, which grew to a lower density of approximately 1×10^8 CFU mL⁻¹. *S. aureus* populations generally stabilised at approximately 1×10^7 CFU mL⁻¹ in all mutant backgrounds. In all triple-species cultures, the titre of *C. albicans* CFUs decreased rapidly from 1×10^5 CFU mL⁻¹ after initial inoculation, with no recoverable colonies after 24-48 hours.

4.5 Discussion

The growth curves in MOPS with acetate with and without nitrate yielded interesting observations. Surprisingly, the Δanr mutant did not appear to have any growth delay or change in growth rate, despite being an important regulator of nitrate respiration (Zumft, 1997). The Δdnr and $\Delta narG$ mutants both appear to have a growth delay in the presence of nitrate, though of these two mutants only the $\Delta narG$ mutant had a change in growth rate. The $\Delta norB$ mutant also had a change in growth rate in the presence of nitrate. The $\Delta roxSR$ mutant had a lower growth rate than the wild type, and though this was not statistically significant, it was expected as the culture conditions were highly aerobic, and the RoxSR two-component system positively regulates the expression of four of the five terminal oxidases.

The result that the Δdnr mutant was patently different to the Δanr mutant was surprising, especially considering that *dnr* expression is under the control of Anr, and that the Δanr mutant was relatively similar to the wild type. Adding another layer of complexity is the differences between the $\Delta narG$, $\Delta nirS$, and $\Delta norB$ mutants. Interestingly, the $\Delta nirS$ mutant did not show any significant changes in growth rate in the presence of nitrate or compared with the wild type, yet the $\Delta narG$ and $\Delta norB$ mutants did, and were significantly different to growth in medium without the addition of nitrate. This distribution of growth rates means that in the presence of nitrate, the wild type, Δanr , and $\Delta nirS$ form one group, and the Δdnr , $\Delta narG$, and $\Delta norB$ mutants form another. This grouping is suggestive that there may be a $NO_2^-:NO$ “node point”, in which growth is attenuated if *P. aeruginosa* cannot sufficiently reduce nitric oxide or utilise nitrate during exponential growth. A previous study has linked an accumulation of nitric oxide with biofilm dispersal and increased cell death (Barraud *et al.*, 2006). Whilst *P. aeruginosa* may be able to cycle nitric oxide back to nitrate via flavohaemoglobin (nitric oxide dioxygenase), this may be only a short-term fix since more nitric oxide will be generated and the same problem reoccurs. Given that the Δanr mutant seems relatively unaffected by the presence of nitrate, this “node point” is likely predominantly regulated through the concerted activities of Dnr, Fhp, and NarXL to control nitric oxide production. The NarXL two-component system has a switching action between kinase/phosphatase activity, mediated by nitrate, and alongside Dnr has activity on the *nar* and *nirS/nirQ* operons. If nitrate levels decrease, expression of the *nar* and *nirQ* operons ceases to be induced by NarL, and therefore subsequent production of NorCB and NirQ (which activates NirS and NorCB activity) is decreased. If *dnr* is absent, there may be decreased reduction of nitrite to nitric oxide, since *nirS/nirQ* operon expression is also induced by Dnr. The expression of *fhp* is induced by multiple entities (FhpR, AsrA, and PA3697) but is likely insufficient on its own to mitigate the effects of decreased nitric oxide reductase expression.

Of all the mutants and conditions tested, the Δdnr , $\Delta narG$, $\Delta norB$, and $\Delta roxSR$ mutants

in the presence of nitrate had the slowest growth rate. These growth rates may be explained with reference to the membrane occupancy hypothesis, which states that as the cell grows in preparation for division, the volume of the cell increases at a faster rate than the membrane surface area increases, limiting the number of respiratory complexes that may insert into the membrane (Zhuang, Vemuri and Mahadevan, 2011; Szenk, Dill and de Graff, 2017). Anr, Dnr and NarXL together induce the expression of all denitrification genes required to convert nitrate to dinitrogen gas. Since NarXL only gives negative feedback to *nar* operon expression through the accumulation of nitrite, all the sensory signals in the presence of nitrate point to continued expression and activity of the nitrate, nitrite, nitric oxide, and nitrous oxide reductases.

When *narG* is missing, there is still no mechanism to directly detect a defect in nitrate reduction, and the cell will produce the full (or nearly full) denitrification apparatus and occupy membrane space. Considering that denitrification requires nitrate reductase activity to initiate the reduction cascade, it is entirely useless unless supplemented with NapA activity, which is not expressed in exponential phase growth. Therefore, the cell is partially crippled by a non-functioning respiratory branch and growth is decreased. Supporting this model is the Δ_{roxSR} data. In a Δ_{roxSR} mutant, CcoN1—the dominant terminal oxidase under aerobic conditions—is not expressed. Whilst the remaining terminal oxidases have routes to expression, the arguably most crucial oxidase is not present, therefore greatly decreasing aerobic respiration and the subsequent growth rate to near $\Delta_{dnr}/\Delta_{narG}$ levels. In artificial sputum medium, it appears that an abundance of nutrients is able to alleviate the effects of a truncated denitrification cascade. Together, these data highlight the fine sensitivity and regulation of the branched respiratory system of *P. aeruginosa*.

The triple-species cultures gave interesting insight into the relative ‘aggressiveness’ of different *P. aeruginosa* mutants. It was expected that the Δ_{dnr} , Δ_{narG} , and Δ_{roxSR} mutants would be less competitive in that they might maintain higher titres of *C. albicans* and *S. aureus*; however, this did not appear to be strictly true, in fact the titre of *P. aeruginosa* decreased (in the case of Δ_{narG} and Δ_{roxSR}). This highlights that the population dynamics between the species are regulated and reflected in a more complicated manner that cannot be deconstructed by simple CFU enumeration. Further investigation into secreted molecules and quorum sensing networks in *P. aeruginosa* will give valuable insight into this and will be elaborated later in this dissertation.

Expression of respiration associated genes

5.1 Background and rationale

RNA-seq data previously collected in the Welch lab indicated the strong up-regulation of denitrification genes during growth on MOPS with 40 mM acetate. In this section, I sought to investigate the relative importance of the major denitrification regulators, Anr and Dnr, on the expression of denitrification genes during growth in MOPS with 40 mM acetate. Based on the growth rates presented in Section 4.2, I hypothesised that denitrification gene expression may be lower in a Δdnr mutant compared with the wild type and Δanr mutant, and that denitrification gene expression may be higher in a $\Delta roxSR$ mutant compared with the wild type, to compensate for a decrease in terminal oxidase expression. To test this hypothesis, I used a Tn7-based transposable vector to insert single, orientation- and location-specific, stable, promoter::*lux* transcriptional fusions into the *P. aeruginosa* genome for a number of genes of interest (Choi and Schweizer, 2006).

By creating a transcriptional fusion between the promoters of genes of interest and the *lux-CDABE* cassette, the expression of genes can generally be correlated with light output, providing an affordable and easy system to implement. Nevertheless, the luciferase system has drawbacks that must be considered. In the context of this project, the system's reliance on molecular oxygen is somewhat of a hindrance to its utility. Importantly, the requirement of oxygen to generate light means that we know that the cultures are indeed aerobic if there is a light signal. However, the requirement of molecular oxygen has two negatives: LuxAB depletes the culture medium of molecular oxygen, and the generation of light ceases once molecular oxygen is depleted. With these considerations in mind, the data in this section is reliable with respect to aerobic regulation of denitrification and cannot be used to comment on anaerobic regulation.

In this section I tested for the expression of *acsA*, *ccoN1*, *anr*, *dnr*, *narK1*, *nirS*, *norC*, *nosR*, *fhp*, and *stb*. The expression of *acsA* was used as a control for validating that a graded response could

be obtained from the construct based on the culture medium used, given that AcsA is likely to have the highest activity during growth in a medium containing its substrate, acetate. To support the hypothesis that during growth in medium containing acetate as the sole carbon source *P. aeruginosa* experiences some respiratory pressure due to a fast growth rate, *ccoN1* was investigated since it encodes the dominant terminal oxidase under high oxygen conditions.

The promoters for *anr* and *dnr*, encoding two major regulators of denitrification, were examined for their impact on each other, given that expression of *dnr* is under the control of Anr. I hypothesised that in a Δanr mutant I would observe a decrease in the expression of *dnr*, and also that in a $\Delta roxSR$ mutant I might see an increase in the expression of Anr to counteract a loss of terminal oxidase expression. The expression of denitrification enzyme promoters (*narK1*, *nirS*, *norC*, and *nosR*) were also investigated in mutant backgrounds to determine the relative importance of the two regulators—Anr and Dnr—to their expression.

P. aeruginosa can also convert nitric oxide to nitrate via Fhp, therefore *fhp* expression was measured to establish the relevance of nitric oxide cycling under these conditions and whether the conversion of nitric oxide to nitrate was a significant consideration in the context of growth on acetate. Finally, *sth* expression was explored to ascertain if the transfer of hydride between pyridine nucleotides was heavily utilised by *P. aeruginosa* to maintain redox homeostasis—something that I predicted may be disrupted during growth on acetate.

5.2 Differential expression of *acsA* and *ccoN1*

Promoter fusions were made for *acsA* and *ccoN1*, which encode acetyl-CoA synthetase and a constitutively-expressed high-affinity terminal oxidase, respectively (Comolli and Donohue, 2004; Arai *et al.*, 2014). The data showed that *acsA* is strongly expressed when cultured in MOPS with 40 mM acetate, and since acetate is a primary substrate of AcsA one would expect expression to be high; however, when cultured in MOPS glycerol, for example, *acsA* is expressed at a much lower level, with a peak normalised RLU value approximately ten times lower than during growth on acetate (Figure 19). The CcoN1 terminal oxidase was also strongly expressed during growth on MOPS with 40 mM acetate compared with the other carbon sources tested, and was significantly greater than that of cells grown in glucose ($p = 0.0073$), succinate ($p = 0.0010$), and glycerol ($p = 0.009$), demonstrating that a graded response can be achieved with the luciferase system.

5.3 Expression of *anr* and *dnr*

Given the strongest expression of terminal oxidases occurred during growth with acetate as the sole carbon source, experiments from this point forward focused on the effects of gene deletions

on expression during growth on MOPS with 40 mM acetate only. The promoters of *anr* and *dnr* were investigated in the wild type, Δanr , and $\Delta roxSR$ backgrounds (Figure 20). The expression of *anr* was significantly lower in $\Delta roxSR$ ($p = 0.0015$) compared with the wild type, in contrast to my predictions. The expression of Δdnr was also significantly lower in the Δanr and $\Delta roxSR$ mutants ($p = 0.0001$ and $p = 0.0023$, respectively).

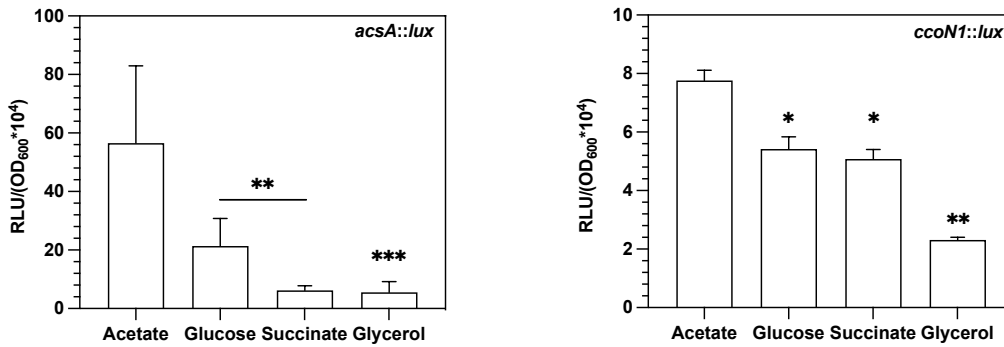


FIGURE 19. Luminescence from promoter::lux transcriptional fusions of *acsA* and *ccoN1* in *P. aeruginosa* when cultured in MOPS with different carbon sources. Mean and standard deviation of at least three biological replicates.

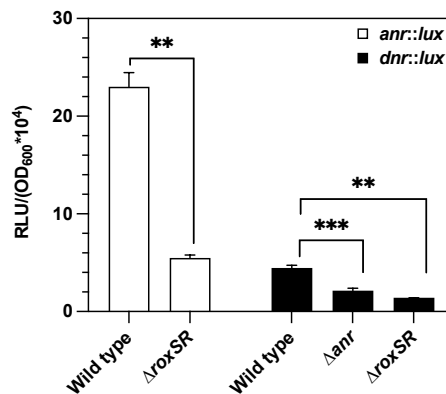


FIGURE 20. Luminescence from promoter::lux transcriptional fusions of *anr* and *dnr* in different genetic backgrounds when cultured in MOPS with 40 mM acetate. Mean and standard deviation of at least three biological replicates.

5.4 Expression of N-oxide reductases

Promoter fusions were made for each of the N-oxide reductases (*narK1*, *nirS*, *norC*, and *nosR*) and introduced into Δanr , Δdnr , and $\Delta roxSR$ mutants (Figure 21).

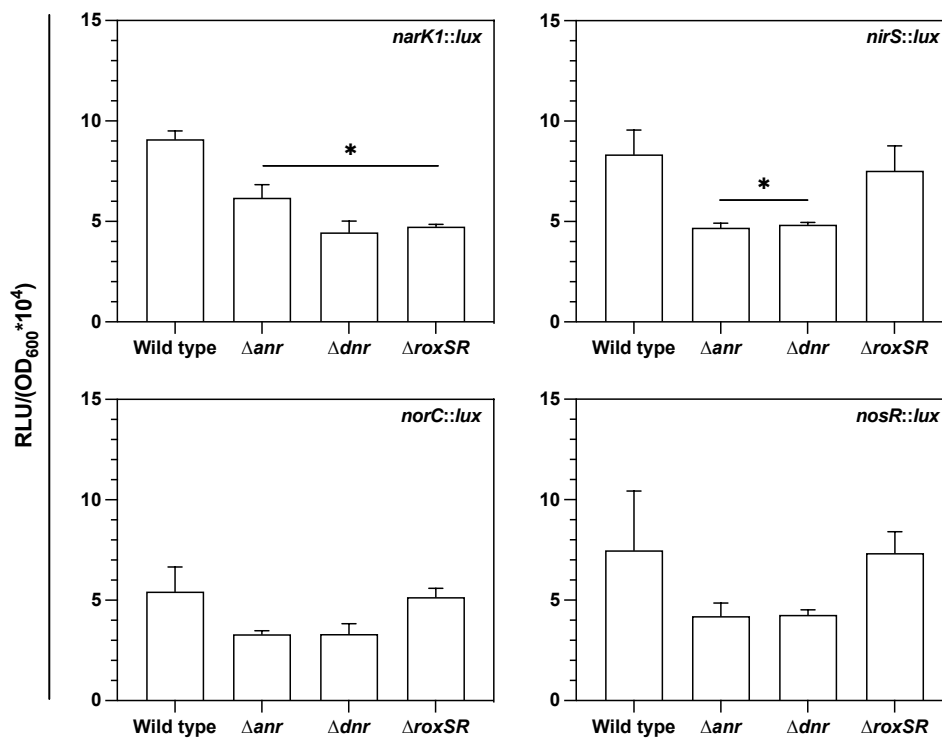


FIGURE 21. Luminescence from promoter::lux transcriptional fusions of *narK1* (Δanr $p = 0.0420$, Δdnr $p = 0.0145$, and $\Delta roxSR$ $p = 0.0021$), *nirS* (Δanr $p = 0.0353$ and Δdnr $p = 0.0387$), *norC*, and *nosR* in different genetic backgrounds when cultured in MOPS with 40 mM acetate. Mean and standard deviation of at least three biological replicates.

The expression of all N-oxide reductases was lower in the Δanr and Δdnr mutants compared the wild type, as expected. However, the differences in expression between the Δanr and Δdnr mutant were negligible, in contrast to my initial hypothesis. Although the expression of *norC* and *nosR* appeared lower in both Δanr and Δdnr compared with the wild type, there were no significant differences. In contrast to my initial hypothesis that denitrification would be up-regulated to compensate for a loss of terminal oxidase expression in $\Delta roxSR$, there were no significant differences in expression of any of the N-oxide reductases compared with the wild type.

5.5 Expression of *fbp* and *sth*

No significant differences were found in the expression of *fbp* and *sth* between the wild type and any of the mutants tested (Figure 22).

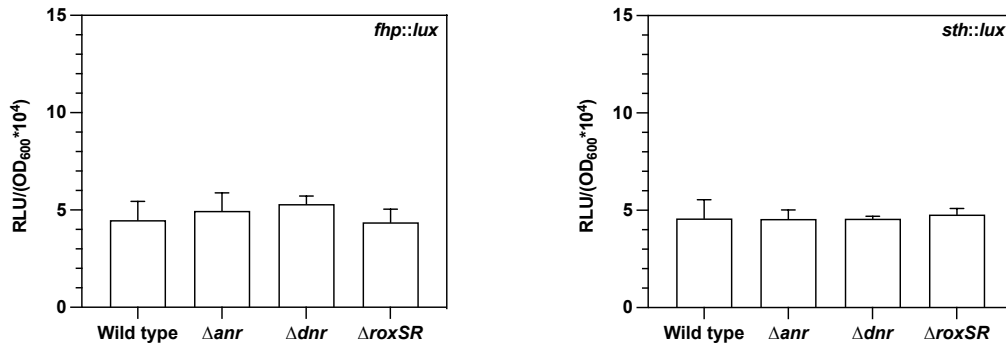


FIGURE 22. Luminescence from promoter::*lux* transcriptional fusions of *fhp* and *sth* in different genetic backgrounds when cultured in MOPS with 40 mM acetate. Mean and standard deviation of at least three biological replicates.

5.6 Discussion

Previous proteomic analysis showed up-regulation of a number of denitrification genes during growth in MOPS with 40 mM acetate (Dolan, Kohlstedt, *et al.*, 2020). In this section, transcriptional fusions were made to determine the exact nature of these changes, i.e. are the changes due to predictable transcriptional regulation by known entities (that is, Anr and Dnr), or could there be other factors at play, for example loss of RoxSR function.

It should be noted that although the cultures used in this experimental format are not anaerobic, the degree of oxygenation of the cultures is unknown. Considering the dimensional characteristics of a 96-well microtitre plate and the orbital settings, it was assumed that the surface-to-volume ratio of the culture medium was equal enough to preclude steep oxygen gradients in the plate wells.

Surprisingly, an increase in neither *anr* nor *dnr* expression was not observed in the Δ *roxSR* mutant. In aerobic conditions, RoxSR promotes expression of four out of five terminal oxidases and represses the expression of the *coxB* terminal oxidase. Therefore, it was expected that denitrification may be up-regulated to counteract a loss of terminal oxidase function. It is possible, however, that a lack of repression of *caa3* resulted in sufficient activity of *cox* to mitigate the need for denitrification, especially since *caa3* is a high-affinity oxidase that generates the most ATP per molecule of nutrient of any of the terminal oxidases (Schuster *et al.*, 2004; Kawakami *et al.*, 2010; Arai *et al.*, 2014). As was expected, there was a decrease in the expression of *dnr* in an Δ *anr* mutant, and surprisingly in the Δ *roxSR* mutant, too. As previously stated, it was expected that in the absence of RoxSR-mediated expression of terminal oxidases, the denitrification branch of respiration would be up-regulated to accommodate for a decrease in aerobic respiration.

The only N-oxide reductases affected by the loss of *anr*, *dnr*, or *roxSR*, were the nitrate and nitrite reductases. This was somewhat surprising, considering both *nar* and *nir* operons have multiple routes to expression and do not necessarily depend on a single regulator. However, it does serve to highlight that a concerted action by multiple partners is required for full expression of *nar* and *nir*, and that the top-level regulator, Anr, is not necessarily essential for transcription of denitrification genes. In contrast, *nosR* expression was not significantly lower than the wild type in either the *anr* or *dnr* mutant, which was unexpected given that, according to the existing literature, *nos* may only be expressed through Dnr activity.

The lack of change in expression of *fhp* and *sth*, was not surprising, given that these genes are all controlled outside of the Anr/Dnr regulon. However, it was anticipated that there may be higher expression of *sth* in denitrification mutants considering the prediction that denitrification may be used to supplement aerobic respiration during times of potential redox imbalance, and Sth can be used to rebalance the redox pool by reducing $\text{NAD}^+/\text{NADP}^+$.

In summary, the data in this section underscores *P. aeruginosa*'s remarkable ability to adapt its respiratory composition under diverse conditions, and, importantly, highlights gaps in the current knowledge of how denitrification may be regulated under aerobic conditions.

Measurement of redox ratios

6.1 Background and rationale

The results presented in Section 4.2, 5.3 and 5.4 showed that some of the mutants tested have growth defects during growth on MOPS with 40 mM acetate and 20 mM nitrate (Δdnr , $\Delta narG$, $\Delta norB$, and $\Delta roxSR$), and also showed that the expression of denitrification genes is lower in Δanr and Δdnr mutants compared with the wild type. Previous work has also demonstrated that a loss of the production of phenazines (which are redox active compounds) resulted in an increase in the NADH:NAD⁺ ratio and expression of denitrification enzymes (Price-Whelan, Dietrich and Newman, 2007; Dietrich *et al.*, 2013; Y.-C. Lin *et al.*, 2018).

Based on these findings, I anticipated that denitrification is used to mitigate redox imbalance, and that denitrification mutants might have an impaired respiratory capacity that manifests as an accumulation of intracellular NADH. This is relevant since during respiration the oxidation of NADH is coupled to reduction of N-oxides or oxygen via the ubiquinone pool. To test this hypothesis, ratios of NAD(P)H to NAD(P)⁺ ratios and absolute NAD(P)(H) concentrations were quantified both in the absence and presence of nitrate in MOPS with acetate for *P. aeruginosa* wild type and a range of respiration mutants.[†] An $\Delta aceK$ mutant was included in this section as a control, considering that AceK regulates the branch point between the complete citric acid cycle and the glyoxylate shunt, and therefore a loss of this regulation could affect NAD(P)(H) levels.

The growth rate with acetate as a sole carbon source was comparable to that of growth on glucose (Figure 13), despite only having a supply of only 2 carbons per acetate instead of 6 carbons per glucose. It has been shown that the three *P. aeruginosa* NADH dehydrogenases (NDH-1, NDH-2, and Nqr) and the pyridine nucleotide transhydrogenase Sth, are all significantly up-regulated during growth with acetate as the sole carbon source (Dolan, Kohlstedt, *et al.*, 2020). Sth catalyses the reduction of NAD⁺ or NADP⁺ by NADPH or NADH, respectively, and is thought to

[†]Part of this work was published in Dolan *et al.* (2020).

be primarily designated to the reoxidation of NADPH by NAD⁺ (Nikel, Pérez-Pantoja and de Lorenzo, 2016). In *E. coli*, growth on acetate is known to generate more NADPH than is required for biosynthesis, then it follows that there may be a strong need to dissipate the reductive power of high NADPH levels (Sauer *et al.*, 2004). Furthermore, if the rate at which the cell volume increases outpaces the rate at which the membrane surface area increases, then cytosolic NADH generation will outpace the rate of oxidation of NADH at the cell membrane.

In extreme cases, if the rate of respiration is elevated to such an extent that it shifts the balance of NADH to NAD⁺ to a more reduced ratio, this could then trigger overflow metabolism to counteract a shift in the redox state of the cell (Szenk, Dill and de Graff, 2017). Aerobic denitrification may be utilised as a form of overflow metabolism by attempting to use as many potential electron acceptors as possible to increase NADH oxidation (Vemuri *et al.*, 2007). These data, in addition to the expression of denitrification genes aerobically, suggests that *P. aeruginosa* may be employing aerobic denitrification as a redox balancing mechanism.

6.2 NAD(H) concentrations

At 24 hours of growth, the total NAD(H) concentration was quantified for the *P. aeruginosa* wild type and each mutant (Figure 23). At the 24-hour point, the majority of NAD(H) was the oxidised form (Appendix A, Figure A3). In MOPS with 40 mM acetate, only the Δ_{roxSR} mutant had significantly higher ($p = 0.0446$) levels of NAD(H) at 24 hours of growth compared with the wild type. Comparing MOPS with 40 mM acetate with MOPS with 40 mM acetate and 20 mM nitrate, only the Δ_{norB} mutant had a significantly higher NAD(H) concentration ($p = 0.0182$). However, when comparing MOPS with 40 mM acetate and 20 mM nitrate final concentrations, the Δ_{dnr} ($p = 0.0265$), Δ_{narG} ($p = 0.0005$), Δ_{nirS} ($p = 0.0033$), and Δ_{norB} ($p = 0.0485$) mutants all had significantly higher total NAD(H) concentrations than the wild type. In these instances, the increase in total NAD(H) concentration was attributable to an excess of the NAD⁺ fraction.

6.3 NADP(H) concentrations

The concentration of total NADP(H) was also measured and compared at 24 hours of growth (Figure 24). Three of the mutants had significantly different total NADP(H) to the wild type: Δ_{nirS} (lower, $p = 0.0020$) Δ_{norB} (lower, $p = 0.0232$), and Δ_{aceK} (higher, $p = 0.0117$). During growth in the presence of nitrate, only the Δ_{nirS} ($p = 0.0096$) and Δ_{norB} ($p = 0.0335$) mutants exhibited a lower NADP(H) concentration. Only the Δ_{nirS} mutant showed a significant difference in NADP(H) concentration between the two media used, with Δ_{nirS} maintaining a higher

NADP(H) concentration during growth in the presence of nitrate ($p = 0.0022$).

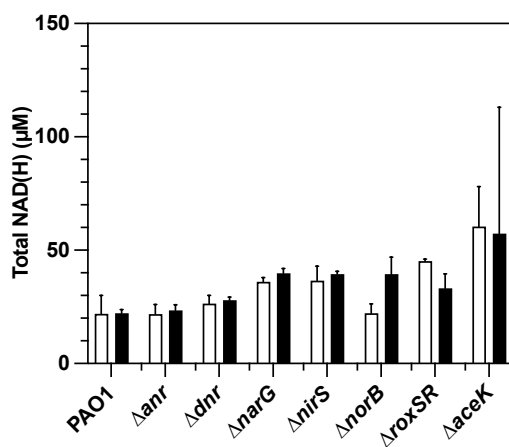


FIGURE 23. Total NAD(H) concentration at 24 hours of growth. *P. aeruginosa* cultured in MOPS with 40 mM acetate (white bars) or MOPS with 40 mM acetate and 20 mM KNO₃ (black bars). Mean and standard deviation of at least three biological replicates.

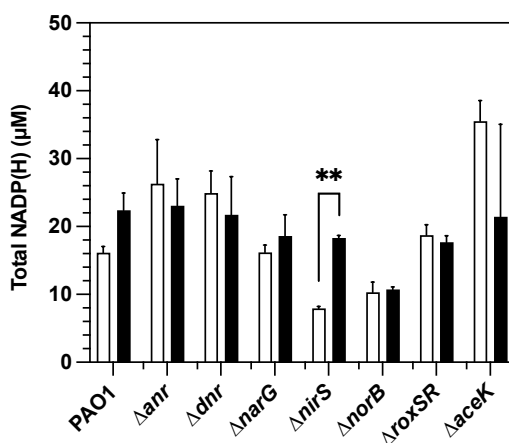


FIGURE 24. Total NADP(H) concentration at 24 hours of growth. *P. aeruginosa* cultured in MOPS with 40 mM acetate (white bars) or MOPS with 40 mM acetate and 20 mM KNO₃ (black bars). Mean and standard deviation of at least three biological replicates.

6.4 NAD(H) ratios

NAD(H) was extracted hourly from aerobically grown MOPS cultures with differing carbon sources. It was found that the carbon source alone was sufficient to induce changes in the intracellular redox ratio of the *P. aeruginosa* wild type (Appendix A, Figure A1). Next, the *P. aeruginosa*

wild type and a range of mutants were assessed to determine a baseline NADH:NAD⁺ ratio when electron acceptors are limited (i.e. without nitrate) and whether aerobic denitrification was the cause of the decrease in NADH:NAD⁺ ratios during growth with nitrate, respectively.

The wild type and all mutants exhibited transient NADH:NAD⁺ ratios greater than 1:1 in MOPS with 40 mM acetate (Figure 25). A gradual increase towards a peak in the ratio was observed generally at approximately 5-6 hours of growth, at the point at which the wild type and most mutants were in late exponential phase, followed by a rapid decrease in the NADH:NAD⁺ ratio (Figure 26). Nitrate was included in the medium to ascertain if *P. aeruginosa* may be utilising aerobic denitrification to modulate its redox pool; that is, is *P. aeruginosa* attempting to use denitrification to reoxidise the NADH cofactor and lower the NADH:NAD⁺ ratio?

All strains tested—except for the Δdnr ($p = 0.3598$) and $\Delta norB$ ($p = 0.3628$) mutants—were able to significantly decrease the peak NADH:NAD⁺ ratio. This suggests that if *P. aeruginosa* is unable to express the full complement of denitrification enzymes (such as in Δdnr) or is unable to reduce nitric oxide and therefore nitric oxide inhibits denitrification enzymes, then *P. aeruginosa* is also unable to sufficiently oxidise NADH. In some instances, the peak NADH:NAD⁺ ratio exhibited during growth on MOPS with 40 mM acetate does not align with the peak during growth on MOPS with 40 mM acetate and 20 mM nitrate. The most likely reason for this is the slight delay in growth shown by some of the mutants (Figure 14).

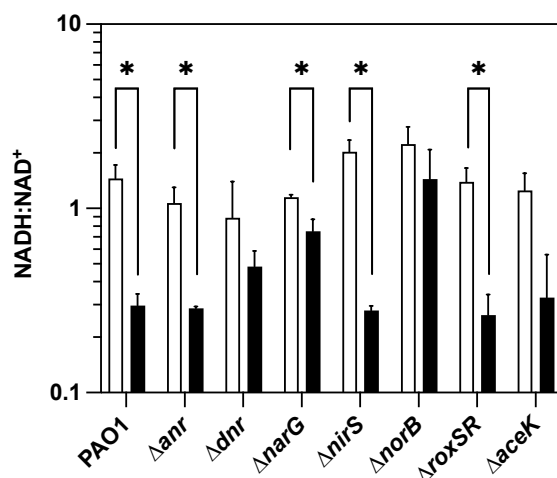


FIGURE 25. Peak NADH:NAD⁺ ratios of *P. aeruginosa* wild type and respiratory mutants cultured in MOPS with 40 mM acetate (white bars) or MOPS with 40 mM acetate and 20 mM KNO₃ (black bars). Mean and standard deviation of at least three biological replicates.

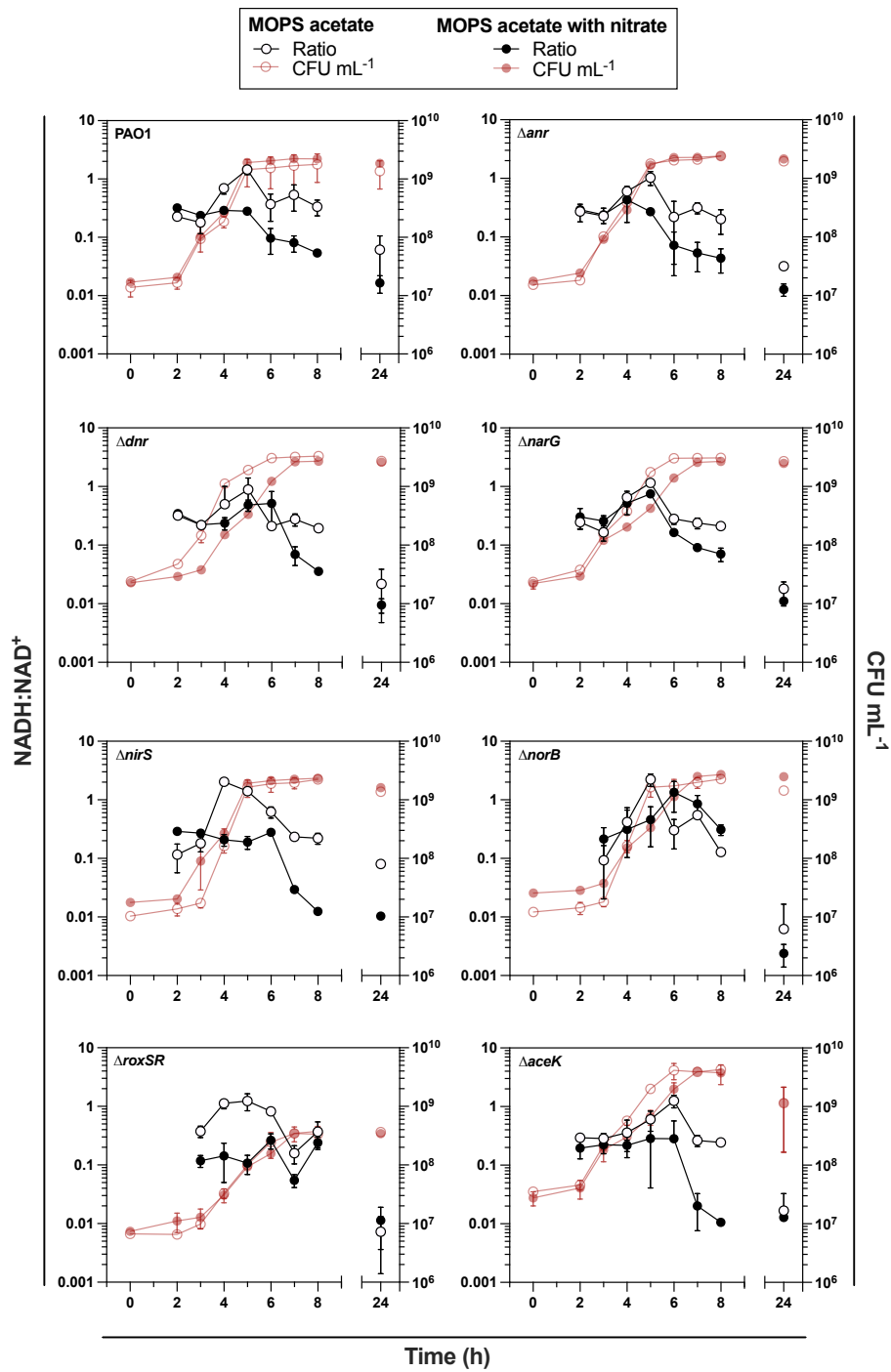


FIGURE 26. NADH:NAD⁺ ratios of *P. aeruginosa* wild type and respiratory mutants cultured in MOPS with 40 mM acetate or MOPS with 40 mM acetate and 20 mM KNO₃. Mean and standard deviation of at least three biological replicates.

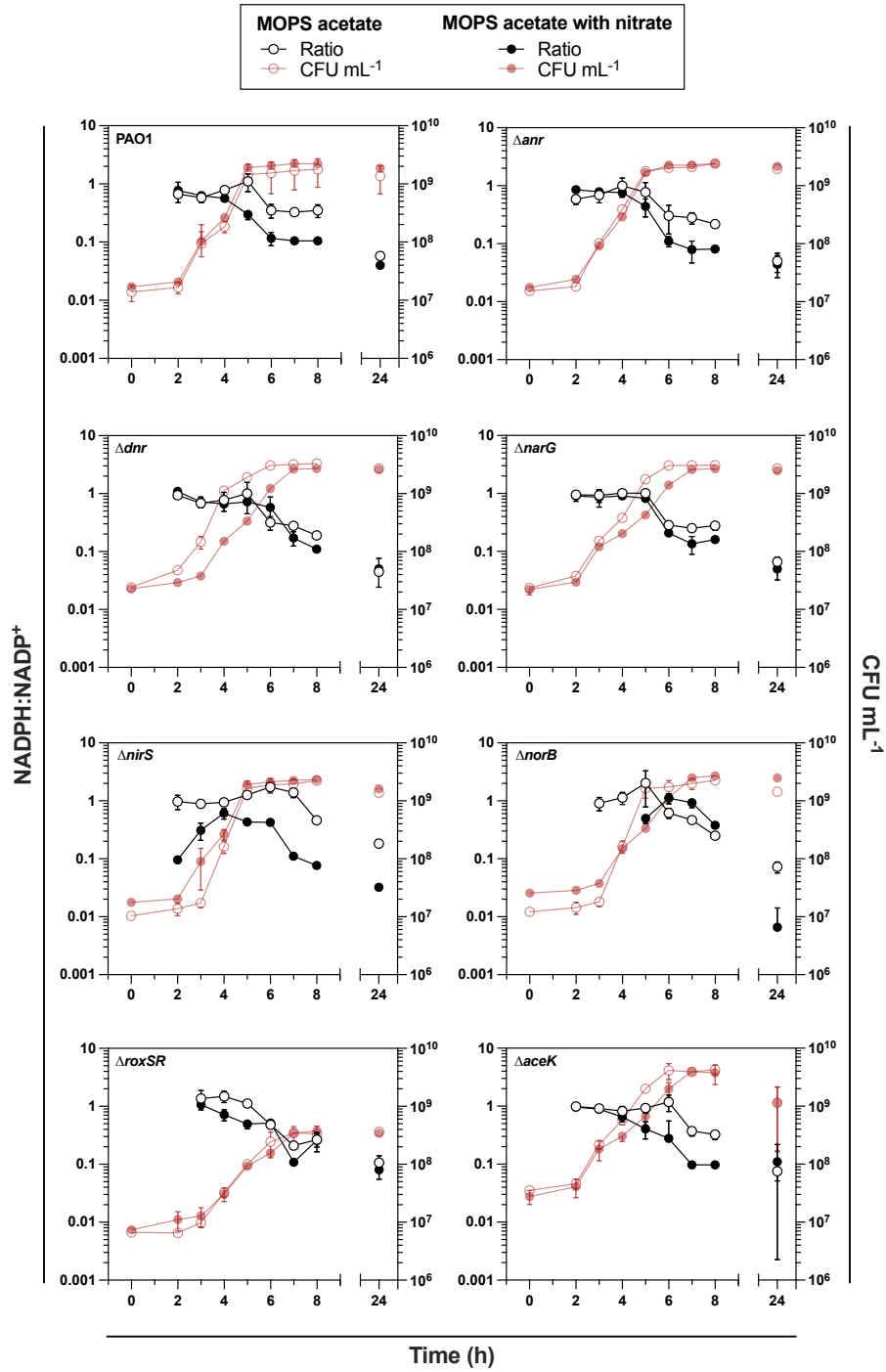


FIGURE 27. NADPH:NADP⁺ ratios of *P. aeruginosa* wild type and respiratory mutants cultured in MOPS with 40 mM acetate or MOPS with 40 mM acetate and 20 mM KNO₃. Mean and standard deviation of at least three biological replicates. Missing time points are due to no detection of NADP(H).

6.5 NADP(H) ratios

The NADPH:NADP⁺ ratios of the wild type and all mutants adhered to the same pattern: a starting ratio of approximately 1:1 followed by a gradual decline (Figure 27).

6.6 Discussion

During growth on MOPS acetate, it has been observed that cells have an increased NADH:NAD⁺ ratio (Dolan, Kohlstedt, *et al.*, 2020). The results in this section have shown that *P. aeruginosa* seemingly adapts its electron transport chain to include denitrification in conditions that usually preclude expression of denitrification genes. Considering that denitrification is typically associated with anaerobic and microaerobic growth, this was a surprising finding. It appears that the function of this electron transport chain remodelling is to modulate the NADH:NAD⁺ ratio, thus restoring redox balance (Wu and Bauer, 2010). This hypothesis was further supporting by the lack of redox ratio modulation in Δdnr and $\Delta norB$ mutants in the presence of nitrate. The data collected thus far highlights the relative importance of Anr and Dnr in activating denitrification gene expression. In contrast to the usual depiction of Anr as being the key regulator of denitrification, it seems that Dnr is even more crucial.

It appears that the reduction of nitrate is the key step in the denitrification cascade, especially considering that this reaction is coupled to the oxidation of NADH (Cava *et al.*, 2004; Gates *et al.*, 2011). The importance of nitrate reduction becomes even more apparent when the growth rates are taken into consideration alongside the increase in NAD(H) concentrations by the denitrification mutants. The Δdnr , $\Delta narG$, $\Delta nirS$, and $\Delta norB$ all have an increased 24-hour NAD(H) concentration compared with the wild type during growth in MOPS with 40 mM acetate and 20 mM nitrate, and all (except $\Delta nirS$) have a slower growth rate. This suggests that an inability to modulate the redox state directly through denitrification-coupled NADH oxidation has significant impacts on growth. From these data, we can infer that the function of NirS is least important in the hierarchy of denitrification-dependent redox modulation, as there seems to be little effect on growth and the redox ratio is still significantly lowered in the presence of nitrate. The ratio data for the $\Delta norB$ mutant was anticipated, considering that an accumulation of nitric oxide would lead to inhibition of the other N-oxide reductases, further supporting the importance of managing a balance of nitric oxide levels.

Interestingly, the $\Delta aceK$ mutant provided somewhat surprising results. As previously discussed, AceK regulates the branch point between the glyoxylate shunt and continuing flux through the complete citric acid cycle. The lack of significant peak NADH:NAD⁺ ratio modulation suggests potential involvement of AceK in regulation of denitrification, though possibly indirectly.

The significant accumulation of NADP(H) was expected, since the ICD-catalysed generation of NADPH is excessive during growth on acetate, and would likely be accentuated without AceK-mediated inactivation of ICD (Sauer *et al.*, 2004). It appears that Sth activity is not sufficient to transfer H⁺ from NADH to NADP⁺ in considerable enough amounts to decrease the NADH:NAD⁺ ratio, though this is perhaps not surprising considering its primary function is to perform the direct opposite reaction.

The data in this section begins to highlight the complexity around the regulation of aerobic and “anaerobic” respiratory branches and the redox status of the cell. Additionally, the data presented shows that *P. aeruginosa* effectively employs aerobic denitrification to adjust its intracellular redox balance, and this seems to be tied to growth on acetate (and therefore flux through the glyoxylate shunt). Future work using isocitrate dehydrogenase mutants would assist in expanding this hypothesis. The utilisation of nitrate to maintain redox homeostasis may be representative of an as-yet-unclarified mechanism of overflow metabolism in *P. aeruginosa*, placing further emphasis on the considerable metabolic flexibility of this important pathogen (Vemuri *et al.*, 2006).

Nitrate reduction

7.1 Background and rationale

The data presented thus far indicates that denitrification-associated genes are expressed aerobically, largely regardless of the presence of nitrate, and the measured redox ratios (i.e. the balance of reduced NAD species to oxidised NAD species) suggest that nitrate reduction is coupled to the oxidation of NADH/NADPH. Furthermore, it appears that there are significant differences in the expression of denitrification genes in Δanr and Δdnr mutants, and likewise differences in redox ratios.

To gain further insight into the proposed link between denitrification and redox balancing, I measured nitrite concentrations over the same time course as the redox experiments to determine if NADH oxidation was concomitant with nitrite production. This investigation aimed to complement the work of Price Whelan *et al.* 2007), which demonstrated that the addition of nitrate to phenazine-null mutants rescued an increased NADH:NAD⁺ ratio phenotype (Price-Whelan, Dietrich and Newman, 2007).

MOPS with 40 mM acetate was supplemented with 20 mM nitrate, far in excess of physiological levels (Grasemann *et al.*, 1998; Palmer, Aye and Whiteley, 2007; Kolpen *et al.*, 2014; Line *et al.*, 2014). It was expected that providing an excess of nitrate would remove any constraints on denitrification arising from precursor limitation. I then repeated this experiment in artificial sputum medium, which contains nitrate concentrations close to that of CF sputa, to assess the extent to which denitrification is used under more physiologically relevant conditions. I hypothesised that during growth on artificial sputum medium, nitrate would be consumed relatively quickly compared with growth on MOPS with 40 mM acetate and 20 mM nitrate, considering that artificial sputum medium contains far less nitrate, but that this consumption would not start until later in the growth curve (for example in stationary phase when there is increased competition between cells for oxygen). The hypothesis behind this is that, based on previously published

data detailing how cell morphology changes depending on carbon source (Dolan, Kohlstedt, *et al.*, 2020), growth on a rich medium would not skew the cell morphology in favour of increasing cell volume relative to membrane space as is seen during growth on MOPS acetate. Therefore, *P. aeruginosa* would not attempt to use denitrification as a form of overflow metabolism to cope with increased NADH concentration relative to NAD⁺ concentration.

Furthermore, to date there have been no publications detailing the time-resolved utilisation of nitrate (i.e. denitrification) by *P. aeruginosa* in an artificial sputum medium. This section therefore sought to also provide insight into the potential importance of denitrification in the context of a chronic lung infection or lung condition, such as CF.

7.2 MOPS acetate with nitrate

The production of nitrite by the *P. aeruginosa* wild type did not exceed 37 μM nitrite at any point in the measured time period and maintained this approximate concentration throughout stationary phase (Figure 28). Surprisingly, the Δdnr and $\Delta narG$ mutants both produced nitrite, peaking at approximately 42 μM and 18 μM , respectively. The $\Delta nirS$ mutant maintained a higher concentration of nitrite, as expected. In contrast to the wild type and other mutants, the $\Delta norB$ mutant produced very little nitrite at its peak, approximately 8 μM . The $\Delta roxSR$ mutant produced nitrite early in its growth curve, maintaining a concentration of between 40-60 μM for every measured time point throughout the experiment. Statistically, the peak nitrite concentration produced by the Δanr , $\Delta narG$, and $\Delta norB$ mutants was significantly lower than the wild type, and the Δdnr , $\Delta nirS$ and $\Delta roxSR$ mutants, produced significantly more (p values; Δanr 0.0216, Δdnr 0.0078, $\Delta narG$ 0.0002, $\Delta nirS$ 0.0007, $\Delta norB$ 0.0002, $\Delta roxSR$ 0.0027).

7.3 Artificial sputum medium

The same measurements were made when cultured in artificial sputum medium (Figure 29) containing 348 μM nitrate, an approximation of physiological levels of nitrate found in CF sputum (Grasemann *et al.*, 1998; Palmer, Brown and Whiteley, 2007; Kolpen *et al.*, 2014; Line *et al.*, 2014).

The wild type and mutants did not behave as they did in a limited-nutrient medium with an excess of nitrate availability. The general trend was that nitrite production began far later in the growth curve, with no considerable concentrations of nitrite produced and maintained before 7 hours. All of the peaks were observed in stationary phase at the 7- or 8-hour time point, much later than observed when grown in a minimal medium.

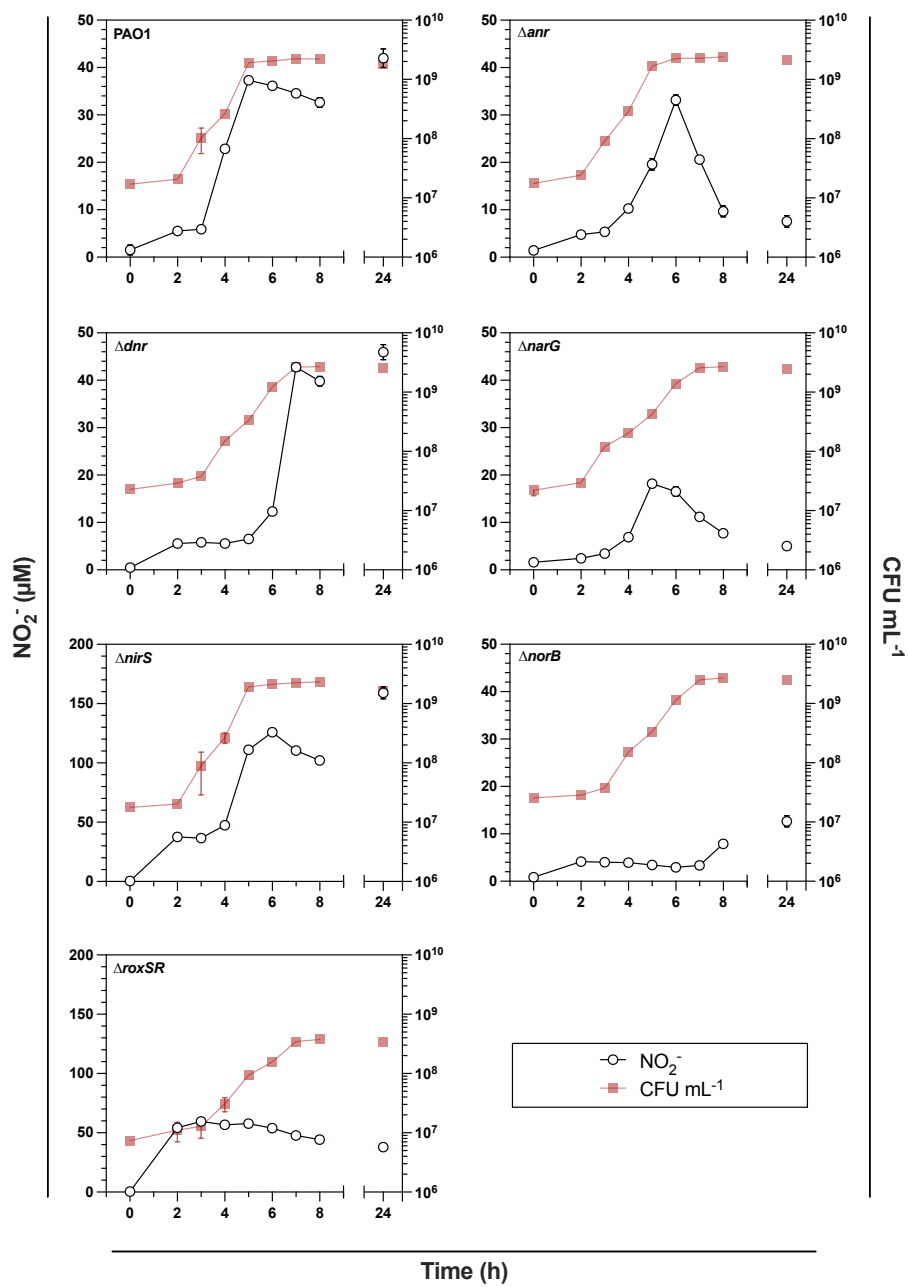


FIGURE 28. Measurement of nitrite concentrations of *P. aeruginosa* wild type and respiratory mutants cultured in MOPS with 40 mM acetate and 20 mM KNO₃. Mean and standard deviation of at least three biological replicates.

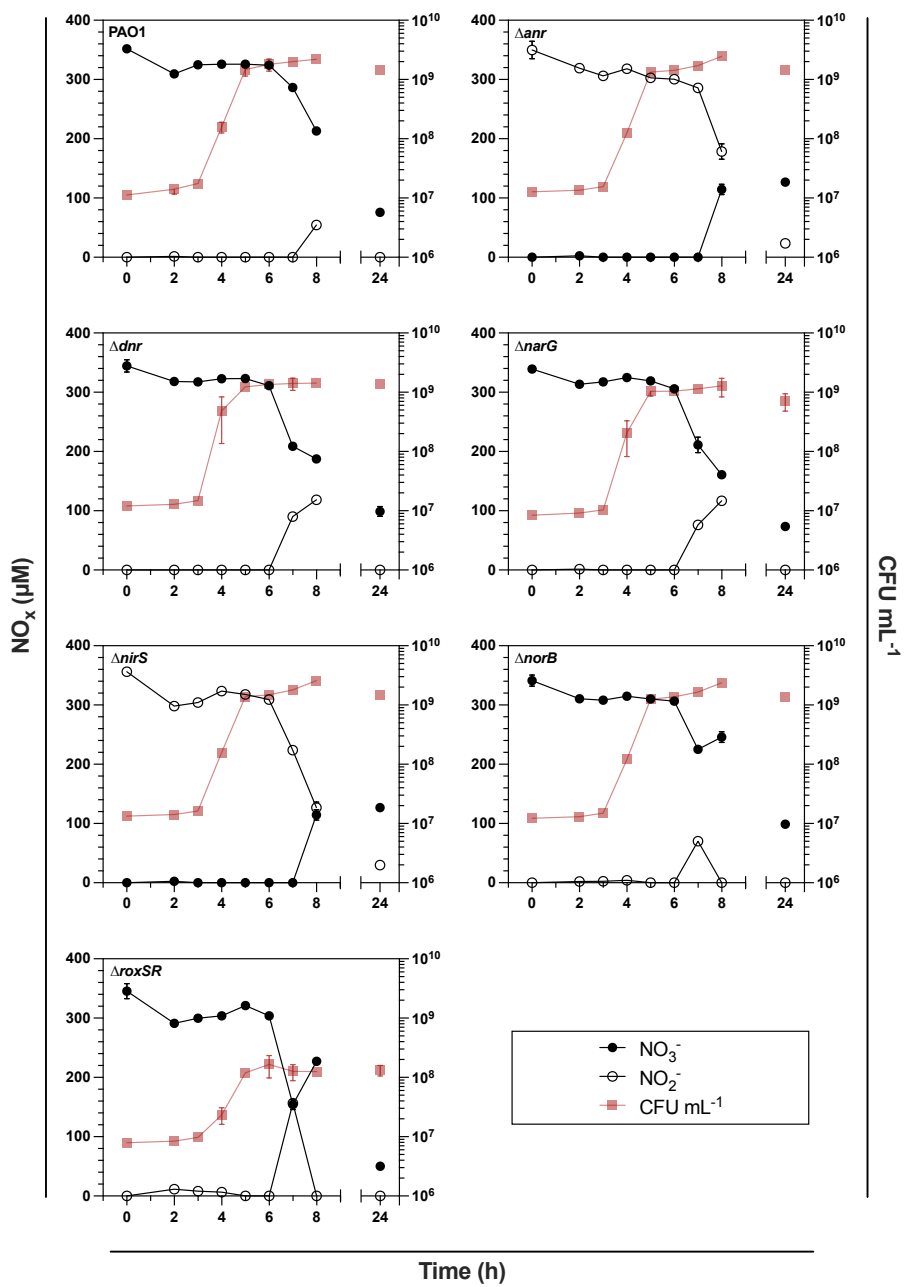


FIGURE 29. Measurement of nitrate and nitrite concentrations of *P. aeruginosa* wild type and respiratory mutants cultured in artificial sputum medium. Mean and standard deviation of at least three biological replicates.

7.4 Discussion

In this chapter, I set out to quantify nitrite production by *P. aeruginosa*, and to determine if nitrite production could be associated with a decrease in the NADH:NAD⁺ ratio shown in Section 6.4. Based on the observations in the NAD(P)(H) measurement experiments, I anticipated that when grown in MOPS with 40 mM acetate and 20 mM nitrate, I would observe substantial nitrite production in the wild type and most of the mutants considering the excess of nitrate provided. Furthermore, I expected to see that the peak in nitrite production would coincide with the lowering of the NADH:NAD⁺ ratio in those mutants that could significantly alter this ratio. If these two observations were indeed simultaneous (or near to), it would further reinforce the hypothesis developed in previous sections that denitrification is used to correct redox imbalance. Additionally, I aimed to examine the extent to which denitrification is used in artificial sputum medium in order to contextualise denitrification in a more physiologically relevant condition. I predicted that denitrification would be used to a smaller extent than in a less physiologically relevant condition such as MOPS with 40 mM acetate.

Interestingly, there seemed to be no strong pattern in the amount of nitrite produced relative to the degree of denitrification impairment in the mutants. In contrast to the literature-perceived importance of specific genes to denitrification (for example, *anr* compared with *dnr*), it appeared that this importance does not correlate with changes in nitrite production. The exception to this is the $\Delta nirS$ mutant, which produced and accumulated a greater concentration of nitrite, since it cannot convert nitrite to nitric oxide. The Δanr mutant produced a comparable amount of nitrite to the wild type, though the peak concentration measured was not maintained at a comparable level to the wild type and rapidly decreased in stationary phase. The $\Delta narG$ and Δdnr mutants were also able to produce nitrite, though much later in its growth curve in the case of the Δdnr mutant. This activity may be attributable to NapA, the periplasmic nitrate reductase, which is regulated entirely separately to NarG—through RpoS—and is reported to be expressed in stationary phase only (Van Alst *et al.*, 2009).

In contrast, when grown in a rich medium (i.e. artificial sputum medium), it appeared that there were three rough groups of different levels of nitrite production: the wild type and $\Delta norB$ mutant in one, the Δanr , Δdnr , and $\Delta narG$ mutants in a second, and the $\Delta nirS$ and $\Delta roxSR$ mutants in a third. It is not clear why the Δanr , Δdnr , and $\Delta narG$ mutants reduced more nitrate than the wild type, but it could be posited that a dysregulation by loss of either Anr or Dnr control could lead to increased expression mediated through the other regulatory partners and thus less stringent control over nitrite production. Again, the reduction of nitrate in the $\Delta narG$ mutant is likely attributable to NapA activity (Van Alst *et al.*, 2009). It may be that the feedback mechanisms for regulating *napA* expression are less stringent than those of the Anr/Dnr/NarXL

system and this leads to increased nitrite production compared with the wild type. As in the minimal medium cultures, the $\Delta nirS$ mutant produced increased amounts of nitrite compared with the wild type.

In both media, $\Delta norB$ and $\Delta roxSR$ mutants produced very distinct phenotypes compared with the other mutants. The $\Delta norB$ mutant produced only low levels of nitrite throughout the growth curve despite having the ability to fully activate expression of the *nar* operon. This data could represent another manifestation of the $NO_2^-:NO$ “node point”. The elevated levels of nitrite from early in the growth curve of the $\Delta roxSR$ mutant could be indicative of denitrification being used as a compensatory mechanism to mitigate a loss of *ccoNI* expression. It also could support the hypothesis that RoxSR somehow regulates denitrification in times of redox stress—perhaps functioning as a repressor until a stress-related signal is received—and a complete absence of RoxSR lifts all repression indiscriminately.

Surprisingly, compared with growth in a minimal medium with an abundance of nitrate (20 mM), *P. aeruginosa* utilises more nitrate in artificial sputum medium which contains a relatively low amount of nitrate (348 μM). Despite an apparent limit to available nitrate for use in denitrification, the growth rates and CFU densities are comparable in both media (Section 4.2 and 4.3). This may be explained by the different cell shape and volume differences when grown in minimal media (Dolan, Kohlstedt, *et al.*, 2020), however this has not been investigated in artificial sputum medium.

In summary, the work presented in Section 4-7 describes that for efficient aerobic growth on acetate, denitrification is required, is dependent on having at least nitrate reductase and nitric oxide reductase, and Dnr-mediated regulation is critical. Without these components of the denitrification respiratory network, the intracellular redox ratio increases, and the growth rate is attenuated (Figure 30). Moreover, the work in these sections also complements existing work investigating *P. aeruginosa* and redox ratios, further expanding our knowledge of denitrification utilisation and how this relates to other aspects of *P. aeruginosa* physiology that can manage redox homeostasis.

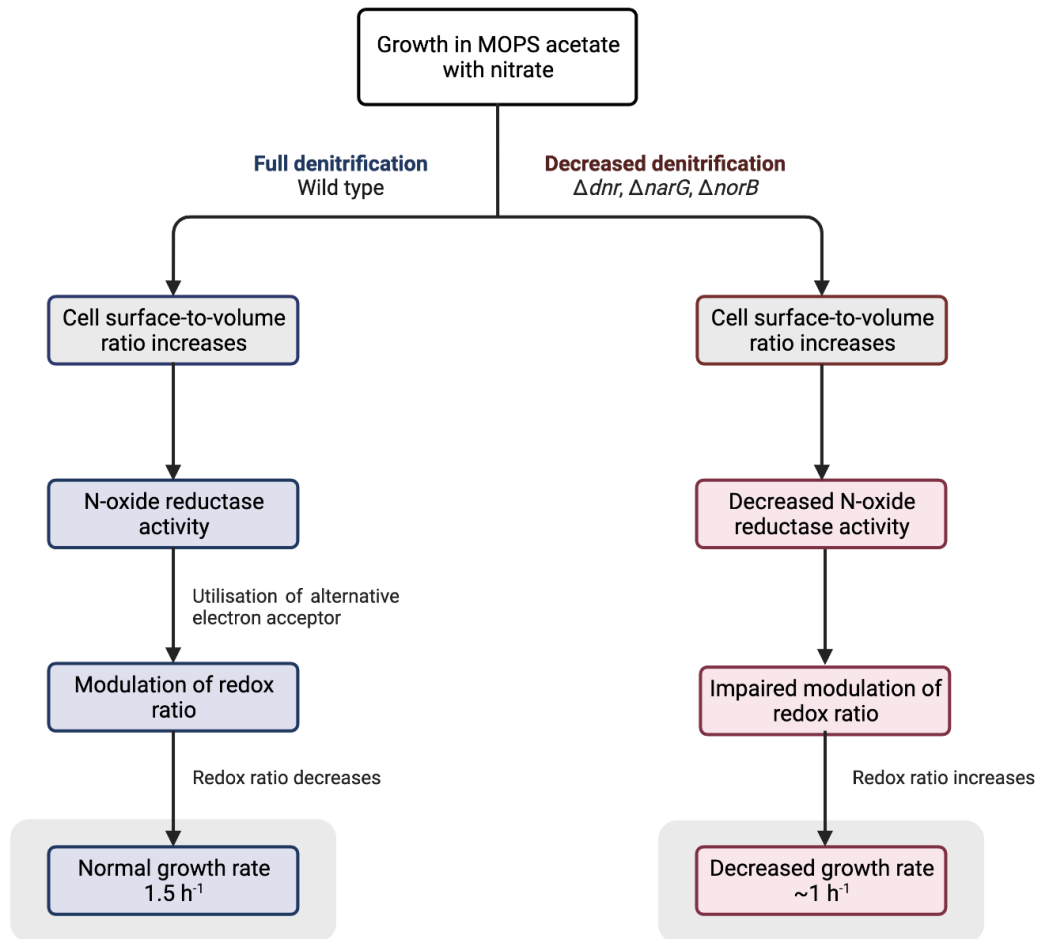


FIGURE 30. Dnr-dependent denitrification facilitates efficient growth when cultured with a short chain fatty acid (acetate) as the sole carbon source by employing denitrification to maintain redox homeostasis.

SIGNALLING, VIRULENCE, AND BIOFILMS

Extracellular profile

8.1 Quorum sensing

8.1.1 Background and rationale

Previous work investigating QS and denitrification, and how these relate to biofilms, has firmly established that QS regulates denitrification. Yoon *et al.* (2002) showed that in a $\Delta rhlR$ mutant, the activity of nitrate reductase, nitrite reductase, and nitric oxide reductase all increased in a biofilm setup (Yoon *et al.*, 2002). The effect of PQS on managing the interface between anaerobic and aerobic respiration through inhibition of denitrification has been comprehensively explored by Toyofuku *et al.*, who first showed that both $\Delta lasI$ and $\Delta rhlII$ mutants exhibited increased nitrate reduction activity, and that this activity could be restored to wild-type levels through the addition of exogenous OdDHL or BHL (Toyofuku *et al.*, 2007). These authors then continued to demonstrate that the activity of all denitrification enzymes could be decreased in these mutants with the addition of BHL—suggesting that denitrification is regulated through the *rhl* system—and also showed that PQS inhibits denitrification enzyme activity through its iron-chelating action, since iron is essential to denitrification enzymes, and that the addition of iron rescues denitrification capabilities (Toyofuku *et al.*, 2007, 2008). More recently, it has been shown that nitrate removal

under aerobic conditions is higher in *las* and *rhl* mutants, and that the addition of an acylase to the wild type also results in the $\Delta lasI$ and $\Delta rhlI$ phenotypes observed by Toyofuku *et al.* (Zhu *et al.*, 2020; Cui *et al.*, 2021).

In this section, I measured the promoter activity of genes involved in the production of quorum sensing molecules (using luminescent biosensor strains) to identify if any potential major changes in OdDHL, BHL, or PQS production could be observed in mutants defective in denitrification. I hypothesised that in mutants defective in denitrification, I would observe lower BHL and PQS levels compared with the wild type, since there would be a lower level of denitrification gene expression and thus a lower QS-mediated inhibition. However, in a $\Delta norB$ mutant I anticipated that an accumulation of nitric oxide may lead to increased QS-mediated repression of denitrification (namely through PQS), to preclude further generation of nitric oxide. I also hypothesised that during growth with other microbial species (in this project, *C. albicans* and *S. aureus*), there may be an increase in quorum sensing activity, for example to increase virulence factor production, in order to remain competitive.

All quorum sensing molecule analysis in this section was made using the raw luminescence values due to an issue with generating reliable standard curves from our synthetic quorum sensing molecules, which at times return concentrations of less than zero at points in growth where it is known that quorum sensing molecules should be quantifiable. Samples analysed on different plates were not compared due to plate-to-plate variation. This subsection will primarily focus on PQS. Gene expression was also measured for OdDHL and BHL synthesis, and the data from these experiments is included in Appendix B.

8.1.2 Batch culture (MOPS acetate \pm nitrate)

P. aeruginosa and respiration mutants were cultured axenically for 24 hours in MOPS with 40 mM acetate with and without 20 mM nitrate (Figure 31). The Δanr ($p = 0.0047$) and Δdnr ($p = 0.0008$) mutants both consistently produced significantly less PQS compared with the wild type. In the presence of nitrate, only the $\Delta norB$ ($p = 0.0355$) mutant was significantly different compared with the wild type, producing significantly more PQS during the first 8 hours.

In general, the Δanr and Δdnr data support the hypothesis that less expression of denitrification genes results in less PQS production. Additionally, the $\Delta norB$ data also suggests that PQS might be used to inhibit denitrification genes in order to prevent an accumulation of nitric oxide. For better visualisation, values were then adjusted to reflect a percentage of PQS production relative to the wild type, which was set at a value of 100. To preserve the error in wild-type data, statistical comparisons were made using the raw data, not the percentage adjusted values.

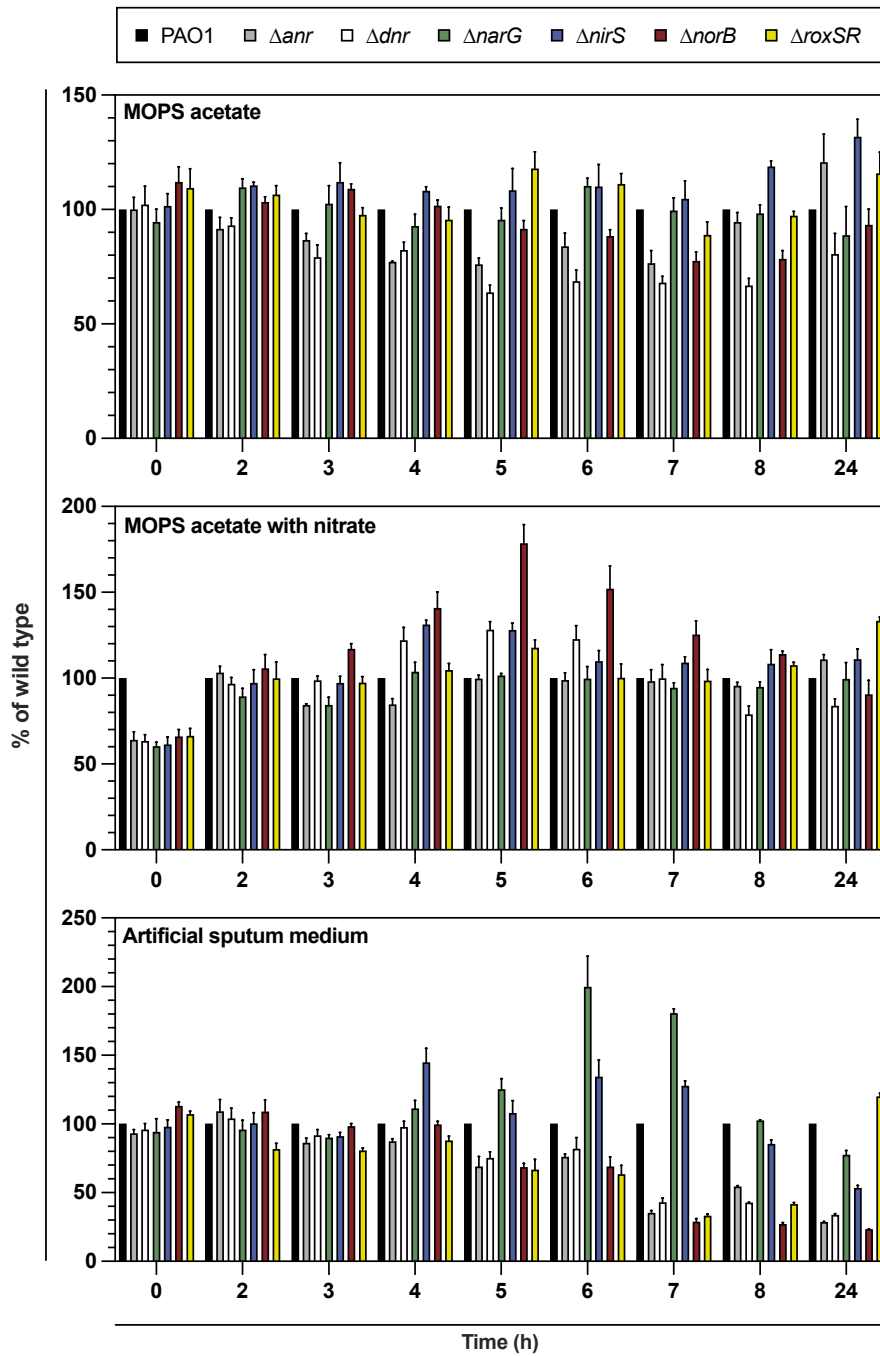


FIGURE 31. *P. aeruginosa* wild type and denitrification mutant PQS promoter activity when cultured in a range of media. TOP MOPS with 40 mM acetate. MIDDLE MOPS with 40 mM acetate and 20 mM KNO_3 . BOTTOM Artificial sputum medium. Mean and standard deviation of at least three biological replicates.

8.1.3 Batch culture (artificial sputum medium)

During growth in artificial sputum medium over 24 hours, with hourly sampling for the first 8 hours, there were no statistically significant differences observed during the first 8 hours (Figure 31). However, there was a general trend of the Δanr , Δdnr , and $\Delta norB$ mutants producing less PQS compared with the wild type over this time period, and the $\Delta narG$ and $\Delta nirS$ mutants producing more PQS.

By 24 hours every denitrification mutant produced significantly less PQS compared with the wild type. Interestingly, the $\Delta roxSR$ ($p = 0.0011$) mutant produced significantly more PQS, perhaps to stimulate increased pyocyanin production in order to counteract reduced terminal oxidase expression and the subsequent potential redox imbalance associated with impaired respiration. It is not clear why the $\Delta narG$ and $\Delta nirS$ mutants appear to produce more PQS compared with the wild type, but the remainder of the data does support the hypothesis that lower denitrification gene expression results in lower PQS production.

A smaller pool of mutants (Δanr , Δdnr , $\Delta narG$, $\Delta roxSR$) were then selected for growth in longer single- and triple-species-species experiments. In single-species experiments, compared with the wild type under the same conditions, the Δanr ($p = 0.0095$) and Δdnr ($p = 0.0124$) mutants both produced significantly less PQS and the $\Delta roxSR$ ($p = 0.0324$) mutant produced significantly more. In the triple-species experiments, only the $\Delta roxSR$ mutant was significantly different to the wild type, producing significantly more PQS ($p = 0.0008$). When comparing the single- and triple-species-species experiments to each other, the wild type and $\Delta narG$ mutant both produced significantly lower levels of PQS in triple species-format, and the Δanr and $\Delta roxSR$ mutants produced more (Figure 32).

8.1.4 Continuous-flow system culture (artificial sputum medium)

Using the continuous-flow system, *P. aeruginosa* (and *C. albicans* and *S. aureus*) were cultured over 96 hours. Samples were taken in both single- and triple-species-species experiments every 24 hours. In single-species experiments, the Δanr ($p = 0.0278$), Δdnr ($p = 0.0416$), and $\Delta roxSR$ ($p = 0.0347$) mutants all produced less PQS than the wild type. In triple-species experiments there were no significant differences. Comparing the single- and triple-species-species experiments showed that generally the wild type and mutants produced PQS in a similar pattern to that observed in the batch culture experiments, with the wild type and $\Delta narG$ mutants producing less PQS in triple-species format, and the Δanr and $\Delta roxSR$ mutants producing more PQS in triple-species format (Figure 33).

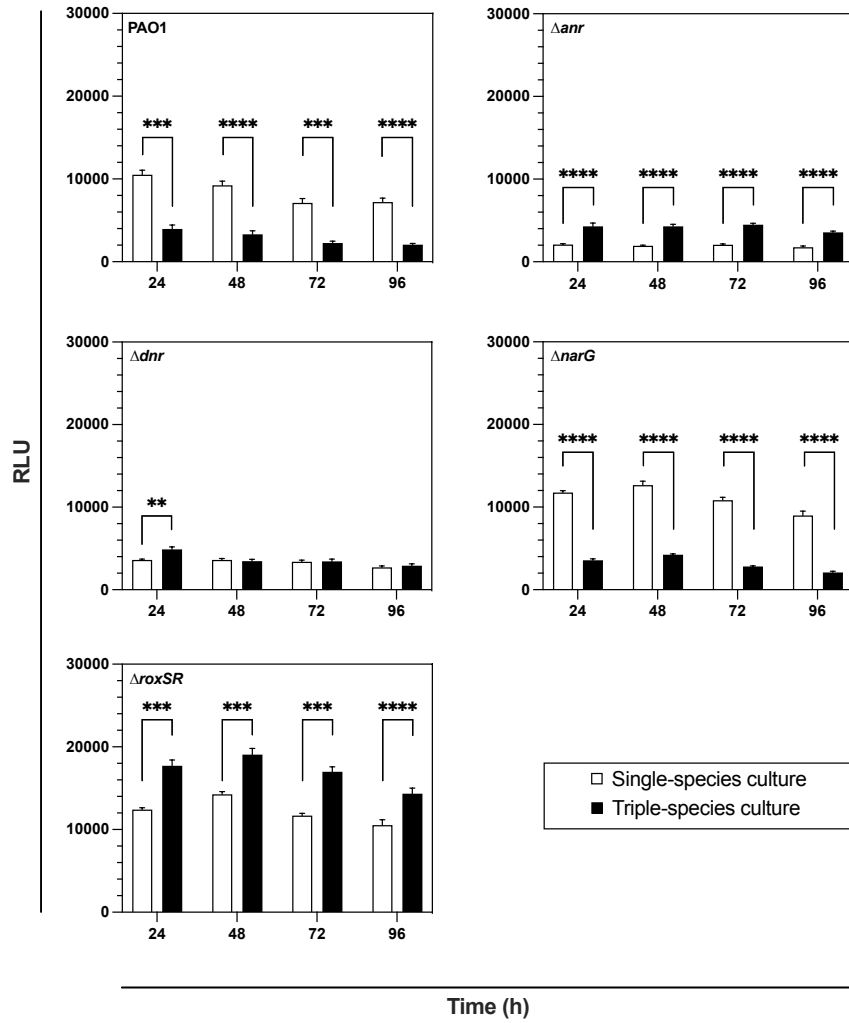


FIGURE 32. Comparison of single- and triple-species PQS promoter activity when cultured in artificial sputum medium batch culture. Mean and standard deviation of at least three biological replicates.

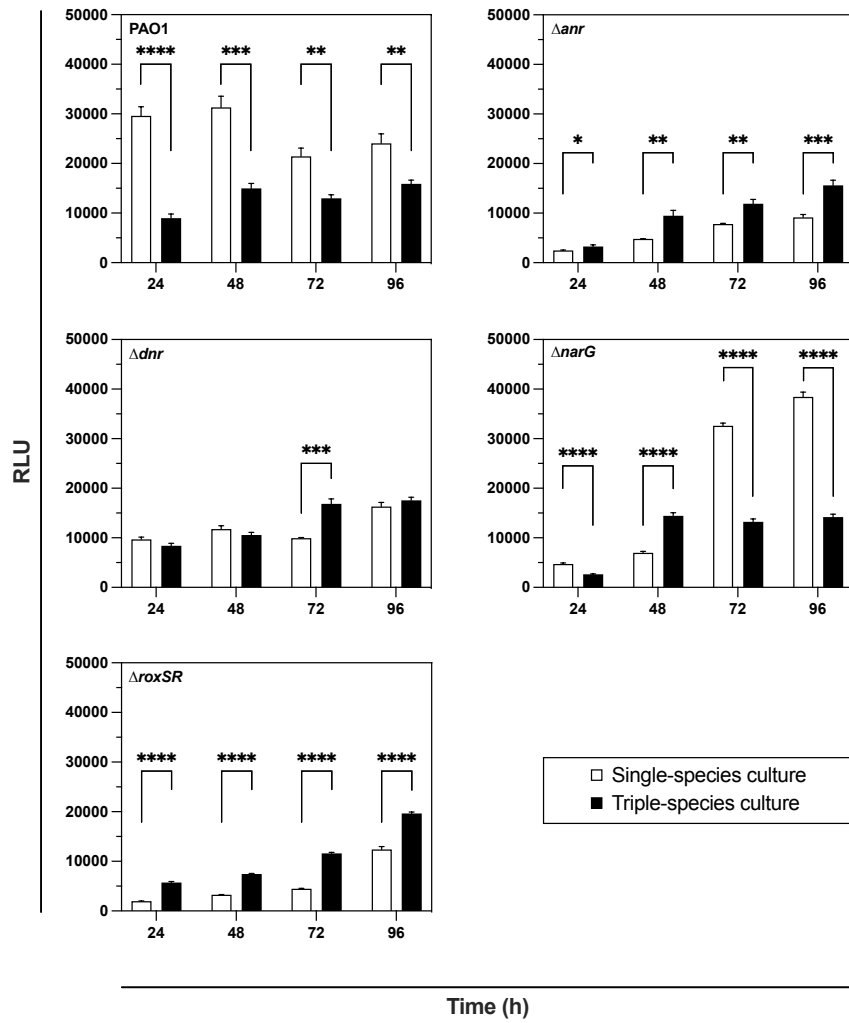


FIGURE 33. Comparison of single- and triple-species PQS promoter activity when cultured in artificial sputum medium continuous-flow culture. Mean and standard deviation of at least three biological replicates.

8.1.5 Discussion

The results in this section highlight the need for accurate, reproducible assays. Unfortunately, for many of the experiments presented here there was a large standard deviation in the results. This, coupled with a lack of reliable synthetic molecules (possibly due to degradation) to use as a reference curve, made it difficult to determine true effects of denitrification gene deletions as no absolute concentrations could be calculated. The inability to quantify quorum sensing molecule concentrations also made it difficult to compare two key media relevant to denitrification activity in *P. aeruginosa*, MOPS with 40 mM acetate and MOPS with 40 mM acetate and 20 mM nitrate, as their measurements were made using different 96-well plates and were therefore subject to plate-to-plate variation. However, broad comparisons can still be made and discussed in the wider context of biological respiration and its link to *P. aeruginosa* respiration.

Though the *las* and *rhl* systems have been thoroughly demonstrated to be involved in anaerobic and aerobic denitrification, because they transcriptionally repress the expression of denitrification enzymes (Toyofuku *et al.*, 2007; Cui *et al.*, 2021), it was perhaps ambitious to be able to draw conclusions about these systems in the inverse situation, i.e. the absence of denitrification enzymes. However, a lower level of BHL was observed in the Δdnr and $\Delta norB$ mutants compared with the wild type during growth on MOPS with 40 mM acetate and 20 mM nitrate (Appendix B, Figure B4), presumably to de-repress transcription of denitrification genes in these mutants, since the Δdnr mutant would have an impaired respiratory chain, and the $\Delta norB$ mutant would accumulate nitric oxide and further impair its respiratory chain.

It has been previously shown that PQS overproduction also inhibits denitrification—specifically the activities of nitrate reductase, nitrite reductase, and nitric oxide reductase—by chelating iron, which is an essential metal at the catalytic centre of these enzymes (Toyofuku *et al.*, 2008; Zhu *et al.*, 2020). Additionally, a raft of work centred on the myriad functionalities of PQS highlighted its role in iron trapping and concomitant induction of siderophore expression (Diggle *et al.*, 2007; J. Lin *et al.*, 2018). It is not difficult to imagine a finely tuned balance of entities—quorum sensing molecules (for example, PQS), iron availability, siderophores, and a suitable electron acceptor—would determine denitrification activity in a concerted manner, or vice-versa. Therefore, it was hypothesised that a lack of one of these entities may induce observable changes in the expression of the remainder.

In this section it has been shown that respiration mutants exhibited different PQS levels compared with the wild type when grown in a range of media (MOPS with 40 mM acetate, MOPS with 40 mM acetate and 20 mM nitrate, and artificial sputum medium) with the following general pattern: PQS levels are lower in denitrification mutants that may accumulate nitric oxide compared with the wild type (once again highlighting this intermediate as a potential regulatory

node point), but in contrast PQS is higher than the wild type in a $\Delta roxSR$ mutant, which may be more reliant on denitrification as a form of respiration. Thus, it can be inferred that PQS (and BHL) readily balances the expression of denitrification enzymes in response to nitric oxide levels. However, this is a broad generalisation, and we must also remember the inhibitory function of nitric oxide on denitrification enzymes.

Based on previously published findings using the continuous-flow system in single- and triple-species formats, it would be assumed that quorum sensing molecule accumulation would be lower in a continuous-flow model compared with batch culture (O'Brien and Welch, 2019), given the continuous replacement of artificial sputum medium in the continuous-flow system. Additionally, a general trend of lower quorum sensing molecule concentration was observed in triple-species cultures compared with single species cultures, except for PQS levels in Δanr and $\Delta roxSR$ mutants, which displayed the opposite. If, as previously posited in this dissertation, RoxSR acts as a repressor of denitrification, it may be rational to expect increases in PQS levels in a $\Delta roxSR$ mutant to modulate increased denitrification gene expression.

It was hoped that the work in this section would support and expand on the comprehensive quorum sensing measurements carried out previously determined in the Welch laboratory, however further work will be needed to truly complement the existing literature (O'Brien and Welch, 2019).

8.2 Siderophore production

8.2.1 Background and rationale

In this section, I quantified supernatant siderophore concentration throughout growth, both in minimal medium and artificial sputum medium, to assess *P. aeruginosa*'s demand for iron, which should be especially pronounced when there is a strong need for maintaining the appropriate intracellular redox balance (i.e. when growing rapidly on acetate) or when grown in competition with *C. albicans* and *S. aureus*. I expected that siderophore concentration may increase in conditions that promote increased denitrification gene expression, since denitrification enzymes require iron for their catalytic function. Siderophore production by *P. aeruginosa* has also been shown to increase during growth on a synthetic cystic fibrosis sputum medium, and siderophore production is also an important aspect of community function, either as a cooperative, competitive, or cheating tactic employed by polymicrobial communities (Hare *et al.*, 2012; Cornelis and Dingemans, 2013; Kramer, Özkaya and Kümmerli, 2020). Therefore, I also expected to see elevated siderophore levels during growth in triple-species cultures compared with single species cultures.

Iron is an essential metal in all organisms, often found in catalytic centres of enzymes. Iron is used most by biological organisms in two oxidation states, Fe^{2+} and Fe^{3+} , with the former most common in anaerobic environments, and the latter in aerobic environments. This positioning of the oxidation state of iron makes it perfectly suited for oxido-reduction reactions. However, Fe^{3+} has low solubility in oxygenated environments, presenting availability issues for this vital element (Andrews, Robinson and Rodríguez-Quiñones, 2003).

Pseudomonas, like many organisms, has evolved its own iron acquisition strategies, involving both extracellular reduction of Fe^{3+} to Fe^{2+} to improve solubility (for example by phenazines and the Feo system), or siderophore-mediated Fe^{3+} uptake (Andrews, Robinson and Rodríguez-Quiñones, 2003; Cornelis, 2010). *Pseudomonas* produces two iron-chelating siderophores, pyoverdine (high affinity) and pyochelin (low affinity), which bind specifically to Fe^{3+} and are then imported to the cell by the cytoplasmic membrane protein TonB (Cornelis and Dingemans, 2013). The affinity of pyoverdine is strong enough to remove iron from transferrin, a vertebrate blood-plasma glycoprotein used for iron transport, and alongside TonB has been demonstrated to be essential for infection in a mouse model (Takase *et al.*, 2000). In contrast, pyochelin has a low affinity for iron and is typically produced before environmental iron is critically low, at which point *P. aeruginosa* switches to pyoverdine production, providing another example of the fine balancing of complementary systems in *P. aeruginosa* (Dumas, Ross-Gillespie and Kümmerli, 2013). However, the pyochelin-iron complex has been demonstrated to be active in redox cycling and, in conjunction with the presence of pyocyanin, generates hydroxyl radicals that damage the lung epithelium, so whilst its utility in iron acquisition may be limited, its relevance in infections is pronounced (Coffman *et al.*, 1990; Britigan *et al.*, 1992; Lyczak, Cannon and Pier, 2002).

S. aureus also produces two iron-chelating siderophores, appropriately named staphyloferrin A and staphyloferrin B (Skaar and Hammer, 2011). *C. albicans* does not produce its own siderophores, but has cunningly evolved strategies to acquire iron through the uptake of iron-bound siderophores produced by other species through its Sti1/Arn1 transporter complex (Ardon *et al.*, 2001; Heymann *et al.*, 2002; Haas, 2003).

8.2.2 Batch culture (MOPS acetate \pm nitrate)

P. aeruginosa wild type and respiration mutants were cultured in MOPS with 40 mM acetate with and without 20 mM nitrate for 24 hours, with hourly extraction and quantification of siderophores during the first 2-8 hours of growth (Figure 34). Growth in MOPS with 40 mM acetate showed no statistical differences in siderophore production between any of the mutants and the wild type. However, when grown in MOPS with 40 mM acetate and 20 mM nitrate added, the Δdnr mutant produced significantly lower siderophore concentration than the wild type dur-

ing the first 8 hours of the measured duration ($p = 0.0058$). Interestingly, the $\Delta norB$ mutant's siderophore production was not significantly different compared with the wild type. This was unexpected, since of all the mutants investigated thus far, the $\Delta norB$ mutant appears to have the lowest denitrification activity, behaving similarly to the Δdnr mutant.

8.2.3 Batch culture (artificial sputum medium)

P. aeruginosa wild type and respiration mutants were also cultured in artificial sputum medium in single- and triple-species aerobic batch cultures. First, the wild type and all respiration mutants used in this study were cultured axenically for 24 hours (Figure 34). There were no significant differences in siderophore production between the wild type and any of the mutants tested.

The *P. aeruginosa* wild type and a smaller pool of mutants were also cultured axenically and in triple-species batch format for 96 hours, with samples removed for quantification every 24 hours (Figure 35). This allowed for a direct comparison with the same experiments performed in the continuous-flow system. Surprisingly, when cultured in artificial sputum medium, the concentration of siderophores produced increased approximately two-fold compared with the minimal media (Figure 34), despite their growth rates being similar (Section 4.2 and 4.3).

When cultured axenically, both the Δanr and $\Delta roxSR$ mutants were significantly different to the wild type ($p = 0.0004$ and $p = 0.0003$, respectively), with both mutants producing a lower concentration of siderophores. In contrast, when cultured in triple-species format none of the mutants showed any significant differences compared with the wild type throughout the duration of the experiment. In the triple-species cultures, there was a general trend of lower siderophore production. Comparing the single- and triple-species batch cultures revealed that the *P. aeruginosa* wild type and $\Delta narG$ mutant triple-species cultures both produced a significantly lower siderophore concentration than their related single species cultures across all time points (both $p < 0.001$).

8.2.4 Continuous-flow system culture (artificial sputum medium)

The same comparisons as in Section 8.2.3 were made using data obtained from samples taken from continuous-flow system cultures (Figure 36). The single- and triple-species culture siderophore concentration was not significantly different to each other. Only the $\Delta narG$ mutant was significantly different to the wild type (single species culture $p = 0.0419$, triple-species culture $p = 0.0236$). The differences observed between the wild type and $\Delta narG$ mutant cultures may be attributable to the lack of data with which to make statistical analyses. In all time points, except the 96-hour time point, the siderophore concentration was below the detection limit in either the single species culture, triple-species culture, or both.

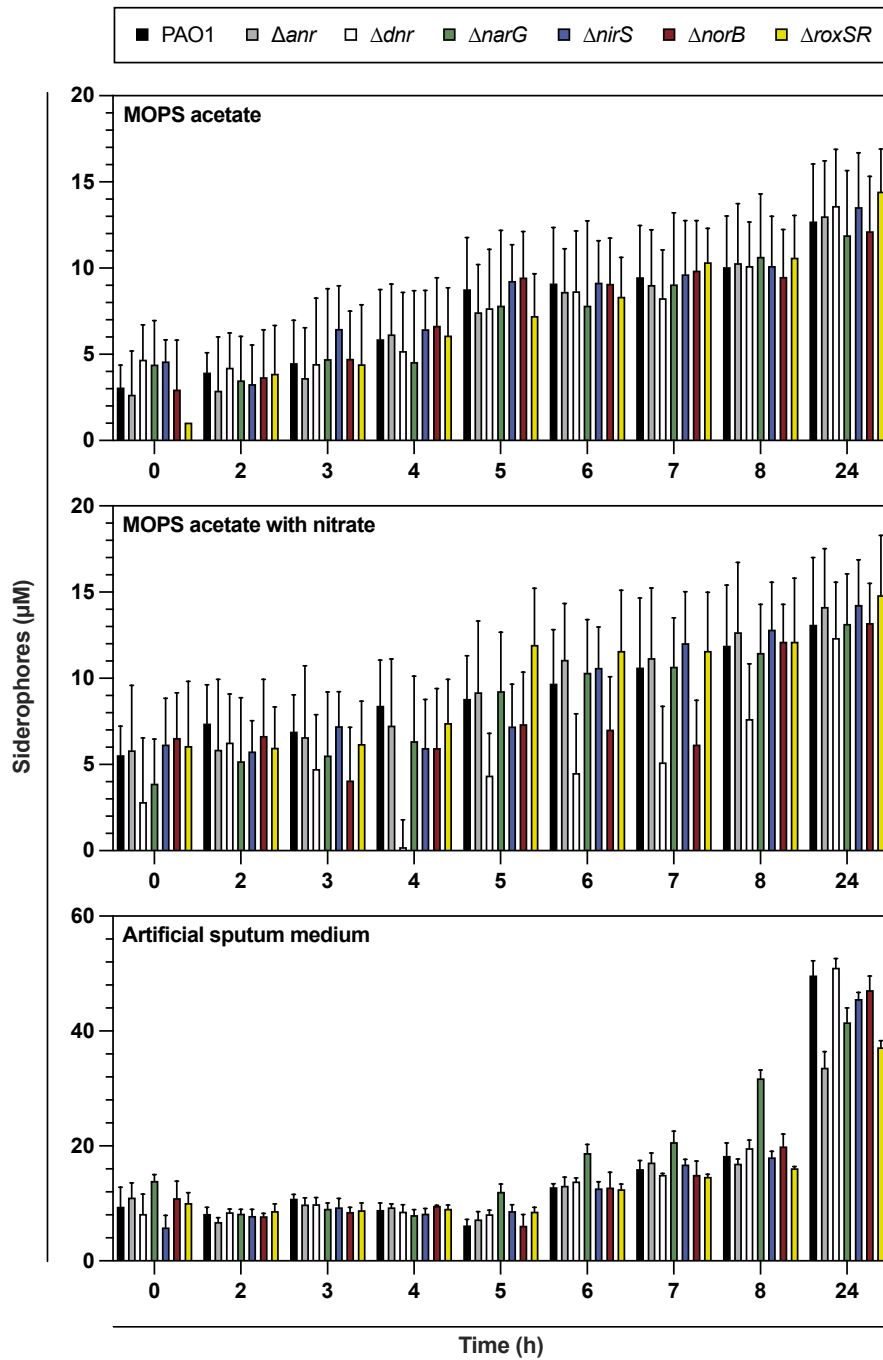


FIGURE 34. *P. aeruginosa* wild type and denitrification mutant PQS promoter activity when cultured in a range of media. TOP MOPS with 40 mM acetate. MIDDLE MOPS with 40 mM acetate and 20 mM KNO_3 . BOTTOM Artificial sputum medium. Mean and standard deviation of at least three biological replicates.

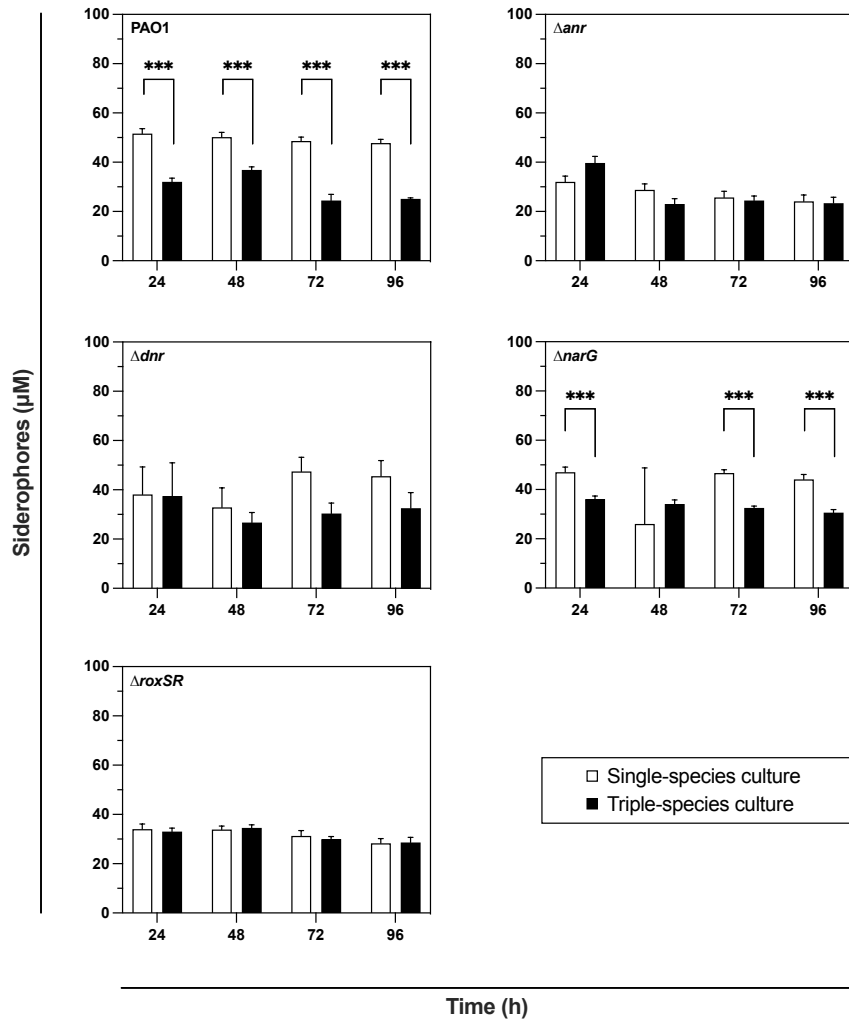


FIGURE 35. Comparison of single- and triple-species siderophore production when cultured in artificial sputum medium batch culture. Mean and standard deviation of at least three biological replicates.

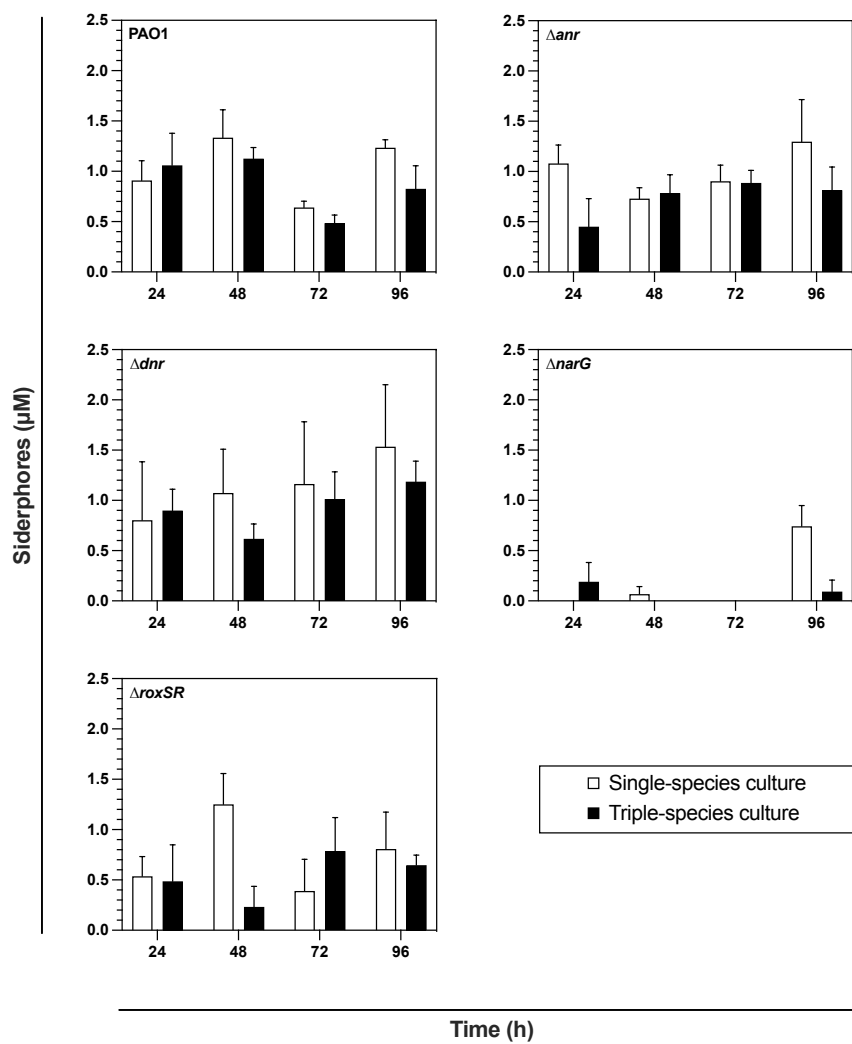


FIGURE 36. Comparison of single- and triple-species siderophore production when cultured in artificial sputum medium continuous-flow culture. Mean and standard deviation of at least three biological replicates.

8.2.5 Discussion

In the 0-to-24-hour batch culture experiments, as expected, a gradual increase in siderophore concentration was observed. In the context of growth this is logical, as one would expect to not only see an increase in siderophores proportional to cell density, but iron availability would decrease as competition for resources increases. It was hypothesised that some mutants may show decreased siderophore production, namely the Δdnr , $\Delta narG$, and $\Delta norB$ mutants. If Δdnr is not able to effectively express denitrification enzymes, for example $\Delta narG$ or $\Delta nirS$, then nitric oxide production would be curtailed. This in turn, may decrease production of siderophores, since there would be less demand for iron at the catalytic centres of these enzymes, and the iron-binding activity of nitric oxide would be negligible since there would be no active production of nitric oxide by NirS. This hypothesis proved somewhat true in the single species batch culture experiments, although could not be fully supported statistically.

When grown in MOPS with 40 mM acetate, there were no significant differences between the wild type and any of the mutants, however, when MOPS with 40 mM acetate and 20 mM nitrate was used as the culture medium, the Δdnr mutant produced significantly lower concentrations of siderophores compared with the wild type. If, based on the data previously presented in this dissertation, we are to proclaim Dnr as the single most important regulator of aerobic denitrification, then this result is supportive of the idea that low denitrification activity equals low iron-acquisition activity, and thus may be clinically relevant in the context of inflammation. It has previously been shown that interplay between iron availability and nitric oxide influences biofilm formation via Psl, though the authors state they do not yet know the exact mechanism (Zhu, Rice and Barraud, 2019). The same study also found that exogenously added nitric oxide inhibited the expression of siderophore production and other iron acquisition-related genes. It has also previously been reported that a lack of nitric oxide reductase activity increases iron scavenging activity, perhaps in an attempt to sequester iron from the denitrification enzymes with an ultimate goal of decreasing nitric oxide production (Yoon *et al.*, 2007; Borrero-de Acuña *et al.*, 2016). With the roles of nitric oxide and iron scavenging in mind, it was hoped that the $\Delta nirS$ and $\Delta norB$ mutants may have distinct and contrasting phenotypes; disappointingly however, these mutants did not show any significant differences compared with the wild type. There was also no significant difference between the wild type and any of the mutants when comparing growth in MOPS with 40 mM acetate compared with MOPS with 40 mM acetate and 20 mM nitrate. It must be noted that the standard deviation in these data was large, therefore any possible differences could potentially be obscured by error.

In the artificial sputum medium batch cultures (0–24-hour experiments), there were no statistically defined differences in siderophore production between any of the mutants and the wild

type. However, in the 0-96-hour single species artificial sputum medium experiments, both the Δanr and $\Delta roxSR$ mutants produced significantly lower siderophore concentrations than the wild type. Furthermore, we do not know the transcriptomic profile of *P. aeruginosa* wild type, Δanr , and Δdnr mutants when cultured under our specific aerobic conditions in artificial sputum medium, so we are therefore unable to fully comment on the induction of denitrification gene expression. The 0-96-hour single species experimental results thus may be explained in very simple terms: no Anr or RoxSR activity decreases expression of iron-containing reductases/oxidases, and subsequently iron acquisition is not as pertinent.

In the 0-96-hour triple-species experiments, there was no statistical difference in siderophore production between the wild type and any of the mutants, with all cultures containing approximately 25-30 μM siderophore concentration. Both the wild type and $\Delta narG$ mutant siderophore concentrations were significantly lower than in single-species experiments. The lower supernatant concentrations of siderophores in the triple-species experiments may be explained by the known activities of *C. albicans* iron acquisition through internalising siderophores produced by other species or by the siderophore mediated-acquisition of iron by *S. aureus* (Ardon *et al.*, 2001; Heymann *et al.*, 2002; Haas, 2003; Skaar and Hammer, 2011). Additionally, *P. aeruginosa* is known to acquire iron via active lysis of *S. aureus* and therefore down-regulates its own production of siderophores (Mashburn *et al.*, 2005). An additional consideration that must be noted is that in the triple-species batch culture experiments, *C. albicans* was quickly outcompeted and eliminated from the culture vessel and may act as an additional source of iron.

The supernatant siderophore concentration in the continuous-flow system cultures was 2-4% of the measured concentration in the batch culture experiments. This may be attributed to the constant supply of fresh medium, which theoretically provides unlimited iron and negates the need for high concentrations of siderophores, and the constant elimination of siderophores from the culture vessel during waste removal.

An important point to consider is that the concentrations determined were nearing the limit of sensitivity for the detection method used, evidenced by the larger relative standard deviation compared with batch culture experiments, thereby potentially muting any differences between the wild type and mutants. But perhaps most importantly is that under these conditions, all three species were maintained for the duration of the experiment, and so the constantly supply of fresh media coupled with the synergistic interactions between *P. aeruginosa*, *C. albicans*, and *S. aureus* may have defined an effective 'functional limit' to siderophore production.

8.3 Pyocyanin production

8.3.1 Background and rationale

P. aeruginosa produces four phenazines: pyocyanin, phenazine-1-carboxylic acid, phenazine-1-carboxamide, and 1-hydroxyphenazine. Pyocyanin, which is responsible for the blue colour of *P. aeruginosa* stationary-phase cultures, is the most abundant phenazine produced and has antimicrobial and redox-active properties (Kerr *et al.*, 1999; Mavrodi *et al.*, 2001; Price-Whelan, Dietrich and Newman, 2006, 2007; Das *et al.*, 2013; Raji El Feghali and Nawas, 2018). Pyocyanin's low molecular weight and zwitterionic state enable it to permeate cells with relative ease and cause widespread oxidative stress and inflammation in multiple organ systems during an infection, further reinforcing its relevance as an important virulence factor (Hall *et al.*, 2016).

I anticipated that, given the redox activity of pyocyanin and the apparent lack of denitrification in some of the mutants investigated so far, some of the denitrification mutants could possibly overproduce pyocyanin to mitigate the redox stresses attributed to increased NADH:NAD⁺ ratios (Price-Whelan, Dietrich and Newman, 2007). I also expected increased pyocyanin production during growth with other species, *C. albicans* and *S. aureus*, and that this would also be elevated in denitrification mutants in order to remain competitive as oxygen availability becomes limited (Wang, Kern and Newman, 2010).

8.3.2 Batch culture (artificial sputum medium)

When comparing pyocyanin production in single-species culture to triple-species culture (Figure 37), generally, *P. aeruginosa* wild type and mutants all produced more pyocyanin in triple-species culture. The wild type produced significantly more at every sample point in the 96-hour duration of the experiment (p values; 24h <0.0001, 48h <0.0001, 72h <0.0001, 96h <0.0001). The Δanr mutant only showed a significant difference at 24 hours (p = 0.0005). The Δdnr mutant was only significantly different at 72 and 96 hours (p = 0.0019 and p = 0.0053, respectively). Compared with the wild type, the $\Delta narG$ mutant produced significantly more pyocyanin at every sample point in the 96-hour duration of the experiment (p values; 24h <0.0001, 48h 0.0001, 72h <0.0001, 96h <0.0001). The $\Delta roxSR$ mutant was only significantly different at 96 hours (p = 0.0005), producing more pyocyanin in triple-species culture. In single species culture all mutants produced significantly less pyocyanin compared with the wild type across the time series (p values; Δanr 0.0049, Δdnr 0.0008, $\Delta narG$ 0.0080, $\Delta roxSR$ 0.0489). In triple-species culture, the Δanr , Δdnr , and $\Delta roxSR$ mutants all produced significantly less pyocyanin (p = 0.0002, p = 0.0002, and p = 0.116, respectively), whilst the $\Delta narG$ mutant produced significantly more (p = 0.0063).

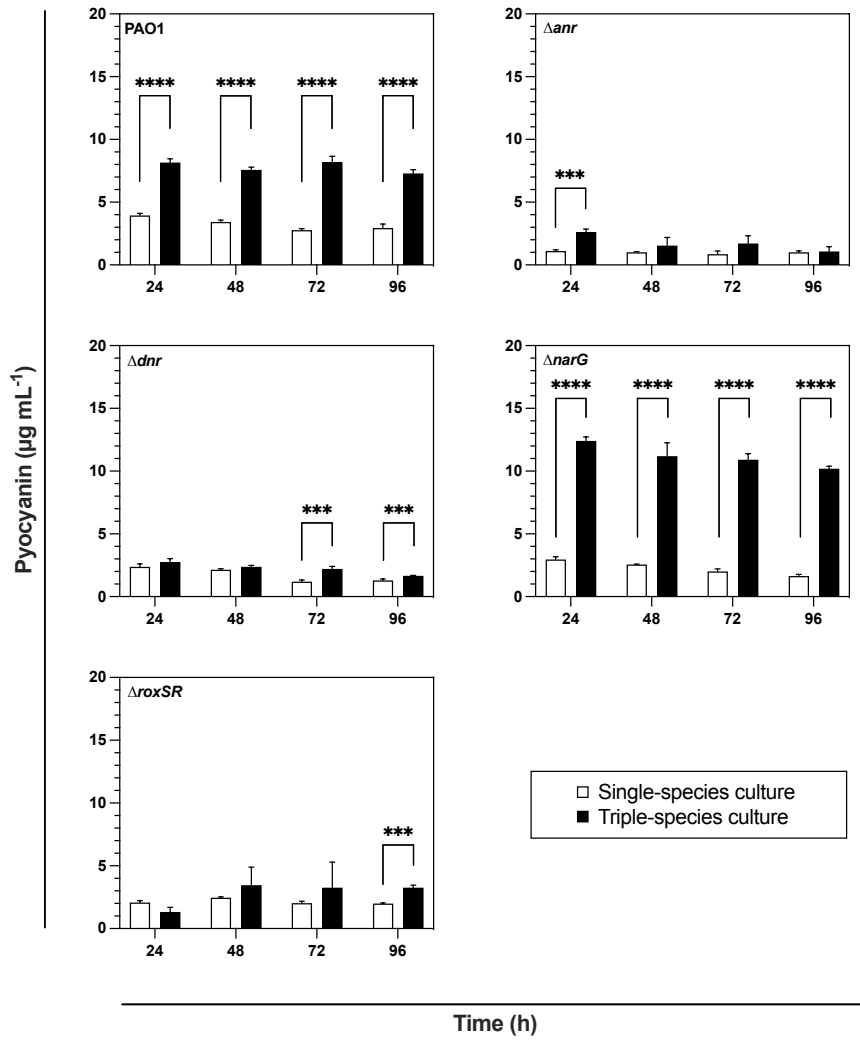


FIGURE 37. Comparison of single- and triple-species pyocyanin production by *P. aeruginosa* when cultured in artificial sputum medium batch culture. Mean and standard deviation of at least three biological replicates..

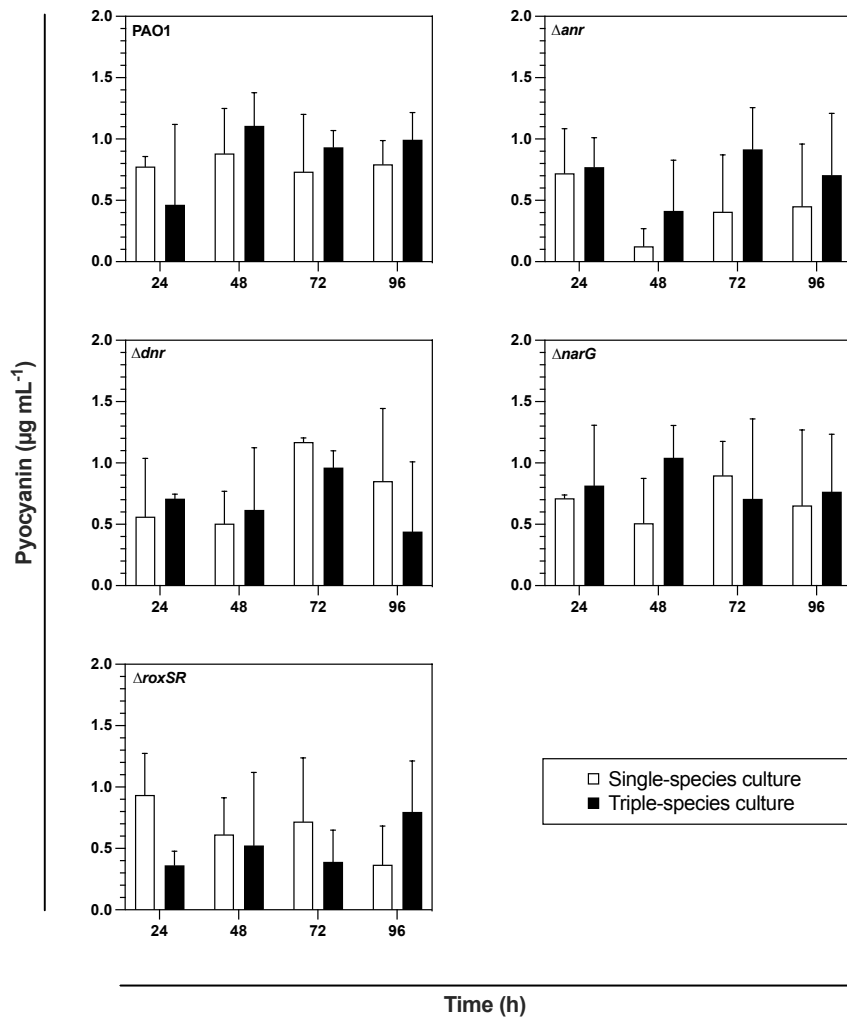


FIGURE 38. Comparison of single- and triple-species pyocyanin production by *P. aeruginosa* when cultured in artificial sputum medium continuous-flow culture. Mean and standard deviation of at least three biological replicates.

8.3.3 Continuous-flow system culture (artificial sputum medium)

Pyocyanin was also extracted from the continuous-flow system single- and triple-species cultures (Figure 38). In all comparisons there were no statistically significant differences in pyocyanin production, though there was a large amount of error in the calculated concentrations.

8.3.4 Discussion

During growth in MOPS with 40 mM acetate and 20 mM nitrate, *P. aeruginosa* wild type and mutants created from the parental strain did not produce a measurable amount of pyocyanin using the chloroform extraction method, despite these same strains producing very measurable quantities of pyocyanin in artificial sputum medium. This was unexpected given the reported pyocyanin production in the same base medium (Dietrich *et al.*, 2006), however in this publication *P. aeruginosa* PA14 and HPLC analyses were used and perhaps this can account for the difference in observations. Additionally, the end-point pH of *P. aeruginosa* cultures in MOPS with 40 mM acetate and 20 mM nitrate was 8.1, a considerable increase from the starting pH of 7.4. Over the same time period, artificial sputum medium increased from a starting pH of 6.7 to 7.7. Given that high pH can result in non-enzymatic degradation of lactone rings, it is possible that a decrease of *las/rhl* quorum sensing molecules—and thus downstream effects on the *pqs* system and *phz* expression production—might be a more appropriate explanation for the lack of detectable pyocyanin (Yates *et al.*, 2002; Frederix and Downie, 2011; Della Sala *et al.*, 2019). Furthermore, it has been shown that limiting oxygen and growth rate also increases pyocyanin production (Whooley and McLoughlin, 1982). In contrast to the conditions used by Whooley and McLoughlin, the culture conditions used in this section were highly aerobic and the *P. aeruginosa* growth rate was not limited, which you might when comparing a nutrient-poor medium (i.e. MOPS with 40 mM acetate and 20 mM nitrate) with a nutrient-rich medium (i.e. artificial sputum medium).

It has previously been reported that *S. aureus* increases pyocyanin production by *P. aeruginosa*, triggered by *N*-acetylglucosamine in the cell wall of *S. aureus* (Korgaonkar and Whiteley, 2011). Interestingly, *C. albicans* has been reported to both increase and decrease pyocyanin production through the secretion of farnesol. At low cell densities, a direct interaction between PqsR and farnesol inhibits expression of the *pqs* operon, thus decreasing pyocyanin production (Cugini *et al.*, 2007). Farnesol also promotes the generation of reactive oxygen species in fungi and bacteria (Machida *et al.*, 1998; Semighini *et al.*, 2006; Gomes *et al.*, 2009; Shirtliff *et al.*, 2009). It has also been reported that in $\Delta lasR$ mutants, increased pyocyanin production may be stimulated by farnesol through increased PQS and BHL production, subsequently inducing oxidative stress responses mediated through RhIR (Cugini, Morales and Hogan, 2010).

The stable concentration of pyocyanin in the batch culture conditions throughout the experimental duration was somewhat surprising, as it was predicted that as the cultures approached 96 hours of growth pyocyanin would accumulate. In contrast, it was observed that the concentrations remained remarkably constant. The same trend was also observed in triple-species cultures, although these cultures also typically had an increased concentration of pyocyanin. This was to be expected, given the increased competition between *P. aeruginosa*, *C. albicans*, and *S. aureus*. It must be noted that the triple species CFU enumeration indicated that *C. albicans* is rapidly eliminated from batch cultures, therefore, the effect of *C. albicans* may not be relevant when explaining the production of pyocyanin in these data.

Interestingly, there was a substantial difference in pyocyanin production between the Δdnr and $\Delta narG$ mutants, despite their similarities in previous experiments (for example, their growth rates and redox ratios). It was expected that their behaviour would be similar, though when considering that (in terms of nitrate-reducing capabilities) the loss of Dnr can be somewhat mitigated by Anr and NarXL, but the loss of NarG may only be relieved by NapA, perhaps it is not surprising that the loss of NarG is extremely pronounced. It has been previously reported that NapA-dependent nitrate reduction is coupled to phenazine oxidation, and both nitrate reduction and phenazine oxidation are mechanisms by which the intracellular NADH-NAD⁺ ratio can be decreased (Price-Whelan, Dietrich and Newman, 2007; Y.-C. Lin *et al.*, 2018; Dolan, Kohlstedt, *et al.*, 2020). Whilst NapA has also been shown to compensate for a loss of NarG in anaerobic survival (Van Alst *et al.*, 2009), I expect that the loss of NarG is too great for NapA to overcome, and pyocyanin production is up-regulated in an attempt to relieve redox stress under these conditions.

In the continuous-flow system cultures, a much lower concentration of pyocyanin was observed, and there were no significant differences between single- and triple-species cultures. This may be explained by three potential mechanisms. First, in the continuous-flow system there is a constant supply of fresh medium to the culture vessel and “waste medium” is removed from the culture vessel at the same rate. This may lead to “washout” of pyocyanin from the active culture. Second, the constant supply of fresh medium and the effective removal of cells from the culture vessel allows the cells to reach a steady state rate of growth, potentially at a point in growth where production of pyocyanin is not maximal. And third, the continuous-flow system flow rate is optimized to preserve populations of all three species, therefore *C. albicans* populations are better able to modulate pyocyanin production through its farnesol production. One caveat in the calculation of pyocyanin concentration extracted from the continuous-flow system is that the raw absorbance readings given by the spectrophotometer were very low, meaning that the values returned were more prone to variation due to the intrinsic measurement error of the machine, and the extraction procedure is not well suited to low concentrations of pyocyanin. This may explain

the large standard deviation in the collected data and may obscure some of the finer differences in pyocyanin production between the *P. aeruginosa* and mutants, and between the single- and triple-species cultures. The collection of data for all dual-species combinations may have enabled a more thorough analysis of the species-specific effects on pyocyanin production. However, the data presented here highlights the complex nature of polymicrobial interactions and generates many further avenues of investigation.

The concentrations of pyocyanin extracted from both batch and continuous-flow system cultures were comparable to and within the range of pyocyanin concentrations detected in the CF lung (Rada and Leto, 2013).

Biofilm formation

9.1 Background and rationale

Biofilms are often quoted as being the predominant reason for either ineffective clearance of an infection by the host immune system or poor treatment outcomes after chemotherapeutic intervention in a clinical setting. In medical literature, *P. aeruginosa* biofilms in the context of CF infection are the best described example of biofilm formation (Costerton, Stewart and Greenberg, 1999). However, single-species biofilms are rare in nature and the polymicrobial composition of biofilms and the interactions between the contained species are being recognised as increasingly important as our knowledge of polymicrobial communities expands.

Studies using a physiologically relevant medium (for example, synthetic cystic fibrosis medium, artificial sputum medium) with a specific focus on polymicrobial biofilms are limited, and to date only a handful of papers focus on the co-culture of *P. aeruginosa* and other CF biofilm-associated species in this context (Sriramulu *et al.*, 2005; Haley, Colmer-Hamood and Hamood, 2012; DeLeon *et al.*, 2014; Iglesias *et al.*, 2020; Kasetty *et al.*, 2021; O'Brien *et al.*, 2021), with the remainder predominantly focusing on either the evolution of *P. aeruginosa* in biofilms or the effects of therapeutics on the biofilm (Davies *et al.*, 2017; Grassi *et al.*, 2019; Kosztolowicz *et al.*, 2020; Maisetta *et al.*, 2020).

I predicted that denitrification mutants would be defective in biofilm formation, and that they could possibly be outcompeted by other species when grown in polymicrobial culture, based on previous work establishing the importance of denitrification in biofilm formation and morphology (Yoon *et al.*, 2002; Livingston *et al.*, 2022; Schwermer, Beer and Stoodley, 2022). The work in this section focuses on the biofilm dynamics of *P. aeruginosa* under a nutrient-limited batch culture condition, in single-species and in combination with either *C. albicans* or *S. aureus*, or both. To gain an overview of the biofilm properties, three techniques were used XTT assays, crystal violet staining, and CFU enumeration. The XTT assay aims to differentiate this data

into discrete groups: metabolically active cells, and dead cells/extracellular components. XTT is converted by respiring cells to an orange-coloured formazan product. However, the XTT assay does not discriminate between species. Crystal violet staining has historically been the archetypal tool for investigation of biofilms; however, it is limited in that it only gives information about all biological matter as one group, with no discrimination between cell or extracellular matter. Therefore, CFU enumeration using species-selective media was used to quantify the individual populations of the different species in the biofilm or planktonic fraction. Together, these three techniques afford a comprehensive overview of polymicrobial biofilm dynamics.

9.2 XTT assay

Metabolic activity was determined using the XTT assay. Briefly, normalised measurements were obtained by measuring absorbance of the XTT-solubilized biofilm mixture at 450 nm and subtracting a background measurement of medium-only controls. Biofilm metabolic activity measurements were made after 48 hours of incubation. For better visualisation, values were then adjusted to reflect a percentage of XTT reduction relative to the wild type, which was set at a value of 100. In order to preserve the error in wild-type data, statistical comparisons were made to the raw data, not the percentage adjusted values.

Comparing the wild-type performances of *P. aeruginosa*, *S. aureus*, and *C. albicans* in single-, dual-, and triple-species culture (Figure 39) showed that both *C. albicans* and *S. aureus* single-species biofilms have significantly higher metabolic activity than *P. aeruginosa* single-species biofilms ($p = 0.0067$ and $p = 0.0125$, respectively).

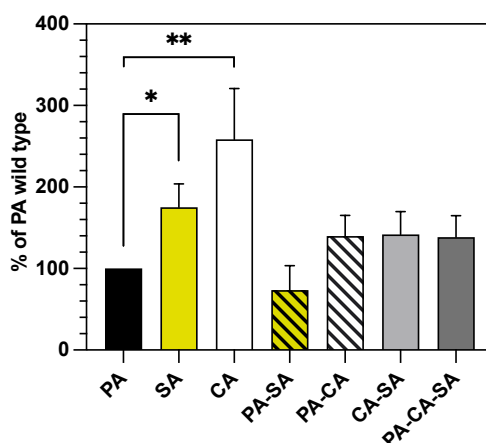


FIGURE 39. XTT assay of single-, dual-, and triple-species wild-type (PA = *P. aeruginosa*, SA = *S. aureus*, CA = *C. albicans*) biofilms in artificial sputum medium microtitre plate batch cultures. Mean and standard deviation of at least three biological replicates.

Next, mutants defective in denitrification were used to investigate if denitrification ability may impact on the metabolic activity of *P. aeruginosa* in both single species and polymicrobial biofilms (Figure 40). In the *P. aeruginosa* single species experiment, the $\Delta narG$ and $\Delta norB$ mutants both showed significantly higher metabolic activity compared with the *P. aeruginosa* wild type ($p = 0.0140$ and $p = 0.0355$, respectively). In the PA-SA dual-species culture, the Δanr and $\Delta roxSR$ mutants both showed a significant increase in metabolic activity compared with the *P. aeruginosa* wild type dual-species culture ($p = 0.0314$ and $p = 0.0260$, respectively). Comparison between the *P. aeruginosa* wild type dual-species culture and the PA-CA dual-species culture showed that the Δanr , Δdnr , and $\Delta norB$ mutants all exhibit significantly less metabolic activity ($p = 0.0068$, $p = 0.0188$ and $p = 0.0103$, respectively). In the triple-species culture, only the Δdnr and $\Delta narG$ mutants both showed a significant difference compared with the *P. aeruginosa* wild type, with significant decrease ($p = 0.0440$) and a significant increase ($p = 0.0029$) in metabolic activity, respectively.

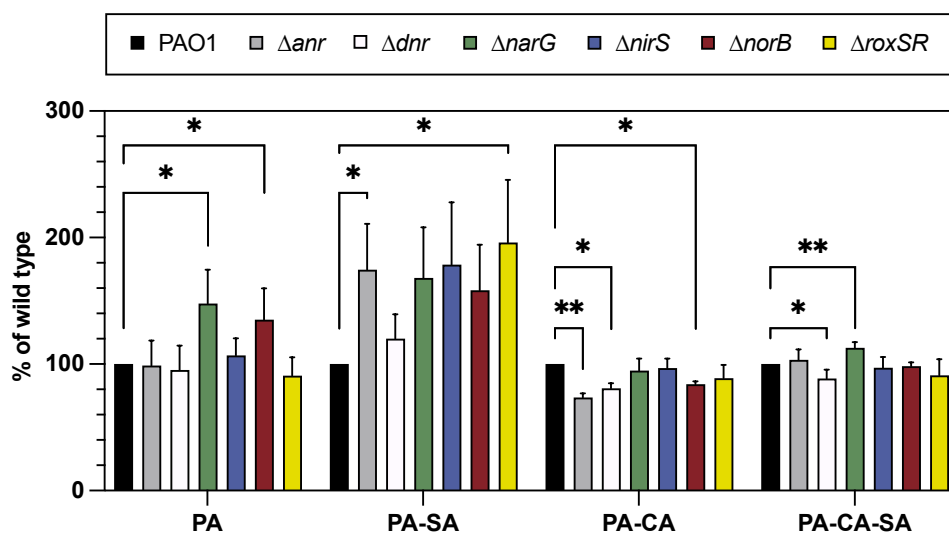


FIGURE 40. XTT assay of single-, dual-, and triple-species (PA = *P. aeruginosa*, SA = *S. aureus*, CA = *C. albicans*) biofilms in artificial sputum medium microtitre plate batch cultures. Mean and standard deviation of at least three biological replicates.

9.3 Crystal violet staining

Biofilm formation was also measured using the crystal violet staining technique. Briefly, normalised measurements were obtained by measuring absorbance of the crystal violet-stained biofilm at 570 nm and subtracting a background measurement of medium-only controls. Measurements were made after 48 hours of incubation. For better visualisation, values were then adjusted to

reflect a percentage of biofilm formation relative to the wild type, which was set at a value of 100. In order to preserve the error in wild-type data, statistical comparisons were made to the raw data, not the percentage adjusted values.

First, a comparisons were made between the wild-type performances of *P. aeruginosa*, *S. aureus*, and *C. albicans* in single-, dual-, and triple-species culture with *C. albicans* or *S. aureus* (Figure 41). Compared with *P. aeruginosa*, *S. aureus* formed significantly less biofilm ($p = 0.0170$), and *C. albicans* did not differ significantly in biofilm formation. The PA-SA dual-species culture formed significantly less biofilm than the *P. aeruginosa* grown in single-species culture ($p = 0.0079$). The CA-SA dual-species culture also formed significantly less biofilm than the *P. aeruginosa* grown in single-species culture ($p = 0.0054$).

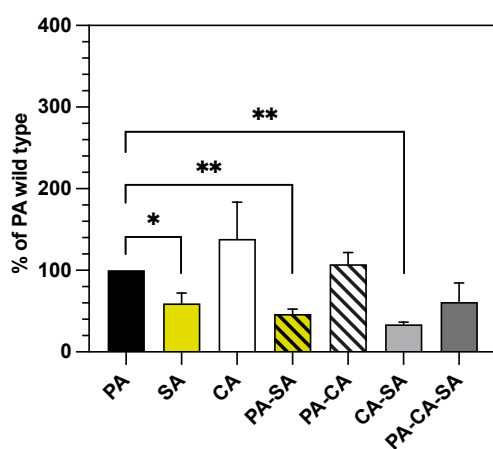


FIGURE 41. Crystal violet assay of single-, dual-, and triple-species wild-type (PA = *P. aeruginosa*, SA = *S. aureus*, CA = *C. albicans*) biofilms in artificial sputum medium microtitre plate batch cultures. Mean and standard deviation of at least three biological replicates.

To understand how denitrification may impact on the biofilm-forming ability of *P. aeruginosa*, mutants defective in denitrification were investigated using the crystal violet assay in single-, dual-, and triple-species combinations with *C. albicans* and *S. aureus* (Figure 42). In the *P. aeruginosa* single-species experiment, several mutants showed a significant difference in biofilm formation compared with the wild type. A significant decrease was observed in the Δanr ($p < 0.0001$), Δdnr ($p < 0.0001$), and $\Delta roxSR$ mutants ($p = 0.0005$). In the PA-SA dual-species experiment, only the $\Delta nirS$ mutant showed a significant difference to the *P. aeruginosa* wild type dual-species biofilm, with a 253% increase in biofilm formation ($p = 0.0111$). Comparing the *P. aeruginosa* wild type dual-species biofilm with the mutant PA-CA dual-species experiments, a significant decrease in biofilm formation was observed in the Δanr ($p = 0.0073$), Δdnr ($p = 0.0020$), and $\Delta roxSR$ ($p = 0.0005$) mutants. In the triple species experiment, only the Δanr mutant showed a significant

difference to the *P. aeruginosa* wild type, with a significant decrease in biofilm formation ($p = 0.0225$).

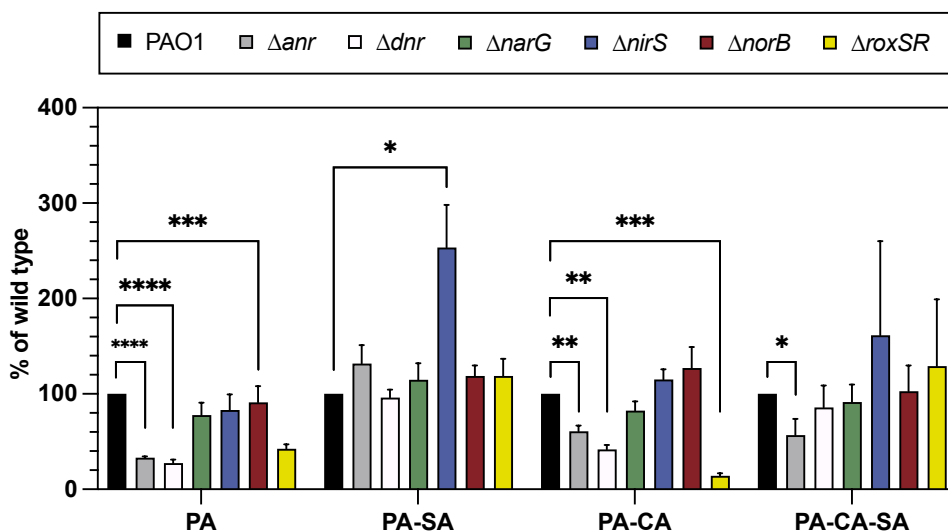


FIGURE 42. Crystal violet assay of single-, dual-, and triple-species (PA = *P. aeruginosa*, SA = *S. aureus*, CA = *C. albicans*) biofilms in artificial sputum medium microtitre plate batch cultures. Mean and standard deviation of at least three biological replicates.

9.4 CFU distribution: biofilm vs planktonic

Many studies centred on biofilm formation rely solely upon measuring the adhered cells, with little attention paid to the planktonic fraction. To gain a holistic view of biofilm dynamics in single-, dual-, and triple-species cultures, the number of CFUs were enumerated for both the biofilm and planktonic fractions of all combinations of *P. aeruginosa* (wild type and mutants), *C. albicans*, and *S. aureus* (Figure 43). One difficulty in enumerating biofilm CFUs is sufficiently breaking up the biofilm without damaging (and killing) cells, therefore the biofilm CFUs presented in this section may not be entirely representative of the biofilm composition.

In single-species cultures, all tested strains were able to form a biofilm and maintained a planktonic population. The CFU enumeration of *P. aeruginosa* Δanr , Δdnr and $\Delta roxSR$ mutants was lower than the wild type and other mutants, though there were no statistically significant differences between any pairing. The planktonic fractions were largely identical between all *P. aeruginosa* strains, though both *C. albicans* and *S. aureus* maintained a lower titre of cells in the planktonic fraction compared with the biofilm fraction.

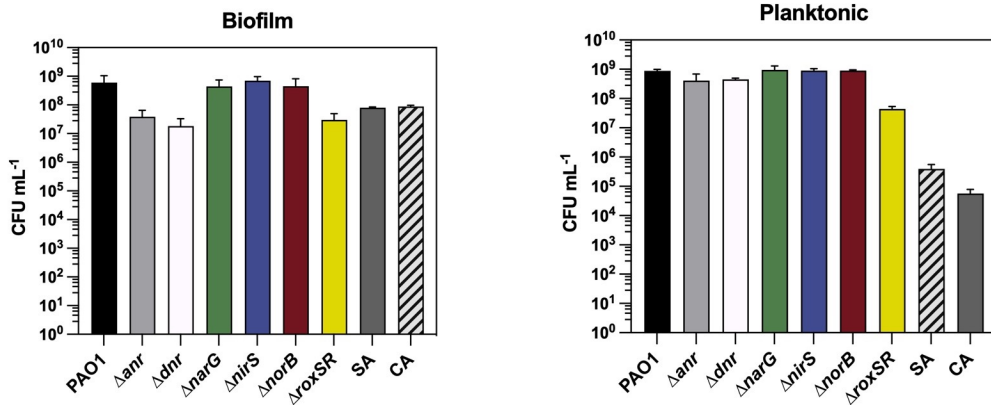


FIGURE 43. CFU enumeration of single-species (SA = *S. aureus*, CA = *C. albicans*) batch culture biofilm plates. Mean and standard deviation of at least three biological replicates.

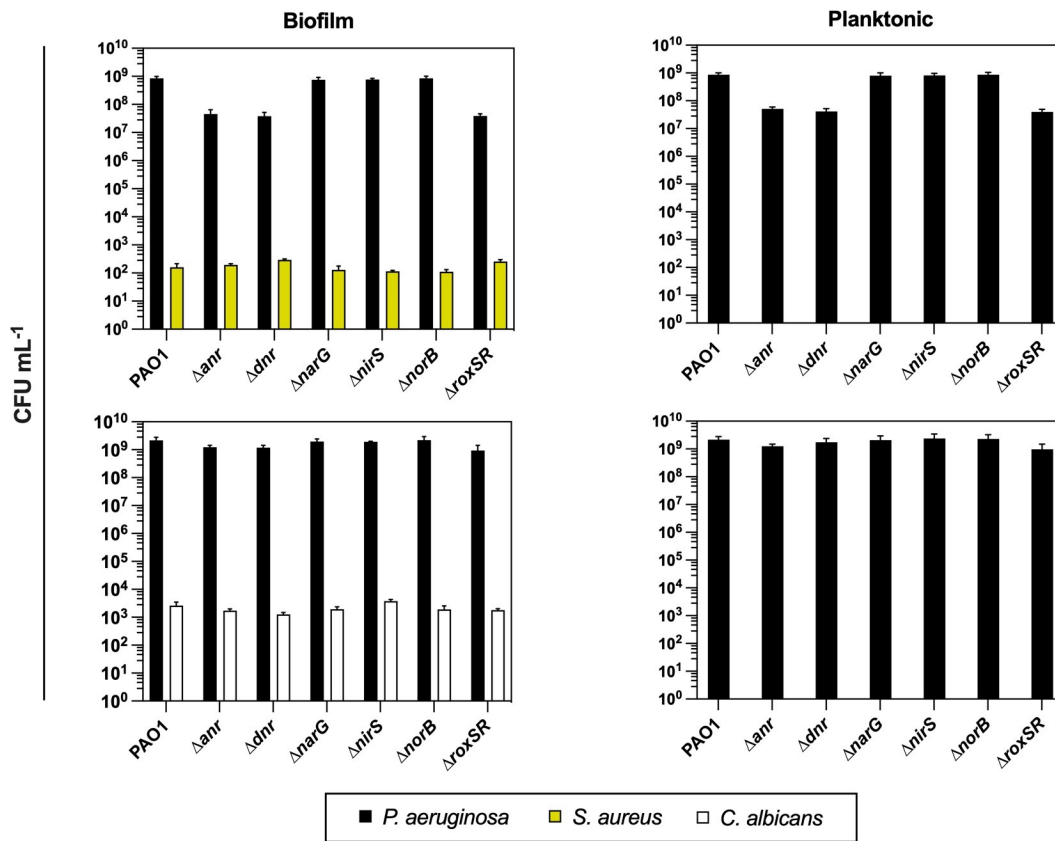


FIGURE 44. CFU enumeration of dual-species batch culture biofilm plates. Mean and standard deviation of at least three biological replicates.

In dual-species cultures, all tested *P. aeruginosa* strains were able to form a biofilm, though in every combination *C. albicans* or *S. aureus* was outcompeted in the planktonic fraction, with exception of the *C. albicans*—*S. aureus* dual-species culture (Figure 43). The general trend shows that *C. albicans* can maintain a higher titre of CFUs than *S. aureus* against *P. aeruginosa*, though in *C. albicans*—*S. aureus* dual-species culture the reverse is true, *S. aureus* dominates the interaction. Again, the *P. aeruginosa* Δanr , Δdnr and $\Delta roxSR$ mutants all had lower CFUs in the biofilm fraction than the wild type and other mutants, but *C. albicans* or *S. aureus* populations remained near identical across all combinations.

In triple-species cultures, the differences between the *P. aeruginosa* wild type and its mutants were eliminated, and all species populations were maintained at a stable titre for all combinations tested, and, like the dual-species cultures, *C. albicans* and *S. aureus* were both eliminated from the planktonic population (Figure 45).

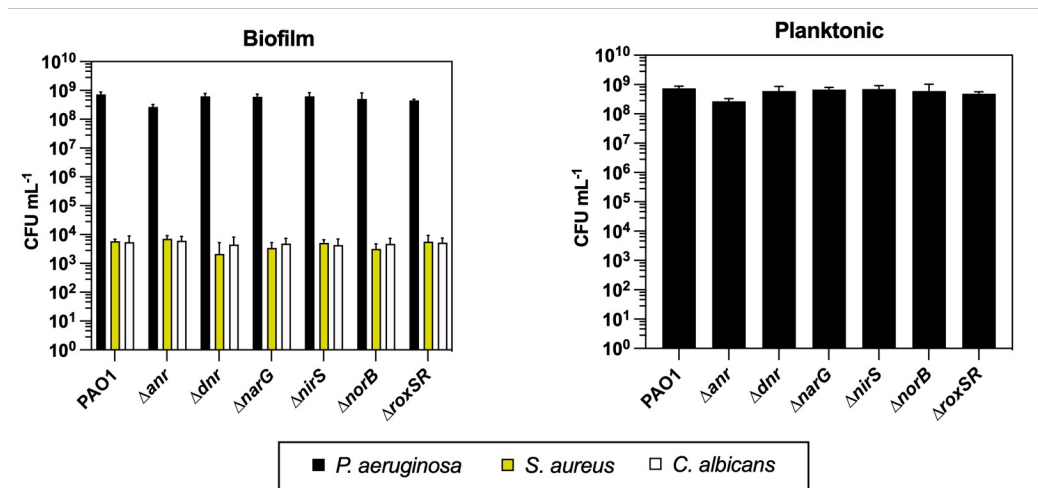


FIGURE 45. CFU enumeration of triple-species batch culture biofilm plates. Mean and standard deviation of at least three biological replicates.

9.5 Discussion

With reference to the crystal violet staining, when comparing wild types between the three species, *S. aureus* forms the least biofilm biomass, and *C. albicans* forms the most biofilm biomass. The dual-species biofilms had the least biomass in all instances involving *S. aureus*. In contrast, all dual-species biofilms involving *C. albicans* had the most biomass. Interestingly, though deficient in biomass, the *S. aureus* biofilms were among the most metabolically active relative to their biomass.

To tease apart the mechanics of the polymicrobial biofilm, the number of CFUs were enumerated for both the biofilm and planktonic fractions. These data revealed that, as expected, the respiration regulatory mutants (Δanr , Δdnr and $\Delta roxSR$) all were slightly biofilm deficient in single-species culture. Previous studies have shown that in the biofilm architecture there is a steep oxygen gradient, therefore the Δanr and Δdnr mutants would be expected to underperform in the depths of a biofilm. The RoxSR system has been linked to cell-density phenotypes in *P. putida* (Fernández-Piñar *et al.*, 2008). Anecdotally, I have observed that when grown on LB agar plates, the $\Delta roxSR$ mutant does not grow well and prefers to form distinct colonies rather than a more 'close-knit lawn', even at the initial inoculation point on the plate. Additionally, overnight cultures often yielded the lowest optical density compared with the other mutants tested, even in rich media. Interestingly, the total biomass, metabolic activity, and CFUs for dual and triple species biofilms were comparable to the single species biofilms. This is suggestive of a maximum carrying capacity for the given conditions and cooperative regulation between species to maximise utilisation of this. The presence of *C. albicans* appears to also support the maintenance of *S. aureus* in the triple species biofilm, as the titre of *S. aureus* increases in the triple species biofilm compared with the dual-species biofilms in combination with *P. aeruginosa*. The loss of both *C. albicans* and *S. aureus* from dual and triple species planktonic fractions suggests that it is due to the secretion of an extracellular factor by *P. aeruginosa*. However, this effect seems to largely be limited to the planktonic fraction, as no decrease in population titres was observed for the biofilm fraction when comparing dual and triple species biofilms. This can perhaps be attributed to the protection conferred by being part of a biofilm, where it may be harder for *P. aeruginosa* to outcompete these species.

These results may be explained by the very nature of biofilms; a dense population of cells suspended in a complex meshwork of extracellular DNA, polymeric substances, and other secreted particles. It is possible that the complex mesh-like component of a biofilm is acting as a net that can trap entities secreted by the three species, and this trapping is able to partially neuter their killing effect on competitors. Indeed, the diffusion coefficient of biofilms vs an aqueous solution is lower, supporting this hypothesis (Stewart, 2003). Whilst *P. aeruginosa* is the dominant organism in the triple and dual-species biofilms, it seems that there is some benefit conferred to *P. aeruginosa* by the presence of *C. albicans* and *S. aureus*, exemplified by the increase of *P. aeruginosa* titres of the Δanr , Δdnr , and $\Delta roxSR$ mutants. It seems that the negative effects of these mutations in single-species biofilm formation are mitigated by the presence of other species, suggesting community cooperativity, though the exact mechanism behind this remains to be elucidated. A more high-resolution investigation of the structure of the biofilm cross-section would aid in observing how different mutations alter the biofilm architecture, and localisation of species in the biofilm.

POLYMICROBIAL INTERACTIONS

Continuous-flow system population dynamics

10.1 Background and rationale

In this section[†], I hypothesised that a loss of *P. aeruginosa* denitrification in a polymicrobial culture may lead to behavioural changes in *P. aeruginosa* in order to remain ecologically competitive. I predicted that a loss of denitrification may negatively impact the fitness of *P. aeruginosa*. Therefore, I sought to enumerate the individual population numbers of three species (*P. aeruginosa*, *C. albicans*, and *S. aureus*) grown in a polymicrobial culture. To mimic a physiologically relevant environment, I used an *in vitro* continuous-flow system previously developed by Dr Thomas O'Brien, and maintained these three species in stable steady-state culture in artificial sputum medium (O'Brien and Welch, 2019). To determine the effect of defects in respiration on community composition, I also used *P. aeruginosa* Δanr , Δdnr , $\Delta narG$ and $\Delta roxSR$ mutants in single- and triple-species formats, representing the first time that defined mutants have been studied in this way. Sections 8.1.4, 8.2.4, and 8.3.3 contain the extracellular profile analyses of these steady state polymicrobial cultures.

The vast majority of microbiological research is conducted with axenically cultured species,

[†]The work in this section was conducted in collaboration with Dr Éva Bényei (preparation and maintenance of the continuous-flow system) and Pok-Man Ho (computational aspects).

with very few studies using co-culture systems. Furthermore, batch culture experiments have limited relevance when the research question is framed around an infection scenario, where resources may be renewed or depleted, or the microenvironment may vary dramatically with the flux of diverse species. The metabolic diversity of *P. aeruginosa* highlighted thus far is testament to the adaptability of *P. aeruginosa* to a range of conditions and with differing genetic backgrounds.

However, very little is known about how genetic—and therefore metabolic changes—in *P. aeruginosa* could affect species-species interactions and the consequential population dynamics. Historically, the Lotka-Volterra predator-prey model was developed by Alfred J. Lotka and Vito Volterra independently, who were studying autocatalytic chemical reactions and predatory fish populations, respectively. The model was later expanded to accommodate prey-density and how that pertains to growth and was famously applied to the study of *Lynx canadensis* and *Lepus americanus* populations based on the number of pelts collected (Lotka, 1925; Volterra, 1926; Gilpin, 1973). In this section, a Lotka-Volterra competition model used the experimentally-collected data to predict higher-order multi-species population dynamics and determine pairwise behavioural categorisation of *P. aeruginosa*, *C. albicans*, and *S. aureus* interactions (Lotka, 1932).

10.2 CFU enumeration

First, the *P. aeruginosa* wild type and a smaller pool of respiration mutants (Δanr , Δdnr , $\Delta narG$, $\Delta roxSR$) were cultured axenically in the continuous-flow system to ensure that they were able to grow and maintain a stable population for the duration of the experiment in absence of any competition from other species (Appendix C, Figure C1). The wild type and Δanr , Δdnr , and $\Delta narG$ mutants all reached a density of approximately 2×10^8 CFU mL⁻¹. The $\Delta roxSR$ mutant reach a density approximately 1-log lower, at 2×10^7 CFU mL⁻¹.

The *P. aeruginosa* wild type and selected respiration mutants were then co-cultured with *C. albicans* and *S. aureus* in artificial sputum medium, with samples removed every three hours during the first 12 hours of growth, and then every 24 hours from time 0 (Figure 46). The final densities of *P. aeruginosa* were approximately the same as when cultured axenically. The *P. aeruginosa* wild type triple species co-culture CFU enumeration yielded numbers in line with those previously reported using this system (O'Brien and Welch, 2019).

The Δanr , Δdnr , $\Delta narG$, and $\Delta roxSR$ mutants all appear to have an effect on titres of both *C. albicans* and *S. aureus* compared with the wild type, with titres of these species approximately 1-2-log lower and 1-1.5-log lower, respectively. The Δanr mutant co-culture showed slightly decreased *S. aureus* titres but showed a larger decrease in *C. albicans* titres. The most remarkable effect was observed in the Δdnr mutant co-culture, which showed a large decrease of both *C. albicans* and *S. aureus* titres, and a concomitant increase in *P. aeruginosa* titres from the outset of

the experiment. The $\Delta narG$ mutant co-culture showed titres for all three species that were in an approximate middle ground between the wild Δnar and Δdnr mutants. The $\Delta roxSR$ mutant co-culture titres remained approximately the same as the starting inoculation, except for a 1-log reduction in *C. albicans* titres.

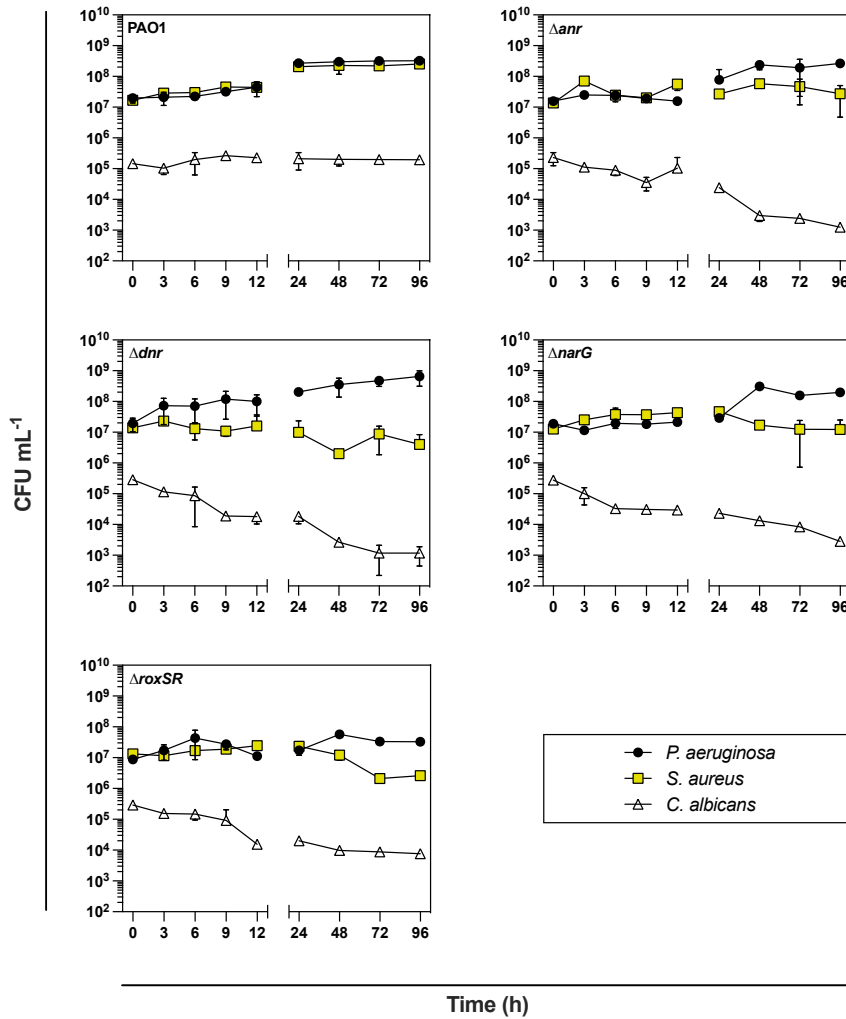


FIGURE 46. CFU enumeration of *P. aeruginosa* (wild type and respiratory mutants), *C. albicans*, and *S. aureus* triple-species culture in artificial sputum medium continuous-flow culture. Mean and standard deviation of at least three biological replicates.

10.3 Lotka-Volterra Markov Chain Monte Carlo analysis

The CFU enumeration data were analysed using a Lotka-Volterra competition model to discriminate the behaviours of *P. aeruginosa*, *C. albicans*, and *S. aureus*. In brief, the experimentally collected data was used to as a starting point to build a model that could simulate the polymicrobial setup used in this section and derive interspecies interactions. The simulation was repeatedly refined by accounting for deviation from the experimental data and updating the model parameters every 50 iterations of the simulation, up to a maximum of 10,000 iterations. Of the total number of iterations, the top 100 that best fit the experimentally collected data were then used to arrange pairwise interactions between the three species into nine ecological relationships: neutral, competitor, mutualistic partner, predator or parasite, prey or host, commensal, commensal host, harmed by, and harming other.

The model in its current state proved viable for all data sets and highlighted clear differences in the ecological relationships between the three species (Table 16). The analysis of the Δdnr mutant was restricted to using the first 48 hours of data. For the Δdnr mutant, inclusion of the 72-hour (or also the 96 hour) time-points violated the model limits and all pairwise interactions in the simulated data defaulted to “neutral”. Due to the lack of higher resolution data between 48 hours and 96 hours, further investigations were impossible; hence only the first 48 hours were included in downstream ecological investigations in this dissertation. For all datasets the output values only fell into four of the nine categories (predator or parasite, prey or host, competitor, and mutualistic partner). Further statistical exploration of interactions is included in Appendix D (Tables D1-10).

10.3.1 Wild type analysis

S. aureus' relationship with the *P. aeruginosa* wild type (SA-PA) is inconclusive between whether the former is the prey or host of *P. aeruginosa* or if they are in a mutualistic relationship ($\chi^2 = 0.04$, $p > 0.1$). Nevertheless, *S. aureus* is likely to be the weaker species in the relationship regardless of whether the *P. aeruginosa* wild type is harming *S. aureus* or not. The *C. albicans*-*P. aeruginosa* (CA-PA) interaction values ($\chi^2 = 67$, $p \ll 0.01$) indicate that there is at least one relationship that is likely to be significantly different from the others. Further analysis of the CA-PA interactions showed *C. albicans* is likely to be either the predator or parasite of *P. aeruginosa*, or both are in a competition relationship ($\chi^2 = 0.01$, $\text{adj } p > 0.1$). In either case, the *P. aeruginosa* wild type is likely to be harmed by *C. albicans* in the ecosystem, regardless of whether *P. aeruginosa* harms or benefits *C. albicans* in return. The CA-SA relationship is inconclusive ($\chi^2 = 6$, $p = 0.1$). The distribution of counts between the four ecological relationships showed ambiguity, however, this species pair is unlikely interact in a net-neutral way.

TABLE 16. Distribution of 100 simulated pairwise interspecies interactions between *P. aeruginosa* (PA; wild type and mutants), *C. albicans* (CA), and *S. aureus* (SA) based on experimentally collected CFU data from a polymicrobial continuous-flow system setup with artificial sputum medium. The order of species in the “Pair” column indicates the direction of the interaction, e.g. SA-PA means that *S. aureus* is ... of *P. aeruginosa*. In this context, « 0.01 should be understood to mean less than 0.0001.

PA strain	Pair	Prey or host	Predator or parasite	Competitor	Mutualistic partner	χ^2	p value
Wild type	SA-PA	51	0	0	49	0.04	0.841
	CA-PA	3	46	45	6	67	« 0.01
	CA-SA	34	27	22	17	6	0.097
Δanr	SA-PA	25	11	14	50	38	« 0.01
	CA-PA	24	21	0	55	21	« 0.01
	CA-SA	94	1	4	1	254	« 0.01
Δdnr	SA-PA	0	17	83	0	44	« 0.01
	CA-PA	22	0	2	76	88	« 0.01
	CA-SA	25	8	66	1	102	« 0.01
$\Delta narG$	SA-PA	40	0	60	0	4	0.045
	CA-PA	16	13	66	5	92	« 0.01
	CA-SA	92	0	0	8	71	« 0.01
$\Delta roxSR$	SA-PA	36	21	37	6	25	« 0.01
	CA-PA	25	7	65	3	96	« 0.01
	CA-SA	37	19	21	23	8	0.046

10.3.2 Δanr analysis

The Δanr mutant SA-PA competition model results indicate that the most likely interaction is mutualistic ($\chi^2 = 38$, $p \ll 0.01$), with the largest number of best-fit models were allocated to the mutualistic partner category. The Δanr mutant CA-PA competition model results indicate that the most likely interaction is mutualistic ($\chi^2 = 21$, $p \ll 0.01$), as the largest number of best-fit models were distributed to the mutualistic partner category. The Δanr mutant CA-SA competition model results indicate that the most likely interaction is that *C. albicans* is the prey or host of *S. aureus* ($\chi^2 = 254$, $p \ll 0.01$), also demonstrated by the overwhelming allocation of best-fit models to the predator or parasite category (94/100).

10.3.3 Δdnr analysis

The most likely interaction between the Δdnr mutant and *S. aureus* was competition ($\chi^2 = 44$, $p \ll 0.01$), with 83/100 best-fit models allocated to this category. The Δdnr mutant CA-PA compe-

tion model results indicate that the most likely interaction is that these species are mutualistic partners ($\chi^2 = 88$, $p \ll 0.01$), given that 76/100 best-fit models were distributed to this category. The Δdnr mutant CA-SA competition model results indicate that the most likely interaction is that *C. albicans* and *S. aureus* are competitors ($\chi^2 = 102$, $p \ll 0.01$), with the largest allocation of best-fit models to the competitor category (66/100).

10.3.4 $\Delta narG$ analysis

The relationship between the $\Delta narG$ mutant and *S. aureus* is inconclusive as there is an almost equal split between *S. aureus* being the prey or host of *P. aeruginosa* and the two species being in competition. The most likely interaction between the $\Delta narG$ mutant and *C. albicans* is that *C. albicans* is the competitor of *P. aeruginosa* ($\chi^2 = 92$, $p \ll 0.01$), with 66/100 of the best-fit models being distributed to this category. The most likely interaction between *C. albicans* and *S. aureus* is that *C. albicans* is the prey or host of *S. aureus* ($\chi^2 = 71$, $p \ll 0.01$), with 92/100 best-fit models being allocated to this category.

10.3.5 $\Delta roxSR$ analysis

The results for the *P. aeruginosa* $\Delta roxSR$ mutant were relatively evenly distributed across categories compared with the other respiration mutants tested. The SA-PA competition model results in Table 16 indicate that the most likely interaction is either *S. aureus* is the prey or host of *P. aeruginosa*, or that *S. aureus* and *P. aeruginosa* are competitors; however, the expanded analysis cannot determine which of these is most likely ($\chi^2 = 0.014$, adj $p = 5.441$). The most likely interaction between the $\Delta roxSR$ mutant and *C. albicans* is that they are competitors ($\chi^2 = 96$, $p \ll 0.01$), with 65/100 of the best-fit models being distributed to this category. The $\Delta roxSR$ mutant CA-SA interactions were relatively evenly distributed amongst all categories, therefore it is inconclusive what the overall most likely ecological relationship is.

10.4 Discussion

The work in this section constitutes the first time a continuous-flow model has been used to (i) determine population titres of defined mutants in polymicrobial cultures and to (ii) then analyse the population dynamics and determine behavioural categorisation of a polymicrobial culture using a Lotka-Volterra competition model. Previous attempts to utilise Lotka-Volterra competition models to determine ecological relationships between microbial species have had mixed success, as might be expected from trying to determine extremely complex interspecies interactions. However, the field is rapidly expanding (Bucci and Xavier, 2014; Carrara *et al.*, 2015;

Fronhofer *et al.*, 2015; Quinn *et al.*, 2016; Bucci *et al.*, 2016; Momeni, Xie and Shou, 2017; Abreu, Ortiz Lopez and Gore, 2018; Aguirre de Cárcer, 2020; Xu *et al.*, 2020; Dimas Martins and Gjini, 2020; Joseph *et al.*, 2020; Li *et al.*, 2021).

The *P. aeruginosa* wild type triple-species culture shows all three species maintaining a stable population, albeit in different titres. The competition model determined that the interaction between *P. aeruginosa* and *S. aureus* was the prey or host of *P. aeruginosa* or that they were in a mutualistic relationship, *C. albicans* was either the predator or parasite of *P. aeruginosa* or they were competitors, and the interaction between *C. albicans* and *S. aureus* was inconclusive, that is, it could not be determined which of the four categories were most likely and not that no categories were defined.

When examining the denitrification regulation mutants, Δanr and Δdnr , a shift in behaviour can be observed as we see a progression down the denitrification regulatory cascade outlined in Figure 7. In the Δanr mutant, it was observed that both *S. aureus* and *C. albicans* CFU titres decreased, which could perhaps be attributed to the change in behaviour of *C. albicans*. Compared with the wild-type culture, *C. albicans* switches from being the predator or parasite of *P. aeruginosa* to being mutualistic, suggesting that the Δanr mutant is “stronger” than the wild type when interacting with *C. albicans*. This shift in relationship means that *C. albicans* now effectively only gains a limited benefit from the mutualistic relationship and as a consequence *C. albicans* is less able to defend itself against *S. aureus*. In the *C. albicans* and *S. aureus* interaction, the change in *C. albicans* to prey or host behaviour is demonstrated as a decrease in the experimentally observed *C. albicans* titres. Perhaps this may also be attributed to *P. aeruginosa* no longer being classified as prey or host of *C. albicans*. If *P. aeruginosa* and *C. albicans* are in a mutualistic relationship, then *C. albicans* is also contributing to maintenance of the *P. aeruginosa* population. This allocation of resources may mean that *C. albicans* can only be maintained at a much lower titre.

The shift in behavioural categorisation is most dramatic in the Δdnr mutant, with each pairwise interaction changing relative to the wild type and becoming less “tolerant” of other species compared with the Δanr mutant. The relationship between *P. aeruginosa* and *S. aureus* changes from *S. aureus* being the prey or host of *P. aeruginosa* (or a mutualistic partner), to a competitive relationship between the two species. The drawbacks of being on the “submissive” side of an interaction, i.e. giving without gaining, are lost, and one could predict that *S. aureus* should now fare better in terms of population numbers. However, with the two species now in competition, *S. aureus* must allocate resources to being competitive instead of growth to support *P. aeruginosa*. Also, *P. aeruginosa* and *C. albicans* change to being mutualistic partners. *C. albicans* and *S. aureus* also become competitors. The CFU titres of all three species change in this combination, with *P. aeruginosa* titres increasing and *C. albicans* and *S. aureus* titres decreasing. This is likely due to increased competition in the system, generally, with *S. aureus* facing competition from both *P.*

aeruginosa and *C. albicans*. These changes in interspecies interactions perhaps afford *P. aeruginosa* the opportunity to dominate the polymicrobial culture. The *P. aeruginosa* Δ *dnr* mutant has effectively decreased stressful interactions with *C. albicans* (i.e. being no longer predator or prey), and can reallocate resources to share the burden of competition with *S. aureus*. The Δ *dnr* mutant culture analysis highlights how finely balanced polymicrobial communities are, with the loss of a single gene sufficient to initiate a complete restructuring of the interspecies interactions. When considering potential therapeutic treatments for microbial infections, for example synthetic RNA silencing, it is important to consider how the whole community may respond. It must be noted that the Lotka-Volterra competition model could only analyse the first 48 hours of data before failing to accurately categorise the interactions between species. It is hoped that future work will aim to further refine the model to include dual-species interactions and single species data, to more accurately interpret the effects that the three species have on each other.

The Δ *narG* mutant behaved similarly to the Δ *anr* and Δ *roxSR* mutants at first glance of the CFU enumeration data. The Δ *narG* competition model defined all three pairwise relationships differently compared with the wild type. The exact interaction between *S. aureus* and *P. aeruginosa* was inconclusive, *C. albicans* became the competitor of *P. aeruginosa*, and in turn *C. albicans* became the prey or host of *S. aureus*. These shifts in interactions may explain how the titres of *P. aeruginosa* Δ *narG* remained comparable to the wild type whereas the other two species' titres decreased. That is, *P. aeruginosa* is no longer in a potentially mutualistic partnership with *S. aureus* and is also now in competition with *C. albicans*. At the same time, *C. albicans* is now the prey or host of *S. aureus*. With *S. aureus* under attack from *P. aeruginosa*, *C. albicans* under attack from *S. aureus* and also facing competition from *P. aeruginosa*, the outcome is that *P. aeruginosa* has the greatest potential benefit from this arrangement of interactions and can dominate the culture.

Finally, the Δ *roxSR* mutant also behaved differently compared the wild type or any other mutant. The titres of *C. albicans* and *S. aureus* decreased compared with the *P. aeruginosa* wild type culture, but the *P. aeruginosa* titre also decreased. However, the titre of *P. aeruginosa* in triple-species culture was not significantly different compared with the single species culture, suggesting that neither *C. albicans* nor *S. aureus* are responsible for the decreased population levels of *P. aeruginosa*. The inconclusive nature of the analysis of interactions between *S. aureus* and *P. aeruginosa* (although in either case it appears that *P. aeruginosa* is on the stronger side of their interaction), the shift of *C. albicans* and *P. aeruginosa* to competitors, and the ambiguity between *C. albicans* and *S. aureus* interactions make it difficult to judge the effect of the loss of RoxSR function on the polymicrobial community. Interestingly, despite only being able to obtain a 1×10^7 CFU mL⁻¹ population density, it could be argued that per CFU there is a greater effect on the behavioural ecology of the triple-species culture due to the loss of *roxSR* than there is in any of the other genotypes analysed.

Most previous studies focus on the implementation of a generalised Lotka-Volterra model. Here we have applied a Lotka-Volterra competition model, incorporating the carrying capacity of the system to further expand the range of information available in triple-species culture comparisons that may not be available from single species data. Additionally, the previously mentioned publications generally assume that there is only one “true” ecological interaction type. By incorporating Bayesian inference methods into the Lotka-Volterra competition model analysis we challenge the “one true type” dogma previously presented and demonstrate—to our knowledge for the first time—that complex relationships can be predicted, mathematically, that also hold true from a biological standpoint. This is further supported by our observations that despite having the same starting point (i.e. the same raw data to inform the model), populations may finish up in very different end points (i.e. the distribution of behavioural classification into discrete groups). Furthermore, the model acknowledges the ambiguity present in many biological interactions and it is hoped that future approaches will be able to characterise these grey areas more adequately.

Despite the current limitations of the model, it is clear that the respiratory mutants begin to dominate the polymicrobial culture, although the nature of their interactions varies widely (Figure 47). The mechanism behind this is unclear. It was hypothesised that *P. aeruginosa* respiration mutants may seek to scavenge alternative electron acceptors or use redox active molecules to relieve some of the oxidative stress caused by high NADH levels, and as a result may produce greater quantities of siderophores and phenazines which may in turn have a killing effect on other species. However, measuring siderophores and pyocyanin in cultures paired to the CFU enumeration in this section did not support this, and in fact the levels of siderophores and pyocyanin produced by these mutants was lower than the wild type (though not significantly). It is possible that without the ability to properly produce the complete denitrification architecture, these resources are instead allocated elsewhere and confer a fitness advantage. Future work including transcriptomic or proteomic analysis of these cultures would assist greatly in unveiling the exact nature of *P. aeruginosa*'s role in a continuous-flow system polymicrobial community.

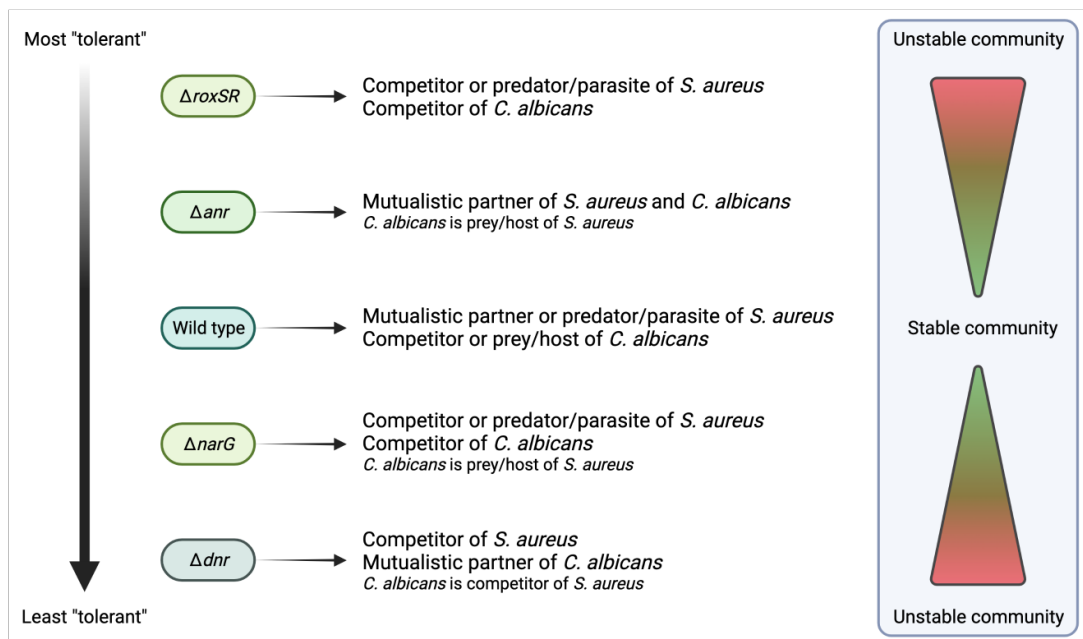


FIGURE 47. Summary of simulated interspecies interactions between *P. aeruginosa*, *C. albicans*, and *S. aureus* based on polymicrobial data obtained from continuous-flow system triple-species cultures using artificial sputum medium.

Final conclusions

P. aeruginosa's comprehensive ability to adapt to a wide range of environmental niches is an extremely real threat to the health and economy of the human population. Due to the high level of intrinsic antibiotic resistance, *P. aeruginosa* infections are notoriously difficult to treat and place a significant burden on public health systems (Bodey *et al.*, 1983; Lister, Wolter and Hanson, 2009). Moreover, to the detriment of those unfortunate enough to be colonised by *P. aeruginosa*, these infections often require intensive chemotherapeutic intervention to eliminate from the body. *P. aeruginosa* is especially relevant in CF patients; adaptation to the lung occurs extremely early on and by the time patients reach 18 years of age more than 90% have a chronic *P. aeruginosa* infection (Döring, 1997).

Colonisation of specific niches, such as the CF lung, often requires *P. aeruginosa* to be able to thrive on a wide range of nutrients. The CF lung is generally nutrient-poor and lacks easy provision of rich carbon sources such as glucose. This imposes an existential threat to *P. aeruginosa*—adapt or die. Fortunately (at least for *Pseudomonas*), a large genome harbouring a multitude of survival-supporting options provides ample opportunity for *P. aeruginosa* to make the best use of what is available, and indeed *P. aeruginosa* readily rewires its metabolic network to utilise even the poorest of nutrients. One of the most significant examples of this is the use of the glyoxylate shunt, a convenient carbon-economic shortcut through the citric acid cycle. This pathway is up-regulated during growth on fatty acids, such as acetate, and is a dominant adaptation of central carbon metabolism in CF lung isolates (Rossi *et al.*, 2018; Wu *et al.*, 2019).

Considering the importance of central carbon metabolism in infection, and key pathways such as the glyoxylate shunt, the Welch laboratory has as strong focus on *P. aeruginosa* metabolic networks. In reference to fatty acids, we observed a concomitant up-regulation of denitrification transcripts when grown in a highly aerobic culture medium containing acetate as the sole source of carbon (Dolan, Kohlstedt, *et al.*, 2020). Denitrification is, canonically, an anaerobic process controlled by oxygen-sensitive regulators, therefore we were surprised to see *P. aeruginosa* seemingly using what should be a totally unnecessary branch of respiration. This piqued our interest,

as fatty acids such as acetate are known to be readily available in the lung and there are also very steep oxygen gradients present in the mucus build-up that is so characteristic of CF lung (Stutts *et al.*, 1986; Worlitzsch *et al.*, 2002).

Several questions were raised by these observations. How does *P. aeruginosa* regulate denitrification in aerobic conditions? What is the benefit of aerobic denitrification? How might denitrification mutants behave in a physiologically relevant condition, and could this be used to inform future therapeutic treatments? In this dissertation, I believe that I have contributed to the fundamental understanding of what might drive an organism that has abundant oxygen availability to scavenge for alternative electron acceptors and what the benefits of this may be. A summary of the observations described in Sections 4-8 of this dissertation can be found in Table 17 at the end of this chapter.

11.1 Regulation of denitrification genes

During growth with acetate as the sole carbon source, *P. aeruginosa* restructures its metabolic network to drive carbon flux through the glyoxylate shunt. This allows *P. aeruginosa* to maintain a similar growth rate on a carbon-poor nutrient to a carbon-rich nutrient, such as glucose (Section 4.2). Using denitrification mutants, I have shown that the growth rate is only affected by the loss of two of the five denitrification genes tested: *dnr* and *norB* (Section 4.2). The most plausible explanations are that (a) in a Δdnr mutant the denitrification genes may not be strongly expressed enough, and (b) when the full regulatory network is available, as we know it, the accumulation of nitric oxide in the $\Delta norB$ mutant leads to inhibition of the remaining denitrification enzymes. The consequence of this is that without full denitrification, growth on short chain fatty acids is impeded. I proposed that the reduction in growth rate of the $\Delta roxSR$ mutant is more likely due to RoxSR's involvement in aerobic (O_2 -based) respiration.

In terms of regulation of expression, I have shown that *dnr* expression is decreased in both an Δanr mutant and a $\Delta roxSR$ mutant (Section 5.3). A decrease in *dnr* expression in an Δanr mutant is not surprising, however the $\Delta roxSR$ result was surprising, as without the majority of terminal oxidases being expressed through the action of their primary regulator, I believed that there would be a compensatory up-regulation of denitrification. I have also shown that in a Δdnr mutant, the expression of all N-oxide reductases is lower than the wild type (Section 5.4). Again, this is not necessarily a surprising finding, although it was expected that in a Δdnr mutant the expression of *nosR* would be completely abolished considering that Dnr is the only known positive regulator of the *nos* operon. However, Western blot analyses in the Welch laboratory have shown no detection of NirS in an Δanr or Δdnr mutant. Reasons for the indication of expression in the luciferase assay may be attributed to sensitivity (i.e. gain settings), post-transcriptional control, or simply

some level of background expression. We acknowledge that this technique has its caveats, as previously discussed in Section 5.1.

11.2 Denitrification in redox homeostasis

When *P. aeruginosa* is cultured with acetate as a carbon source, we have observed that alongside the rapid growth on what is a nutrient-poor medium, *P. aeruginosa* cells change morphology and become elongated, consistent with other findings describing increases in cell length concomitant with faster growth (Deforet, Van Ditmarsch and Xavier, 2015; Dolan, Kohlstedt, *et al.*, 2020). As cells elongate, their cell surface-to-volume ratio changes such that the cell volume exceeds the cell membrane's capacity for respiratory complexes that can support the bioenergetic needs of the cell (Szenk, Dill and de Graff, 2017).

I hypothesised that a result of this would be an increase in NADH accumulation, and that *P. aeruginosa* was employing aerobic denitrification to assuage the effects of this by offering a hybrid respiratory chain that could optimise the use of potential available terminal electron acceptors. To test this hypothesis, I extracted NAD(P)(H) species throughout exponential growth in a minimal medium containing acetate as the sole carbon source and the same media with an excess of nitrate, and it was observed that decrease in the NADH:NAD⁺ ratio is synchronous with nitrite production (Sections 6.4 and 7.2). Therefore, I have shown that aerobic denitrification is an effective modulator of redox pools in *P. aeruginosa*. To further confirm this, I used denitrification mutants and determined that both Δdnr and $\Delta norB$ mutants cannot significantly alter their NADH levels in the presence of nitrate, once again highlighting the interplay between regulation and nitric oxide production, and the irrelevance of Anr in aerobic denitrification. I also found that a $\Delta narG$ mutant behaves similarly to the Δdnr and $\Delta norB$ mutants in that it also shows a diminished capacity to decrease NADH:NAD⁺ ratios. Whilst I did not find any statistical significance to assert that decreased *narG* expression might be the true cause of a Δdnr mutant's phenotype, this would be the logical deduction considering that NarG is the only nitrate reductase under the regulatory control of Dnr.

The nitrite produced by the $\Delta narG$ mutant must also be acknowledged (Figures 28 and 29). I believe that the source of nitrite production could be attributed to the periplasmic nitrate reductase, NapA, considering that the production of nitrite in this mutant occurs at the approximate transition into stationary phase. NapA is regulated outside of the Anr/Dnr/NarXL system, by RpoS, and is thought to be only expressed in stationary phase. Furthermore, NapA does not translocate protons to contribute to ATP generation, therefore is unlikely to be expressed during rapid growth in exponential phase as a compensatory device to relieve the $\Delta narG$ phenotype (Kawakami *et al.*, 2010; Arai *et al.*, 2014; Kirchoff *et al.*, 2018). Additionally, I have also shown

that $\Delta norB$ nitrite production is markedly lower than the wild type or any other mutant during growth in MOPS with 40 mM acetate and 20 mM nitrate, once again highlighting the role of nitric oxide in inhibiting denitrification, and thus inferring that substantial conversion of nitrate to nitrite must be occurring in order to reach a threshold nitric oxide concentration. In Section 7.3, I demonstrate that in artificial sputum medium there is a lower utilisation of nitrate in exponential phase, and nitrite production does not occur until stationary phase, therefore this is most probably attributable to NapA activity.

In Section 8.1.2, I determined that during exponential growth in MOPS with 40 mM acetate there was a decrease in exponential-phase PQS production in a Δdnr mutant, and that in MOPS with 40 mM acetate and 20 mM nitrate there was an increase in PQS production in a $\Delta norB$ mutant. In Section 8.2.2, I showed that siderophore production is decreased in the presence of nitrate in a Δdnr mutant. These data together highlight the indirect effect of denitrification on quorum sensing, specifically in the production of PQS, complementing previous work demonstrating the effect of quorum sensing on denitrification (Toyofuku *et al.*, 2008; Cui *et al.*, 2021) and that a decrease in N-oxide reductases that contain iron at their catalytic centre results in a cut of the demand for iron (Zumft, 1997; Toyofuku *et al.*, 2008; Zhu *et al.*, 2020). It has been previously shown that NADH levels are modulated by pyocyanin in nitrate-dependent-oxygen-depleted cultures, therefore highlighting the role of pyocyanin in maintaining redox homeostasis (Price-Whelan, Dietrich and Newman, 2007). In Section 8.3.4, I suggest that the lack of pyocyanin production during growth on MOPS with 40 mM acetate excludes redox balancing via pyocyanin and emphasises the importance of denitrification in redox balancing irrelevant of phenazine participation.

In summary, I have shown that *P. aeruginosa* uses aerobic denitrification during growth on a short-chain fatty acid to decrease its NADH:NAD⁺ ratio. It also appears that this activity is dependent on Dnr and thus is highly probable to be NarG-dependent. Therefore, I propose that aerobic denitrification is very likely to be a form overflow metabolism, requiring the restructuring of *P. aeruginosa* metabolism to produce a hybrid electron transport chain, ultimately resulting in the most efficient utilisation of electron acceptors whilst preserving redox homeostasis, growth, and carbon consumption.

11.3 Denitrification and fitness in a polymicrobial community

The majority of microbiological research is conducted by studying subject species in the absence of other microbiological competition. In addition to this, many studies rely on just a few commonly used media (such as Luria-Bertani, MOPS-based, or M9-based media), which are not representative of natural conditions. Whilst this does generate a wealth of insight in areas such

as metabolism or virulence factors production, it does little to truly replicate the complexities of real-world scenarios. To this end, I sought to explore the inter-species relationships between *P. aeruginosa* and two other species commonly associated with the CF airway, *C. albicans* and *S. aureus*, in a physiologically relevant medium. Considering that *P. aeruginosa* is the archetypal biofilm-forming bacteria, I began by investigating the biofilm-forming ability of *P. aeruginosa* and respiration mutants both in single-species culture and in triple-species culture.

In Section 9.3, I showed that the Δanr , Δdnr and $\Delta roxSR$ mutants all form significantly less biofilm-associated biomass than the wild type when grown in batch culture conditions. RoxSR has been reported to be involved in population density sensing (Fernández-Piñar *et al.*, 2008), and Anr regulates *dnr* expression and is the well-known anaerobic regulator of denitrification in *P. aeruginosa*. With this in mind, it was expected that these three mutants would be defective in biofilm formation. The defect in biofilm formation of these mutants is also perhaps not surprising when we consider the architecture of a biofilm, a typically dense mixture of dead and living cells, matrix exopolysaccharides, eDNA and other secreted elements, that gives rise to a steep oxygen gradient in the cross-section of the biofilm. In contrast, when cultured alongside *C. albicans* and *S. aureus* the difference in biofilm-forming ability of the Δanr , Δdnr , and $\Delta roxSR$ mutants compared with the wild type were abolished. Perhaps this could be attributed to metabolic cross-feeding between species, a common phenomenon in biofilms (Williamson *et al.*, 2012; Schiessl *et al.*, 2019; Smith *et al.*, 2019; Joshi, Gunawan and Mann, 2021). One drawback to these insights is the fact that the absolute conditions in which biofilm assays were cultured was not anaerobic from the outset of the experiment, though it is likely that the condition of the microtitre plate was close to anaerobic after 48 hours.

In Section 10.2, I used artificial sputum medium in a continuous-flow system developed in the Welch laboratory (O'Brien and Welch, 2019) to investigate the polymicrobial population composition of cultures containing *P. aeruginosa* wild type or *P. aeruginosa* respiration mutants cultured alongside *C. albicans* and *S. aureus*. I found that depending on the “severity” of the gene deletion, that is, how far down the denitrification cascade the missing gene is, the more *P. aeruginosa* appears to dominate the polymicrobial culture. This was unexpected as, based on the data presented earlier in this dissertation, I predicted that these mutants might fare worse in a polymicrobial community than the wild type in light of a major branch of respiration being unusable. It is still not entirely clear what the mechanism is behind this, though perhaps it may be attributable to the antibiotic activity of pyocyanin. In Section 8.3.2, I showed that under batch culture conditions, *P. aeruginosa* produces more pyocyanin in triple-species culture than in single species culture. However, the same difference could not be detected in the continuous-flow system culture, but this may be because of the constant dilution of culture medium.

I also worked with Pok-Man Ho to use mathematical modelling to effectively sort pairwise

interactions between species into ecological roles (Section 10.3), and from these data further determine how aggressive or tolerant *P. aeruginosa* mutants may be towards other species. To our knowledge, this is the first time Bayesian methods have been incorporated into a Lotka-Volterra competition model and applied to the study of defined *P. aeruginosa* mutants in a polymicrobial culture using a continuous-flow system and a physiologically relevant medium. In brief, the analysis revealed that compared with the wild type, the deletion of *anr* resulted in stronger interactions from *P. aeruginosa*, the deletion of *dnr* resulted in even stronger interactions from *P. aeruginosa*, and the deletion of *narG* resulted in population dynamics that fell somewhere between the Δanr mutant and the Δdnr mutant. Whilst these classifications are oversimplifications of a more complex hierarchy of polymicrobial interactions, I believe they are a good summary of the most likely biological conclusion from the mathematic simulations. These data and the subsequent analysis also highlight an issue with the oft-cited aspirational outcome from microbiological research of “potential as a therapeutic target”. Based on the data presented here, it may not necessarily be wise to target the anaerobic respiration of *P. aeruginosa* considering that in the experimentally collected data we see the perturbation of an otherwise stable community of CF-associated pathogens, giving rise to different species dominating. In a clinical context, this could have negative implications for patient health, potentially exacerbating an already undesirable situation. Of course, the answer is not to not treat a *P. aeruginosa* infection, but this model allows for the use of projected outcomes to potentially inform a treatment regimen.

11.4 Future perspectives

Moving forward, further work investigating the transcriptomic and proteomic changes in Δanr and Δdnr would likely provide novel candidates for the regulation of aerobic denitrification in the absence of Anr, and will shed light on the changes brought about by a loss of Dnr that make it more competitive in a polymicrobial setting. Additionally, complementation of deletion mutants would be absolutely necessary to confirm the phenotypes presented in this dissertation. Expanding the number of species in the continuous-flow system to include other members of the CF consortia could also yield a more in depth understanding of the dynamics of diverse respiratory capabilities in a polymicrobial community. Furthermore, expanding the Lotka-Volterra competition model to incorporate known virulence factors or cross-feeding of commonly shared metabolites will give valuable insight into the chemical warfare and cooperativity of species in the CF lung, and the ramifications that this may have on the human health. Finally, studies centred around phenotypic and/or genotypic heterogeneity within species’ subpopulations—and how these subpopulations may assume different roles with respect to denitrification—would likely provide fascinating illumination of cooperativity within microbial cultures.

TABLE 17. Summary of phenotypes observed in Chapters 4-8. *P. aeruginosa* mutants compared with the PAO1 wild type grown in MOPS with 40 mM acetate and 20 mM nitrate. N.D. = no difference.

<i>P. aeruginosa</i> strain	Growth		Expression			Redox modulation	Nitrite production	BHL production	PQS production	Siderophore production
	rate	<i>nar</i>	<i>nir</i>	<i>nor</i>	<i>nos</i>					
Δnar	N.D.	Lower	Lower	N.D.	N.D.	N.D.	N.D.	N.D.	N.D.	N.D.
Δdnr	Lower	Lower	Lower	N.D.	N.D.	None	Lower	Lower	N.D.	Lower
$\Delta narG$	Lower					Lower	Lower	N.D.	N.D.	N.D.
$\Delta nirS$	N.D.		Not tested			N.D.	Higher	N.D.	N.D.	N.D.
$\Delta norB$	Lower					None	Lower	Lower	Higher	N.D.
$\Delta roxSR$	Lower	Lower	N.D.	N.D.	N.D.	N.D.	N.D.	N.D.	N.D.	N.D.

References

Abdelhamid, Y. *et al.* (2019) 'Evolutionary plasticity in the allosteric regulator-binding site of pyruvate kinase isoform PykA from *Pseudomonas aeruginosa*', *Journal of Biological Chemistry*, 294(42), pp. 15505–15516.

Abdelhamid, Y. *et al.* (2021) 'Structure, function and regulation of a second pyruvate kinase isozyme in *Pseudomonas aeruginosa*', *Frontiers in Microbiology*, 12(790742).

Abreu, C., Ortiz Lopez, A. and Gore, J. (2018) 'Pairing off: a bottom-up approach to the human gut microbiome', *Molecular Systems Biology*, 14(e8425).

Aguirre de Cárcer, D. (2020) 'Experimental and computational approaches to unravel microbial community assembly', *Computational and Structural Biotechnology Journal*, 18, pp. 4071–4081.

Ahearn, D. G. *et al.* (1999) 'Primary adhesion of *Pseudomonas aeruginosa* to inanimate surfaces including biomaterials', *Methods in Enzymology*, 310, pp. 551–557.

Ahmed, S. A. K. S. *et al.* (2019) 'Natural quorum sensing inhibitors effectively downregulate gene expression of *Pseudomonas aeruginosa* virulence factors'. *Applied Microbiology and Biotechnology*, 103, pp. 3521–3535.

Van Alst, N. E. *et al.* (2009) 'Compensatory periplasmic nitrate reductase activity supports anaerobic growth of *Pseudomonas aeruginosa* PAO1 in the absence of membrane nitrate reductase', *Canadian Journal of Microbiology*, 55(10), pp. 1133–1144.

Alvarez-Ortega, C. and Harwood, C. S. (2007) 'Responses of *Pseudomonas aeruginosa* to low oxygen indicate that growth in the cystic fibrosis lung is by aerobic respiration', *Molecular Microbiology*, 65(1), pp. 153–165.

- Anderson, R. D. *et al.* (2010) 'Biosignificance of bacterial cyanogenesis in the CF lung', *Journal of Cystic Fibrosis*, 9(3), pp. 158–164.
- Anderson, R. M., Zimprich, C. A. and Rust, L. (1999) 'A second operator is involved in *Pseudomonas aeruginosa* elastase (*lasB*) activation.', *Journal of Bacteriology*, 181(20), pp. 6264–70.
- Andrews, S. C., Robinson, A. K. and Rodríguez-Quinones, F. (2003) 'Bacterial iron homeostasis', *FEMS Microbiology Reviews*, 27, pp. 215–237.
- Arai, H. *et al.* (2005) 'Transcriptional regulation of the flavohemoglobin gene for aerobic nitric oxide detoxification by the second nitric oxide-responsive regulator of *Pseudomonas aeruginosa*', *Journal of Bacteriology*, 187(12), pp. 3960–3968.
- Arai, H. *et al.* (2014) 'Enzymatic characterization and *in vivo* function of five terminal oxidases in *Pseudomonas aeruginosa*', *Journal of Bacteriology*, 196(24), pp. 4206–4215.
- Arai, H., Kodama, T. and Igarashi, Y. (1997) 'Cascade regulation of the two CBP/FNR-related transcriptional regulators (ANR and DNR) and the denitrification enzymes in *Pseudomonas aeruginosa*', *Molecular Microbiology*, 25(6), pp. 1141–1148.
- Arai, H., Kodama, T. and Igarashi, Y. (1999) 'Effect of nitrogen oxides on expression of the *nir* and *nor* genes for denitrification in *Pseudomonas aeruginosa*', *FEMS Microbiology Letters*, 170, pp. 19–24.
- Arai, H., Mizutani, M. and Igarashi, Y. (2003) 'Transcriptional regulation of the *nos* genes for nitrous oxide reductase in *Pseudomonas aeruginosa*', *Microbiology*, 149, pp. 29–36.
- Ardon, O. *et al.* (2001) 'Identification of a *Candida albicans* ferrichrome transporter and its characterization by expression in *Saccharomyces cerevisiae*', *Journal of Biological Chemistry*, 276(46), pp. 43049–43055.
- Barraud, N. *et al.* (2006) 'Involvement of nitric oxide in biofilm dispersal of *Pseudomonas aeruginosa*', *Journal of Bacteriology*, 188(21), pp. 7344–7353.
- Barraud, N. *et al.* (2009) 'Nitric oxide signaling in *Pseudomonas aeruginosa* biofilms mediates phosphodiesterase activity, decreased cyclic di-GMP levels, and enhanced dispersal', *Journal of*

Bacteriology, 191(23), pp. 7333–7342.

De Bentzmann, S. and Plésiat, P. (2011) ‘The *Pseudomonas aeruginosa* opportunistic pathogen and human infections’, *Environmental Microbiology*, 13(7), pp. 1655–1665.

Berks, B. C. *et al.* (1995) ‘Enzymes and associated electron transport systems that catalyse the respiratory reduction of nitrogen oxides and oxyanions’, *Biochimica et Biophysica Acta*, 1232(3), pp. 97–173.

Bittar, F. and Rolain, J. M. (2010) ‘Detection and accurate identification of new or emerging bacteria in cystic fibrosis patients’, *Clinical Microbiology and Infection*, 16(7), pp. 809–820.

Bjarnsholt, T. *et al.* (2009) ‘*Pseudomonas aeruginosa* biofilms in the respiratory tract of cystic fibrosis patients’, *Pediatric Pulmonology*, 44(6), pp. 547–558.

Bjornson, H. S. *et al.* (1982) ‘Association between microorganism growth at the catheter insertion site and colonization of the catheter in patients receiving total parenteral nutrition’, *Surgery*, 92(4), pp. 720–727.

Blumer, C. and Haas, D. (2000) ‘Mechanism, regulation, and ecological role of bacterial cyanide biosynthesis’, *Archives of Microbiology*, 173(3), pp. 170–177.

Bodey, G. P. *et al.* (1983) ‘Infections caused by *Pseudomonas aeruginosa*’, *Reviews of Infectious Diseases*, 5(2), pp. 279–313.

Boon, E. M. and Marletta, M. A. (2005) ‘Ligand discrimination in soluble guanylate cyclase and the H-NOX family of heme sensor proteins’, *Current Opinion in Chemical Biology*, 9, pp. 441–446.

Borlee, B. R. *et al.* (2010) ‘*Pseudomonas aeruginosa* uses a cyclic di-GMP-regulated adhesin to reinforce the biofilm extracellular matrix’, *Molecular Microbiology*, 75(4), pp. 827–842.

Borrero-de Acuña, J. M. *et al.* (2016) ‘Protein network of the *Pseudomonas aeruginosa* denitrification apparatus’, *Journal of Bacteriology*, 198(9), pp. 1401–1413.

Borthwick, A. C., Holms, W. H. and Nimmo, H. G. (1984) ‘The phosphorylation of *Escherichia*

coli isocitrate dehydrogenase in intact cells', *The Biochemical Journal*, 222, pp. 797–804.

Bouchard, C. (1889) 'L'influence qu'exerce sur la maladie charbonneuse l'inoculation du bacille pyocanique', *Comptes rendus de l'Académie des Sciences*, 108, pp. 713–714.

Boyle, M. P. and De Boeck, K. (2013) 'A new era in the treatment of cystic fibrosis: correction of the underlying CFTR defect', *The Lancet Respiratory Medicine*, 1(2), pp. 158–163.

Briaud, P. *et al.* (2019) 'Coexistence with *Pseudomonas aeruginosa* alters *Staphylococcus aureus* transcriptome, antibiotic resistance and internalization into epithelial cells', *Scientific Reports*, 9(16364).

Brint, J. M. and Ohman, D. E. (1995) 'Synthesis of multiple exoproducts in *Pseudomonas aeruginosa* is under the control of RhlR-RhlI, another set of regulators in strain PAO1 with homology to the autoinducer-responsive LuxR-LuxI family', *Journal of Bacteriology*, 177(24), pp. 7155–63.

Britigan, B. E. *et al.* (1992) 'Interaction of the *Pseudomonas aeruginosa* secretory products pyocyanin and pyochelin generates hydroxyl radical and causes synergistic damage to endothelial cells: implications for *Pseudomonas*-associated tissue injury', *Journal of Clinical Investigation*, 90(6), pp. 2187–2196.

Brodl, E., Winkler, A. and Macheroux, P. (2018) 'Molecular mechanisms of bacterial bioluminescence', *Computational and Structural Biotechnology Journal*, 16, pp. 551–564.

Brown, G. C. and Cooper, C. E. (1994) 'Nanomolar concentrations of nitric oxide reversibly inhibit synaptosomal respiration by competing with oxygen at cytochrome oxidase', *FEBS Letters*, 356, pp. 295–298.

Bucci, V. *et al.* (2016) 'MDSINE: Microbial Dynamical Systems INference Engine for microbiome time-series analyses', *Genome Biology*, 17(121).

Bucci, V. and Xavier, J. B. (2014) 'Towards predictive models of the human gut microbiome', *Journal of Molecular Biology*, 426(23), pp. 3907–3916.

Button, B. *et al.* (2012) 'A periciliary brush promotes the lung health by separating the mucus layer from airway epithelia', *Science*, 337(6097), pp. 937–941.

Button, B. M. and Button, B. (2013) 'Structure and function of the mucus clearance system of the lung', *Cold Spring Harbor Perspectives in Medicine*, 3(8).

Campbell, J. J. R. and Stokes, F. N. (1951) 'Tricarboxylic acid cycle in *Pseudomonas aeruginosa*', *Journal of Biological Chemistry*, 190(2), pp. 853–858.

Cao, H. *et al.* (2001) 'A quorum sensing-associated virulence gene of *Pseudomonas aeruginosa* encodes a LysR-like transcription regulator with a unique self-regulatory mechanism', *Proceedings of the National Academy of Sciences of the United States of America*, 98(25), pp. 14613–14618.

Carloni, S. *et al.* (2017) 'The small RNA ReaL: a novel regulatory element embedded in the *Pseudomonas aeruginosa* quorum sensing networks', *Environmental Microbiology*, 19(10), pp. 4220–4237.

Carrara, F. *et al.* (2015) 'Inferring species interactions in ecological communities: a comparison of methods at different levels of complexity', *Methods in Ecology and Evolution*, 6, pp. 895–906.

Carrica, M. del C. *et al.* (2013) 'The two-component systems PrrBA and NtrYX co-ordinately regulate the adaptation of *Brucella abortus* to an oxygen-limited environment', *Molecular Microbiology*, 88(2), pp. 222–233.

Castiglione, N. *et al.* (2009) 'The transcription factor DNR from *Pseudomonas aeruginosa* specifically requires nitric oxide and haem for the activation of a target promoter in *Escherichia coli*', *Microbiology*, 155, pp. 2838–2844.

Castric, P. (1994) 'Influence of oxygen on the *Pseudomonas aeruginosa* hydrogen cyanide synthase', *Current Microbiology*, 29(1), pp. 19–21.

Castric, P. A. (1983) 'Hydrogen cyanide production by *Pseudomonas aeruginosa* at reduced oxygen levels', *Canadian Journal of Microbiology*, 29(10), pp. 1344–1349.

Cava, F. *et al.* (2004) 'A new type of NADH dehydrogenase specific for nitrate respiration in the extreme thermophile *Thermus thermophilus*', *Journal of Biological Chemistry*, 279, pp. 45369–45378.

CFTR2 Variant List History (2022) Clinical and Functional Translation of CFTR. Available at: www.cftr2.org.

Charrin, A. and Roger, G. H. (1889) 'Action du sérum des animaux malades ou vaccines sur les microbes pathogènes', *Comptes rendus de l'Académie des Sciences*, 109, pp. 710–713.

Chen, J. and Strous, M. (2013) 'Denitrification and aerobic respiration, hybrid electron transport chains and co-evolution', *Biochimica et Biophysica Acta - Bioenergetics*, 1827(2), pp. 136–144.

Chen, Q., Shen, Y. and Zheng, J. (2021) 'A review of cystic fibrosis: basic and clinical aspects', *Animal Models and Experimental Medicine*, 4(3), pp. 220–232.

Chiappini, E., Taccetti, G. and de Martino, M. (2014) 'Bacterial lung infections in cystic fibrosis patients: an update', *The Pediatric Infectious Disease Journal*, 33(6), pp. 653–654.

Choi, K.-H. and Schweizer, H. P. (2006) 'mini-Tn7 insertion in bacteria with single *attTn7* sites: example *Pseudomonas aeruginosa*', *Nature Protocols*, 1(1), pp. 153–161.

Chung, J. C. S. *et al.* (2013) 'Type III secretion system expression in oxygen-limited *Pseudomonas aeruginosa* cultures is stimulated by isocitrate lyase activity', *Open Biology*, 3(1).

Coffman, T. J. *et al.* (1990) 'Possible role of bacterial siderophores in inflammation: iron bound to the *Pseudomonas* siderophore pyochelin can function as a hydroxyl radical catalyst', *Journal of Clinical Investigation*, 86(4), pp. 1030–1037.

Collman, J. P., Hudson, L., *et al.* (2008) '*Pseudomonas aeruginosa* PqsA is an anthranilate-coenzyme A ligase', *Journal of Bacteriology*, 190(4), pp. 1247–55.

Collman, J. P., Yang, Y., *et al.* (2008) 'A functional nitric oxide reductase model', *Proceedings of the National Academy of Sciences of the United States of America*, 105(41), pp. 15660–15665.

Comolli, J. C. and Donohue, T. J. (2002) '*Pseudomonas aeruginosa* RoxR, a response regulator related to *Rhodobacter sphaeroides* PrrA, activates expression of the cyanide-insensitive terminal oxidase', *Molecular Microbiology*, 45(3), pp. 755–768.

Comolli, J. C. and Donohue, T. J. (2004) 'Differences in two *Pseudomonas aeruginosa* *cbb3* cytochrome oxidases', *Molecular Microbiology*, 51(4), pp. 1193–1203.

Conrad, D. *et al.* (2013) 'Cystic fibrosis therapy: a community ecology perspective', *American Journal of Respiratory Cell and Molecular Biology*, 48(2), pp. 150–156.

Constantinidou, C. *et al.* (2006) 'A reassessment of the FNR regulon and transcriptomic analysis of the effects of nitrate, nitrite, NarXL, and NarQP as *Escherichia coli* K12 adapts from aerobic to anaerobic growth', *Journal of Biological Chemistry*, 281(8), pp. 4802–4815.

Cordas, C. M. *et al.* (2013) 'Electrochemical behaviour of bacterial nitric oxide reductase—evidence of low redox potential non-heme Fe_B gives new perspectives on the catalytic mechanism', *Biochimica et Biophysica Acta - Bioenergetics*, 1827(3), pp. 233–238.

Cornelis, P. (2010) 'Iron uptake and metabolism in pseudomonads', *Applied Microbiology and Biotechnology*, 86(6), pp. 1637–1645.

Cornelis, P. (2020) 'Putting an end to the *Pseudomonas aeruginosa* IQS controversy', *MicrobiologyOpen*, 9(e962).

Cornelis, P. and Dingemans, J. (2013) '*Pseudomonas aeruginosa* adapts its iron uptake strategies in function of the type of infections', *Frontiers in Cellular and Infection Microbiology*, 3(75).

Costerton, J. W., Stewart, P. S. and Greenberg, E. P. (1999) 'Bacterial biofilms: a common cause of persistent infections', *Science*, 284(5418), pp. 1318–1322.

Crousilles, A. *et al.* (2018) 'Gluconeogenic precursor availability regulates flux through the glyoxylate shunt in *Pseudomonas aeruginosa*', *Journal of Biological Chemistry*, 293(37), pp. 14260–14269.

Cugini, C. *et al.* (2007) 'Farnesol, a common sesquiterpene, inhibits PQS production in *Pseudomonas aeruginosa*', *Molecular Microbiology*, 65(4), pp. 896–906.

Cugini, C., Morales, D. K. and Hogan, D. A. (2010) '*Candida albicans*-produced farnesol stimulates *Pseudomonas* quinolone signal production in LasR-defective *Pseudomonas aeruginosa* strains', *Microbiology*, 156(10), pp. 3096–3107.

Cui, X. *et al.* (2021) 'Regulation of *las* and *rhl* quorum sensing on aerobic denitrification in *Pseudomonas aeruginosa* PAO1', *Current Microbiology*, 78, pp. 659–667.

- Cutruzzolà, F. and Frankenberg-Dinkel, N. (2016) 'Origin and impact of nitric oxide in *Pseudomonas aeruginosa* biofilms', *Journal of Bacteriology*, 198(1), pp. 55–65.
- D'Autréaux, B. *et al.* (2002) 'Direct inhibition by nitric oxide of the transcriptional ferric uptake regulation protein via nitrosylation of the iron', *Proceedings of the National Academy of Sciences of the United States of America*, 99(26), pp. 16619–16624.
- Damron, F. H. *et al.* (2013) 'Construction of mobilizable mini-Tn7 vectors for bioluminescent detection of Gram-negative bacteria and single-copy promoter *lux* reporter analysis', *Applied and Environmental Microbiology*, 79(13), pp. 4149–4153.
- Darling, K. E. A. and Evans, T. J. (2003) 'Effects of nitric oxide on *Pseudomonas aeruginosa* infection of epithelial cells from a human respiratory cell line derived from a patient with cystic fibrosis', *Infection and Immunity*, 71(5), pp. 2341–2349.
- Das, T. *et al.* (2013) 'Pyocyanin facilitates extracellular DNA binding to *Pseudomonas aeruginosa* influencing cell surface properties and aggregation', *PLOS One*, 8(3), p. e58299.
- Davenport, P. W., Griffin, J. L. and Welch, M. (2015) 'Quorum sensing is accompanied by global metabolic changes in the opportunistic human pathogen *Pseudomonas aeruginosa*', *Journal of Bacteriology*, 197(12), pp. 2072–2082.
- Davies, E. V. *et al.* (2017) 'Evolutionary diversification of *Pseudomonas aeruginosa* in an artificial sputum model', *BMC Microbiology*, 17(3).
- Deforet, M., Van Ditmarsch, D. and Xavier, J. B. (2015) 'Cell-size homeostasis and the incremental rule in a bacterial pathogen', *Biophysical Journal*, 109(3), pp. 521–528.
- Van Delden, C. *et al.* (1998) 'Starvation selection restores elastase and rhamnolipid production in a *Pseudomonas aeruginosa* quorum-sensing mutant', *Infection and Immunity*, 66(9), pp. 4499–4502.
- DeLeon, S. *et al.* (2014) 'Synergistic interactions of *Pseudomonas aeruginosa* and *Staphylococcus aureus* in an *in vitro* wound model', *Infection and Immunity*, 82(11), pp. 4718–4728.
- Derichs, N. (2013) 'Targeting a genetic defect: cystic fibrosis transmembrane conductance regu-

lator modulators in cystic fibrosis', *European Respiratory Review*, 22(127), pp. 58–65.

Déziel, E. *et al.* (2004) 'Analysis of *Pseudomonas aeruginosa* 4-hydroxy-2-alkylquinolines (HAQs) reveals a role for 4-hydroxy-2-heptylquinoline in cell-to-cell communication', *Proceedings of the National Academy of Sciences of the United States of America*, 101(5), pp. 1339–1344.

Dietrich, L. E. P. *et al.* (2006) 'The phenazine pyocyanin is a terminal signalling factor in the quorum sensing network of *Pseudomonas aeruginosa*', *Molecular Microbiology*, 61(5), pp. 1308–1321.

Dietrich, L. E. P. *et al.* (2013) 'Bacterial community morphogenesis is intimately linked to the intracellular redox state', *Journal of Bacteriology*, 195(7), pp. 1371–1380.

Diggle, S. P. *et al.* (2003) 'The *Pseudomonas aeruginosa* quinolone signal molecule overcomes the cell density-dependency of the quorum sensing hierarchy, regulates *rhl*-dependent genes at the onset of stationary phase and can be produced in the absence of LasR', *Molecular Microbiology*, 50(1), pp. 29–43.

Diggle, S. P. *et al.* (2007) 'The *Pseudomonas aeruginosa* 4-quinolone signal molecules HHQ and PQS play multifunctional roles in quorum sensing and iron entrapment', *Chemistry & Biology*, 14(1), pp. 87–96.

Dimas Martins, A. and Gjini, E. (2020) 'Modeling competitive mixtures with the Lotka-Volterra framework for more complex fitness assessment between strains', *Frontiers in Microbiology*, 11 (572487).

Dolan, S. K., Kohlstedt, M., *et al.* (2020) 'Contextual flexibility in *Pseudomonas aeruginosa* central carbon metabolism during growth in single carbon sources', *mBio*, 11(e02684-19).

Dolan, S. K., Pereira, G., *et al.* (2020) 'Transcriptional regulation of central carbon metabolism in *Pseudomonas aeruginosa*', *Microbial Biotechnology*, 13(1), pp. 285–289.

Dolan, S. K. and Welch, M. (2018) 'The glyoxylate shunt, 60 years on', *Annual Review of Microbiology*, 72(1), pp. 309–330.

Donlan, R. M. (2002) 'Biofilms: microbial life on surfaces', *Emerging Infectious Diseases*, 8(9), pp. 881–890.

- Döring, G. (1997) 'Cystic fibrosis respiratory infections: interactions between bacteria and host defence', *Monaldi Archives for Chest Disease*, 52(4), pp. 363–366.
- Drees, S. L. and Fetzner, S. (2015) 'PqsE of *Pseudomonas aeruginosa* acts as pathway-specific thioesterase in the biosynthesis of alkylquinolone signaling molecules', *Chemistry & Biology*, 22(5), pp. 611–618.
- Dumas, Z., Ross-Gillespie, A. and Kümmerli, R. (2013) 'Switching between apparently redundant iron-uptake mechanisms benefits bacteria in changeable environments', *Proceedings of the Royal Society B: Biological Sciences*, 280(21031055).
- Durand, S. and Guillier, M. (2021) 'Transcriptional and post-transcriptional control of the nitrate respiration in bacteria', *Frontiers in Molecular Biosciences*, 8(667758).
- Emmerich, R. and Löw, O. (1899) 'Bakteriolytische Enzyme als Ursache der erworbenen Immunität und die Heilung von Infektionskrankheiten durch dieselben', *Zeitschrift für Hygiene und Infektionskrankheiten*, 31.
- Essar, D. W. *et al.* (1990) 'Identification and characterization of genes for a second anthranilate synthase in *Pseudomonas aeruginosa*: interchangeability of the two anthranilate synthases and evolutionary implications', *Journal of Bacteriology*, 172(2), pp. 884–900.
- Fang, F. C. (1997) 'Mechanisms of nitric oxide-related antimicrobial activity', *The Journal of Clinical Investigation*, 99(12), pp. 2818–2825.
- Fang, F. C. (2004) 'Antimicrobial reactive oxygen and nitrogen species: concepts and controversies', *Nature Reviews Microbiology*, 2(10), pp. 820–832.
- Farrow, J. M. *et al.* (2008) 'PqsE functions independently of PqsR-*Pseudomonas* quinolone signal and enhances the *rhl* quorum-sensing system', *Journal of Bacteriology*, 190(21), pp. 7043–7051.
- Feltner, J. B. *et al.* (2016) 'LasR variant cystic fibrosis isolates reveal an adaptable quorum-sensing hierarchy in *Pseudomonas aeruginosa*', *mBio*, 7(e01513-16).
- Fernández-Piñar, R. *et al.* (2008) 'A two-component regulatory system integrates redox state and

- population density sensing in *Pseudomonas putida*', *Journal of Bacteriology*, 190(23), pp. 7666–7674.
- Field, T. R. *et al.* (2010) 'The genus *Prevotella* in cystic fibrosis airways', *Anaerobe*, 16(4), pp. 337–344.
- Fletcher, M. P. *et al.* (2007) 'Biosensor-based assays for PQS, HHQ and related 2-alkyl-4-quinolone quorum sensing signal molecules', *Nature Protocols*, 2(5), pp. 1254–1262.
- Fordos, M. J. (1860) 'Recherches sur la matière colorante des suppurations bleues: pyocyanine', *Comptes rendus de l'Académie des Sciences*, 51, pp. 215–217.
- Frayman, K. B. *et al.* (2017) 'The lower airway microbiota in early cystic fibrosis lung disease: a longitudinal analysis', *Thorax*, 72(12), pp. 1104–1112.
- Frederix, M. and Downie, A. J. (2011) 'Quorum sensing: regulating the regulators', *Advances in Microbial Physiology*, 58, pp. 23–80.
- Friedman, L. and Kolter, R. (2004) 'Two genetic loci produce distinct carbohydrate-rich structural components of the *Pseudomonas aeruginosa* biofilm matrix', *Journal of Bacteriology*, 186(14), pp. 4457–4465.
- Fronhofer, E. A. *et al.* (2015) 'Condition-dependent movement and dispersal in experimental metacommunities', *Ecology Letters*, 18(9), pp. 954–963.
- Fuqua, W. C., Winans, S. C. and Greenberg, E. P. (1994) 'Quorum sensing in bacteria: the LuxR-LuxI family of cell density-responsive transcriptional regulators', *Journal of Bacteriology*, 176(2), pp. 269–275.
- Gallagher, L. A. *et al.* (2002) 'Functions required for extracellular quinolone signaling by *Pseudomonas aeruginosa*', *Journal of Bacteriology*, 184(23), pp. 6472–6480.
- Gambello, M. J. and Iglewski, B. H. (1991) 'Cloning and characterization of the *Pseudomonas aeruginosa lasR* gene, a transcriptional activator of elastase expression', *Journal of Bacteriology*, 173(9), pp. 3000–3009.
- Gamper, M., Zimmermann, A. and Haas, D. (1991) 'Anaerobic regulation of transcription ini-

tiation in the *arcDABC* operon of *Pseudomonas aeruginosa*', *Journal of Bacteriology*, 173(15), pp. 4742–4750.

Gaston, B. *et al.* (2002) 'Nitrogen redox balance in the cystic fibrosis airway: effects of anti-pseudomonal therapy', *American Journal of Respiratory and Critical Care Medicine*, 165(3), pp. 387–390.

Gates, A. J. *et al.* (2011) 'A composite biochemical system for bacterial nitrate and nitrite assimilation as exemplified by *Paracoccus denitrificans*', *Biochemical Journal*, 435(3), pp. 743–753.

Gayon, U. and Dupetit, G. (1886) 'Recherches sur la reduction des nitrates par les infinement petits', *Mémoires de la Société des Sciences Physiques et Naturelles de Bordeaux*, 3(2), pp. 201–307.

Gentzsch, M. and Mall, M. A. (2018) 'Ion channel modulators in cystic fibrosis', *Chest*, 154(2), pp. 383–393.

Gessard, C. (1882) 'Sur les colorations bleue et verte des linges à pansements', *Comptes rendus de l'Académie des Sciences*, 94, pp. 536–538.

Giardina, G. *et al.* (2008) 'NO sensing in *Pseudomonas aeruginosa*: structure of the transcriptional regulator DNR', *Journal of Molecular Biology*, 378(5), pp. 1002–1015.

Giardina, G. *et al.* (2009) 'A dramatic conformational rearrangement is necessary for the activation of DNR from *Pseudomonas aeruginosa*', *Proteins: Structure, Function and Bioinformatics*, 77(1), pp. 174–180.

Gilchrist, F. J. *et al.* (2015) 'Exhaled breath hydrogen cyanide as a marker of early *Pseudomonas aeruginosa* infection in children with cystic fibrosis', *ERJ Open Research*, 1(00044–2015).

Gillum, A. M., Tsay, E. Y. H. and Kirsch, D. R. (1984) 'Isolation of the *Candida albicans* gene for orotidine-5'-phosphate decarboxylase by complementation of *S. cerevisiae ura3* and *E. coli pyrF* mutations', *MGG Molecular & General Genetics*, 198, pp. 179–182.

Glasser, J. R. and Mallampalli, R. K. (2012) 'Surfactant and its role in the pathobiology of pulmonary infection', *Microbes and Infection*, 14(1), pp. 17–25.

- Glasser, N. R., Kern, S. E. and Newman, D. K. (2014) 'Phenazine redox cycling enhances anaerobic survival in *Pseudomonas aeruginosa* by facilitating generation of ATP and a proton-motive force', *Molecular Microbiology*, 92(2), pp. 399–412.
- Gomes, F. I. A. *et al.* (2009) 'Effect of farnesol on planktonic and biofilm cells of *Staphylococcus epidermidis*', *Current Microbiology*, 59(2), pp. 118–122.
- Goretski, J., Zafiriou, O. C. and Hollocher, T. C. (1990) 'Steady-state nitric oxide concentrations during denitrification', *Journal of Biological Chemistry*, 265(20), pp. 11535–11538.
- Govan, J. R. W. and Deretic, V. (1996) 'Microbial pathogenesis in cystic fibrosis: mucoid *Pseudomonas aeruginosa* and *Burkholderia cepacia*', *Microbiological Reviews*, 60(3), pp. 539–574.
- Grasemann, H. *et al.* (1998) 'Nitric oxide metabolites in cystic fibrosis lung disease', *Archives of Disease in Childhood*, 78, pp. 49–53.
- Grasemann, H. *et al.* (2000) 'Airway nitric oxide levels in cystic fibrosis are related to a polymorphism in the neuronal nitric oxide synthase gene', *American Journal of Respiratory and Critical Care Medicine*, 162(6), pp. 2172–2176.
- Grassi, L. *et al.* (2019) 'The antimicrobial peptide lin-SB056-1 and its dendrimeric derivative prevent *Pseudomonas aeruginosa* biofilm formation in physiologically relevant models of chronic infections', *Frontiers in Microbiology*, 10(198).
- Greenberg, D. P. and Stutman, H. R. (1991) 'Cystic fibrosis: infection and immunity to *Staphylococcus aureus* and *Haemophilus influenzae*', *Clinical Reviews in Allergy*, 9(1–2), pp. 75–86.
- Gupta, A. B. (1997) '*Thiosphaera pantotropha*: a sulphur bacterium capable of simultaneous heterotrophic nitrification and aerobic denitrification', *Enzyme and Microbial Technology*, 21(8), pp. 589–595.
- Haas, H. (2003) 'Molecular genetics of fungal siderophore biosynthesis and uptake: the role of siderophores in iron uptake and storage', *Applied Microbiology and Biotechnology*, 62(4), pp. 316–330.
- Haiko, J. *et al.* (2019) 'Coexistence of *Candida* species and bacteria in patients with cystic fi-

brosis', *European Journal of Clinical Microbiology & Infectious Diseases*, 38(6), pp. 1071–1077.

Haley, C. L., Colmer-Hamood, J. A. and Hamood, A. N. (2012) 'Characterization of biofilm-like structures formed by *Pseudomonas aeruginosa* in a synthetic mucus medium', *BMC Microbiology*, 12(181).

Hall, S. *et al.* (2016) 'Cellular effects of pyocyanin, a secreted virulence factor of *Pseudomonas aeruginosa*', *Toxins*, 8(236).

Hammond, J. H. *et al.* (2015) 'Links between Anr and quorum sensing in *Pseudomonas aeruginosa* biofilms', *Journal of Bacteriology*, 197(17), pp. 2810–2820.

Hardalo, C. and Edberg, S. C. (1997) '*Pseudomonas aeruginosa*: assessment of risk from drinking water', *Critical Reviews in Microbiology*, 23(1), pp. 47–75.

Hare, N. J. *et al.* (2012) 'Proteomics of *Pseudomonas aeruginosa* Australian epidemic strain 1 (AES-1) cultured under conditions mimicking the cystic fibrosis lung reveals increased iron acquisition via the siderophore pyochelin', *Journal of Proteome Research*, 11(2), pp. 776–795.

Härtig, E. *et al.* (1999) 'Nitrate and nitrite control of respiratory nitrate reduction in denitrifying *Pseudomonas stutzeri* by a two-component regulatory system homologous to NarXL of *Escherichia coli*', *Journal of Bacteriology*, 181(12), pp. 3658–3665.

Härtig, E. and Zumft, W. G. (1999) 'Kinetics of *nirS* expression (cytochrome *cd*₁ nitrite reductase) in *Pseudomonas stutzeri* during the transition from aerobic respiration to denitrification: evidence for a denitrification-specific nitrate- and nitrite-responsive regulator', *Journal of Bacteriology*, 181(1), pp. 161–166.

Hasegawa, N., Arai, H. and Igarashi, Y. (1998) 'Activation of a consensus FNR-dependent promoter by DNR of *Pseudomonas aeruginosa* in response to nitrite', *FEMS Microbiology Letters*, 166, pp. 213–217.

Hayashi, N. R. *et al.* (1998) 'The *nirQ* gene, which is required for denitrification of *Pseudomonas aeruginosa*, can activate the RubisCO from *Pseudomonas hydrogothermophila*', *Biochimica et Biophysica Acta*, 1381, pp. 347–350.

- Hays, E. E. *et al.* (1945) 'Antibiotic substances produced by *Pseudomonas aeruginosa*', *Journal of Biological Chemistry*, 159(3), pp. 725–750.
- Henderson, A. G. *et al.* (2014) 'Cystic fibrosis airway secretions exhibit mucin hyperconcentration and increased osmotic pressure', *Journal of Clinical Investigation*, 124(7), pp. 3047–3060.
- Henry, Y. and Bessières, P. (1984) 'Denitrification and nitrite reduction: *Pseudomonas aeruginosa* nitrite reductase', *Biochimie*, 66(4), pp. 259–289.
- Heymann, P. *et al.* (2002) 'The siderophore iron transporter of *Candida albicans* (Sit1p/Arn1p) mediates uptake of ferrichrome-type siderophores and is required for epithelial invasion', *Infection and Immunity*, 70(9), pp. 5246–5255.
- Hino, T. *et al.* (2010) 'Structural basis of biological N₂O generation by bacterial nitric oxide reductase', *Science*, 330(6011), pp. 1666–1670.
- Hogardt, M. *et al.* (2007) 'Stage-specific adaptation of hypermutable *Pseudomonas aeruginosa* isolates during chronic pulmonary infection in patients with cystic fibrosis', *The Journal of Infectious Diseases*, 195, pp. 70–80.
- Holloway, B. W. (1955) 'Genetic recombination in *Pseudomonas aeruginosa*', *Journal of General Microbiology*, 13(3), pp. 572–581.
- Huang, W. and Wilks, A. (2017) 'A rapid seamless method for gene knockout in *Pseudomonas aeruginosa*', *BMC Microbiology*, 17(199).
- Hurley, B. P. *et al.* (2011) 'The two-component sensor response regulator RoxS/RoxR plays a role in *Pseudomonas aeruginosa* interactions with airway epithelial cells', *Microbes and Infection*, 12(3), pp. 190–198.
- Ibberson, C. B. *et al.* (2017) 'Co-infecting microbes dramatically alter pathogen gene essentiality during polymicrobial infection', *Nature Microbiology*, 2(17079).
- Iglesias, Y. D. *et al.* (2020) 'Activity of antibiotics against *Staphylococcus aureus* in an *in vitro* model of biofilms in the context of cystic fibrosis: influence of the culture medium', *Antimicrobial Agents and Chemotherapy*, 63(7).

- Jackson, A. A. *et al.* (2013) 'Anr and its activation by PlcH activity in *Pseudomonas aeruginosa* host colonization and virulence', *Journal of Bacteriology*, 195(13), pp. 3093–3104.
- Jackson, A. A. *et al.* (2014) 'Global regulator Anr represses PlcH phospholipase activity in *Pseudomonas aeruginosa* when oxygen is limiting', *Microbiology*, 160, pp. 2215–2225.
- Jormakka, M. *et al.* (2004) 'Architecture of NarGH reveals a structural classification of Mo-bisMGD enzymes', *Structure*, 12, pp. 95–104.
- Joseph, T. A. *et al.* (2020) 'Compositional Lotka-Volterra describes microbial dynamics in the simplex', *PLOS Computational Biology*, 16(5).
- Joshi, R. V., Gunawan, C. and Mann, R. (2021) 'We are one: multispecies metabolism of a biofilm consortium and their treatment strategies', *Frontiers in Microbiology*, 12(635432).
- Juhas, M., Eberl, L. and Tümmler, B. (2005) 'Quorum sensing: the power of cooperation in the world of *Pseudomonas*', *Environmental Microbiology*, 7(4), pp. 459–471.
- Kakishima, K. *et al.* (2007) 'Participation of nitric oxide reductase in survival of *Pseudomonas aeruginosa* in LPS-activated macrophages', *Biochemical and Biophysical Research Communications*, 355(2), pp. 587–591.
- Kasetty, S. *et al.* (2021) 'Both *Pseudomonas aeruginosa* and *Candida albicans* accumulate greater biomass in dual-species biofilms under flow', *mSphere*, 6(3).
- Katsir, G. *et al.* (2015) 'The *Escherichia coli* NarL receiver domain regulates transcription through promoter specific functions', *BMC Microbiology*, 15(174).
- Kawakami, T. *et al.* (2010) 'Differential expression of multiple terminal oxidases for aerobic respiration in *Pseudomonas aeruginosa*', *Environmental Microbiology*, 12(6), pp. 1399–1412.
- Kern, S. E., Price-Whelan, A. and Newman, D. K. (2014) *Pseudomonas: Methods and Protocols, Methods in Molecular Biology*. Edited by A. Filloux and J.-L. Ramos. New York: Humana Press.
- Kerr, J. R. *et al.* (1999) '*Pseudomonas aeruginosa* pyocyanin and 1-hydroxyphenazine inhibit fungal

growth', *Journal of Clinical Pathology*, 52(5), pp. 385–387.

Kirchhoff, C. *et al.* (2018) 'Chemiosmotic energy conservation in *Dinoroseobacter shibae*: proton translocation driven by aerobic respiration, denitrification, and photosynthetic light reaction', *Frontiers in Microbiology*, 9(903).

Kirchner, S. *et al.* (2012) 'Use of artificial sputum medium to test antibiotic efficacy against *Pseudomonas aeruginosa* in conditions more relevant to the cystic fibrosis lung', *Journal of Visualized Experiments*, 64(e3857).

Kirketerp-Møller, K. *et al.* (2008) 'Distribution, organization, and ecology of bacteria in chronic wounds', *Journal of Clinical Microbiology*, 46(8), pp. 2717–2722.

Klausen, M. *et al.* (2003) 'Biofilm formation by *Pseudomonas aeruginosa* wild type, flagella and type IV pili mutants', *Molecular Microbiology*, 48(6), pp. 1511–1524.

Klepac-Ceraj, V. *et al.* (2010) 'Relationship between cystic fibrosis respiratory tract bacterial communities and age, genotype, antibiotics and *Pseudomonas aeruginosa*', *Environmental Microbiology*, 12(5), pp. 1293–1303.

Kolpen, M. *et al.* (2014) 'Nitrous oxide production in sputum of cystic fibrosis patients with chronic *Pseudomonas aeruginosa* lung infection', *PLOS One*, 9(e84353).

Konstan, M. W. *et al.* (2017) 'Assessment of safety and efficacy of long-term treatment with combination lumacaftor and ivacaftor therapy in patients with cystic fibrosis homozygous for the F508del-CFTR mutation (PROGRESS): a phase 3, extension study', *The Lancet Respiratory Medicine*, 5(2), pp. 107–118.

Korgaonkar, A. K. and Whiteley, M. (2011) '*Pseudomonas aeruginosa* enhances production of an antimicrobial in response to *N*-acetylglucosamine and peptidoglycan', *Journal of Bacteriology*, 193(4), pp. 909–917.

Kornberg, H. L. (1966) 'The role and control of the glyoxylate cycle in *Escherichia coli*', *The Biochemical Journal*, 99(1), pp. 1–11.

Kornberg, H. L. and Krebs, H. A. (1957) 'Synthesis of cell constituents from C₂-units by a mod-

ified tricarboxylic acid cycle', *Nature*, 179(4568), pp. 988–991.

Kornberg, H. L. and Madsen, N. B. (1958) 'The metabolism of C₂ compounds in microorganisms.', *The Biochemical Journal*, 68(3), pp. 549–557.

Kosztolowicz, T. *et al.* (2020) 'Modelling experimentally measured of ciprofloxacin antibiotic diffusion in *Pseudomonas aeruginosa* biofilm formed in artificial sputum medium', *PLOS One*, 15(12).

Kramer, J., Özkaya, Ö. and Kümmerli, R. (2020) 'Bacterial siderophores in community and host interactions', *Nature Reviews Microbiology*, 18, pp. 152–163.

Krebs, H. A. (1970a) 'Rate control of the tricarboxylic acid cycle', *Advances in Enzyme Regulation*, 8, pp. 335–353.

Krebs, H. A. (1970b) 'The history of the tricarboxylic acid cycle', *Perspectives in Biology and Medicine*, 14(1), pp. 154–170.

Kurachi, M. (1958) 'Studies on the biosynthesis of pyocyanine', *Bulletin of the Institute for Chemical Research, Kyoto University*, 36(6), pp. 174–187.

Kuroki, M. *et al.* (2014) 'Fine-tuned regulation of the dissimilatory nitrite reductase gene by oxygen and nitric oxide in *Pseudomonas aeruginosa*', *Environmental Microbiology Reports*, 6(6), pp. 792–801.

LaBauve, A. E. and Wargo, M. J. (2013) 'Growth and laboratory maintenance of *Pseudomonas aeruginosa*', *Current Protocols in Microbiology*, 31(9), pp. 1713–1723.

Lamont, I. L. *et al.* (2002) 'Siderophore-mediated signaling regulates virulence factor production in *Pseudomonas aeruginosa*', *Proceedings of the National Academy of Sciences of the United States of America*, 99(10), pp. 7072–7077.

LaPorte, D. C., Walsh, K. and Koshland, D. E. (1984) 'The branch point effect', *Journal of Biological Chemistry*, 259(22), pp. 14068–14075.

Laratta, W. P. *et al.* (2002) 'Involvement of the PrrB/PrrA two-component system in nitrite respiration in *Rhodobacter sphaeroides* 2.4.3: evidence for transcriptional regulation', *Journal of*

Bacteriology, 184(13), pp. 3521–3529.

Lau, C. K. Y., Krewulak, K. D. and Vogel, H. J. (2016) 'Bacterial ferrous iron transport: the Feo system', *FEMS Microbiology Reviews*, 40(2), pp. 273–298.

Lau, G. W. *et al.* (2004) 'The role of pyocyanin in *Pseudomonas aeruginosa* infection', *Trends in Molecular Medicine*, 10(12), pp. 599–606.

Laville, J. *et al.* (1998) 'Characterization of the *hcnABC* gene cluster encoding hydrogen cyanide synthase and anaerobic regulation by ANR in the strictly aerobic biocontrol agent *Pseudomonas fluorescens* CHA0', *Journal of Bacteriology*, 180(12), pp. 3187–3196.

Lazazzera, B. A. *et al.* (1996) 'DNA binding and dimerization of the Fe-S-containing FNR protein from *Escherichia coli* are regulated by oxygen', *Journal of Biological Chemistry*, 271(5), pp. 2762–2768.

Li, J. *et al.* (2021) 'Antibiotic intervention redispersed bacterial interspecific interacting dynamics in competitive environments', *Environmental Microbiology*, 23(12), pp. 7432–7444.

Lin, J. *et al.* (2018) 'The *Pseudomonas* quinolone signal (PQS): not just for quorum sensing anymore', *Frontiers in Cellular and Infection Microbiology*, 8(230).

Lin, Y.-C. *et al.* (2018) 'Phenazines regulate Nap-dependent denitrification in *Pseudomonas aeruginosa* biofilms', *Journal of Bacteriology*, 200(9).

Line, L. *et al.* (2014) 'Physiological levels of nitrate support anoxic growth by denitrification of *Pseudomonas aeruginosa* at growth rates reported in cystic fibrosis lungs and sputum', *Frontiers in Microbiology*, 5(554).

LiPuma, J. J. (2010) 'The changing microbial epidemiology in cystic fibrosis', *Clinical Microbiology Reviews*, 23(2), pp. 299–323.

Lister, P. D., Wolter, D. J. and Hanson, N. D. (2009) 'Antibacterial-resistant *Pseudomonas aeruginosa*: clinical impact and complex regulation of chromosomally encoded resistance mechanisms', *Clinical Microbiology Reviews*, 22(4), pp. 582–610.

Livingston, J. *et al.* (2022) 'Visualization of mRNA expression in *Pseudomonas aeruginosa* aggregates reveals spatial patterns of fermentative and denitrifying metabolism', *Applied and Environmental Microbiology*, 88(11), e00439-22.

Lotka, A. J. (1932) 'Contribution to the mathematical theory of capture', *Proceedings of the National Academy of Sciences of the United States of America*, 18(2), pp. 172–178.

Lücke, G. A. (1862) 'Pus bleu', *Virchows Archiv: European Journal of Pathology*.

Lyczak, J. B., Cannon, C. L. and Pier, G. B. (2000) 'Establishment of *Pseudomonas aeruginosa* infection: lessons from a versatile opportunist', *Microbes and Infection*, 2(9), pp. 1051–1060.

Lyczak, J. B., Cannon, C. L. and Pier, G. B. (2002) 'Lung infections associated with cystic fibrosis', *Clinical Microbiology Reviews*, 15(2), pp. 194–222.

Machida, K. *et al.* (1998) 'Farnesol-induced generation of reactive oxygen species via indirect inhibition of the mitochondrial electron transport chain in the yeast *Saccharomyces cerevisiae*', *Journal of Bacteriology*, 180(17), pp. 4460–4465.

Maisetta, G. *et al.* (2020) 'Targeting *Pseudomonas aeruginosa* in the sputum of primary ciliary dyskinesia patients with a combinatorial strategy having antibacterial and anti-virulence potential', *International Journal of Molecular Sciences*, 21(69).

Mashburn, L. M. *et al.* (2005) '*Staphylococcus aureus* serves as an iron source for *Pseudomonas aeruginosa* during *in vivo* coculture', *Journal of Bacteriology*, 187(2), pp. 554–566.

Maunder, E. and Welch, M. (2017) 'Matrix exopolysaccharides; the sticky side of biofilm formation', *FEMS Microbiology Letters*, 364(13).

Mavrodi, D. V. *et al.* (2001) 'Functional analysis of genes for biosynthesis of pyocyanin and phenazine-1-carboxamide from *Pseudomonas aeruginosa* PAO1', *Journal of Bacteriology*, 183(21), pp. 6454–6465.

Mayburd, A. L. and Kassner, R. J. (2002) 'Mechanism and biological role of nitric oxide binding to cytochrome *c*', *Biochemistry*, 41(39), pp. 11582–11591.

- McGuirl, M. A. *et al.* (2001) 'Expression, purification, and characterization of NosL, a novel Cu(I) protein of the nitrous oxide reductase (*nos*) gene cluster', *Journal of Biological Inorganic Chemistry*, 6(2), pp. 189–195.
- McKnight, S. L., Iglewski, B. H. and Pesci, E. C. (2000) 'The *Pseudomonas* quinolone signal regulates *rhl* quorum sensing in *Pseudomonas aeruginosa*', *Journal of Bacteriology*, 182(10), pp. 2702–2708.
- McVey, A. C. *et al.* (2020) '2-Aminopyridine analogs inhibit both enzymes of the glyoxylate shunt in *Pseudomonas aeruginosa*', *International Journal of Molecular Sciences*, 21(2490).
- Medina, G. *et al.* (2003) 'Mechanism of *Pseudomonas aeruginosa* RhlR transcriptional regulation of the *rhlAB* promoter', *Journal of Bacteriology*, 185(20), pp. 5976–5983.
- Möker, N., Dean, C. R. and Tao, J. (2010) '*Pseudomonas aeruginosa* increases formation of multi-drug-tolerant persister cells in response to quorum-sensing signaling molecules', *Journal of Bacteriology*, 192(7), pp. 1946–1955.
- Momeni, B., Xie, L. and Shou, W. (2017) 'Lotka-Volterra pairwise modeling fails to capture diverse pairwise microbial interactions', *eLife*, 6(e25051).
- Moore, E. G. and Gibson, Q. H. (1976) 'Cooperativity in the dissociation of nitric oxide from hemoglobin', *Journal of Biological Chemistry*, 251(9), pp. 2788–2794.
- Mukherjee, S. *et al.* (2017) 'The RhlR quorum-sensing receptor controls *Pseudomonas aeruginosa* pathogenesis and biofilm development independently of its canonical homoserine lactone autoinducer', *PLOS Pathogens*, 13(7).
- Murima, P. *et al.* (2016) 'A rheostat mechanism governs the bifurcation of carbon flux in mycobacteria', *Nature Communications*, 7, p. 12527.
- Müsken, M. *et al.* (2010) 'Genetic determinants of *Pseudomonas aeruginosa* biofilm establishment', *Microbiology*, 156(2), pp. 431–441.
- Neve, R. L., Carrillo, B. D. and Phelan, V. V. (2021) 'Impact of artificial sputum medium formulation on *Pseudomonas aeruginosa* secondary metabolite production', *Journal of Bacteriology*,

203(21), pp. 1–18.

Nikel, P. I., Pérez-Pantoja, D. and de Lorenzo, V. (2016) 'Pyridine nucleotide transhydrogenases enable redox balance of *Pseudomonas putida* during biodegradation of aromatic compounds', *Environmental Microbiology*, 18(10), pp. 3565–3582.

Nowak, E. *et al.* (2006) 'The structural basis of signal transduction for the response regulator PrrA from *Mycobacterium tuberculosis*', *Journal of Biological Chemistry*, 281(14), pp. 9659–9666.

O'Brien, T. J. *et al.* (2021) 'An *in vitro* model for the cultivation of polymicrobial biofilms under continuous-flow conditions', *F1000Research*, 10(801).

O'Brien, T. J. and Welch, M. (2019) 'A continuous-flow model for *in vitro* cultivation of mixed microbial populations associated with cystic fibrosis airway infections', *Frontiers in Microbiology*, 10(2713).

O'Neal, W. K. and Knowles, M. R. (2018) 'Cystic fibrosis disease modifiers: complex genetics defines the phenotypic diversity in a monogenic disease', *Annual Review of Genomics and Human Genetics*, 19, pp. 201–222.

Ochsner, U. A. and Reiser, J. (1995) 'Autoinducer-mediated regulation of rhamnolipid biosurfactant synthesis in *Pseudomonas aeruginosa*', *Proceedings of the National Academy of Sciences of the United States of America*, 92(14), pp. 6424–6428.

Oh, J.-I. and Kaplan, S. (2000) 'Redox signaling: globalization of gene expression', *The EMBO Journal*, 19(16), pp. 4237–4247.

Oliver, A. and Mena, A. (2010) 'Bacterial hypermutation in cystic fibrosis, not only for antibiotic resistance', *Clinical Microbiology and Infection*, 16(7), pp. 798–808.

Osamura, T. *et al.* (2017) 'Specific expression and function of the A-type cytochrome *c* oxidase under starvation conditions in *Pseudomonas aeruginosa*', *PLOS One*, 12(5).

Palmer, K. L., Aye, L. M. and Whiteley, M. (2007) 'Nutritional cues control *Pseudomonas aeruginosa* multicellular behavior in cystic fibrosis sputum', *Journal of Bacteriology*, 189(22), pp. 8079–8087.

- Palmer, K. L., Brown, S. A. and Whiteley, M. (2007) 'Membrane-bound nitrate reductase is required for anaerobic growth in cystic fibrosis sputum', *Journal of Bacteriology*, 189(12), pp. 4449–4455.
- Paranjape, S. M. and Mogayzel, P. J. J. (2014) 'Cystic fibrosis', *Pediatrics In Review*, 35(5), pp. 194–205.
- Parkins, M. D. and Floto, R. A. (2015) 'Emerging bacterial pathogens and changing concepts of bacterial pathogenesis in cystic fibrosis', *Journal of Cystic Fibrosis*, 14(3), pp. 293–304.
- Parsek, M. R. and Singh, P. K. (2003) 'Bacterial biofilms: an emerging link to disease pathogenesis', *Annual Review of Microbiology*, 57, pp. 677–701.
- Pasqua, M. *et al.* (2017) 'Ferric uptake regulator Fur is conditionally essential in *Pseudomonas aeruginosa*', *Journal of Bacteriology*, 199(22).
- Pauleta, S. R., Dell'Acqua, S. and Moura, I. (2013) 'Nitrous oxide reductase', *Coordination Chemistry Reviews*, 257(2), pp. 332–349.
- Payne, S. M. (1994) 'Detection, isolation, and characterization of siderophores', *Methods in Enzymology*, 235, pp. 329–344.
- Pearson, J. P. *et al.* (1994) 'Structure of the autoinducer required for expression of *Pseudomonas aeruginosa* virulence genes', *Proceedings of the National Academy of Sciences of the United States of America*, 91(1), pp. 197–201.
- Pearson, J. P. *et al.* (1995) 'A second *N*-acylhomoserine lactone signal produced by *Pseudomonas aeruginosa*', *Proceedings of the National Academy of Sciences of the United States of America*, 92(5), pp. 1490–1494.
- Pesci, E. C. *et al.* (1999) 'Quinolone signaling in the cell-to-cell communication system of *Pseudomonas aeruginosa*', *Proceedings of the National Academy of Sciences of the United States of America*, 96(20), pp. 11229–11234.
- Pihet, M. *et al.* (2009) 'Occurrence and relevance of filamentous fungi in respiratory secretions of patients with cystic fibrosis — a review', *Medical Mycology*, 47(4), pp. 387–397.

- Poole, K. (2001) 'Multidrug efflux pumps and antimicrobial resistance in *Pseudomonas aeruginosa* and related organisms', *Journal of Molecular Microbiology and Biotechnology*, 3(2), pp. 255–264.
- Price-Whelan, A., Dietrich, L. E. P. and Newman, D. K. (2006) 'Rethinking “secondary” metabolism: physiological roles for phenazine antibiotics', *Nature Chemical Biology*, 2(2), pp. 71–78.
- Price-Whelan, A., Dietrich, L. E. P. and Newman, D. K. (2007) 'Pyocyanin alters redox homeostasis and carbon flux through central metabolic pathways in *Pseudomonas aeruginosa* PA14', *Journal of Bacteriology*, 189(17), pp. 6372–6381.
- Pulcrano, G. *et al.* (2012) 'Different mutations in *mucA* gene of *Pseudomonas aeruginosa* mucoid strains in cystic fibrosis patients and their effect on *algU* gene expression', *New Microbiologica*, 35(3), pp. 295–305.
- Quinn, R. A. *et al.* (2014) 'Biogeochemical forces shape the composition and physiology of polymicrobial communities in the cystic fibrosis lung', *mBio*, 5(2).
- Quinn, R. A. *et al.* (2016) 'Ecological networking of cystic fibrosis lung infections', *npj Biofilms and Microbiomes*, 2(4).
- Rada, B. and Leto, T. L. (2013) 'Pyocyanin effects on respiratory epithelium: relevance in *Pseudomonas aeruginosa* airway infections', *Trends in Microbiology*, 21(2), pp. 73–81.
- Raji El Feghali, P. A. and Nawas, T. (2018) 'Pyocyanin: a powerful inhibitor of bacterial growth and biofilm formation', *Madridge Journal of Case Reports and Studies*, 3(1), pp. 101–107.
- Ratjen, F. and Döring, G. (2003) 'Cystic fibrosis', *The Lancet*, 361, pp. 681–689.
- Renilla, S. *et al.* (2012) 'Acetate scavenging activity in *Escherichia coli*: interplay of acetyl-CoA synthetase and the PEP-glyoxylate cycle in chemostat cultures', *Applied Microbiology and Biotechnology*, 93(5), pp. 2109–2124.
- Rigauts, C. *et al.* (2021) '*Rothia mucilaginosa* is an anti-inflammatory bacterium in the respiratory tract of patients with chronic lung disease', *European Respiratory Journal*, 59(5), p. 2101293.

- Rinaldo, S. *et al.* (2011) 'Observation of fast release of NO from ferrous d_1 haem allows formulation of a unified reaction mechanism for cytochrome cd_1 nitrite reductases', *Biochemical Journal*, 435(1), pp. 217–225.
- Rinaldo S, Cutruzzolà F. (2007) 'Nitrite reductases in denitrification'. In: Bothe H, Ferguson SJ, Newton WE, Eds. *Biology of the Nitrogen Cycle*. Amsterdam: Elsevier. 37–55.
- Riordan, J. R. *et al.* (1989) 'Identification of the cystic fibrosis gene: cloning and characterization of complementary DNA', *Science*, 245, pp. 1066–1073.
- Rossi, E. *et al.* (2018) 'High-resolution in situ transcriptomics of *Pseudomonas aeruginosa* unveils genotype independent patho-phenotypes in cystic fibrosis lungs', *Nature Communications*, 9(3459).
- Rust, L., Pesci, E. C. and Iglewski, B. H. (1996) 'Analysis of the *Pseudomonas aeruginosa* elastase (*lasB*) regulatory region', *Journal of Bacteriology*, 178(4), pp. 1134–1140.
- Ryall, B. *et al.* (2008) '*Pseudomonas aeruginosa*, cyanide accumulation and lung function in CF and non-CF bronchiectasis patients', *European Respiratory Journal*, 32(3), pp. 740–747.
- Sajjan, U. *et al.* (2001) 'Enhanced susceptibility to pulmonary infection with *Burkholderia cepacia* in *Cftr*^{-/-} mice', *Infection and Immunity*, 69(8), pp. 5138–5150.
- Della Sala, G. *et al.* (2019) 'The chemical language of Gram-negative bacteria'. In Tommonaro G, Ed. *Quorum Sensing*. Cambridge, MA, USA: Academic Press. 3–28.
- Sauer, U. *et al.* (2004) 'The soluble and membrane-bound transhydrogenases UdhA and PntAB have divergent functions in NADPH metabolism of *Escherichia coli*', *Journal of Biological Chemistry*, 279(8), pp. 6613–6619.
- Sawers, R. G. (1991) 'Identification and molecular characterization of a transcriptional regulator from *Pseudomonas aeruginosa* PAO1 exhibiting structural and functional similarity to the FNR protein of *Escherichia coli*', *Molecular Microbiology*, 5(6), pp. 1469–1481.
- Schertzer, J. W., Boulette, M. L. and Whiteley, M. (2009) 'More than a signal: non-signaling properties of quorum sensing molecules', *Trends in Microbiology*, 17(5), pp. 189–195.

- Schiessl, K. T. *et al.* (2019) 'Phenazine production promotes antibiotic tolerance and metabolic heterogeneity in *Pseudomonas aeruginosa* biofilms', *Nature Communications*, 10(762).
- Schobert, M. and Jahn, D. (2010) 'Anaerobic physiology of *Pseudomonas aeruginosa* in the cystic fibrosis lung', *International Journal of Medical Microbiology*, 300(8), pp. 549–556.
- Schreiber, K. *et al.* (2007) 'The anaerobic regulatory network required for *Pseudomonas aeruginosa* nitrate respiration', *Journal of Bacteriology*, 189(11), pp. 4310–4314.
- Schroder, I. *et al.* (1994) 'Phosphorylation and dephosphorylation of the NarQ, NarX, and NarL proteins of the nitrate-dependent two-component regulatory system of *Escherichia coli*', *Journal of Bacteriology*, 176(16), pp. 4985–4992.
- Schuster, M. *et al.* (2004) 'The *Pseudomonas aeruginosa* RpoS regulon and its relationship to quorum sensing', *Molecular Microbiology*, 51(4), pp. 973–985.
- Schweizer, H. P. and Po, C. (1996) 'Regulation of glycerol metabolism in *Pseudomonas aeruginosa*: characterization of the *glpR* repressor gene', *Journal of Bacteriology*, 178(17), pp. 5215–5221.
- Schwermer, C. U., Beer, D. de and Stoodley, P. (2022) 'Nitrate respiration occurs throughout the depth of mucoid and non-mucoid *Pseudomonas aeruginosa* submerged agar colony biofilms including the oxic zone', *Scientific Reports*, 12(8557).
- Scofield, J. A. and Wu, H. (2016) 'Nitrite reductase is critical for *Pseudomonas aeruginosa* survival during co-infection with the oral commensal *Streptococcus parasanguinis*', *Microbiology*, 162(2), pp. 376–383.
- Sédillot, C.-E. (1849) *De l'infection purulente ou pyoémie*. Paris: Jean-Baptiste Baillière.
- Semighini, C. P. *et al.* (2006) 'Farnesol-induced apoptosis in *Aspergillus nidulans* reveals a possible mechanism for antagonistic interactions between fungi', *Molecular Microbiology*, 59(3), pp. 753–764.
- Sharma, V., Noriega, C. E. and Rowe, J. J. (2006) 'Involvement of NarK1 and NarK2 proteins in transport of nitrate and nitrite in the denitrifying bacterium *Pseudomonas aeruginosa* PAO1',

Applied and Environmental Microbiology, 72(1), pp. 695–701.

Shiro, Y. (2012) 'Structure and function of bacterial nitric oxide reductases', *Biochimica et Biophysica Acta - Bioenergetics*, 1817(10), pp. 1907–1913.

Shirtliff, M. E. *et al.* (2009) 'Farnesol-induced apoptosis in *Candida albicans*', *Antimicrobial Agents and Chemotherapy*, 53(6), pp. 2392–2401.

Skaar, E. P. and Hammer, N. D. (2011) 'Molecular mechanisms of *Staphylococcus aureus* iron acquisition', *Annual Review of Microbiology*, 65(10), pp. 129–147.

Smith, D. *et al.* (2013) 'Hydrogen cyanide, a volatile biomarker of *Pseudomonas aeruginosa* infection', *Journal of Breath Research*, 7(4).

Smith, E. E. *et al.* (2006) 'Genetic adaptation by *Pseudomonas aeruginosa* to the airways of cystic fibrosis patients', *Proceedings of the National Academy of Sciences of the United States of America*, 103(22), pp. 8487–8492.

Smith, N. W. *et al.* (2019) 'The classification and evolution of bacterial cross-feeding', *Frontiers in Ecology and Evolution*, 7(153).

Soum, E. and Drapier, J. C. (2003) 'Nitric oxide and peroxy nitrite promote complete disruption of the [4Fe-4S] cluster of recombinant human iron regulatory protein 1', *Journal of Biological Inorganic Chemistry*, 8(1–2), pp. 226–232.

Sriramulu, D. D. *et al.* (2005) 'Microcolony formation: a novel biofilm model of *Pseudomonas aeruginosa* for the cystic fibrosis lung', *Journal of Medical Microbiology*, 54(7), pp. 667–676.

Stewart, P. S. (2003) 'Diffusion in biofilms', *Journal of Bacteriology*, 185(5), pp. 1485–1491.

Stover, C. K. *et al.* (2000) 'Complete genome sequence of *Pseudomonas aeruginosa* PAO1, an opportunistic pathogen', *Nature*, 406(6799), pp. 959–964.

Stutts, M. J. *et al.* (1986) 'Oxygen consumption and ouabain binding sites in cystic fibrosis nasal epithelium', *Pediatric Research*, 20(12), pp. 1316–1320.

- Sugishima, M. *et al.* (2007) 'Alternative cyanide-binding modes to the haem iron in haem oxygenase', *Acta Crystallographica Section F: Structural Biology and Crystallization Communications*, 63(6), pp. 471–474.
- Sun, Z. *et al.* (2014) 'Blocking phosphatidylcholine utilization in *Pseudomonas aeruginosa*, via mutagenesis of fatty acid, glycerol and choline degradation pathways, confirms the importance of this nutrient source *in vivo*', *PLOS One*, 9(7).
- Swift, S. *et al.* (1997) 'Quorum sensing in *Aeromonas hydrophila* and *Aeromonas salmonicida*: identification of the LuxRI homologs AhyRI and AsaRI and their cognate *N*-acylhomoserine lactone signal molecules', *Journal of Bacteriology*, 179(17), pp. 5271–5281.
- Szenk, M., Dill, K. A. and de Graff, A. M. R. (2017) 'Why do fast-growing bacteria enter overflow metabolism? Testing the membrane real estate hypothesis', *Cell Systems*, 5(2), pp. 95–104.
- Takase, H. *et al.* (2000) 'Requirement of the *Pseudomonas aeruginosa tonB* gene for high-affinity iron acquisition and infection', *Infection and Immunity*, 68(8), pp. 4498–4504.
- Tang, A. C. *et al.* (2014) 'Current concepts: host-pathogen interactions in cystic fibrosis airways disease', *European Respiratory Review*, 23(133), pp. 320–332.
- Thomas, P. *et al.* (2015) 'Optimization of single plate-serial dilution spotting (SP-SDS) with sample anchoring as an assured method for bacterial and yeast CFU enumeration and single colony isolation from diverse samples', *Biotechnology Reports*, 8, pp. 45–55.
- Toole, G. O., Kaplan, H. B. and Kolter, R. (2000) 'Biofilm formation as microbial development', *Annual Review of Microbiology*, 54, pp. 49–79.
- Toyofuku, M. *et al.* (2007) 'Quorum sensing regulates denitrification in *Pseudomonas aeruginosa* PAO1', *Journal of Bacteriology*, 189(13), pp. 4969–4972.
- Toyofuku, M. *et al.* (2008) 'Influence of the *Pseudomonas* quinolone signal on denitrification in *Pseudomonas aeruginosa*', *Journal of Bacteriology*, 190(24), pp. 7947–7956.
- Treangen, T. J. *et al.* (2014) 'Complete genome sequence of the quality control strain *Staphylococcus aureus* subsp. *aureus* ATCC 25923', *Genome Announcements*, 2(6), p. 25923.

Troxell, B. and Hassan, H. M. (2013) 'Transcriptional regulation by Ferric Uptake Regulator (Fur) in pathogenic bacteria', *Frontiers in Cellular and Infection Microbiology*, 3(59).

Turner, K. H. *et al.* (2015) 'Essential genome of *Pseudomonas aeruginosa* in cystic fibrosis sputum', *Proceedings of the National Academy of Sciences of the United States of America*, 112(13), pp. 4110–4115.

Vallières, E. and Elborn, J. S. (2014) 'Cystic fibrosis gene mutations: evaluation and assessment of disease severity', *Advances in Genomics and Genetics*, 4, p. 161.

Vemuri, G. N. *et al.* (2006) 'Overflow metabolism in *Escherichia coli* during steady-state growth: transcriptional regulation and effect of the redox ratio', *Applied and Environmental Microbiology*, 72(5), pp. 3653–3661.

Vemuri, G. N. *et al.* (2007) 'Increasing NADH oxidation reduces overflow metabolism in *Saccharomyces cerevisiae*', *Proceedings of the National Academy of Sciences of the United States of America*, 104(7), pp. 2402–2407.

Visca, P., Imperi, F. and Lamont, I. L. (2007) 'Pyoverdine siderophores: from biogenesis to biosignificance', *Trends in Microbiology*, 15(1), pp. 22–30.

Waksman, S. A. (1973) 'History of the Word "Antibiotic"', *Journal of the History of Medicine and Allied Sciences*, XXVIII(3), pp. 284–286.

Walsh, K. and Koshland, D. E. (1984) 'Determination of flux through the branch point of two metabolic cycles', *Journal of Biological Chemistry*, 259(15), pp. 9646–9654.

Walsh, K. and Koshland, D. E. (1985) 'Branch point control by the phosphorylation state of isocitrate dehydrogenase: a quantitative examination of fluxes during a regulatory transition', *Journal of Biological Chemistry*, 260(14), pp. 8430–8437.

Wang, S. *et al.* (2013) 'A spider web strategy of type IV pili-mediated migration to build a fibre-like Psl polysaccharide matrix in *Pseudomonas aeruginosa* biofilms', *Environmental Microbiology*, 15(8), pp. 2238–2253.

Wang, S. *et al.* (2015) 'The exopolysaccharide PsI-eDNA interaction enables the formation of a biofilm skeleton in *Pseudomonas aeruginosa*', *Environmental Microbiology Reports*, 7(2), pp. 330–340.

Wang, Y. *et al.* (2011) 'Phenazine-1-carboxylic acid promotes bacterial biofilm development via ferrous iron acquisition', *Journal of Bacteriology*, 193(14), pp. 3606–3617.

Wang, Y., Kern, S. E. and Newman, D. K. (2010) 'Endogenous phenazine antibiotics promote anaerobic survival of *Pseudomonas aeruginosa* via extracellular electron transfer', *Journal of Bacteriology*, 192(1), pp. 365–369.

Wells, I. C. (1952) 'Antibiotic substances produced by *Pseudomonas aeruginosa*; syntheses of Pyo Ib, Pyo Ic, and Pyo III', *Journal of Biological Chemistry*, 196(1), pp. 331–340.

Whiteley, M. and Greenberg, E. P. (2001) 'Promoter specificity elements in *Pseudomonas aeruginosa* quorum-sensing-controlled genes', *Journal of Bacteriology*, 183(19), pp. 5529–5534.

Whooley, M. A. and McLoughlin, A. J. (1982) 'The regulation of pyocyanin production in *Pseudomonas aeruginosa*', *European Journal of Applied Microbiology and Biotechnology*, 15(3), pp. 161–166.

Wilderman, P. J. *et al.* (2001) 'Characterization of an endoprotease (PrpL) encoded by a PvdS-regulated gene in *Pseudomonas aeruginosa*', *Infection and Immunity*, 69(9), pp. 5385–5394.

Williams, H. D., Zlosnik, J. E. A. and Ryall, B. (2006) 'Oxygen, cyanide and energy generation in the cystic fibrosis pathogen *Pseudomonas aeruginosa*', *Advances in Microbial Physiology*, 52(6), pp. 1–71.

Williamson, K. S. *et al.* (2012) 'Heterogeneity in *Pseudomonas aeruginosa* biofilms includes expression of ribosome hibernation factors in the antibiotic-tolerant subpopulation and hypoxia-induced stress response in the metabolically active population', *Journal of Bacteriology*, 194(8), pp. 2062–2073.

Wilton, M. *et al.* (2016) 'Extracellular DNA acidifies biofilms and induces aminoglycoside resistance in *Pseudomonas aeruginosa*', *Antimicrobial Agents and Chemotherapy*, 60(1), pp. 544–553.

Winson, M. K. *et al.* (1998) 'Construction and analysis of *luxCDABE*-based plasmid sensors for

investigating *N*-acylhomoserine lactone-mediated quorum sensing', *FEMS Microbiology Letters*, 163(2), pp. 185–192.

Withers, H., Swift, S. and Williams, P. (2001) 'Quorum sensing as an integral component of gene regulatory networks in Gram-negative bacteria', *Current Opinion in Microbiology*, 4(2), pp. 186–193.

Woodhead, G. S. and Wood, G. E. C. (1889) 'De l'action antidotique exercée par les liquides pyocyaniques sur le cours de la maladie charbonneuse', *Comptes rendus de l'Académie des Sciences*.

Woodmansee, A. N. and Imlay, J. A. (2003) 'A mechanism by which nitric oxide accelerates the rate of oxidative DNA damage in *Escherichia coli*', *Molecular Microbiology*, 49(1), pp. 11–22.

Worlitzsch, D. *et al.* (2002) 'Effects of reduced mucus oxygen concentration in airway *Pseudomonas* infections of cystic fibrosis patients', *The Journal of Clinical Investigation*, 109(3), pp. 317–325.

Wu, J. and Bauer, C. E. (2010) 'RegB kinase activity is controlled in part by monitoring the ratio of oxidized to reduced ubiquinones in the ubiquinone pool', *mBio*, 1(5).

Wu, X. *et al.* (2019) '*In vivo* proteome of *Pseudomonas aeruginosa* in airways of cystic fibrosis patients', *Journal of Proteome Research*, 18(6), pp. 2601–2612.

Xu, K. D. *et al.* (1998) 'Spatial physiological heterogeneity in *Pseudomonas aeruginosa* biofilm is determined by oxygen availability', *Applied and Environmental Microbiology*, 64(10), pp. 4035–4039.

Xu, L. *et al.* (2020) 'Stochastic generalized Lotka-Volterra model with an application to learning microbial community structures', *arXiv:2009.10922*.

Yamamoto, K. *et al.* (2005) 'Functional characterization *in vitro* of all two-component signal transduction systems from *Escherichia coli*', *Journal of Biological Chemistry*, 280(2), pp. 1448–1456.

Yates, E. A. *et al.* (2002) '*N*-acylhomoserine lactones undergo lactonolysis in a pH-, temperature-, and acyl chain length-dependent manner during growth of *Yersinia pseudotuberculosis* and *Pseudomonas aeruginosa*', *Infection and Immunity*, 70(10), pp. 5635–5646.

- Ye, R. W. *et al.* (1995) 'Anaerobic activation of the entire denitrification pathway in *Pseudomonas aeruginosa* requires Anr, an analog of Fnr', *Journal of Bacteriology*, 177(12), pp. 3606–3609.
- Yoon, S. S. *et al.* (2002) '*Pseudomonas aeruginosa* anaerobic respiration in biofilms: relationships to cystic fibrosis pathogenesis', *Developmental Cell*, 3(4), pp. 593–603.
- Yoon, S. S. *et al.* (2006) 'Anaerobic killing of mucoid *Pseudomonas aeruginosa* by acidified nitrite derivatives under cystic fibrosis airway conditions', *Journal of Clinical Investigation*, 116(2), pp. 436–446.
- Yoon, S. S. *et al.* (2007) 'Two-pronged survival strategy for the major cystic fibrosis pathogen, *Pseudomonas aeruginosa*, lacking the capacity to degrade nitric oxide during anaerobic respiration', *The EMBO Journal*, 26(15), pp. 3662–3672.
- Youard, Z. A., Wenner, N. and Reimann, C. (2011) 'Iron acquisition with the natural siderophore enantiomers pyochelin and enantio-pyochelin in *Pseudomonas aeruginosa*', *Biometals*, 24(3), pp. 513–522.
- Yung, D. B. Y., Sircombe, K. J. and Pletzer, D. (2021) 'Friends or enemies? The complicated relationship between *Pseudomonas aeruginosa* and *Staphylococcus aureus*', *Molecular Microbiology*, 116.
- Zender, M. *et al.* (2016) 'Dissecting the multiple roles of PqsE in *Pseudomonas aeruginosa* virulence by discovery of small tool compounds', *ACS Chemical Biology*, 11(6), pp. 1755–1763.
- Zhao, K. *et al.* (2013) 'Psl trails guide exploration and microcolony formation in early *P. aeruginosa* biofilms', *Nature*, 497(7449), pp. 388–391.
- Zheng, S. *et al.* (2004) 'Impaired nitric oxide synthase-2 signaling pathway in cystic fibrosis airway epithelium', *American Journal of Physiology - Lung Cellular and Molecular Physiology*, 287, pp. 374–381.
- Zhu, X., Rice, S. A. and Barraud, N. (2019) 'Nitric oxide and iron signaling cues have opposing effects on biofilm development in *Pseudomonas aeruginosa*', *Applied and Environmental Microbiology*, 85(3).

Zhu, Z. *et al.* (2020) 'Quorum sensing systems regulate heterotrophic nitrification-aerobic denitrification by changing the activity of nitrogen-cycling enzymes', *Environmental Science and Ecotechnology*, 2(100026).

Zhuang, K., Vemuri, G. N. and Mahadevan, R. (2011) 'Economics of membrane occupancy and respiro-fermentation', *Molecular Systems Biology*, 7(500).

Zimmermann, A. *et al.* (1991) 'Anaerobic growth and cyanide synthesis of *Pseudomonas aeruginosa* depend on *anr*, a regulatory gene homologous with *fnr* of *Escherichia coli*', *Molecular Microbiology*, 5(6), pp. 1483–1490.

Zumft, W. G. (1997) 'Cell biology and molecular basis of denitrification', *Microbiology and Molecular Biology Reviews*, 61(4), pp. 533–616.

Zumft, W. G. and Kroneck, P. M. H. (2006) 'Respiratory transformation of nitrous oxide (N₂O) to dinitrogen by bacteria and archaea', *Advances in Microbial Physiology*, 52, pp. 107–227.

Appendices

Appendix A: NAD(P)(H) measurements

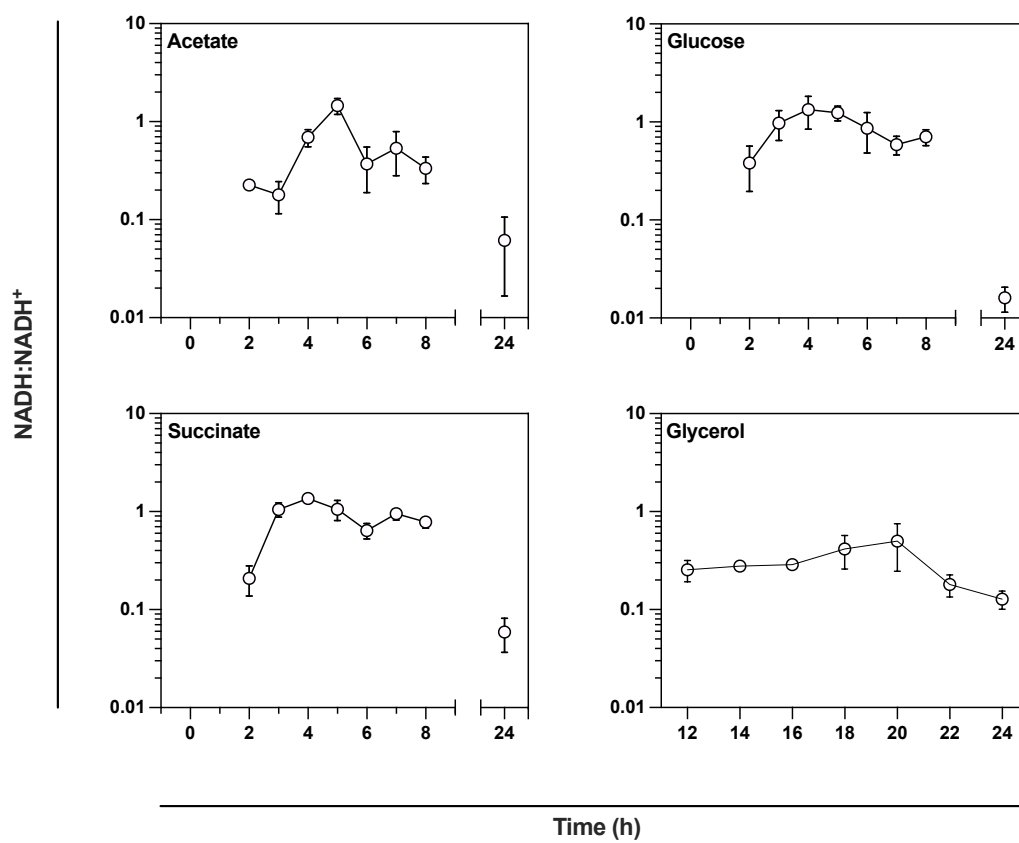


FIGURE A1. NADH:NAD⁺ ratios of *P. aeruginosa* wild type cultured in MOPS with 40 mM acetate, 15 mM glucose, 30 mM succinate, or 30 mM glycerol. Mean and standard deviation of at least three biological replicates.

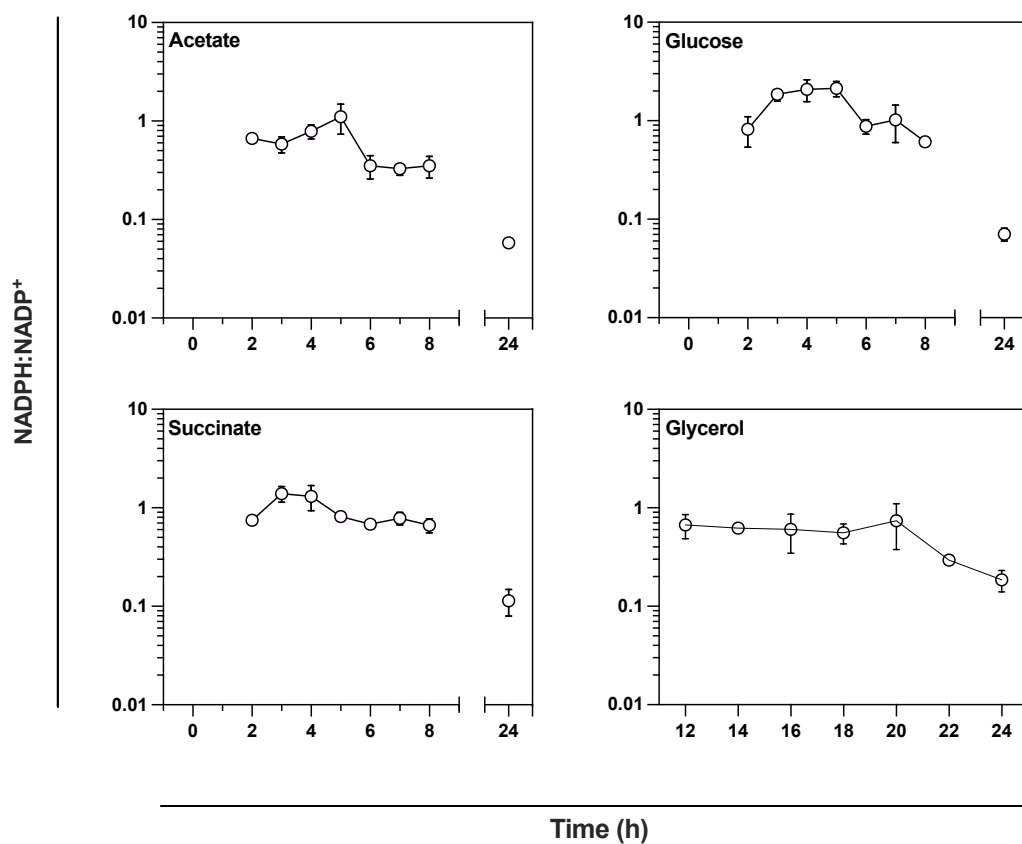


FIGURE A2. NADPH:NADP⁺ ratios of *P. aeruginosa* wild type cultured in MOPS with 40 mM acetate, 15 mM glucose, 30 mM succinate, or 30 mM glycerol. Mean and standard deviation of at least three biological replicates.

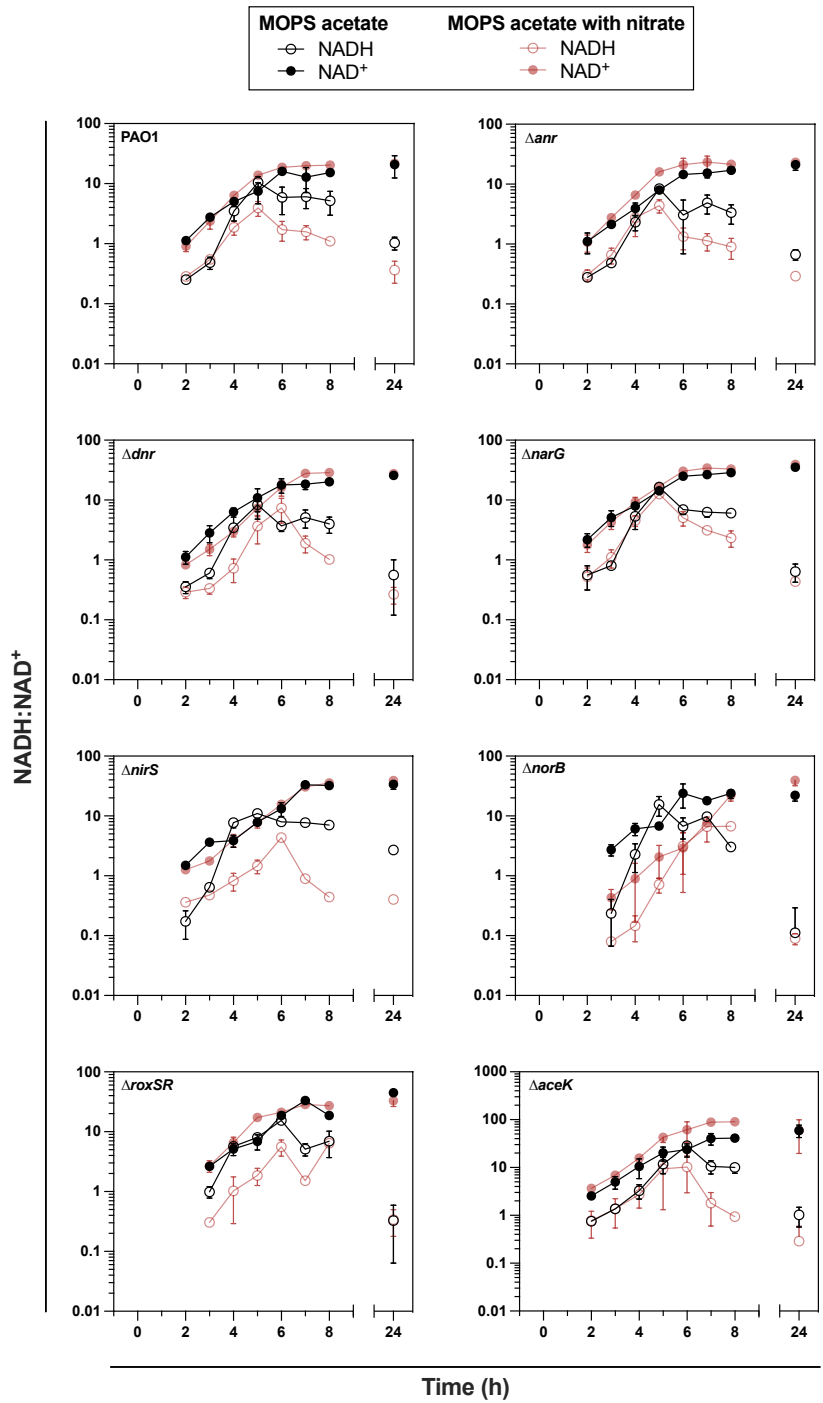


FIGURE A3. Split NAD(H) concentrations during 24 hours of growth of *P. aeruginosa* cultured in MOPS with 40 mM acetate or MOPS with 40 mM acetate and 20 mM KNO₃. Mean and standard deviation of at least three biological replicates.

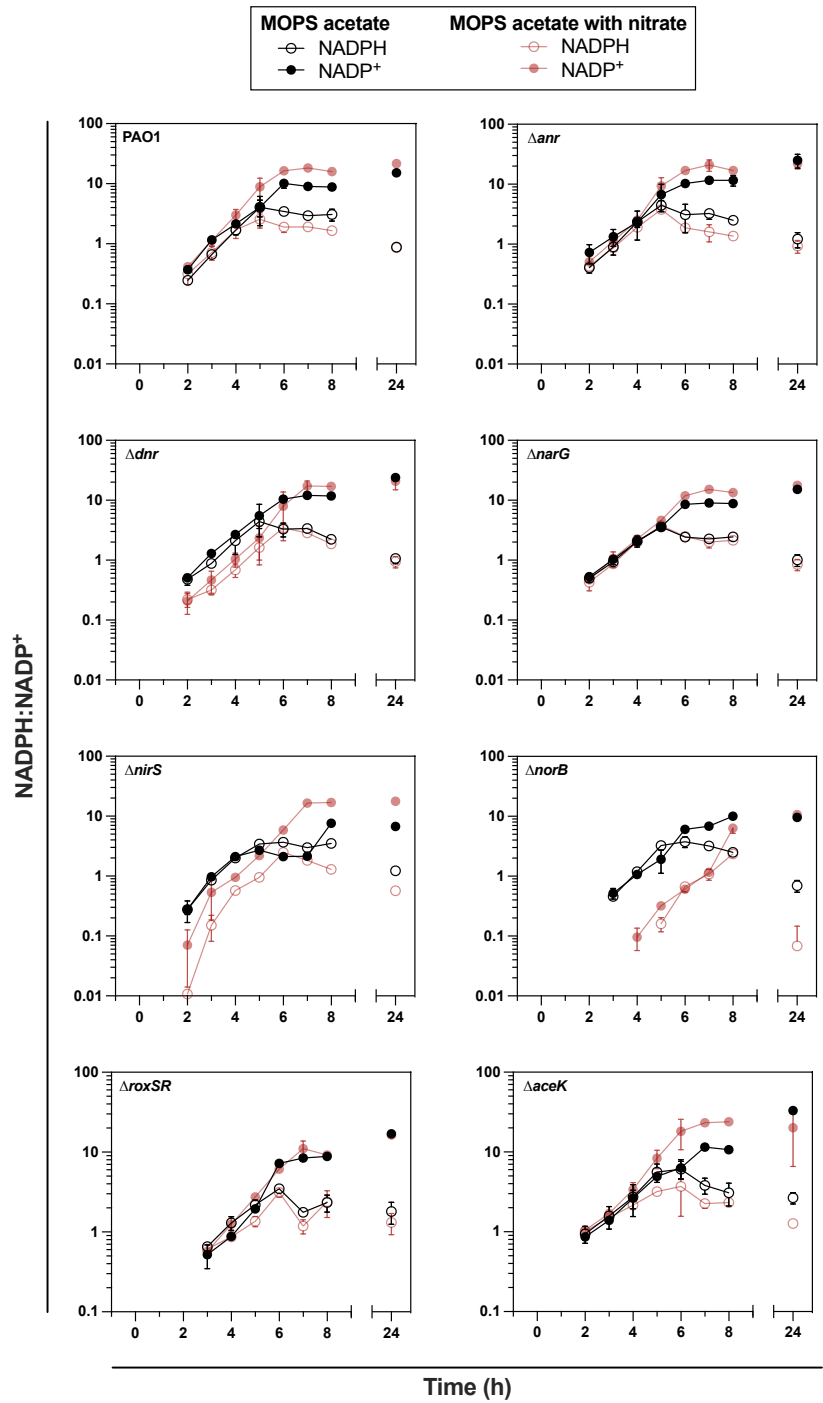


FIGURE A4. Split NADP(H) concentrations during 24 hours of growth of *P. aeruginosa* cultured in MOPS with 40 mM acetate or MOPS with 40 mM acetate and 20 mM KNO₃. Mean and standard deviation of at least three biological replicates.

Appendix B: quorum sensing gene promoter activity measurements

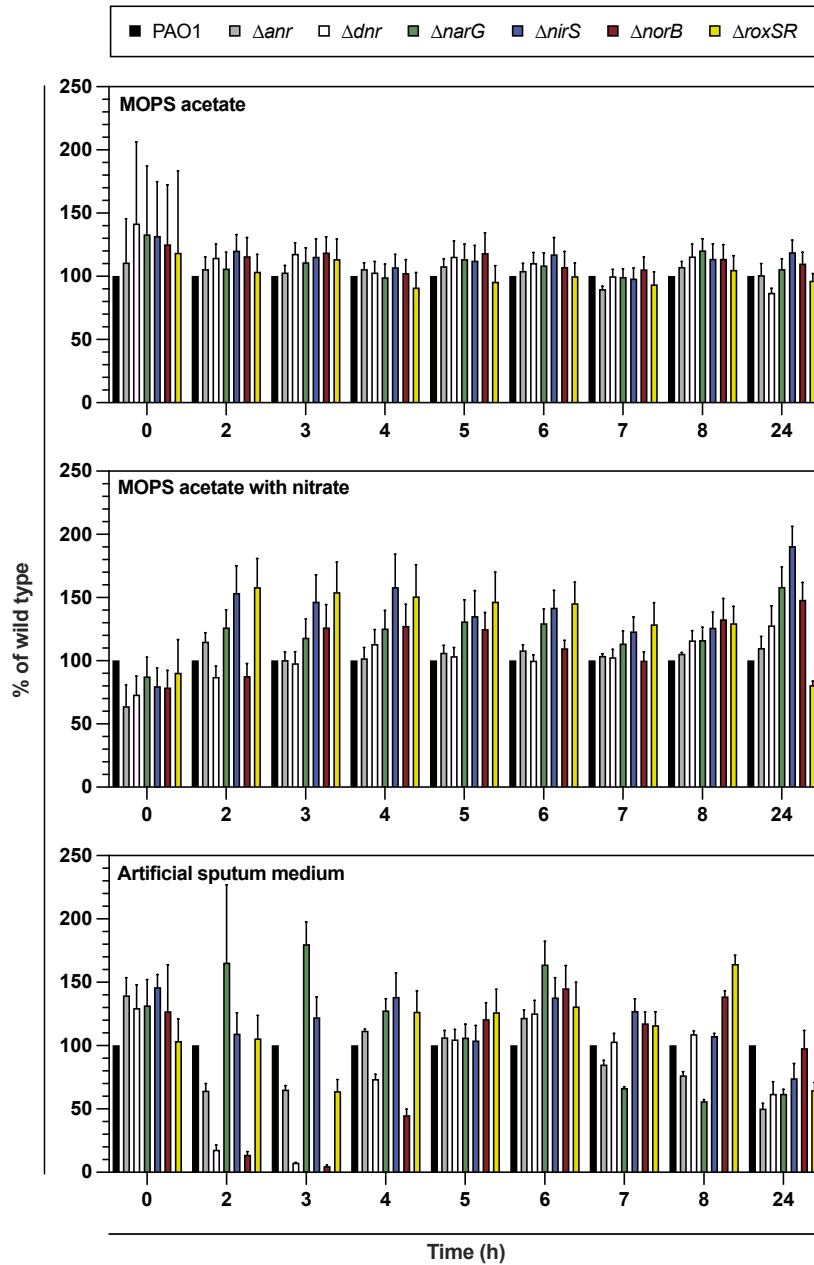


FIGURE B1. *P. aeruginosa* wild type and denitrification mutant OddHL promoter activity when cultured in a range of media. **TOP** MOPS with 40 mM acetate. **MIDDLE** MOPS with 40 mM acetate and 20 mM KNO_3 . **BOTTOM** Artificial sputum medium. Mean and standard deviation of at least three biological replicates.

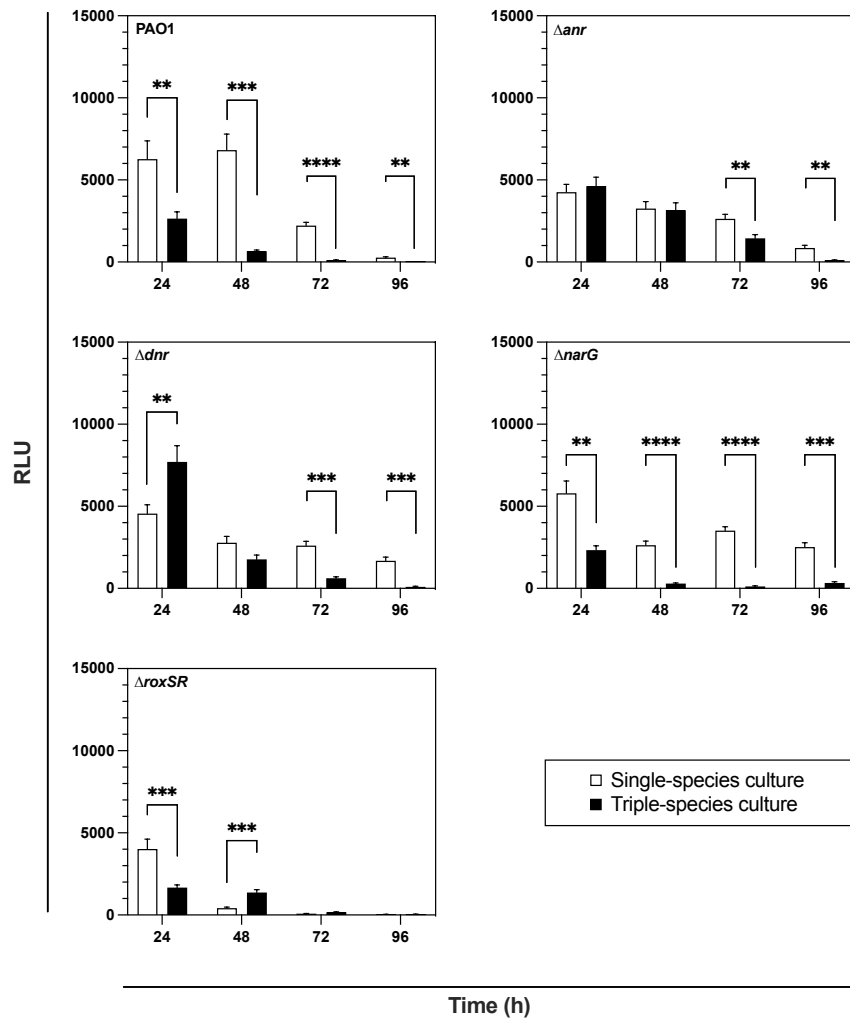


FIGURE B2. Comparison of single- and triple-species OdDHL promoter activity when cultured in artificial sputum medium batch culture. Mean and standard deviation of at least three biological replicates.

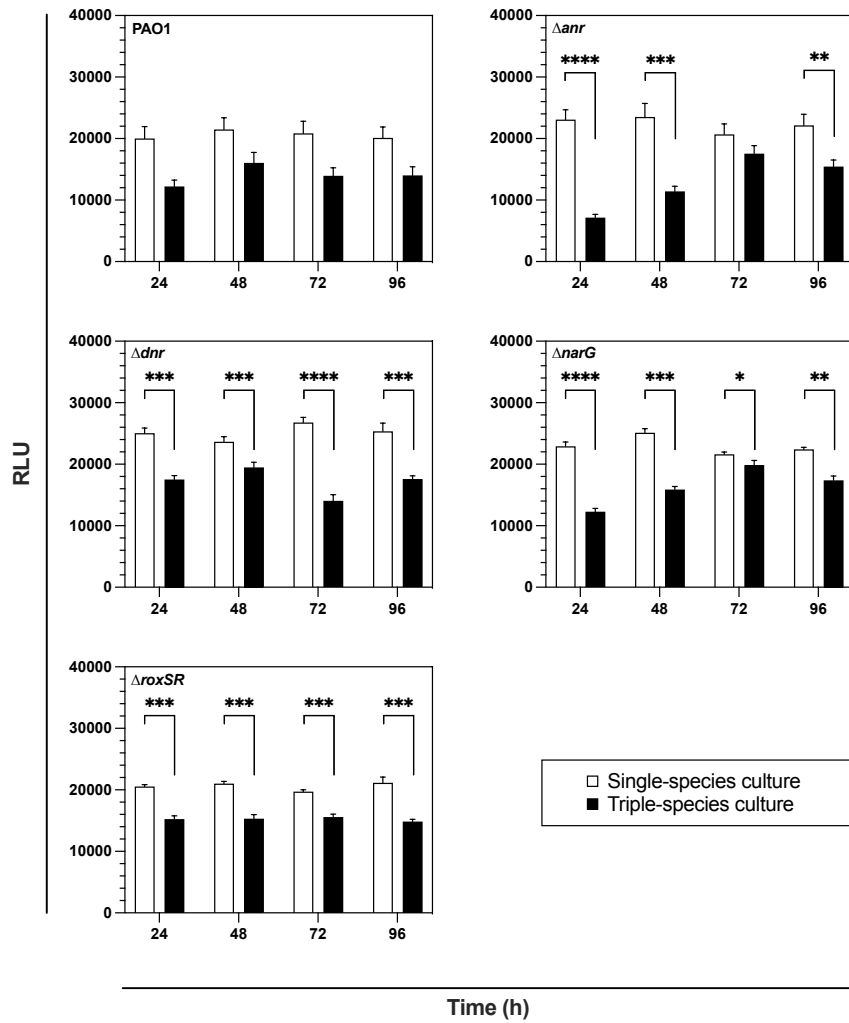


FIGURE B3. Comparison of single- and triple-species O₂DHL promoter activity when cultured in artificial sputum medium continuous-flow culture. Mean and standard deviation of at least three biological replicates.

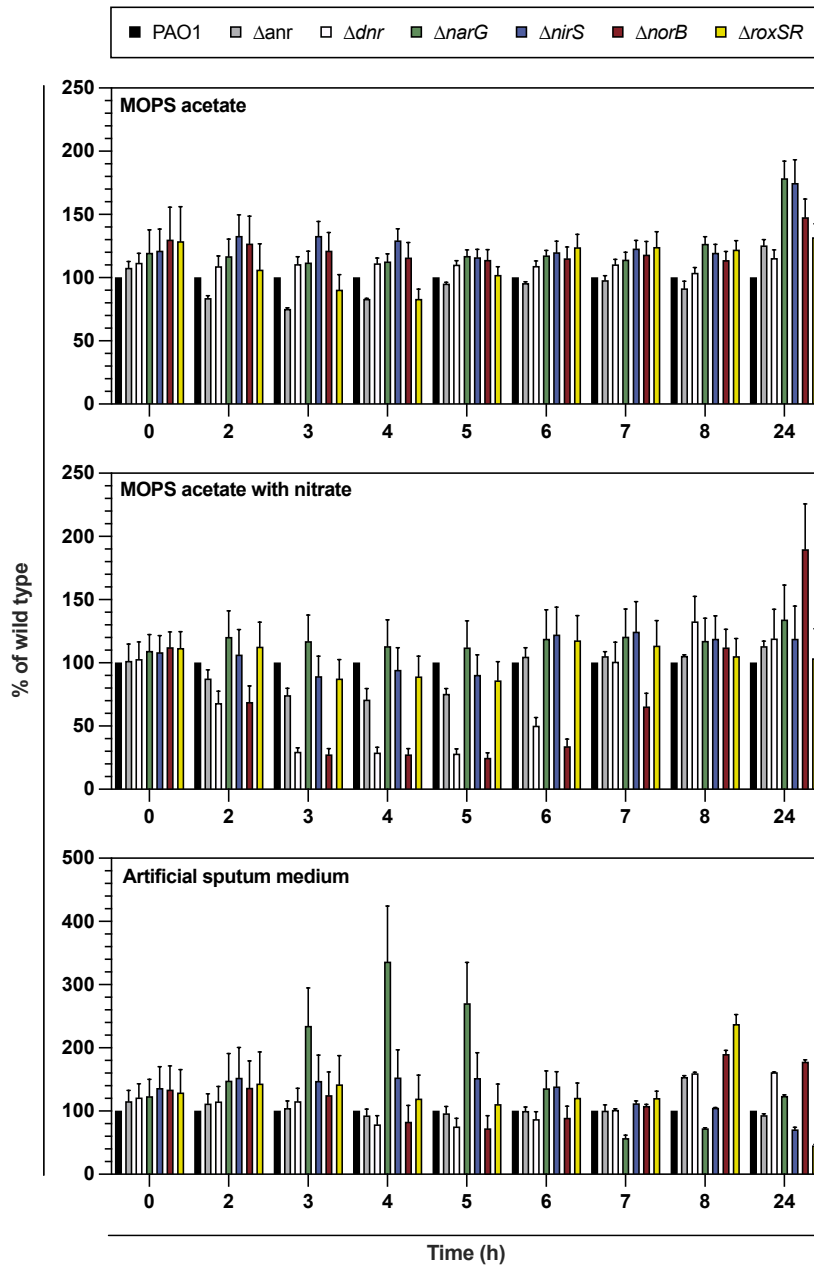


FIGURE B4. *P. aeruginosa* wild type and denitrification mutant BHL promoter activity when cultured in a range of media. **TOP** MOPS with 40 mM acetate. **MIDDLE** MOPS with 40 mM acetate and 20 mM KNO_3 . **BOTTOM** Artificial sputum medium. Mean and standard deviation of at least three biological replicates.

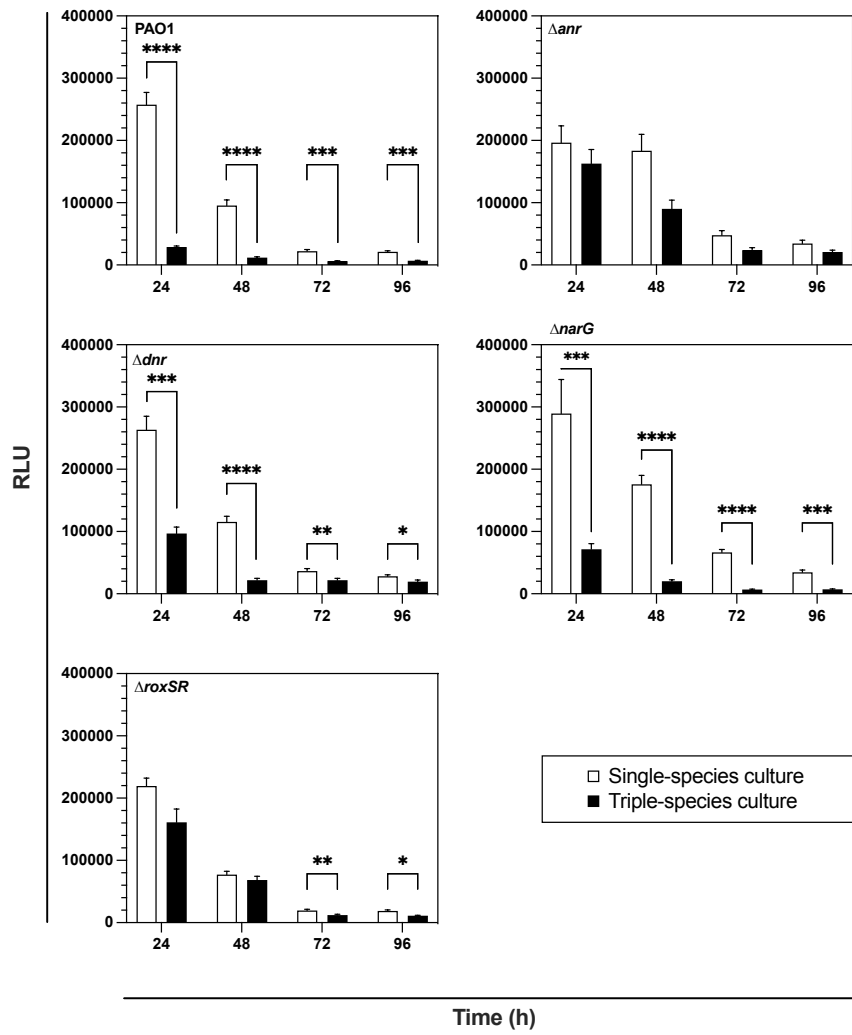


FIGURE B5. Comparison of single- and triple-species BHL promoter activity when cultured in artificial sputum medium batch culture. Mean and standard deviation of at least three biological replicates.

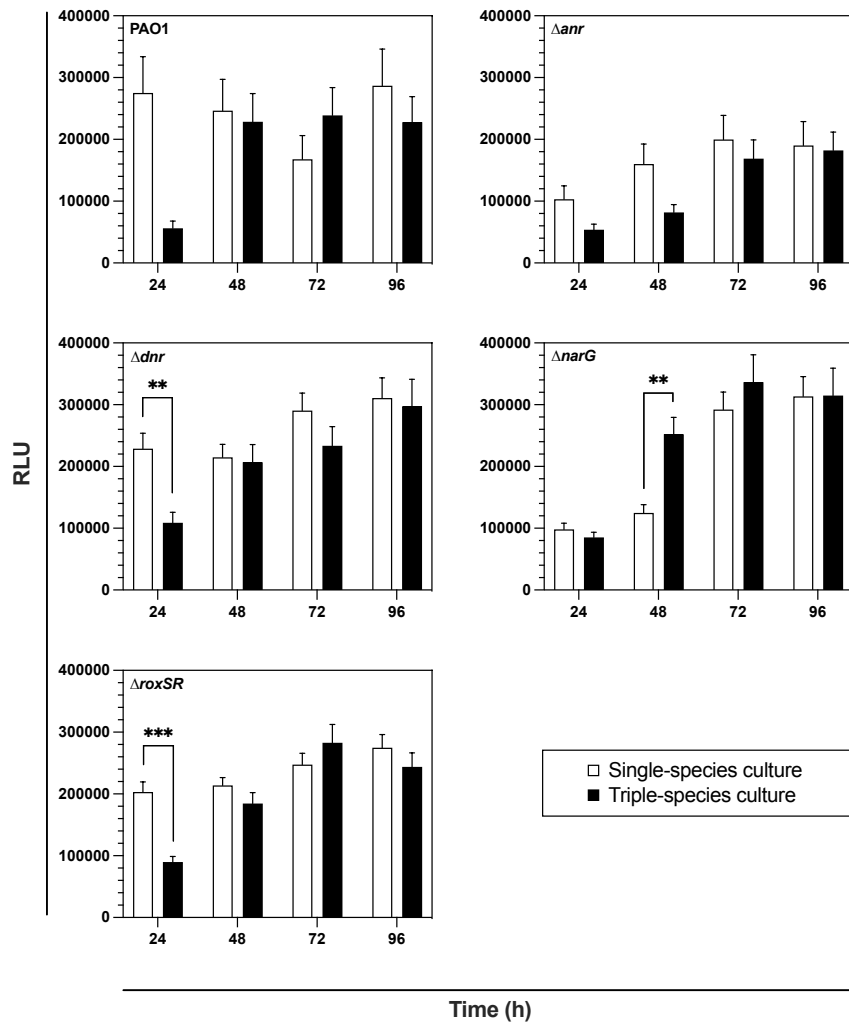


FIGURE B6. Comparison of single- and triple-species BHL promoter activity when cultured in artificial sputum medium continuous-flow culture. Mean and standard deviation of at least three biological replicates.

Appendix C: continuous-flow system CFUs (single species) and additional statistical analyses of LVC model interactions (triple species)

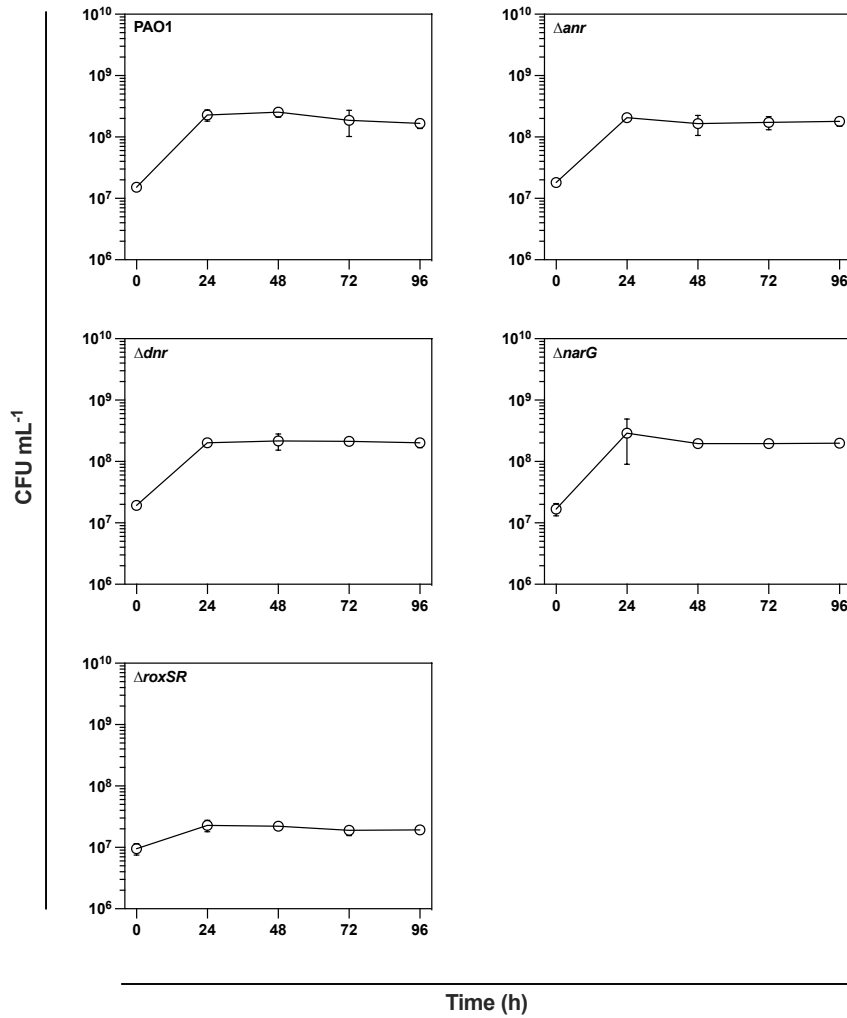


FIGURE C1. CFU enumeration of *P. aeruginosa* wild type and respiratory mutants in artificial sputum medium continuous-flow culture. Mean and standard deviation of at least three biological replicates.

TABLE C1. Statistical testing of LVC model *P. aeruginosa* wild type and *C. albicans* interactions. P values are Bonferroni corrected and compared against a 0.05 p value threshold.

Interaction 1	Interaction 2	χ^2	p value
Competitor	Mutualistic partner	30	< 0.0001
Competitor	Prey/host of PA	37	< 0.0001
Competitor	Predator/parasite of PA	0.01	5.499
Mutualistic partner	Prey/host of PA	1	1.904
Mutualistic partner	Predator/parasite of PA	31	< 0.0001
Prey/host of PA	Predator/parasite of PA	38	< 0.0001

TABLE C2. Statistical testing of LVC model *P. aeruginosa* Δanr and *S. aureus* interactions. P values are Bonferroni corrected and compared against a 0.05 p value threshold.

Interaction 1	Interaction 2	χ^2	p value
Competitor	Mutualistic partner	20	< 0.0001
Competitor	Prey/host of PA	3	0.469
Competitor	Predator/parasite of PA	0.36	3.291
Mutualistic partner	Prey/host of PA	8	0.023
Mutualistic partner	Predator/parasite of PA	25	< 0.0001
Prey/host of PA	Predator/parasite of PA	5	0.118

TABLE C3. Statistical testing of LVC model *P. aeruginosa* Δanr and *C. albicans* interactions. P values are Bonferroni corrected and compared against a 0.05 p value threshold.

Interaction 1	Interaction 2	χ^2	p value
Mutualistic partner	Prey/host of PA	12	0.0014
Mutualistic partner	Predator/parasite of PA	15	0.0002
Prey/host of PA	Predator/parasite of PA	0.2	0.023

TABLE C4. Statistical testing of LVC model *S. aureus* and *C. albicans* interactions (*P. aeruginosa* Δ *anr* co-culture). P values are Bonferroni corrected and compared against a 0.05 p value threshold.

Interaction 1	Interaction 2	χ^2	p value
Competitor	Mutualistic partner	2	1.078
Competitor	Prey/host of SA	83	< 0.0001
Competitor	Predator/parasite of SA	2	1.078
Mutualistic partner	Prey/host of SA	91	< 0.0001
Mutualistic partner	Predator/parasite of SA	0	6
Prey/host of SA	Predator/parasite of SA	91	< 0.0001

TABLE C5. Statistical testing of LVC model *P. aeruginosa* Δ *dnr* and *C. albicans* interactions. P values are Bonferroni corrected and compared against a 0.05 p value threshold.

Interaction 1	Interaction 2	χ^2	p value
Competitor	Mutualistic partner	70	< 0.0001
Competitor	Prey/host of PA	17	0.0001
Mutualistic partner	Prey/host of PA	30	< 0.0001

TABLE C6. Statistical testing of LVC model *S. aureus* and *C. albicans* interactions (*P. aeruginosa* Δ *dnr* co-culture). P values are Bonferroni corrected and compared against a 0.05 p value threshold.

Interaction 1	Interaction 2	χ^2	p value
Competitor	Mutualistic partner	63	< 0.0001
Competitor	Prey/host of SA	18	0.0001
Competitor	Predator/parasite of SA	45	< 0.0001
Mutualistic partner	Prey/host of SA	22	< 0.0001
Mutualistic partner	Predator/parasite of SA	5	0.1178
Prey/host of SA	Predator/parasite of SA	9	0.0185

TABLE C7. Statistical testing of LVC model *P. aeruginosa* $\Delta narG$ and *C. albicans* interactions. P values are Bonferroni corrected and compared against a 0.05 p value threshold.

Interaction 1	Interaction 2	χ^2	p value
Competitor	Mutualistic partner	52	< 0.0001
Competitor	Prey/host of PA	30	< 0.0001
Competitor	Predator/parasite of PA	36	< 0.0001
Mutualistic partner	Prey/host of PA	6	0.098
Mutualistic partner	Predator/parasite of PA	6	0.356
Prey/host of PA	Predator/parasite of PA	0.31	3.464

TABLE C8. Statistical testing of LVC model *P. aeruginosa* $\Delta roxSR$ and *S. aureus* interactions. P values are Bonferroni corrected and compared against a 0.05 p value threshold.

Interaction 1	Interaction 2	χ^2	p value
Competitor	Mutualistic partner	22	< 0.0001
Competitor	Prey/host of PA	0.014	5.441
Competitor	Predator/parasite of PA	4	0.213
Mutualistic partner	Prey/host of PA	21	< 0.0001
Mutualistic partner	Predator/parasite of PA	8	0.023
Prey/host of PA	Predator/parasite of PA	4	0.281

TABLE C9. Statistical testing of LVC model *P. aeruginosa* $\Delta roxSR$ and *C. albicans* interactions. P values are Bonferroni corrected and compared against a 0.05 p value threshold.

Interaction 1	Interaction 2	χ^2	p value
Competitor	Mutualistic partner	57	< 0.0001
Competitor	Prey/host of PA	18	0.0001
Competitor	Predator/parasite of PA	47	< 0.0001
Mutualistic partner	Prey/host of PA	17	0.0002
Mutualistic partner	Predator/parasite of PA	2	1.235
Prey/host of PA	Predator/parasite of PA	10	0.0088

TABLE C10. Statistical testing of LVC model *S. aureus* and *C. albicans* interactions (*P. aeruginosa* Δ *roxSR* co-culture). P values are Bonferroni corrected and compared against a 0.05 p value threshold.

Interaction 1	Interaction 2	χ^2	p value
Competitor	Mutualistic partner	0.091	4.578
Competitor	Prey/host of SA	4	0.213
Competitor	Predator/parasite of SA	0.1	4.511
Mutualistic partner	Prey/host of SA	3	0.424
Mutualistic partner	Predator/parasite of SA	0.381	3.223
Prey/host of SA	Predator/parasite of SA	6	0.097